



This is to certify that the  
dissertation entitled

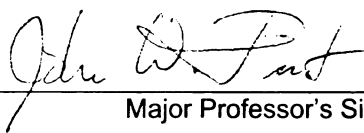
SYNTHESIS AND EVALUATION OF PRECURSORS TO THE  
AMINO- AND ARCHAEL SHIKIMATE PATHWAYS

presented by

Heather A. Stueben

has been accepted towards fulfillment  
of the requirements for the

Ph.D. degree in Chemistry



Major Professor's Signature

04-26-2006

Date

**PLACE IN RETURN BOX** to remove this checkout from your record.  
**TO AVOID FINES** return on or before date due.  
**MAY BE RECALLED** with earlier due date if requested.

DATE DUE	DATE DUE	DATE DUE

SYNTHESIS AND EVALUATION OF PRECURSORS TO THE AMINO- AND  
ARCHAEAL SHIKIMATE PATHWAYS

By

Heather A. Stueben

A DISSERTATION

Submitted to  
Michigan State University  
in partial fulfillment of the requirements  
for the degree of

DOCTOR OF PHILOSOPHY

Department of Chemistry

2006



## ABSTRACT

### SYNTHESIS AND EVALUATION OF PRECURSORS TO THE AMINO- AND ARCHAEAL SHIKIMATE PATHWAYS

By

Heather A. Stueben

Some organisms, in preparation of select metabolites, use variations of the shikimate pathway, an essential metabolic route by which microorganisms and plants synthesize the aromatic amino acids. One such variant, the aminoshikimate pathway, produces 3-amino-5-hydroxybenzoate required for the biosynthesis of the ansamycins and the mitomycins. Another variant, an archaeal shikimate pathway, has been proposed to feature a unique biosynthesis of the intermediate 3-dehydroquinate.

The aminoshikimate pathway of *Amycolatopsis mediterranei* (ATCC 21789) and *Bacillus pumilus* proceeds from the 3-amino derivative of glucose, kanosamine. It has been proposed that the biosynthesis of kanosamine proceeds from uridine 5'-diphospho-D-glucose (UDPG) through the subsequent intermediacy of uridine 5'-diphospho-3-keto-D-glucose (3-ketoUDPG) and uridine 5'-diphospho-D-kanosamine (UDPK). This thesis establishes the intermediacy of 3-ketoUDPG in kanosamine biosynthesis leading to the aminoshikimate pathway. The cell-free lysates of *A. mediterranei* and *B. pumilus* were used to prepare kanosamine from 3-ketoUDPG. RifL from *A. mediterranei*, was established as the dehydrogenase responsible for the oxidation of UDPG to 3-ketoUDPG. It was that RifK from *A. mediterranei* can catalyze the transamination of 3-ketoUDPG to UDPK. The source of nitrogen for the RifK catalyzed transamination of 3-ketoUDPG was established as the  $\alpha$ -amine of either glutamine or glutamic acid.

It has been proposed that the archaeal shikimate pathway of *Methanococcus jannaschii* proceeds from an alternative biosynthesis of the second common shikimate pathway intermediate, 3-dehydroquinic acid (DHQ). This thesis details research performed to provide evidence for a proposed DHQ precursor, 2-amino-2,3,7-trideoxy-6-oxo-4,5-D-*threo*-heptanoic acid (ATTH). The condensation of the proposed precursors to ATTH, 6-deoxy-5-ketofructose 1-phosphate (DKFP) and L-aspartate semialdehyde (ASA), by the proposed aldolase MJ0400 was investigated. Also, this thesis details several routes used in attempts to synthesize ATTH.

Copyright by  
Heather A. Stueben  
2006

**To my family**  
**For always believing in me**

## ACKNOWLEDGEMENTS

First, I would like to thank Prof. John Frost for his guidance and encouragement throughout my graduate career. I would also like to thank the members of my graduate committee, Prof. Babak Borhan, Prof. James Geiger, and Prof. Mitch Smith, for their input in both the preparation of this thesis and at other times during my stay as a graduate student.

I would like to thank Dr. Karen Frost for all her advice and encouragement. I would like to express thanks to past members of my research group, including Dr. Chad Hansen, Dr. Dave Knop, and Dr. Padmesh Venkitasubramanian for their patience and guidance during the early stages of my graduate career. I am also grateful to other past group members Dr. Wei Niu, Dr. Jian Yi, and Dr. Mapitso Molefe, and Dr. Jihane Achkar for their invaluable input and advice. I would like to show my gratitude to Dr. Jiantao Guo for his input and advice throughout my work on the aminoshikimate project. I am thankful as well to the remaining present Frost Group members, Dr. Ningqing Ran, Wengsheng Li, ManKit Lau, Justas Jancauskas, Jinsong Yang, and Brad Cox for their friendship and support.

I would also like to express gratitude to my family. Their perseverance in life's trials, while providing unending love, support, and encouragement, has been invaluable to me throughout my life as well as my graduate career.

# TABLE OF CONTENTS

LIST OF TABLES .....	XI
LIST OF FIGURES.....	XIII
LIST OF ABBREVIATIONS.....	XVII
CHAPTER ONE .....	1
INTRODUCTION.....	1
The Aminoshikimate Pathway and Ansamycin Biosynthesis.....	3
Archaeal Aromatic Amino Acid Biosynthesis.....	15
<i>Archaea</i> : an overview .....	15
Ribose biosynthesis and the shikimate pathway of archaeal methanogens .....	17
The “missing” genes of archaeal aromatic amino acid biosynthesis.....	24
CHAPTER TWO .....	31
UDP-3-KETOGLUCOSE INTERMEDIACY IN KANOSAMINE BIOSYNTHESIS ...	31
Introduction .....	31
Synthesis of 3-ketoUDPG .....	36
Overview .....	36
Synthesis of 3-ketoUDPG using partially purified glucoside-3-dehydrogenase...	38
Synthesis of 3-ketoglucose-1-phosphate using <i>A. tumefaciens</i> standing cells.....	40
Synthesis of 3-ketoUDPG from 3-ketoglucose-1-phosphate .....	41
Synthesis of 3-ketoUDPG from UDPG using the standing cells of <i>A. tumefaciens</i> .....	42
Reaction of 3-ketoUDPG with the cell-free extract of <i>A. mediterranei</i> .....	43
Role of NAD in <i>A. mediterranei</i> kanosamine biosynthesis .....	44
Overview .....	44
Synthesis of [3- <sup>3</sup> H]-glucose.....	45
Synthesis of [3- <sup>3</sup> H]-UDPG.....	46
Reaction of [3- <sup>3</sup> H]-UDPG with <i>A. mediterranei</i> cell-free lysate .....	48
NADH “trapping”.....	49
Expression and Analysis of RifL and RifK .....	51
Overview .....	51
Reaction of UDPG and 3-ketoUDPG with the cells free-lysates of RifL and RifK <i>A. mediterranei</i> mutants.....	53
Heterologous expression and purification of RifL .....	55
Specific activity of RifL.....	58
Initial attempts to produce UDPK using RifK or a combination of RifK/RifL ....	60
Optimization of RifK expression in <i>E. coli</i> .....	65
Specific activity of RifK .....	68
The source of nitrogen in <i>A. mediterranei</i> kanosamine biosynthesis.....	69
Overview .....	69
Investigation of the kanosamine biosynthetic nitrogen source using 3-ketoUDPG and heterologously expressed RifK .....	70

Kanosamine biosynthesis through 3-ketoUDPG by <i>B. pumilus</i> .....	73
Discussion .....	75
CHAPTER THREE.....	93
3-DEHYDROQUINATE BIOSYNTHESIS VIA THE ARCHAEL SHIKIMATE PATHWAY OF METHANOCALDOCOCUS JANNASCHII .....	93
Introduction .....	93
L-Aspartate semialdehyde intermediacy.....	97
Preparation of ASA.....	98
Preparation of DKFP .....	100
Preparation of MJ0400.....	101
Reaction of ASA and DKFP with MJ0400.....	102
Expression of <i>hdhI</i> and <i>thrA</i> .....	104
Expression of <i>mjl602</i> .....	106
Expression of <i>mjl249</i> .....	107
ATTH intermediacy.....	108
Overview .....	108
Synthesis of ATTH from <i>N</i> -Cbz-Aspartic acid.....	109
Synthesis of ATTH from <i>N</i> -Boc-Asp(Obz)-OH .....	120
Synthesis of ATTH from D-tartaric acid through deoxy-xylose intermediacy....	124
Discussion .....	126
CHAPTER FOUR.....	137
EXPERIMENTALS .....	137
GENERAL METHODS.....	137
General Chemistry .....	137
Chromatography .....	138
Spectroscopic measurements.....	139
Chemical Assays.....	141
Organic and Inorganic Phosphate Assay.....	141
Ninhydrin assay .....	142
Bacterial Strains and Plasmids .....	143
Storage of Bacterial Strains and Plasmids .....	143
Culture Medium.....	144
Analysis of culture supernatant .....	145
Genetic Manipulations .....	146
General procedures .....	146
Determination of DNA concentration.....	147
Large scale purification of plasmid DNA .....	147
Small scale purification of plasmid DNA .....	149
Restriction enzyme digest of DNA .....	150
Agarose gel electrophoresis.....	151
Isolation of DNA from agarose .....	151
Treatment of vector DNA with calf intestinal alkaline phosphatase (CIAP) .....	152
Ligation of DNA.....	152
Preparation and transformation of <i>E. coli</i> competent cells .....	152

General Enzymology .....	154
General information .....	154
<i>E. coli</i> UGPase (GalU) assay.....	155
<i>A. tumefaciens</i> glucoside-3-dehydrogenase activity assay.....	155
<i>A. mediterranei</i> UDPG dehydrogenase (RifL) assay.....	156
Assay Condition #1: DCIP/PMS assay .....	156
Assay Condition #2: HPLC assay .....	156
<i>A. mediterranei</i> transaminase (RifK) assay.....	157
<i>A. mediterranei</i> AHBA synthase (RifK) activity .....	158
SDS-PAGE protein gel .....	158
CHAPTER TWO.....	160
Synthetic preparations.....	160
Synthesis of [3- <sup>2</sup> H]-glucose.....	160
Uridine 5'-diphospho-[3- <sup>2</sup> H]-D-glucose .....	162
Genetic manipulations .....	164
Plasmid pHS3.244.....	164
Enzyme purifications .....	164
Overexpressed <i>E. coli galU</i> -encoded UGPase. ....	164
<i>A. tumefaciens</i> glucoside 3-dehydrogenase.....	165
Recombinant RifK .....	167
BL21 Codon Plus RP/pJG7.259 .....	167
JM109/pJG7.259.....	168
In vivo enzymatic reactions.....	169
Oxidation of glucosides to 3-ketoglucosides by <i>A. tumefaciens</i> Whole Cells .....	169
Cell-free lysate preparations.....	170
Cell-free lysate of <i>A. mediterranei</i> .....	170
Cell-free lysate of <i>A. mediterranei</i> RM01 and HGF003.....	171
Cell-free lysate of <i>B. pumilus</i> .....	171
JM109/pJG7.275 and JM109/pJG7.259a Cell-free Lysate. ....	172
BL21(DE3)/pRM030 cell-free lysate.....	172
Preparation of BL21 Codon Plus RP/pJG7.275 Cell-free Lysate (RifL).....	173
Preparation of BL21 Codon Plus RP/pJG7.259 cell-free lysate (RifK) .....	173
In vitro enzymatic reactions .....	174
Kanosamine Biosynthesis from UDPG.....	174
Kanosamine biosynthesis from 3-ketoUDPG .....	174
Kanosamine biosynthesis from [3- <sup>2</sup> H]-UDPG .....	175
Kanosamine biosynthesis from UDPG in the presence of NAD and NADH.....	176
Oxidation of UDPG to 3-ketoUDPG by heterologously expressed RifL .....	176
NAD cofactor.....	176
DCIP/PMS cofactor.....	176
UDPG from 3-ketoUDPG by heterologously expressed RifL .....	177
UDPK from 3-ketoUDPG. ....	177
Heterologously expressed RifK and RifL .....	177
Heterologously expressed RifK .....	178
Chromatography .....	179



HPLC paired-ion chromatography Analysis of UDP-glucosides.....	179
CHAPTER THREE .....	179
Synthetic Preparations .....	179
Synthesis of L-aspartate semialdehyde .....	179
Preparation of DKFP.....	182
Preparation of ATTH from <i>N</i> -Cbz-L-aspartic acid.....	183
Preparation of ATTH from <i>N</i> -tert-butoxycarbonyl-L-aspartic acid $\beta$ -benzyl ester .....	185
ATTH from D-tartaric acid .....	196
Genetic manipulations .....	201
pHS7.098.....	201
pHS8.080.....	201
pHS8.216.....	202
pHS8.240.....	202
pHS8.243.....	203
pHS8.101.....	203
Enzyme Purifications .....	203
<i>E. coli</i> aspartate semialdehyde dehydrogenase (ASADH) .....	203
Enzyme Assays.....	205
ASADH specific activity assay .....	205
In vitro enzyme reactions.....	206
Condensation of ASA and DKFP by MJ0400.....	206
GC-MS analysis.....	207
Analysis of MJ0400 catalyzed condensation of ASA and DKFP. ....	207
REFERENCES.....	208

## LIST OF TABLES

Table 1. Proposed functions of <i>rif</i> biosynthetic gene products.....	11
Table 2. Purification of glucoside-3-dehydrogenase.....	39
Table 3. Methods used to purify [3-H <sup>2</sup> ]-UDPG. ....	48
Table 4. Reactions of UDPG and 3-ketoUDPG with the cell-free lysate of <i>A. mediterranei</i> mutants lacking <i>rifL</i> and <i>rifK</i> . ....	55
Table 5. Arginine and proline codon frequencies of <i>E. coli</i> , <i>A. mediterranei</i> , and <i>rifL</i> ....	57
Table 6. Specific activity determinations of RifL.....	59
Table 7. Reactions of 3-ketoUDPG with heterologously expressed RifK from JM109/pJG7.259a.....	61
Table 8. Reactions of 3-ketoUDPG with RifK obtained from BL21 C+ RP/pJG7.259a..	62
Table 9. Optimization of RifK transamination of 3-ketoUDPG.....	66
Table 10. Optimization of RifK transamination of 3-ketoUDPG.....	67
Table 11. Screening for RifK reducing equivalents.....	68
Table 12. <sup>15</sup> N enrichments in kanosamine produced using <i>A. mediterranei</i> cell-free lysate and in UPDK produced using BL21 C <sup>+</sup> RP/pJG7.259a cell-free lysate. ....	71
Table 13. Nitrogen source and PLP dependence of the RifK catalyzed transamination of 3-ketoUPDG.....	73
Table 14. Reaction of [3- <sup>2</sup> H]-UDPG with <i>B. pumilus</i> cell-free lysate. ....	74
Table 15. <i>B. pumilus</i> NADH trapping experiments. ....	75
Table 16. Varying conditions used to prepare compound A as an intermediate to the <i>N</i> -Cbz-oxazolidine aldehyde.....	110
Table 17. Optimization of oxazolidine aldehyde preparation.....	112
Table 18. Condensation of oxazolidine aldehyde with TPP to produce the enone.....	115

Table 19. Dihydroxylation of the enone.....	117
Table 20. Optimization of enone dihydroxylation. ....	119
Table 21. Protection of protected ATTH in an attempt to separate the diol diastereomers. .....	122

## LIST OF FIGURES

Figure 1. The shikimate pathway.....	6
Figure 2. Labeling patterns of shikimate, 3-amino-5-hydroxybenzoate, and rifamycin from <sup>13</sup> C-labeled glucose and glycerate. ....	7
Figure 3. Labeling pattern of mitomycin C from labeled D-erythrose and pyruvic acid..	9
Figure 4. Rifamycin biosynthetic gene cluster of <i>A. mediterranei</i> S699 and proposed enzyme functions.....	10
Figure 5. The proposed aminoshikimate pathway. ....	12
Figure 6. Proposed pathway for kanosamine biosynthesis.....	15
Figure 7. Non-oxidative Pentose Phosphate Cycle.....	18
Figure 8. Observed <sup>13</sup> C labeling patterns of tyrosine and tryptophan from acetate and pyruvate added to the growing culture of <i>M. thermoautotrophicum</i> .....	20
Figure 9. Observed <sup>13</sup> C labeling patterns of pyruvate, hexoses, pentoses, and tetroses from, <sup>13</sup> C enriched acetate and pyruvate. ....	21
Figure 10. Alternative DHQ precursors as suggested by Frost. ....	27
Figure 11. Alternative DHQ precursors as proposed by White. ....	28
Figure 12. Proposed archaeal shikimate pathway.....	30
Figure 13. Aminoshikimate pathway.....	32
Figure 14. Proposed route for kanosamine biosynthesis from UDPG. ....	34
Figure 15. Mechanism for the oxidation of sucrose to 3-ketosucrose by the glucoside-3- dehydrogenase from <i>A. tumefaciens</i> . ....	37
Figure 16. Preparation of 3-ketoglucose-1-phosphate using the standing cells of <i>A.</i> <i>tumefaciens</i> .....	41
Figure 17. Preparation of 3-ketoUDPG from 3-ketoglucose-1-phosphate.....	42
Figure 18. Preparation of 3-ketoUDPG from UDPG using the standing cells of <i>A.</i> <i>tumefaciens</i> .....	43
Figure 19. Synthesis of [3- <sup>2</sup> H]-glucose from glucose. ....	46

Figure 20. One-pot enzymatic synthesis of [3- $H^2$ ]-UDPG from [3- $H^2$ ]-glucose.....	47
Figure 21. Reaction of [3- $H^2$ ]-UDPG with the cell-free lysate of <i>A. mediterranei</i> . ....	49
Figure 22. Co-factors for the <i>in situ</i> regeneration of NAD from NADH.....	50
Figure 23. Reaction of UDPG with DCIP, PMS, and the cell-free lysate of JM109/pJG7.275.....	56
Figure 24. Preparation of UDPK and the reaction of UDPK with BL21 C <sup>+</sup> RP/pJG7.259a to produce 3-ketoUDPG.....	64
Figure 25. Preparation of DHMP. ....	68
Figure 26. <sup>1</sup> H NMR spectrum of 3-ketoUDPG produced by the oxidation of UDPG by <i>A.</i> <i>tumefaciens</i> .....	80
Figure 27. <sup>13</sup> C NMR spectrum of 3-ketoUDPG produced through the oxidation of UDPG by <i>A. tumefaciens</i> . ....	81
Figure 28. 2D-COSY spectrum of 3-ketoUDPG produced by <i>A. tumefaciens</i> . ....	82
Figure 29. Standard <sup>1</sup> H NMR spectrum of UDPG. ....	83
Figure 30. <sup>1</sup> H NMR spectrum of [3- $^2H$ ]-UDPG. ....	84
Figure 31. <sup>1</sup> H NMR spectrum of kanosamine. ....	85
Figure 32. <sup>1</sup> H NMR spectrum of [3- $^2H$ ]-kanosamine. ....	86
Figure 33. <sup>1</sup> H NMR spectrum of UDPK.....	87
Figure 34. <sup>1</sup> H NMR of the crude product mixture obtained upon the RifK catalyzed transamination of 3-ketoUDPG.....	88
Figure 35. Mass Spectrum of UDPK produced from the RifK catalyzed transamination of 3-ketoUDPG in the presence of L-glutamine.....	89
Figure 36. Mass Spectrum of UDPK produced from the RifK catalyzed transamination of 3-ketoUDPG in the presence of [amide- <sup>15</sup> N]-L-glutamine.....	90
Figure 37. Mass Spectrum of UDPK produced upon the RifK catalyzed transamination of 3-ketoUDPG in the presence of [ $\alpha$ - <sup>15</sup> N]-L-glutamine.....	91
Figure 38. HPLC analysis of UDPK produced by the RifK catalyzed transamination of 3- ketoUDPG. ....	92

Figure 39. Early proposal by Frost for alternate DHQ biosynthetic precursors. ....	94
Figure 40. Predicted <sup>13</sup> C labeling patterns of tyrosine and phenylalanine from acetate and pyruvate through the DHQ biosynthetic route proposed by Frost. ....	95
Figure 41. Hypothetical <i>M. jannaschii</i> biosynthetic route to DHQ proposed by White. ..	97
Figure 42. Preparation of ASA from racemic allyl glycine.....	98
Figure 43. Ozonolysis of Protected allyl glycine.....	99
Figure 44. ASADH activity assay.....	100
Figure 45. Preparation of DKFP. ....	101
Figure 46. Reaction of DKFP and ASA with MJ0400 as proposed by White. ....	103
Figure 47. Reactions catalyzed by homoserine dehydrogenase and aspartate kinase....	105
Figure 48. Division of <i>thrA</i> into different gene segments for individual expression or recombination to produce new bifunctional enzymes. ....	106
Figure 49. Presumed aminotransfer catalyzed by MJ1249 to produce the ketoacid DDTH. ....	107
Figure 50. Preparation of the oxazolidine aldehyde.....	109
Figure 51. Optimized of oxazolidine aldehyde preparation from the acid chloride. ....	113
Figure 52. Synthetic strategy for enone preparation from the oxazolidine aldehyde. ...	114
Figure 53. Simultaneous removal of Cbz group and cleavage of oxazolidine ring.....	118
Figure 54. Possible alternate dihydroxylation products. ....	120
Figure 55. Synthesis of ATTH from <i>N, N</i> -diboc-Asp-OtBu.....	121
Figure 56. ATTH from <i>N</i> -boc-Asp-OBn-OtBu. ....	123
Figure 57. ATTH synthesis from D-tartaric acid through 2-deoxy-xylose intermediacy. ....	126
Figure 58. GC spectrum obtained from the MJ0400 catalyzed condensation of ASA and DKFP. ....	129

Figure 59. Example of a mass spectrum obtained from the GC-MS analysis of the MJ0400 catalyzed condensation of ASA and DKFP.....	130
Figure 60. <sup>1</sup> H NMR spectrum of (4S)-3-carbobenzyloxy-5-oxo-4-(4-oxo-pent-2-enyl)-oxazolidine. ....	131
Figure 61. <sup>1</sup> H NMR spectrum of the product mixture produced upon asymmetric dihydroxylation of (4S)-3-carbobenzyloxy-5-oxo-4-(4-oxo-pent-2-enyl)-oxazolidine. ....	132
Figure 62. <sup>1</sup> H NMR spectrum of the diol mixture obtained upon Sharpless asymmetric dihydroxylation of <i>N,N</i> -Bis( <i>tert</i> -Butoxycarbonyl)amino-6-oxo-hept-4-enoic acid <i>tert</i> -butyl ester. ....	133
Figure 63. <sup>1</sup> H NMR spectrum of diol mixture produced upon Sharpless asymmetric dihydroxylation of <i>N</i> - <i>tert</i> -Butoxycarbonylamino-6-oxo-hept-4-enoic acid <i>tert</i> -butyl ester. ....	134
Figure 64. <sup>1</sup> H NMR spectrum of compound A isolated upon benzylation of the mono-boc protected diol mixture. ....	135
Figure 65. <sup>1</sup> H NMR spectrum of compound B isolated upon the benzylation of the mono-boc protected diol mixture. ....	136

## LIST OF ABBREVIATIONS

3-ketoUDPG	Uridine 5'-diphospho-3-keto-D-glucose
A	Absorbance
Ac <sub>2</sub> O	Acetic anhydride
AcOH	Acetic acid
ADP	Adenine 5'-diphosphate
AHBA	3-amino-5-hydroxybenzoic acid
AminoDAHP	3,4-dideoxy-4-amino-D- <i>arabino</i> -heptulosonic acid 7-phosphate
AminoDHQ	5-deoxy-5-amino-3-dehydroquinic acid
AminoDHS	5-deoxy-5-amino-dehydroshikimic acid
AminoF6P	3-amino-3-deoxy-fructose 6-phosphate
AMINOSA	3-DEOXY-3-AMINO-SHIKIMIC ACID
Amp	Ampicillin
ASADH	L-aspartate semialdehyde dehydrogenase
ATP	Adenosine 5'-triphosphate
ATTH	2-amino-2,3,7-trideoxy-6-oxo-4,5-D- <i>threo</i> -heptanoic acid
Bis-Tris propane	1,3-Bis[Tris(hydroxymethyl)methylamino]propane
BnBr	Benzyl bromide
Boc <sub>2</sub> O	<i>tert</i> -butyloxycarbonyl anhydride
BOP reagent	(Benzotriazol-1-yloxy)Tris(dimethylamino)phosphonium hexafluorophosphate
BSA	Bovine serum albumin



BzCl	Benzoyl chloride
DAHP	3-deoxy-D- <i>arabino</i> -heptulosonic acid 7-phosphate
DCC	Dicyclohexycarbodiimide
DCIP	2,6-dichloroindolphenol
DDTH	3,7-dideoxy-D- <i>threo</i> -heptulo-2,6-diulosonic acid
DEAE	diethylaminoethyl
DHA	Dihydroxy acetone
DHAP	Dihydroxyacetone phosphate
DHMP	5,10-dihydro-5-methyl phenazine
DHS	3-dehydroshikimic acid
(DHQD) <sub>2</sub> PHAL	Hydroquinidine 1,4-phthalazinediyl diether
DIAD	Diisopropyl azo dicarboxylate
DIBAL	Diisobutyl aluminum hydride
DKFP	6-deoxy-5-ketofructose 1-phosphate
DMAP	<i>N,N</i> -Dimethylamino pyridine
DMF	Dimethyl formamide
DMPCA	4,5-dihydroxy-6-methyl-piperidine-2-carboxylic acid
DMSO	Dimethyl sulfoxide
DTT	Dithiothreitol
E4P	Erythrose 4-phosphate
EDTA	Ethylene diamine tetraacetic acid
EPPS (HEPPS)	4-(2-Hydroxyethyl)-1-piperazinepropanesulfonic acid
Et <sub>2</sub> O	Diethyl ether

EtOH	Ethyl alcohol
ETP	Electron transport pathway
EtSH	Ethanethiol
FAD	Flavin adenine dinucleotide
FADH <sub>2</sub>	Flavin adenine dinucleotide reduced
FMN	FLAVIN MONONUCLEOTIDE
G3DH	Glucoside 3-dehydrogenase
GC	Gas chromatography
GK	Glycerol kinase
HEPES	<i>N</i> -(2-Hydroxyethyl)piperazine- <i>N</i> -(2-ethanesulfonic acid)
HK	Hexokinase
HRMS	HI-RES MASS SPECTRAL ANALYSIS
IMINOE4P	1-deoxy-1-imino-D-erythrose 4-phosphate
IPTG	Isopropyl β-D-1-thiogalactopyranoside
K6P	Kanosamine 6-phosphate
ASA	L-aspartate semialdehyde
LB	Luria-Burtani broth
MeI	Methyl iodide
MeOH	Methyl alcohol
MOPS	3-( <i>N</i> -Morpholino)propanesulfonic acid
NAD	Nicotinamide adenine dinucleotide
NADH	Nicotinamide adenine dinucleotide reduced
NADP	Nicotinamide adenine dinucleotide phosphate

NADPH	Nicotinamide adenine dinucleotide phosphate reduced
NaOAc	Sodium acetate
<i>n</i> -BuLi	<i>n</i> -butyl lithium
NTA	Nitrilotriacetic acid
NMO	<i>N</i> -methylmorpholine <i>N</i> -oxide
NMR	Nuclear magnetic resonance
OD	Optical density
PCR	Polymerase chain reaction
PDC	Pyridinium dichromate
PEP	Phosphoenolpyruvate
PGM	Phosphoglucomutase
PhMe	Toluene
Pi	Inorganic phosphate
PIPES	1,4-Piperazinediethanesulfonic acid
PK	Pyruvate kinase
PLP	Pyridoxal 5-phosphate
PMP	Pyridoxamine 5-phosphate
PMS	Phenazine methosulfate
PMSF	Phenyl methyl sulfonyl fluoride
PPase	Inorganic pyrophosphatase
PPh <sub>3</sub>	Triphenylphosphine
PPi	Inorganic pyrophosphate
pTsOH	<i>p</i> -toluenesulfonic acid

Pyr	Pyridine
QA	Quinic acid
Quant.	Quantitative
R5P	Ribose 5-phosphate
RAMA	Rabbit muscle aldolase
S7P	Sedoheptulose 7-phosphate
SA	Shikimic acid
SDS-PAGE	Sodium dodecyl sulfate polyacrylamide gel electrophoresis
TBAF	Tetrabutylammonium fluoride
TBAHC	Tetrabutyl ammonium hydrogen carbonate
TBAHS	Tetrabutyl ammonium hydrogen sulfate
TBDMS	<i>tert</i> -butyl dimethylsilyl
TBDMSCl	<i>tert</i> -butyl dimethylsilyl chloride
<i>t</i> BuOH	<i>tert</i> -butyl alcohol
TEA	Triethylamine
TEAB	Triethylammonium bicarbonate
THF	Tetrahydrofuran
TMSI	Trimethylsilyl iodide
TPAP	Tetrapropylammonium perruthenate
TPP	Triphenylphosphoranyl 2-propanone
Tris	Tris(hydroxymethyl)aminomethane
U	Units
UDP	Uridine 5'-diphosphate

UDPG	Uridine 5'-diphospho-D-glucose
UDPK	Uridine 5'-diphospho-3-amino-3-deoxy-D-glucose or uridine 5'-diphospho-kanosamine
UGPase	Uridine 5'-diphosphoglucose pyrophosphorylase
UMP	Uridine 5'-monophosphate
UTP	Uridine 5'-triphosphate
YMG	Yeast malt glucose media
YT	Yeast tryptone broth

## CHAPTER ONE

### **INTRODUCTION**

The shikimate pathway is an essential metabolic route by which microorganisms and plants synthesize the aromatic amino acids phenylalanine, tyrosine, and tryptophan, in addition to a variety of primary metabolites required to sustain life.<sup>1</sup> The absence of this pathway in animals makes it an attractive target for metabolic intervention in the development of chemotherapeutic agents as well as herbicides. The shikimate pathway is also a source of a wide array of secondary metabolites utilized by both plants and microorganisms to maintain a position in the ecological environment. The majority of these metabolites are produced from the end products of the shikimate pathway, the aromatic amino acids. However, a select few metabolites are produced from variants of the shikimate pathway. These variations can consist of a branching off from any of the main pathway intermediates, a chemical modification of the pathway precursors, or the absence or replacement of common intermediary steps.<sup>2</sup>

The work performed prior to the preparation of this thesis focused on elaborating key intermediates leading to two variations of the shikimate pathway. One such variant, the aminoshikimate pathway, along which the typical intermediates of the shikimate pathway contain an amino group at C-4, produces 3-amino-5-hydroxybenzoate required for the biosynthesis of the ansamycins and the mitomycins. The other variant to be addressed here is an archaeal shikimate pathway featuring a unique biosynthesis of 3-dehydroquinate, which appears to lack the typical requirement of erythrose 4-phosphate

and 3-deoxy-D-*arabino*-heptulosonate 7-phosphate. As well as resolving fundamental biosynthetic questions there are practical incentives to advancing the knowledge of the molecular aspects associated with these two pathway variations. For example, elaboration of the aminoshikimate pathway could lead to the design of strains genetically modified to synthesize medicinally important compounds or analogs in higher than natural concentrations and yields. Through genetic manipulation, the unusual aminoshikimate pathway intermediates could be isolated and used as unique starting points to the synthesis or biosynthesis of novel compounds with intriguing medicinal properties. 5-Amino-5-deoxy-shikimate, which could be produced and isolated through the genetic manipulation of the aminoshikimate pathway, may be a useful starting material for the production of medicinal agents including the neuraminidase inhibitor, Tamiflu, produced currently from shikimate by Roche. Elaboration of the archaeal shikimate pathway could provide an innovative route to the shikimate pathway intermediates. Cells keep the steady-state concentration of erythrose 4-phosphate to a minimum in response to the molecule's inherent instability and propensity towards polymerization. Through genetic manipulation, strains could be designed to produce higher concentrations of shikimate pathway intermediates using the archaeal pathway enzymes.

Chapter One will present an overview of the aminoshikimate pathway and ansamycin biosynthesis as well as an overview of archaeal aromatic amino acid biosynthesis. Chapter Two describes research performed to elaborate the biosynthetic intermediates involved in kanosamine biosynthesis, a short pathway preceding the aminoshikimate pathway during which the famed amine moiety is introduced. Chapter

Three of this manuscript details efforts to delineate the intermediates involved in DHQ biosynthesis by the archaeal shikimate pathway. In order to study these two shikimate pathway variants the putative biosynthetic intermediates were prepared either biosynthetically or chemically. Once prepared the intermediates were incubated with the cell-free lysate of *A. mediterranei* or the alleged enzymes of the pathways heterologously expressed in *E. coli*. The lysate was then analyzed for the formation of the expected products or intermediates.

### The Aminoshikimate Pathway and Ansamycin Biosynthesis

As a class of medicinally significant natural products, each of the ansamycins portray alone or in combination antibacterial, antitumor, and/or antifungal activities.<sup>3</sup> The ansamycins were named for their characteristic structure, which includes an aromatic chromophore joined at two positions with an aliphatic (*ansa*) polyketide chain.<sup>4</sup> The aromatic chromophore contains an amine moiety at which the polyketide chain is connected through an amide linkage. The chromophore is also known to form a quinone-hydroquinone structure in most of the known ansamycins discovered to date (120 naturally-occurring).<sup>5</sup> The ansamycins are divided into two distinct categories based on the aromatic chromophore they contain: naphthalenoid or benzenoid.<sup>3</sup> Of the naphthalenoid ansamycins, the most well known are actamycin, ansathiazin, awamycin, halomycin, naphthomycin, rifamycin, streptovaricin, and tolypomycin. Ansamytocin, ansatrienin, geldanamycin, and the maytansines are some of the more commonly known benzenoid ansamycins.



Produced by *Amycolatopsis mediterranei*, the rifamycins were first isolated by Lepetit Research Laboratories as a mixture containing five distinct structures denoted rifamycin B, G, L, S, and SV.<sup>6</sup> Notably, the rifamycins were the first antibiotics identified whose antibiotic activity was linked to a selective inhibition of RNA synthesis through binding to bacterial RNA polymerase.<sup>7</sup> Due to its stability, ease of isolation, solubility at physiological pH, and spontaneous transformation into the more active rifamycin S, rifamycin B was chosen for development. Rifampicin, a synthetically modified form of rifamycin B<sup>8</sup>, has been used since the 1960's and remains one of the most important treatments of tuberculosis and mycobacterial infections.<sup>9</sup>

The carbon skeletons of the ansamycins share a resemblance with erythromycin-type macrolide antibiotics as the *ansa* chain contains alternating methyl and hydroxyl groups. This feature indicates the *ansa* moiety is produced from a polyketide chain formed via the condensation of methylmalonate units and intermittent malonate units.<sup>10</sup> The biosynthesis of ansamycins began with the study of rifamycin S formation. The formation of rifamycin S was studied through the incorporation of <sup>14</sup>C- and <sup>3</sup>H-labeled precursors. Analysis of the radioactivity of different fragments of the molecule, obtained by chemical degradation, established that propionate and acetate were incorporated head to tail, which is in agreement with the general pattern of a polyketide chain biosynthesis.<sup>11</sup> Through the assimilation of <sup>13</sup>C-enriched precursors followed by <sup>13</sup>C NMR analysis, the biosynthetic origin of the carbon atoms incorporated into the *ansa* chain of rifamycin S was established.<sup>12</sup> Other ansamycins, including geldanamycin,<sup>13</sup> naphthomycin,<sup>14</sup> actamycin,<sup>15</sup> and streptovaricin,<sup>16</sup> have also been used to study *ansa* chain formation.

According to the above labeling studies,<sup>11,12</sup> seven carbon atoms (C-1 to C-7,) of rifamycin S were not derived from propionate and acetate. These seven carbon atoms formed a substituted aromatic chromophore, which appeared to act as the initiator of polyketide synthases in *ansa* chain biosynthesis.<sup>17</sup> This aromatic unit also serves as the biosynthetic precursor of the mitomycin family. Its structure resembles an unusual *meta*-substituted aminobenzoate, as previously known natural aminobenzoates, such as anthranilic acid and *p*-aminobenzoate, are *ortho* or *para* substituted.

Several research groups worked to identify the biosynthetic precursor of this aromatic chromophore. Based on the results of genetic<sup>18</sup> and specific feeding experiments,<sup>19</sup> the biosynthetic precursor of this unique aromatic chromophore was identified as 3-amino-5-hydroxybenzoate (AHBA). Upon addition of AHBA, rifamycin B production was restored in a rifamycin B deficient mutant of *A. mediterranei*.<sup>18</sup> Using <sup>13</sup>C-enriched AHBA, it was determined C-1 of AHBA corresponds to the quinone carbonyl carbon of streptovaricin.<sup>19a</sup> Using [1-<sup>13</sup>C]-AHBA the C-1 of AHBA was also found to correspond to the benzyl methylene of ansamitocin<sup>19b</sup> and the aromatic methyl group of porfiromycin.<sup>19c</sup>

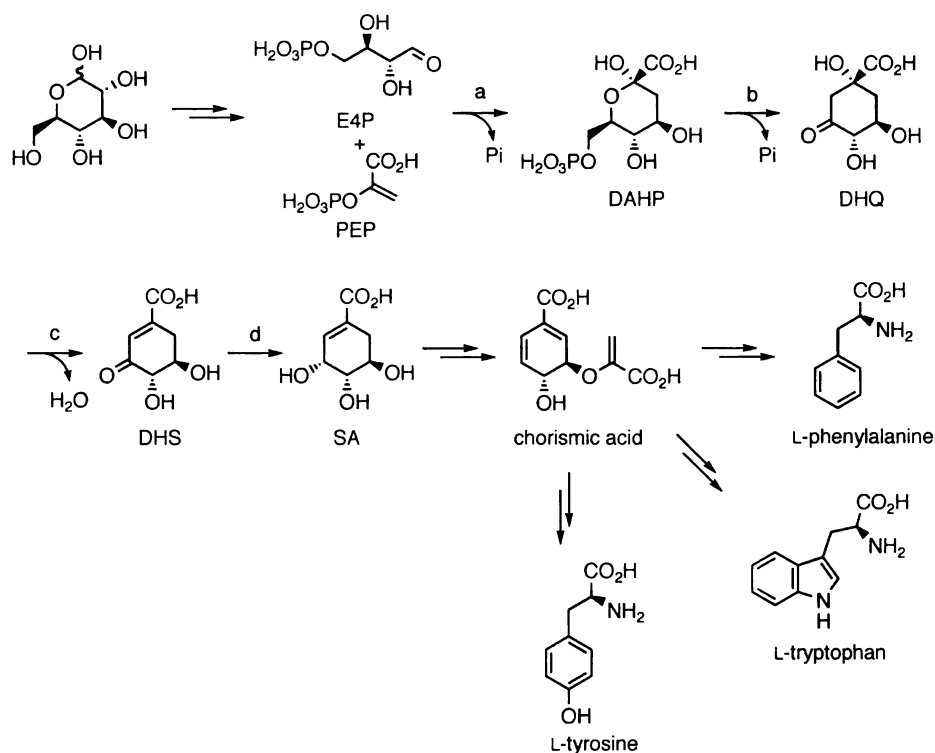


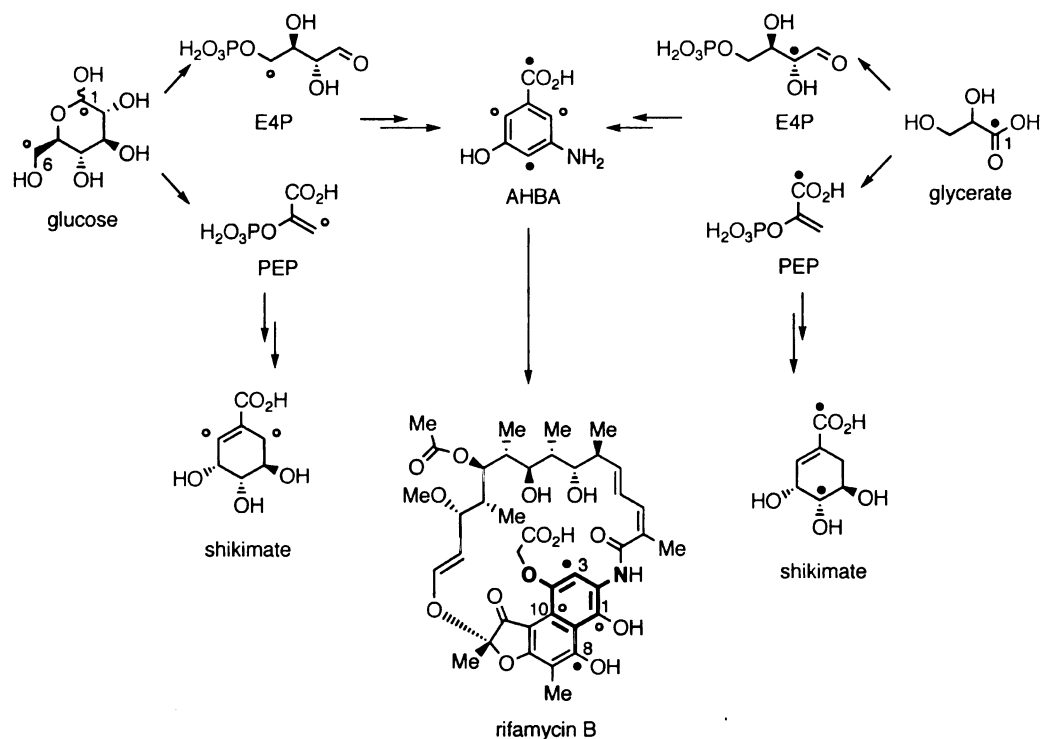
**Figure 1. The shikimate pathway.**

(a) DAHP synthase; (b) 3-dehydroquinate synthase; (c) 3-dehydroquinate dehydratase; (d) shikimate dehydrogenase. Abbreviations: PEP, phosphoenolpyruvate; E4P, D-erythrose 4-phosphate; DAHP, 3-deoxy-D-arabino-heptulosonic acid 7-phosphate; DHQ, 3-dehydroquinate; DHS, 3-dehydroshikimate.

Once AHBA was identified as the biosynthetic precursor of the ansamycin and mitomycin aromatic chromophores, the process of defining AHBA biosynthesis began. Using  $^{13}\text{C}$ -labeled precursors (Figure 2), it was determined AHBA was prepared biosynthetically via the shikimate pathway (Figure 1). Via the shikimate pathway, C-1 of glucose corresponds to C-3 of phosphoenolpyruvate, while C-6 corresponds to C-4 of D-erythrose 4-phosphate, which represent C-3 and C-7 of shikimic acid. Upon addition of [1- $^{13}\text{C}$ ]-D-glucose and [6- $^{13}\text{C}$ ]-D-glucose, the rifamycin B produced contained  $^{13}\text{C}$  enrichment at C-1- and C-10 of the chromophore. The C-1 position of glycerate provides

biosynthetically C-1 of phosphoenolpyruvate as well as C-2 of E4P, which subsequently represent C-1 and C-5 of shikimate. Upon addition of [1-<sup>13</sup>C]-D-glycerate, <sup>13</sup>C enrichment was observed at C-3 and C-8 of the rifamycin B chromophore (Figure 2). These data were consistent with a shikimate pathway origin of the chromophore.<sup>20</sup>

**Figure 2. Labeling patterns of shikimate, 3-amino-5-hydroxybenzoate, and rifamycin from <sup>13</sup>C-labeled glucose and glycerate.**



Although the above labeling experiments implicate the shikimate pathway as the origin of AHBA biosynthesis, further studies indicated that shikimate,<sup>20a-c,21</sup> quinate,<sup>22</sup> and 3-dehydroquinate<sup>20d</sup> were not precursors to AHBA. These results led to the hypothesis that AHBA biosynthesis must branch from the traditional shikimate pathway prior to DHQ biosynthesis. This hypothesis was further exemplified when Gyga and coworkers observed rifamycin production was not effected using *A. mediterranei* A10, a

DHQ synthase deficient strain. Transketolase is necessary for the production of DAHP, the immediate shikimate pathway precursor of DHQ. However a transketolase-deficient mutant, *A. mediterranei* A8, produced no aromatic amino acids and much less rifamycin B relative to the parent strain. This result led Ghisalba and co-workers to suggest AHBA biosynthesis branches from the shikimate pathway prior to DAHP formation.<sup>23</sup>

Hornemann and coworkers, while studying the biosynthesis of mitomycin C, made another important discovery of AHBA biosynthesis (Figure 3).<sup>24</sup> Because the C-3 carbons of DHQ and DHS (Figure 1) are carbonyl carbons, it was hypothesized that the nitrogen might be introduced at C-3 of a shikimate pathway intermediate by a transamination reaction.<sup>20a</sup> Typically C-4 of E4P corresponds to C-2 of DHQ and the other shikimate pathway intermediates. If the amino analogs of DHQ and DHS were prepared via transamination at C-3 then C-4 of E4P would correspond to C-4 of mitomycin C. However, analysis of the labeling pattern of mitomycin C derived from D-[4-<sup>14</sup>C]-erythrose and pyruvic acid showed <sup>14</sup>C enrichment at C-2 of mitomycin C as opposed to C-4 (Figure 3). This result indicated that the amine nitrogen of AHBA was incorporated at the C-4 carbon atom of DAHP to afford 4-amino-3,4-dideoxy-D-arabino-heptulosonic acid 7-phosphate (aminoDAHP) before the formation of 5-amino-5-deoxy-3-dehydroquinate (aminoDHQ, Figure 3). The results led to a hypothesis that aminoDAHP or a closely related molecule was an early precursor in the biosynthesis of AHBA.<sup>24</sup>

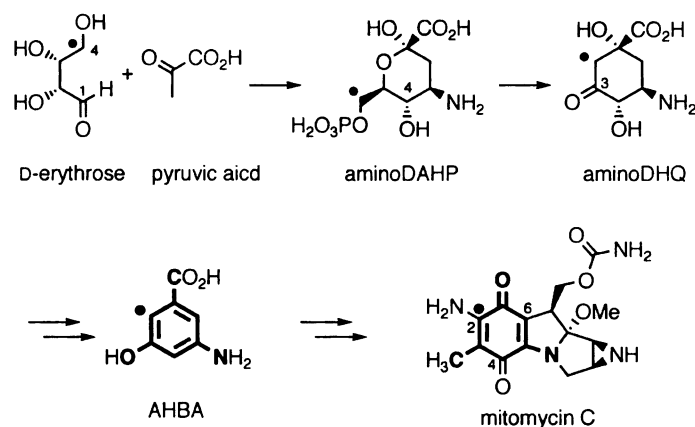
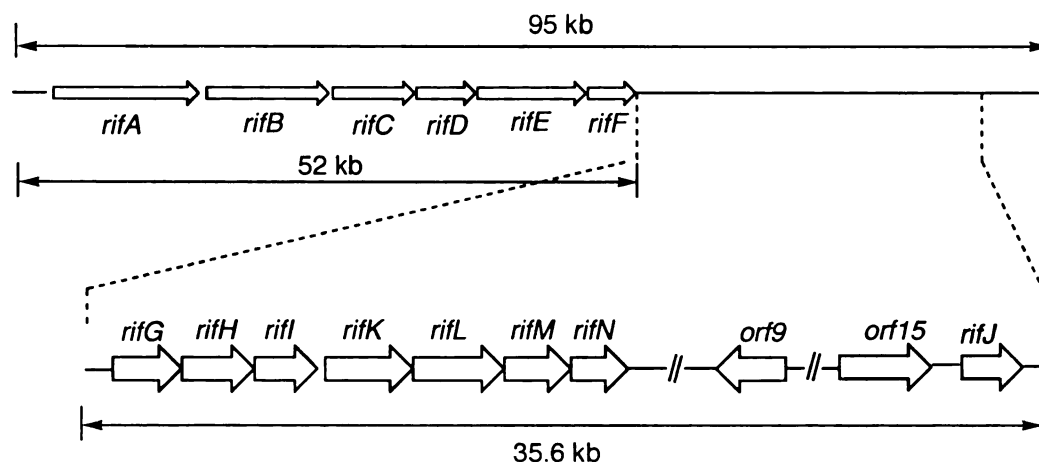


**Figure 3. Labeling pattern of mitomycin C from labeled D-erythrose and pyruvic acid.**

Floss later confirmed aminoDAHP was a precursor of AHBA.<sup>25</sup> Floss synthesized aminoDAHP, 5-amino-5-deoxy-3-dehydroquinone (aminoDHQ), and 5-amino-5-deoxy-3-dehydroshikimate (aminoDHS) and demonstrated that each of these substrates could be used to prepare AHBA with the cell-free lysate of the rifamycin B producer *A. mediterranei*.<sup>25a</sup> Floss and coworkers then isolated and sequenced the AHBA synthase protein from *A. mediterranei*. They further identified the AHBA synthase as the gene product of *rifK*.<sup>26</sup> The *rifK* gene was then used to identify the *rif* biosynthetic gene cluster, a 95-kb region of DNA surrounding *rifK*, required for AHBA biosynthesis from in *A. mediterranei* S699 (Figure 4).<sup>27</sup>

**Figure 4. Rifamycin biosynthetic gene cluster of *A. mediterranei* S699 and proposed enzyme functions.**



The putative function of each gene in the cluster was identified through sequence homology with known enzymes (Table 1). Located immediately upstream of *rifK* three genes, *rifG*, *rifH*, and *rifI*, showed high sequence homology to shikimate pathway genes (Figure 1) encoding DHQ synthase (entry 1, Table 1), a plant-like DAHP synthase (entry 2, Table 1), and shikimate dehydrogenase (entry 3, Table 1), respectively. No gene was found nearby which might encode DHQ dehydratase homology. The closest gene with high sequence homology to a type II DHQ dehydratase (entry 4, Table 1) is *rifJ*, located about 30-kb downstream of *rifK*.<sup>27</sup> Using an *A. mediterranei* mutant with a deactivated *rifJ* gene, Floss and coworkers showed rifamycin B formation was reduced to 10% of wild type levels. However, upon supplementing the culture with AHBA, rifamycin B production by the *A. mediterranei rifJ* mutant was restored. Inactivation experiments also showed the *rifH*-encoded DAHP synthase and *rifG*-encoded 3-dehydroquinate synthase are essential for rifamycin B biosynthesis. However, inactivation of *rifI* had no notable effect on rifamycin B production.<sup>28</sup>

**Table 1. Proposed functions of *rif* biosynthetic gene products.**

Entry	<i>rif</i> biosynthetic gene products	sequence homology (species, homology%/identity%)	proposed function <sup>a</sup>
1	RifG	AroB ( <i>E. coli</i> , 49/33)	aminoDHQ synthase
2	RifH	AroG ( <i>L. esculentum</i> , 54/34)	aminoDAHP synthase
3	RifI	AroE ( <i>Synechocystis</i> sp. 56/29)	Aminoshikimate dehydrogenase
4	RifJ	AroD ( <i>A. pleuropneumoniae</i> , 63/41)	AminoDHQ dehydratase
5	RifK	AHBAS ( <i>S. collinus</i> , 86/70)	AHBA synthase
6	RifL	Pur10 ( <i>S. alboniger</i> , 55/29)	Oxidoreductase
7	RifM	CbbzP ( <i>R. eutropha</i> , 55/32)	Phosphatase
8	RifN	XylR ( <i>Synechocystis</i> sp. 52/29)	Kinase
9	Orf9	YokM ( <i>B. subtilis</i> , 58/30)	Transaminase
10	Orf15	TktA ( <i>E. coli</i> , 58/32)	Transketolase

(a) Abbreviations: aminoshikimate, 5-amino-5-deoxyshikimate; aminoDHQ, 5-amino-5-deoxy-3-dehydroquinone; aminoDAHP, 4-amino-3,4-dideoxy-D-arabino-heptulosonic acid 7-phosphate; AHBA, 3-amino-5-hydroxybenzoate.

Located downstream from the *rifK* gene are five additional genes. The *rifL* gene (Figure 4), annotated as an oxidoreductase (entry 6, Table 1), is translationally coupled to *rifK*. In the same transcription unit with *rifK* and *rifL* are two additional genes, *rifM* and *rifN* (Figure 4), which were annotated as a phosphatase (entry 7, Table 1) and a glucose specific kinase (entry 8, Table 1), respectively.<sup>27</sup> The gene products of *rifL*, *rifM*, and *rifN* were found to be necessary for rifamycin B production since the inactivation of *rifL*, *rifM*, and *rifN* produced mutants incapable of Rifamycin B formation without AHBA



supplementation.<sup>28</sup> AHBA was produced upon heterologous co-expression of *rifG*, *rifH*, *rifK*, *rifL*, *rifM*, *rifN*, and *rifJ* in *Streptomyces coelicolor* YU105, which further indicated these seven genes are required for AHBA production.<sup>28</sup>

Based on the results described above and on a report from the laboratory of Jiao that the amide nitrogen of glutamine is the best source of nitrogen in rifamycin biosynthesis,<sup>29</sup> Floss and co-workers proposed the AHBA biosynthetic pathway shown in Figure 5, which they titled the aminoshikimate pathway. The gene product of *rifH* would catalyze the condensation of iminoE4P with phosphoenolpyruvate to provide aminoDAHP. AminoDAHP would then be cyclized to aminoDHQ, by the action of the *rifG* gene product.<sup>25</sup> The heterologously expressed RifG from *S. lividans* 1326 was found to utilize both DAHP and aminoDAHP as substrates.<sup>30</sup> The *rifJ*-encoded aminoDHQ dehydratase would catalyze the dehydration of aminoDHQ to give aminoDHS, which would be converted into AHBA by dehydration and enolization.<sup>25</sup> The enzymatic activity of RifJ has been demonstrated,<sup>31</sup> as well as the AHBA synthase activity of RifK.<sup>26</sup>

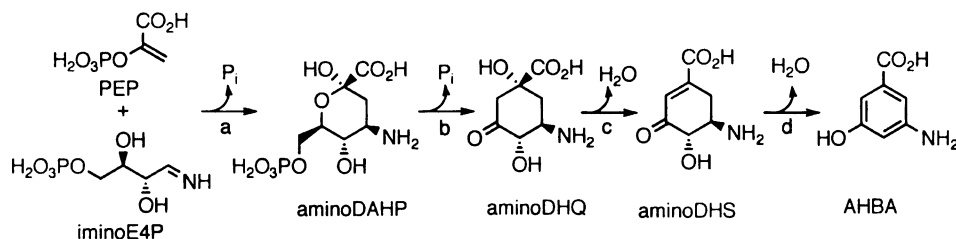


**Figure 5. The proposed aminoshikimate pathway.**

Enzymes (encoding genes): (a) aminoDAHP synthase, *rifH*; (b) 5-amino-5-deoxy-3-dehydroquinase, *rifG*; (c) 5-amino-5-deoxy-3-dehydroquinase dehydratase, *rifJ*; (d) 3-amino-5-hydroxybenzoate synthase, *rifK*.

When expressed in *E. coli*, *rifH*-encoded DAHP synthase can catalyze the synthesis of DAHP from E4P and phosphoenolpyruvate. However, no aminoDAHP was formed when D-erythrose 4-phosphate, phosphoenolpyruvate, and nitrogen sources were incubated with *rifH*-encoded DAHP synthase. Floss suggested that *rifH*-encoded DAHP synthase must combine with another protein in order to synthesize aminoDAHP.<sup>32</sup> However, Frost and Guo suggested transamination of E4P to provide iminoE4P would be unrealistic<sup>33</sup> based on the known chemistry of E4P in solution<sup>34</sup>. They suggested iminoE4P could be prepared biosynthetically from 3-amino-3-deoxy-fructose 6-phosphate (aminoF6P) by the action of a transketolase. Frost and Guo prepared aminoF6P from glucose. They then showed aminoDAHP could be prepared by the action of *A. mediterranei rifH* from aminoF6P in the presence of ribose 5-phosphate (R5P), PEP, and *E. coli* transketolase.<sup>33</sup>

Upon demonstrating aminoDAHP formation from aminoF6P, efforts by Frost and Guo turned toward delineating the biosynthetic precursor of F6P. They suggested the 3-amino derivative of glucose, kanosamine, could be used by *A. mediterranei* to produce aminoF6P. Kanosamine 6-phosphate was prepared and treated with yeast isomerase, *E. coli* transketolase, and *A. mediterranei* RifH in the presence of R5P and PEP to produce aminoDAHP. AminoDAHP production was also demonstrated from kanosamine 6-phosphate using the cell-free lysate of *A. mediterranei*. Quantifiable levels of neither aminoDAHP nor DAHP could be observed when kanosamine 6-phosphate was replaced with kanosamine.<sup>35</sup> However, Floss and coworkers reported the production of kanosamine from kanosamine 6-phosphate by the gene product of *rifN*<sup>36</sup>, originally

annotated as a glucokinase (entry 8, Table 1).<sup>27</sup> These results indicated kanosamine is the precursor to the aminoshikimate pathway and subsequently to AHBA.

With the establishment of kanosamine as the precursor to AHBA biosynthesis, efforts turned towards delineating kanosamine biosynthesis in *A. mediterranei*.<sup>35</sup> Kanosamine biosynthesis was first observed and studied in *Bacillus pumilus* in the 1960's. It was observed that incubation of UDP-[U-<sup>14</sup>C]-glucose in *B. pumilus* cell-free lysate in the presence of NAD and L-glutamine led to the formation of kanosmane.<sup>37</sup> Frost and Guo have demonstrated [6,6'-<sup>2</sup>H<sub>2</sub>]-kanosamine could be produced from UDP-[6,6'-<sup>2</sup>H<sub>2</sub>]-glucose by *A. mediterranei* cell-free lysate in the presence of NAD, and L-glutamine.<sup>35</sup>

The other gene products that are absolutely necessary for AHBA biosynthesis are *rifL*-encoded oxidoreductase, and *rifM*-encoded phosphatase. The functions of these gene products are based on sequence homology with the genetic sequences encoding known enzyme activities.<sup>27</sup> Their actual enzymatic activities have not been experimentally established with enzyme assays. Since they are not required for AHBA biosynthesis after the formation of aminoDAHP according to the proposed aminoshikimate pathway (Figure 5), the enzymes encoded by these genes were originally suggested to be associated with the formation of aminoDAHP by Floss,<sup>28</sup> however they were later suggested to play a role in kanosamine biosynthesis.<sup>35,36</sup> The roles of RifL or RifM in kanosamine biosynthesis had not been demonstrated prior to the initiation of research discussed in this thesis.

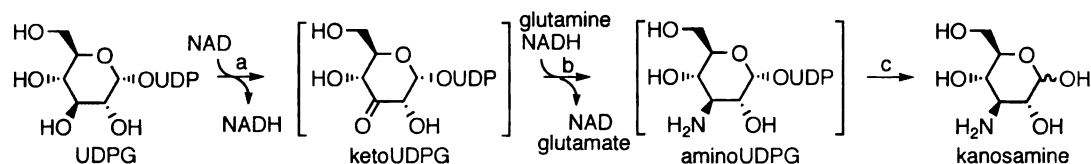


**Figure 6. Proposed pathway for kanosamine biosynthesis.**

Enzymes (encoding genes): (a) Oxidoreductase, *rifL*; (b) transaminase, *rifK*; (c) phosphatase, *rifM*. Abbreviations: UDPG, UDP-glucose; 3-ketoUDPG, UDP-3-keto-glucose; UDPK, UDP-3-amino-3-deoxy-glucose.

## Archaeal Aromatic Amino Acid Biosynthesis

### ***Archaea*: an overview**

Before addressing archaeal amino acid biosynthesis it seems pertinent to give a brief discussion of the *Archaea*, including several differences and similarities between *Archaea* and the other two domains, *Bacteria* and *Eukarya*. For over five decades, scientists were confident in the belief that two basic kinds of organisms existed, eubacteria and eukaryotes. This belief was shattered in 1977 when Woese and co-workers revealed that life consisted of three distinct groups of organisms, eukaryotes and two kinds of prokaryotes, eubacteria and archaeabacteria.<sup>38</sup> In 1990 the bipartite view of life was replaced with a tripartite design to include *Archaea* as a domain separate from *Bacteria* and *Eukarya*.<sup>39</sup> Several arguments have been made, however, against this tripartite view of life, especially by Mayr<sup>40</sup>, Margulis and Guerrero<sup>41</sup>, and Cavalier-Smith<sup>42</sup>. This controversy has resulted in a complex coexistence of old and new terminology. For the sake of simplicity only the older terminology will be used in this report.

According to rRNA phylogenetic trees there are two groups of *Archaea*. The kingdom *Crenarchaeota* consists of hyperthermophiles and thermoacidophiles such as

*Sulfolobus*, *Desulfurococcus*, *Pyrodictium*, *Thermoproteus*, and *Thermofilum*. The second kindom, *Euryarchaeota*, covers a broader ecological range to include hyperthermophiles (some are *Pyrococcus* and *Thermococcus*), methanogens (such as *Methanosarcina*), halophiles (e.g. *Halobacterium* and *Haloferax*), and thermophilic methanogens (such as *Methanothermus*, *Methanobacterium*, and *Methanococcus*).<sup>43</sup>

Several cellular and biochemical features which distinguish *Archaea* from *Bacteria* and *Eukarya* have been identified. The features unique to *Archaea* include isoprenyl ether lipids, flagellar shaft of acid-insoluble glycoproteins related to pilin, modified tRNA molecules, RNA polymerase A split into two proteins, and DNA-binding protein 10b.<sup>44</sup> Other features or combinations of features illustrate the evolutionary relationship between *Archaea* and either *Bacteria* or *Eukarya*. *Archaea* and *Bacteria* share similar general cell sizes, the lack of a nuclear membrane and organelles, and the presence of a large circular chromosome intermittently complemented by one or more small circular plasmids.<sup>43</sup> Although *Archaea* and *Bacteria* look to be very similar based on general genome organization, many archaeal genes display a higher similarity to eukaryotic homologs. Early studies on antibiotic resistance hinted of genetic homology between eukaryotes and archaebacteria as both are resistant to streptomycin (an anti-70S ribosome inhibitor to which eubacteria are sensitive) and sensitive to some anti-80S ribosome inhibitors (such as anisomycin) as well as aphidocolin (a DNA polymerase inhibitor). Later studies revealed significant similarities between archaeal and eukaryotic DNA replication, transcriptional, and translational enzymes. More similarities between *Archaea* and the other two domains have been reported more extensively elsewhere.<sup>43</sup>

## Ribose biosynthesis and the shikimate pathway of archaeal methanogens

Archaeal methanogens typically use  $H_2$  and  $CO_2$  as sole energy and carbon sources, however some require the exogenous presence of acetate or varying amino acids. They can be autotrophic or heterotrophic and have a wide range of optimal growth temperatures (4°C to 85°C). This diversity among the archaeal methanogens is further represented by the variations of common biosynthetic pathways utilized by these organisms.

Early studies, performed mainly with *Methanobacterium thermoautotrophicum*, indicated that the serine, hexulose phosphate, and the reductive pentose phosphate pathways are not utilized by the archaeal methanogens. This suggestion was based on the absence of key biosynthetic enzymes and inconsistencies in the early intermediates formed from one-carbon substrates.<sup>45</sup> The autotrophy of methanogens was investigated and explained by the synthesis of acetate from two  $CO_2$  molecules<sup>46</sup>, which was then linked to an incomplete, acyclic tricarboxylic acid (TCA) cycle. In some archaeal methanogens this non-cyclic TCA cycle produces  $\alpha$ -ketoglutarate in the reductive direction. In *M. thermoautotrophicum*, which uses this reductive non-cyclic TCA cycle, all of the oxidoreductases, with the exception of isocitrate dehydrogenase, have been identified.<sup>47</sup> Other members of the archaeal methanogens, such as *Methanosarcina barkeri*, use an oxidative direction to synthesis  $\alpha$ -ketoglutarate.<sup>48</sup>

Although the common pathway for aromatic amino acid biosynthesis has been well defined in prokaryotes and eukaryotes, among the archaeal methanogens this pathway is less clear. A series of  $^{13}C$  labeling studies were reported examining the amino acid biosynthesis by *Methanospirillum hungatei*, *Methanotheroxothrix concilii*, and

*Methanococcus voltae*. All three methanogens are mesophilic anaerobes, which grow at 35°C under an atmosphere of 4:1 H<sub>2</sub>-CO<sub>2</sub>. All require exogenous acetate as an additional carbon source with CO<sub>2</sub>,<sup>49</sup> however *M. voltae* also requires leucine and isoleucine.<sup>50</sup> Treatment of [1-<sup>13</sup>C]-acetate, [2-<sup>13</sup>C]-acetate, and <sup>13</sup>CO<sub>2</sub> with the cell-free lysate of *M. hungatei* produced phenylalanine and tyrosine with <sup>13</sup>C labeling patterns consistent with the shikimate pathway.<sup>51</sup> Treatment of [1-<sup>13</sup>C]-acetate, [2-<sup>13</sup>C]-acetate, and <sup>13</sup>CO<sub>2</sub> with the cell-free lysate of *M. concilii* or *M. voltae* also provided labeling patterns of phenylalanine and tyrosine which were consistent with the results found using *M. hungataei*.<sup>49</sup>

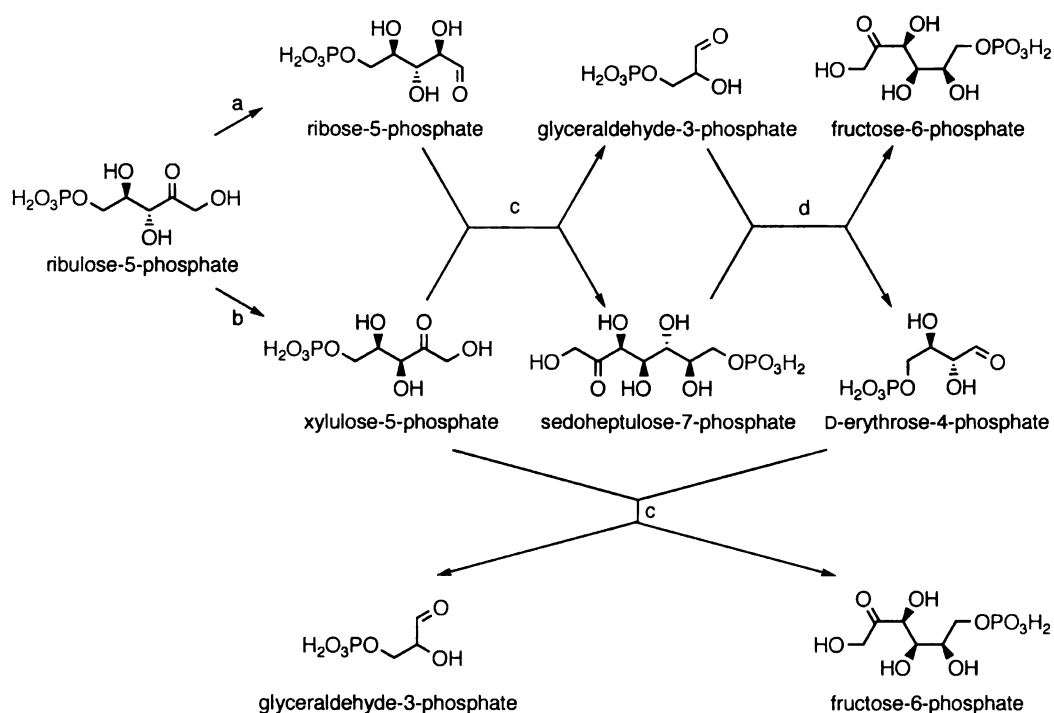


**Figure 7. Non-oxidative Pentose Phosphate Cycle.**

Enzymes: (a) ribulose-5-phosphate isomerase; (b) ribulose-5-phosphate 3-epimerase; (c) transketolase; (d) transaldolase.

*Methanobacterium thermoautotrophicum* is an autotrophic, thermophilic methanogen, which utilizes CO<sub>2</sub> and H<sub>2</sub> as the sole carbon and energy sources.<sup>52</sup> Bacher and co-workers added [1-<sup>13</sup>C]-acetate, [2-<sup>13</sup>C]-acetate, and [1-<sup>13</sup>C]-pyruvate to growing cultures of *M. thermoautotrophicum* to study the biosynthesis of nucleotide, flavin, and deazaflavin coenzymes by the archaeal methanogen. Aside from these coenzymes, several amino acids, including phenylalanine and tyrosine, were isolated and their respective <sup>13</sup>C labeling patterns analyzed. The labeling patterns of both phenylalanine and tyrosine were identical within experimental limits and were consistent with biosynthesis by the shikimate pathway<sup>53</sup>, as had been seen earlier using *M. hungatei*, *M. concilii*, and *M. voltae*.<sup>49</sup> However, it was noted that only the C-7 ring atom of tyrosine and phenylalanine was enriched with <sup>13</sup>C when [1-<sup>13</sup>C]-pyruvate was added to the bacterial culture (Figure 8). This result implies only C-2 of erythrose 4-phosphate contained the <sup>13</sup>C label, not C-1 and C-2 as would be consistent with the biosynthesis of erythrose 4-phosphate from [1-<sup>13</sup>C]-pyruvate by the pentose phosphate cycle. To explain these labeling results, Bacher and Eisenreich suggested *M. thermoautotrophicum* could prepare erythrose 4-phosphate via the carboxylation of pyruvate.<sup>53</sup>



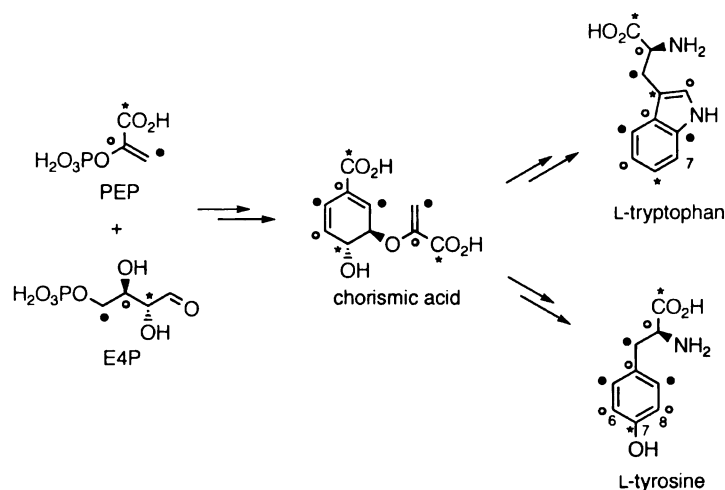


**Figure 8. Observed <sup>13</sup>C labeling patterns of tyrosine and tryptophan from acetate and pyruvate added to the growing culture of *M. thermoautotrophicum*.**

Enrichment Key: (\*), [1-<sup>13</sup>C]-pyruvate; (○), [1-<sup>13</sup>C]-acetate; (●), [2-<sup>13</sup>C]-acetate.

Recognizing a need to further investigate the biosynthesis of different metabolites and especially erythrose 4-phosphate in *M. thermoautotrophicum*, Bacher and Eisenreich performed a systematic comparison between the labeling patterns of varying amino acids and metabolites. To reconstruct the <sup>13</sup>C labeling patterns of central metabolites, Eisenreich and Bacher calculated the average enrichment of carbon atoms supplied to the various downstream metabolites from a specific <sup>13</sup>C-labeled atom position of the respective fundamental precursor. The labeling pattern of pyruvate was calculated from the average labeling patterns of alanine, serine, glycine, and the side chains of phenylalanine and tyrosine. When *M. thermoautotrophicum* was grown with [1,2-<sup>13</sup>C<sub>2</sub>]-acetate only C-2 and C-3 of pyruvate were labeled. Enrichment of <sup>13</sup>C was observed at C-1 of pyruvate only when [1-<sup>13</sup>C]-pyruvate was added to the growing culture (Figure 9).<sup>54</sup> These findings lent credence to an earlier study by Fuchs and Stupperich suggesting some archaeal methanogens form pyruvate by the reductive carboxylation of acetate.<sup>55</sup>

The labeling pattern of pentoses was calculated from the labeling patterns of the ribose

moieties in each of the four RNA nucleosides. Only C-1, C-3, and C-5 were labeled when [1,2- $^{13}\text{C}_2$ ]-acetate was added to the growing culture of *M. thermoautotrophicum*, while C-2 and C-3 were enriched with  $^{13}\text{C}$  when [1- $^{13}\text{C}$ ]-pyruvate was added (Figure 9). These results were consistent with pentose formation by the head-to-head dimerization of two trioses followed by oxidative decarboxylation.<sup>54</sup> These results indicate a tetrose, such as erythrose 4-phosphate, derived from the hexose pool via the pentose phosphate cycle should contain  $^{13}\text{C}$  enrichment at C-1 and C-2 upon addition of [1- $^{13}\text{C}$ ]-pyruvate to the growing culture of *M. thermoautotrophicum* (Figure 9).<sup>54</sup> This result was not consistent with the earlier observation that phenylalanine and tyrosine formation from [1- $^{13}\text{C}$ ]-pyruvate appeared to indicate that only C-2 through C-4 of erythrose 4-phosphate originated from the hexose pool, whereas C-1 seemed originate from  $\text{CO}_2$  (Figure 8).<sup>53</sup>

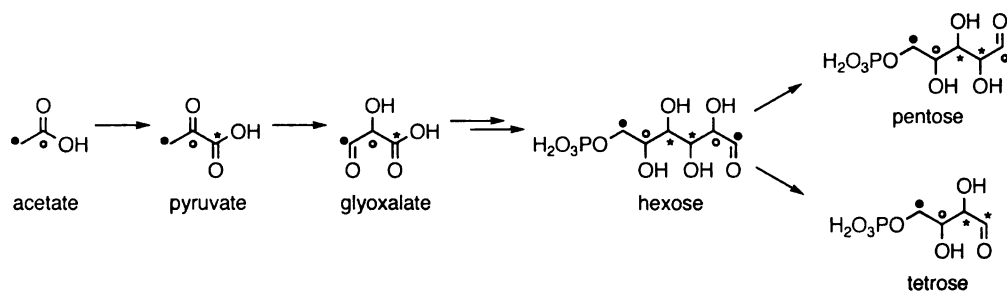


**Figure 9. Observed  $^{13}\text{C}$  labeling patterns of pyruvate, hexoses, pentoses, and tetroses from,  $^{13}\text{C}$  enriched acetate and pyruvate.**

Enrichment Key: (\*), [1- $^{13}\text{C}$ ]-pyruvate; (o), [1- $^{13}\text{C}$ ]-acetate; (•), [2- $^{13}\text{C}$ ]-acetate.

Due to the inherent symmetry of benzene rings, the chemical shifts of C-6 and C-8 of tyrosine and phenylalanine, which represent C-1 and C-3 of erythrose 4-phosphate, degenerate. To further establish the origin of C-1 of erythrose 4-phosphate Bacher and Eisenreich isolated tryptophan produced by the growing culture of *M. thermoautotrophicum* upon addition of [1- $^{13}\text{C}$ ]-acetate, [2- $^{13}\text{C}$ ]-acetate, [1,2- $^{13}\text{C}_2$ ]-acetate,

and [1-<sup>13</sup>C]-pyruvate. No <sup>13</sup>C enrichment was observed at C-7 of tryptophan produced upon the addition of labeled acetate or pyruvate (Figure 8). Had erythrose 4-phosphate been produced via the typical pentose phosphate pathway C-7 of tryptophan should have contained <sup>13</sup>C enrichment. These results further indicate that C-1 of erythrose 4-phosphate did not correspond to C-3 of the hexose pool as would be expected if erythrose 4-phosphate were produced via the pentose phosphate pathway.<sup>54</sup>

Patel and coworkers examined amino acid biosynthesis using yet another archaeal methanogen, *Methanococcus jannaschii*. *M. jannaschii*, originally isolated from a white smoker chimney, is an autotrophic hyperthermophile (optimal growth temperature of 83°C), which utilizes CO<sub>2</sub> and H<sub>2</sub> as sole carbon and energy sources. Unlike the archaeal methanogens discussed thus far, *M. jannaschii* does not adequately uptake acetate from the culture media. As such, Patel and coworkers analyzed amino acid biosynthesis through the addition of exogenous pyruvate enriched with <sup>13</sup>C at C-1, C-2, or C-3. Enrichment at C-6 of phenylalanine and tyrosine was observed when [2-<sup>13</sup>C]-pyruvate was added to the *M. jannaschii* culture, and likewise C-5 was enriched when [3-<sup>13</sup>C]-pyruvate was added.<sup>56</sup> Unlike the previous studies with *M. thermoautotrophicum*,<sup>53,54</sup> Patel and coworkers observed <sup>13</sup>C enrichment at both the C-7 and C-8 ring atoms of phenylalanine and tyrosine when [1-<sup>13</sup>C]-pyruvate was added to the cell culture of *M. jannaschii*. The relative intensity of the enrichment at C-7 and C-8 was much lower than was observed at positions labeled using [2-<sup>13</sup>C]-pyruvate and [3-<sup>13</sup>C]-pyruvate, which led Patel and coworkers to suggest <sup>13</sup>C scrambling had occurred.<sup>56</sup> In a later study Choquet and coworkers re-examined this labeling result through the careful comparison of natural abundance spectra, and observed that as with *M. thermoautotrophicum* only the C-7 ring

atom of phenylalanine and tyrosine was enriched with  $^{13}\text{C}$  when  $[1-^{13}\text{C}]$ -pyruvate was added to the *M. jannaschii* culture.<sup>57</sup>

In the process of studying glycogen biosynthesis by *M. maripaludis*, an autotroph capable of utilizing either  $\text{H}_2$  or formate as an electron donor, Yu and coworkers assayed for the specific activities of enzymes responsible for pentose biosynthesis. High specific activities were observed for transketolase, transaldolase, D-ribose-5-phosphate 3-epimerase, and D-ribulose-5-phosphate isomerase in the cell-free extract of *M. maripaludis*. Fructose-6-phosphate and glyceraldehyde-3-phosphate, intermediates in the Embden-Meyerhoff-Parnas pathway, reacted with transketolase to form xylulose-5-phosphate and erythrose 4-phosphate (Figure 7). Transketolase was also able to catalyze the conversion of xylulose-5-phosphate and ribose-5-phosphate to sedoheptulose-7-phosphate and glyceraldehyde-3-phosphate (Figure 7). Specific activities of glucose-6-phosphate dehydrogenase and 6-phosphogluconate dehydrogenase, however, were not detected in the cell-free lysate of *M. maripaludis*. The high levels of these pentose-biosynthetic enzymes led Yu and coworkers to suggest pentose biosynthesis occurs through a nonoxidative pentose phosphate pathway.<sup>58</sup> However, this suggestion contradicts the earlier  $^{13}\text{C}$  labeling studies of *M. thermoautotrophicum*,<sup>53,54</sup> *M. jannaschii*,<sup>57</sup> and *M. hungatei*,<sup>51</sup> which all indicated the preferential enrichment only at C-7 (not both C-7 and C-8) following labeling with  $[1-^{13}\text{C}]$ -pyruvate.

Due to the above conflicting results, it has been proposed that the biosynthesis of erythrose 4-phosphate by archaeal methanogens may occur via the carboxylation of a triose sugar as opposed to the nonoxidative pentose phosphate pathway (Figure 7).<sup>58</sup> Tumbula and coworkers, however, suggested erythrose 4-phosphate might not be the

precursor of the aromatic amino acids among these archaeal methanogens. The nonoxidative pentose phosphate pathway predicts 66.7% or more of the carbon at the ribose C-1 will originate from the C-2 of acetate. Therefore if erythrose 4-phosphate is not diverted from the pathway for aromatic amino acid biosynthesis, exactly 2/3 of the carbon at the C-1 position of cytidine or uridine would come from the C-2 of acetate. If erythrose 4-phosphate was diverted for aromatic amino acid biosynthesis this fraction would increase. However, if erythrose 4-phosphate was produced by carboxylation of a triose, 50% of the ribose C-1 would be derived from the C-2 of acetate. Using an acetate auxotroph of *M. maripaludis* grown on [2-<sup>13</sup>C]-acetate, the <sup>13</sup>C enrichments of cytidine and uridine were determined. Analysis using <sup>13</sup>C NMR determined the C-1' of cytidine contained a 66.6% enrichment of the <sup>13</sup>C label from the C-2 of acetate. A similar result of 65.3% was observed for the C-1' of uridine. These results were confirmed by mass spectral analysis. Two possibilities could explain these results and the previous results obtained with the aromatic amino acids. One is that erythrose 4-phosphate is biosynthesized from both the nonoxidative pentose phosphate pathway and the carboxylation of a triose. The second, considered to be more probable by Tumbula et al., was that erythrose 4-phosphate is produced only from the pentose phosphate pathway and is not used for aromatic amino acid biosynthesis.<sup>59</sup>

### **The “missing” genes of archaeal aromatic amino acid biosynthesis**

Examination of the ribose biosynthetic products as well as the aromatic amino acids produced by several archaeal methanogens<sup>51,53,54,57,59</sup> has led to the suggestion that in archaeal methanogens, erythrose-4-phosphate may not be the precursor to the shikimate

pathway.<sup>59</sup> If erythrose 4-phosphate is not the precursor to aromatic amino acid biosynthesis by these archaeal methanogens several possibilities exist. One explanation is that the enzyme typically responsible for catalyzing the first step of the shikimate pathway, DAHP synthase, exhibits a high degree of substrate ambiguity. This would be similar to the DS-Co isozyme identified in *Spinacia oleracea*, a DAHP synthase found in the cytosol compartment of the cell. DS-Co from *Spinacia oleracea* is capable of condensing a diose (glycoaldehyde), triose (D-glyceraldehyde, L-glyceraldehyde, and DL-glyceraldehyde phosphate), tetrose (D-erythrose, L-erythrose, D-erythrose 4-phosphate, D-threose, and L-threose) or pentose (D-ribose 5-phosphate, and D-arabinose 5-phosphate) with phosphoenolpyruvate to form the corresponding 2-keto-3-deoxy-sugar acids. Specific activities were not reported for the varying substrates.<sup>60</sup> Another possibility is that the enzyme(s) responsible for the early steps of the shikimate pathway is (are) not present in some archaeal methanogens, causing these microbes to utilize novel enzymes or substrates for the biosynthesis of the aromatic amino acids. This seems to be the case in the halophilic methanogen *Methanohalophilus mahii*. Attempts were made to obtain specific activities for several key shikimate pathway enzymes (DAHP synthase, shikimate dehydrogenase, chorismate mutase, prephenate dehydrogenase, arogenate dehydrogenase, prephenate dehydratase, and arogenate dehydratase). However, after carrying out an extensive series of extract preparation and assays procedures a specific activity for DAHP synthase could not be found.<sup>61</sup>

The first complete genome sequence of an archaeal methanogen was reported for *M. jannaschii* in 1996 at which time only four of the genes required for chorismate biosynthesis were identified.<sup>62</sup> After several other archaeobacterial genomes were

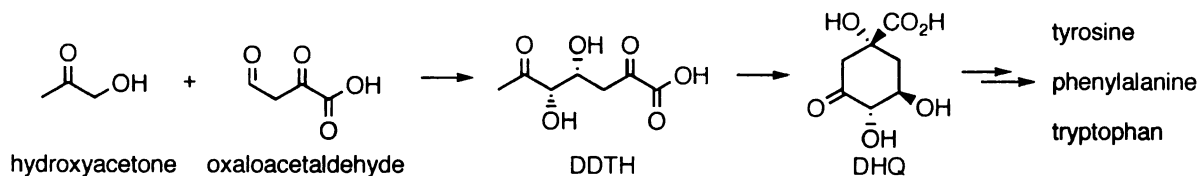
reported Huguchi and coworkers specifically compared the pathways for amino acid biosynthesis through the identification of genes based on their DNA sequence. To perform this comparison they obtained the genomic sequences of seven *archaea*: *M. jannaschii*, *M. thermoautotrophicum*, *Archaeoglobus fulgidus*, *Pyrococcus abyssi*, *Pyrococcus* sp. OT3, *Thermoplasma volcanium*, and *Aeropyrum pernix*. Of the enzymes expected to mediate aromatic amino acid biosynthesis, 14 were not identified in at least one of the *archaea*. The two autotrophs, *M. jannaschii* and *M. thermoautotrophicum*, which would be required to synthesize all 20 amino acids were “missing” only three enzymes expected for aromatic amino acid biosynthesis. DAHP synthase and DHQ synthase were not identified in either of the two autotrophs, *A. fulgidus*, or *P. sp.* OT3. Shikimate kinase was not identified in any of the seven *archaea*,<sup>63</sup> however a novel shikimate kinase, belonging to the GHMP-kinase superfamily, as opposed to the structurally unrelated NMP-kinase superfamily, was later identified in *M. jannaschii*.<sup>64</sup> The apparent absence of genes encoding both DAHP synthase and DHQ synthase in four of the seven archaeal genomes studied would suggest these genes are not required for the biosynthesis of DHQ, or that they are encoded by low-similarity, novel, or “analogous” genes.<sup>65</sup>

In order to determine whether this unique shikimate pathway proceeds from alternate precursors or utilizes a novel DAHP synthase further study was required. Using GC-MS analysis White observed that the reaction of DAHP with the cell-free lysate of *M. jannaschii* did not produce either DHQ or DHS. However, incubation of DHQ with *M. jannaschii* cell-free extract produced DHS quantitatively. These experiments suggested that after DHQ biosynthesis the archaeal shikimate pathway continues as

normal.<sup>66</sup> The inability of *M. jannaschii* cell-free extract to produce DHQ from DAHP in combination with the inability of Fischer and coworkers to detect DAHP synthase activity in *M. mahii* cell free extracts<sup>63</sup> seems to suggest this novel archaeal shikimate pathway proceeds without E4P.

The suggestion that E4P is not a precursor to aromatic amino acid biosynthesis via this archaeal pathway led to the proposition of a variety of alternatives. Frost proposed 3,7-dideoxy-2,6-dioxo-4,5-D-*threo*-heptanoic acid (DDTH) could serve as the immediate precursor of DHQ (Figure 10).<sup>67</sup> DDTH was originally proposed as the first intermediate of the shikimate pathway in *E. coli* until DAHP was identified, and has been prepared synthetically from 2-deoxy-glucose by Sprinson. In solution at physiological pH, DDTH cyclizes spontaneously to DHQ.<sup>68</sup> Frost suggested DDTH could be biosynthesized through the aldol condensation of hydroxyacetone and oxaloacetaldehyde, which would be followed by the cyclization of DDTH to form DHQ.<sup>67</sup> On the other hand, White suggested the formation of an isomer of DAHP, 3-deoxy-D-*ribo*-heptulosonic acid 7-phosphate (DRHP) might be the precursor to archaeal amino acid biosynthesis.

**Figure 10. Alternative DHQ precursors as suggested by Frost.**

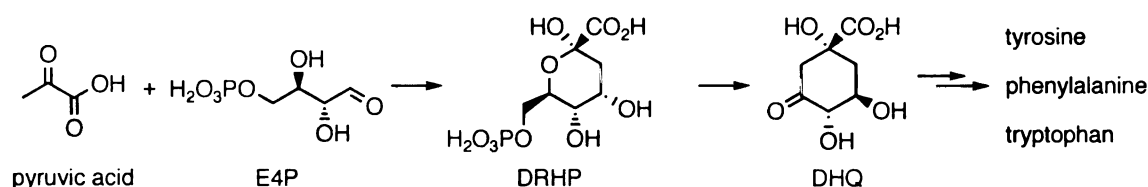


If this archaeal biosynthetic pathway proceeds via different precursors the precursors as well as the enzymes responsible for DHQ biosynthesis needed to be



identified. Using genetic analysis White identified two novel enzymes, MJ0400 and MJ1249, based on their association with other genes required for aromatic amino acid biosynthesis. Both genes were annotated as aldolases. White reacted pyruvate and E4P with the heterologously expressed MJ0400 in an attempt to produce DAHP, however the GC-MS spectra did not correspond to DAHP. Based on this observation he proposed the condensation of pyruvate and E4P produced DRHP (Figure 11). Upon treatment of the presumed DRHP with the cell-free extract of *M. jannaschii* no DHQ or DHS was observed in the product mixture, excluding this condensation product as the DAHP substitute.<sup>66</sup>

**Figure 11. Alternative DHQ precursors as proposed by White.**



To further establish the actual precursors of the archaeal shikimate pathway White performed a series of experiments using the cell-free extract of *M. jannaschii* and the proposed enzymes MJ0400 and MJ1249. White observed no DHQ or DHS was produced upon reacting E4P with pyruvate, oxaloacetaldehyde, or PEP in the presence or absence of coenzymes ( $F_{420}$ ,  $Zn^{2+}$ , and NAD) while using either the cell-free extract of *M. jannaschii* or MJ0400 expressed from *E. coli*. White used these results to eliminate PEP, pyruvate, and E4P as precursors of archaeal amino acid biosynthesis. He then considered the C-3 unit of the condensation to form DHQ might come from glucose 6-phosphate, while the C-4 unit might be derived from homoserine or its possible derivatives.<sup>66</sup>

To test his hypothesis that glucose 6-phosphate and another C-4 unit were the precursors to DHQ biosynthesis by archaeal methanogens, White performed another series of experiments using the cell-free extract of *M. jannaschii*. As the C-3 unit precursor White chose dihydroxyacetone, fructose 1,6-diphosphate, glucose 6-phosphate, glycerol phosphate, dihydroxyacetone phosphate, hydroxyacetone, and 6-deoxy-5-ketofructose 1-phosphate (DKFP). He used pyruvate, homoserine, and aspartate semialdehyde as the C-4 precursors. From the production of DHS and *epi*-shikimate produced from a variety of combinations of these C-3 and C-4 units, White deduced the C-3 unit might be derived from glucose 6-phosphate (most likely DKFP), while the C-4 unit might be derived from homoserine (most likely aspartate semialdehyde) (Figure 12).<sup>66</sup>

To confirm his suspicions, White further examined the condensation of DKFP with aspartate semialdehyde in the presence of one or both enzyme, MJ0400 and MJ1249, and a variety of coenzymes. The highest level of DHQ production achieved was through the condensation of DKFP and aspartate semialdehyde in the presence of both MJ0400 and MJ1249 and NAD. White also observed the production of what he presumed to be 4,5-dihydroxy-6-methylpipercolinic acid upon sodium borohydride reduction of the product mixture obtained when DKFP and aspartate semialdehyde were reacted with MJ0400 alone. These results led White to the conclusion that DKFP and aspartate semialdehyde were the precursors to the shikimate pathway in *M. jannaschii* (Figure 12).

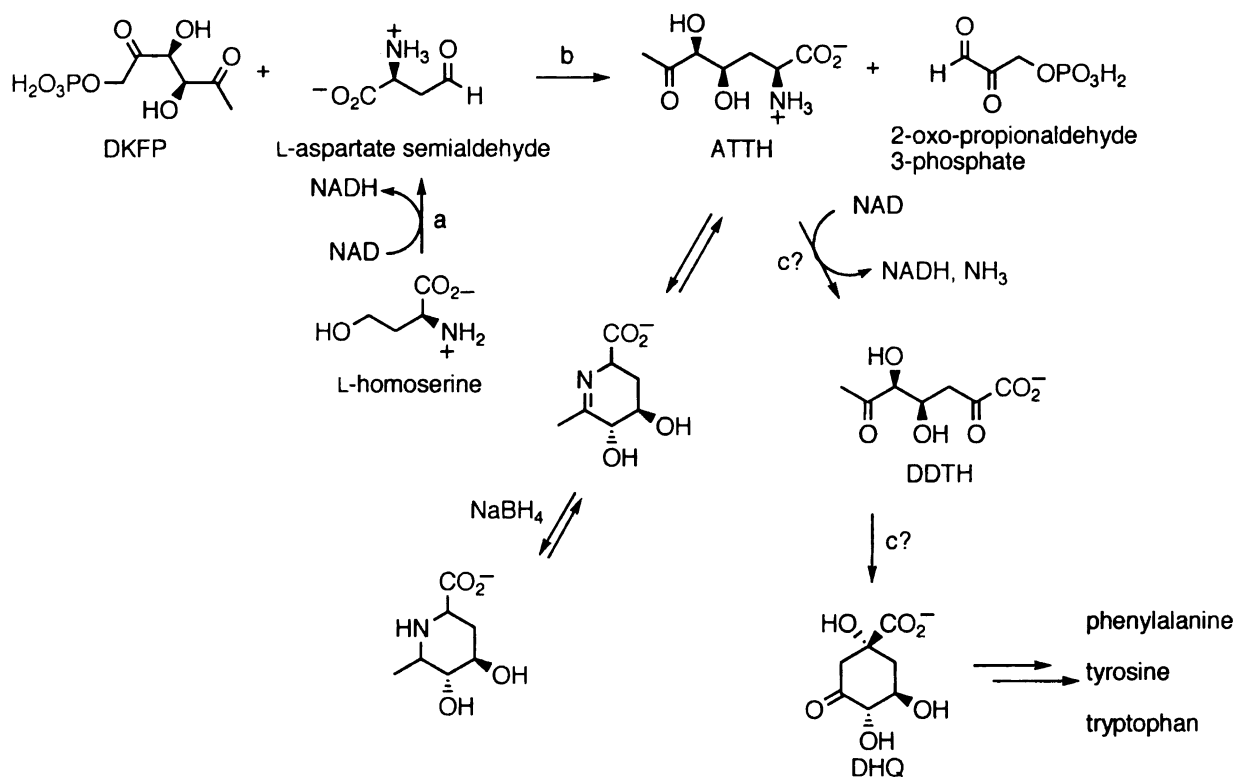


**Figure 12. Proposed archaeal shikimate pathway.**

**Enzymes (genes):** (a) homoserine dehydrogenase, *mj1602*; (b) aldolase, *mj0400*; (c) transaminase, *mj1249*.

## CHAPTER TWO

# **UDP-3-KETOGLUCOSE INTERMEDIACY IN KANOSAMINE BIOSYNTHESIS**

### Introduction

Many biologically active natural products, such as the rifamycin, ansamycin, and mitomycin antibiotics, are derived from a common precursor, 3-amino-5-hydroxybenzoic acid (AHBA). The biosynthesis of AHBA has been studied in a variety of organisms, which produce ansamycin<sup>69</sup> and mitomycin<sup>70</sup> antibiotics. Through labeling studies using <sup>13</sup>C- and <sup>14</sup>C-glucose, glycerate, and other precursors it was hypothesized that AHBA was synthesized via the shikimate pathway.<sup>28</sup> However, studies attempting to incorporate labeled shikimate pathway intermediates (such as shikimic acid (SA), quinic acid (QA), 3-dehydroshikimic acid (DHS)) and 3-deoxy-D-arabino-heptulosonate 7-phosphate (DAHP) failed to yield AHBA.<sup>20</sup> Floss and co-workers proposed an alternative pathway analogous to the early steps of the shikimate pathway, but where a nitrogen atom is incorporated during the first biosynthetic step to produce an amino analog of DAHP (Figure 13). The proposed intermediates aminoDAHP, aminoDHQ, and aminoDHS were synthesized and shown to be precursors to AHBA biosynthesis in *Amycolatopsis mediterranei* S699 cell-free extract.<sup>71</sup>

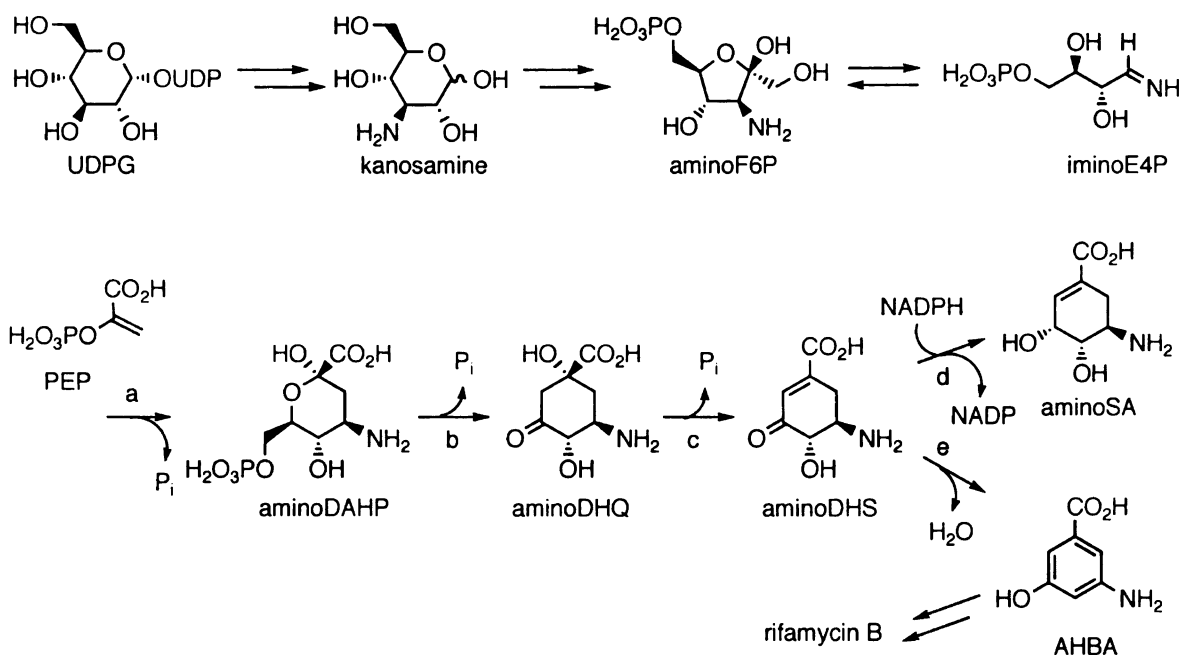


**Figure 13. Aminoshikimate pathway.**

Enzymes (gene designation): (a) DAHP synthase, *rifH*; (b) DHQ synthase, *rifG*; (c) DHQ dehydratase, *rifJ*; shikimate/quinate dehydrogenase, *rifI*; (e) AHBA synthase, *rifK*.

It was originally suggested transamination of E4P could introduce a nitrogen atom to form iminoE4P, which upon condensation with PEP would provide aminoDAHP.<sup>71</sup> However, prone to dimerization, trimerization, and polymerization in solution, nature is forced to keep the steady state concentration of E4P as low as possible.<sup>34</sup> Transamination of E4P then seemed unlikely. Frost and Guo suggested an alternative route for amino introduction where the condensation of aminoF6P with ribose 5-phosphate R5P by transketolase would produce iminoE4P and S7P.<sup>33</sup> AminoF6P was synthesized and treated under varying conditions with *E. coli* transketolase and *A. mediterranei* cell-free extract to produce aminoDAHP and AHBA. Since aminoF6P could be used as a biosynthetic precursor to aminoDAHP, it can be inferred that iminoE4P is an intermediate in this step and aminoF6P is its precursor (Figure 13).<sup>33</sup>

With the establishment of aminoF6P as the precursor to iminoE4P, attention turned toward the origin of aminoF6P. Since F6P is generally prepared biosynthetically via the isomerization of glucose 6-phosphate,<sup>1</sup> it was suggested that a natural product, 3-amino-3-deoxy-D-glucose 6-phosphate (kanosamine 6-phosphate), could act as the precursor to aminoF6P.<sup>35</sup> The phosphorylation of kanosamine by the action of a specific kinase would provide kanosamine 6-phosphate. Kanosamine biosynthesis was first detected and studied in the 1960's.<sup>72</sup> Since the original discovery of kanosamine, various microbes have been found to produce kanosamine as a biosynthetic end product or as an intermediate en route to other natural products,<sup>73</sup> such as kanamycin in *Bacillus aminoglucosidicus* (now known as *Bacillus pumilus*). It was believed that *A. mediterranei* might also make use of kanosamine as a biosynthetic intermediate and possibly as the means for supplying the nitrogen atom into the aminoshikimate pathway.

Using both the cell-free lysate of *A. mediterranei* as well as the putative aminoDAHP synthase from *A. mediterranei*, RifH, aminoDAHP was prepared from kanosamine 6-phosphate (K6P). AHBA was also produced when K6P was treated with *A. mediterranei* cell-free lysate. When K6P was replaced with G6P, however, no AHBA was observed.<sup>35</sup>

Among the genes of the *rif* biosynthetic gene cluster, *rifN*, encodes an enzyme sharing sequence homology with a glucose kinase from *Streptomyces coelicolor* A.<sup>28</sup> Floss and coworkers have shown the gene product of *rifN* is a specific kinase capable of producing K6P from kanosamine in the presence of ATP.<sup>36</sup> These results in combination with the production of aminoDAHP from K6P by the action of RifH indicates

kanosamine is the biosynthetic precursor and nitrogen source of the aminoshikimate pathway (Figure 13).

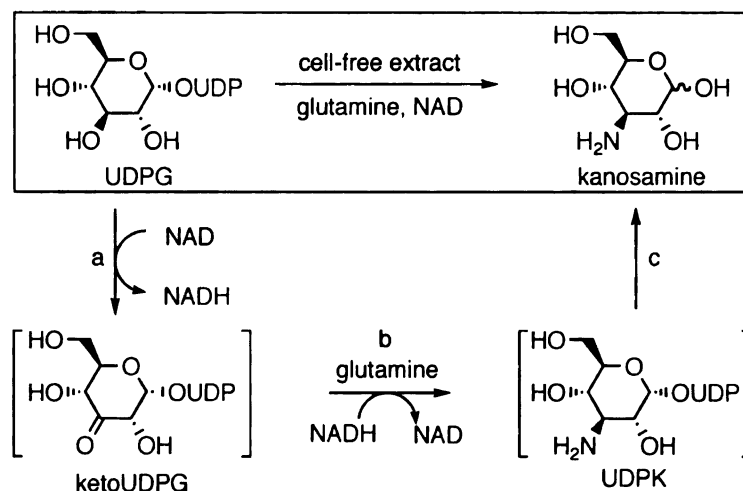


**Figure 14. Proposed route for kanosamine biosynthesis from UDPG.**

Reaction enzymes: (a) oxidoreductase, *rifL*; (b) transaminase, *rifK*, (c) pyrophosphorylase, *rifM*. Abbreviations: UDPG, uridine 5'-diphospho- $\alpha$ -D-glucose; 3-ketoUDPG, uridine 5'-diphospho-3-keto- $\alpha$ -D-glucose; NAD, nicotinamide adenine dinucleotide; NADH nicotinamide adenine dinucleotide reduced; UDPK, uridine 5'-diphospho- $\alpha$ -D-kanosamine.

With the establishment that kanosamine is the source of the amine nitrogen for AHBA biosynthesis, interest shifted to the biosynthesis of kanosamine and the amine nitrogen incorporation. The biosynthesis of kanosamine was originally studied using *Bacillus pumilus* through experiments with  $^{14}\text{C}$  labeled glucose, pyruvate, glycerol, and sodium acetate.<sup>72</sup> It was found that all of the carbons of glucose were present in the kanosamine produced. In *B. pumilus*, kanosamine biosynthesis was found to require glutamine, UTP, NAD,  $\text{MgCl}_2$ , and ATP. From these results, two biosynthetic pathways were proposed. One pathway involved the phosphorylation of glucose to glucose 1-phosphate, followed by pyrophosphorylation to UDPG. The UDPG would then be oxidized to UDP-3-keto-D-glucose (3-ketoUDPG), which would be transformed into

UDP-3-amino-D-glucose or UDP-kanosamine (UDPK). The UDP would be cleaved finally to yield kanosamine (Figure 14). The second pathway entailed the oxidation of glucose to 3-keto-D-glucose followed by kanosamine production through transamination of this keto-intermediate. However, the second pathway was eliminated after kanosamine was not produced upon incubation of 3-keto-D-glucose with the cell-free lysate of *B. pumilus*.<sup>72</sup> In order to show kanosamine is produced from UDPG, UDP-[6,6-<sup>2</sup>H<sub>2</sub>]-glucose was prepared and treated separately with both the cell-free lysate of *A. mediterranei* and *B. pumilus*. In both cases [6,6-<sup>2</sup>H<sub>2</sub>]-kanosamine was produced suggesting that nitrogen incorporation occurs biosynthetically in this step.<sup>35</sup>

Among the enzymes belonging to the *rif* biosynthetic gene cluster are those proposed to catalyze the biosynthesis of kanosamine. By sequence homology, the gene product of *rifL* was found to be similar to a class of oxidoreductases implicated in the interconversion of hydroxyl and carbonyl groups.<sup>28</sup> Specifically, RifL has homology to the gene product of *pur10* found in *Streptomyces alboniger* puromycin biosynthesis, which selectively oxidizes the 3'-hydroxyl group of ATP to a ketone in the presence of NAD.<sup>74</sup> This similarity indicates RifL may be the oxidoreductase responsible for the proposed oxidation of UDPG to 3-ketoUDPG during kanosamine biosynthesis.

The gene product of *rifK* has been identified as AHBA synthase responsible for the catalysis of AHBA from aminoDHS.<sup>26</sup> Database screening using the protein sequence of RifK showed homology to genes implicated in transamination or dehydration/deoxygenation reactions in deoxyhexose biosynthesis as well as those with PLP/PMP dependency. These results led to the proposition of RifK holding a dual role in



AHBA biosynthesis as both AHBA synthase and possibly the aminotransferase catalyzing the production of UDPK from 3-ketoUDPG in kanosamine biosynthesis.<sup>26</sup>

This chapter will focus on the preparation of 3-ketoUDPG as well as its evaluation as a biosynthetic intermediate from UDPG to kanosamine in both *A. mediterranei* and *B. pumilus*. The conversion of 3-ketoUDPG and [3-<sup>3</sup>H]-UDPG to kanosamine was examined using the cell-free extracts of *A. mediterranei* and *B. pumilus* under varying reaction conditions. The oxidation of UDPG to 3-ketoUDPG was examined using the putative oxidoreductase from *A. mediterranei*, RifL. The transamination of 3-ketoUDPG by the putative aminotransferase from *A. mediterranei*, RifK, to produce UDPK was also studied. Finally this chapter will address the source of nitrogen incorporated into kanosamine during its biosynthesis.

## Synthesis of 3-ketoUDPG

### **Overview**

In order to investigate kanosamine biosynthesis and the origin of kanosamine's nitrogen atom, it was determined the intermediates 3-ketoUDPG and UDPK needed to be prepared. Chemoselective modification of carbohydrates tends to be difficult and laborious due to the presence of multiple nearly equivalent hydroxyl groups.<sup>75</sup> The probable instability of the desired 3-ketoUDPG poses another obstacle to chemical synthesis, as elimination of UDP would likely occur under basic conditions. An enzymatic synthesis offered several advantages including regioselectivity and the ability to perform reactions in aqueous media.

*Agrobacterium tumefaciens*, a microbe that induces tumor formation and crown gall disease in plants,<sup>76</sup> has been studied extensively to understand its unique metabolism of polysaccharides, more specifically sucrose (Figure 15). Using this microorganism, Bernaerts and De Ley described the first microbial formation of 3-ketoglycosides.<sup>77</sup> Different groups applying growing bacteria, resting cells of *A. tumefaciens*, or the purified enzyme expanded the use of this microbial oxidation reaction to a variety of sugars.<sup>78</sup> Van Beeuman and De Ley identified the flavin adenine dinucleotide-dependent inducible enzyme responsible for this oxidation reaction as hexopyranoside cytochrome c: oxidoreductase.<sup>79</sup> Hayano and Fukui later proposed use of the simpler name D-glucoside 3-dehydrogenase.<sup>80</sup>

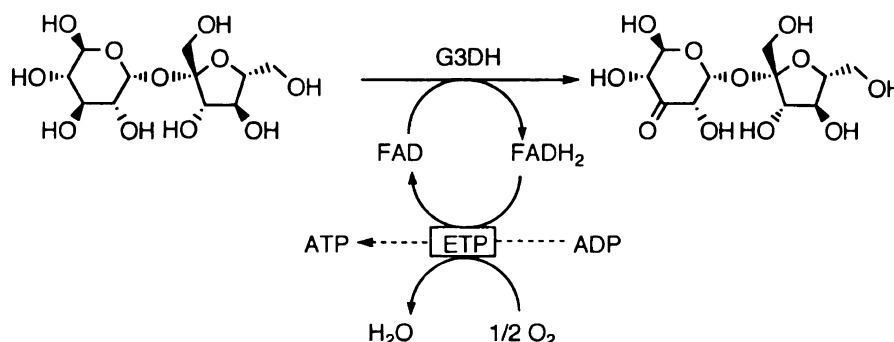


**Figure 15. Mechanism for the oxidation of sucrose to 3-ketosucrose by the glucoside-3-dehydrogenase from *A. tumefaciens*.**

Abbreviations: G3DH, glucoside-3-dehydrogenase; ETP, electron transport pathway.

Fukui, using both the purified enzyme and the standing cells of *A. tumefaciens*, reported the oxidation of glucose-1-phosphate to 3-ketoglucose-1-phosphate.<sup>81</sup> Fukui also identified and reported the whole-cell oxidation was composed of three processes: 1) entry of the substrate into the cells by an active transport mechanism; 2) conversion of the substrate to the product by D-glucoside-3-dehydrogenase; 3) exit of the product into

the reaction media. Fukui also observed the accumulation of phosphate in the culture media as the microbe metabolized 3-ketoglucose-1-phosphate.<sup>81</sup> In order to improve 3-ketoglucose-1-phosphate production Fukui derived a mutant, *A. tumefaciens* M-24, unable to grow on glucose-1-phosphate.<sup>82</sup> The inability of the mutant to utilize glucose-1-phosphate as a carbon source was linked to the inability of the standing cells to degrade 3-ketoglucose-1-phosphate, thus, effectively increasing the levels of 3-ketoglucose-1-phosphate concentrations expelled into the culture media.<sup>82</sup> This mutant was then used to oxidize UDPG to the corresponding 3-ketoUDPG.<sup>83</sup>

### **Synthesis of 3-ketoUDPG using partially purified glucoside-3-dehydrogenase**

When Fukui originally oxidized UDPG to 3-ketoUDPG there was no mention of attempting the oxidation with the native strain of *A. tumefaciens*.<sup>83</sup> Without access to the mutant strain, it was believed that performing the oxidation using the purified enzyme might be more successful. However, the literature purification was lengthy and required a large quantity of cells to provide a small amount of the desired protein.<sup>84</sup> Cells from 4 L of *A. tumefaciens* NCPPB 396 culture were combined and resuspended in 30 mL of a 0.03 M phosphate buffer at pH 7.0. The cells were lysed by two passes through a French pressure cell, and the insoluble, cellular debris was removed by centrifugation. The glucoside-3-dehydrogenase was precipitated at 70% ammonium sulfate saturation. The precipitate was then resuspended in a buffer containing 0.05 M phosphate and 0.01 M sucrose, and absorbed onto a DEAE column pre-equilibrated with 0.01 M phosphate buffer (pH 7.0). Glucoside-3-dehydrogenase was eluted with a linear gradient of 0 – 0.2 M KCl in 0.01 M phosphate/ 0.01 M sucrose buffer. After concentration and dialysis, 1.9

mL of protein solution contained 2.3 units of glucoside-3-dehydrogenase (Table 2). An SDS-PAGE gel of the protein solution contained a band consistent with the literature reported molecular weight of glucose-3-dehydrogenase (68 kDa).<sup>84</sup>

The glucoside-3-dehydrogenase activity was measured using an alkali assay.<sup>85</sup> A known concentration of sucrose was treated with the enzyme solution at 27°C in a phosphate buffer. At 30 minute intervals, 100  $\mu$ L aliquots were removed and added to 3 mL of 0.1 N NaOH solution. After 3 minutes at room temperature, the absorbance of 1 mL of the solution was measured at 340 nm.

**Table 2. Purification of glucoside-3-dehydrogenase.**

Purification step	Vol. (mL)	Tot. Prot. (mg)	Sp. act. <sup>a</sup> (units/mg)	Tot. Act. (units)	Yield (%)
Crude	38	1330	0.03	36	100
Ammonium Sulfate	6.0	120	0.10	10	27
DEAE-cellulose	1.9	8.6	0.28	2.3	6.4

(a) units =  $\mu$ mol/min·mg

Using 2,6-dichloroindolphenol as an electron acceptor, attempts were made to oxidize UDPG to 3-ketoUDPG using the partially purified glucoside-3-dehydrogenase. However, attempts to isolate the desired product failed, and only UDPG was observed. The failure of the reaction to provide 3-ketoUDPG was presumed to be due to the low amount of glucoside-3-dehydrogenase obtained after partial purification from *A. tumefaciens* NCPPB 396.

### Synthesis of 3-ketoglucose-1-phosphate using *A. tumefaciens* standing cells

Although Fukui did not report the preparation of 3-ketoUDPG using the wild-type strain of *A. tumefaciens*, 3-ketoglucose-1-phosphate was isolated from the oxidation of glucose 1-phosphate.<sup>81</sup> It was hypothesized that 3-keto-glucose 1-phosphate, produced from *A. tumefaciens* cells from glucose 1-phosphate, could be condensed with UTP to form 3-ketoUDPG using UDPG pyrophosphorylase (UGPase) in the presence of inorganic pyrophosphatase.

Cultures of *A. tumefaciens* NCPPB 396 were grown on a minimal salts medium (200 mL) containing sucrose as both carbon source and inducer of glucoside-3-dehydrogenase production. The cells were harvested by centrifugation, rinsed with 5 mM Tris-HCl at pH 8.2, and resuspended in 20 mL of the same buffer. Glucose-1-phosphate was added to the suspension and the reaction was incubated in a shaker at 28°C and 250 rpm. Aliquots were removed periodically and analyzed by assay to determine if 3-ketoglucose-1-phosphate was produced. Upon removal of the cells, the product was isolated by ethanol precipitation. 3-Ketoglucose-1-phosphate was identified in the crude product mixture by both <sup>1</sup>H and <sup>31</sup>P NMR. However, purification of the product caused the  $\beta$ -elimination of the phosphate to produce an endiolone (Figure 16), (+)-(2R,3R)-3,5-dihydroxy-2-hydroxymethyl-2,3-dihydro-4H-pyran-4-one. When the purification step was eliminated, the 3-ketoglucose-1-phosphate obtained was still contaminated with the enediolone. Later it was realized that the Tris salts from the oxidation reaction buffer could be catalyzing the  $\beta$ -elimination upon lyophilization. To remove Tris salts, the product solution was absorbed onto a plug of Dowex 50 (H<sup>+</sup> form) followed by elution of

the product with water. The pH of the eluant was adjusted to 4 with NaOH solution and lyophilized to yield 3-ketoglucose-1-phosphate free of the endiolone (Figure 16).

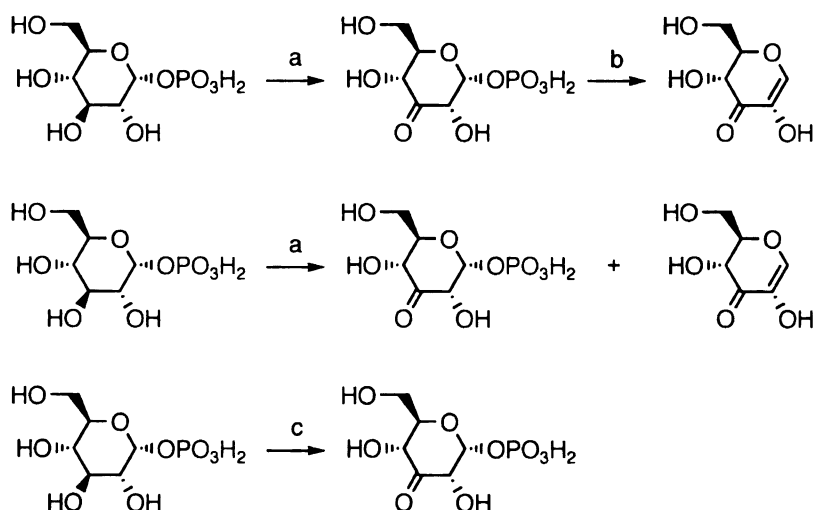


**Figure 16. Preparation of 3-ketoglucose-1-phosphate using the standing cells of *A. tumefaciens*.**

Reaction Conditions: (a) *A. tumefaciens* cells, 5 mM Tris-HCl pH 8.2; (b) Anion exchange column (AG1-X8) followed by cation exchange (Dowex 50 (H<sup>+</sup> form)); (c) *i. A. tumefaciens* cells, 5 mM Tris-HCl pH 8.2; *ii.* Cation exchange column to remove Tris salts (Dowex 50 (H<sup>+</sup> form)).

### Synthesis of 3-ketoUDPG from 3-ketoglucose-1-phosphate

UDPG is prepared from glucose-1-phosphate in several different ways (Figure 17). One method is to treat glucose-1-phosphate with UDPG pyrophosphorylase in the presence of UTP and inorganic pyrophosphatase.<sup>86</sup> The inorganic pyrophosphatase is required in the reaction to convert inorganic pyrophosphate formed into inorganic phosphate. This drives the equilibrium of the reaction toward the formation of UDPG and restricts the reformation of glucose-1-phosphate. However, any attempt to produce 3-ketoUDPG from 3-ketoglucose-1-phosphate under these conditions failed. Presumably, the pyrophosphorylase cannot utilize the keto substrate.

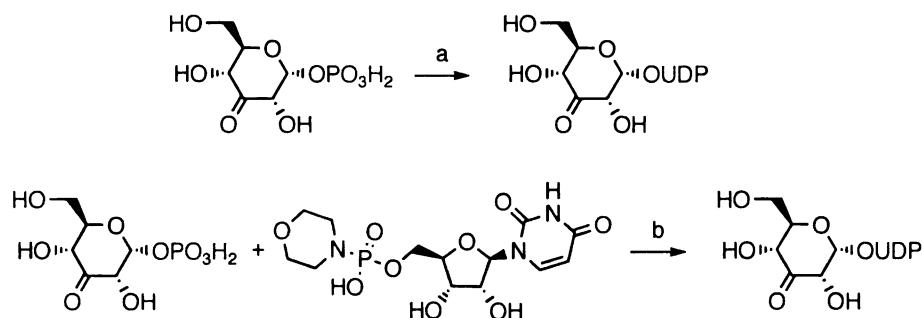


**Figure 17. Preparation of 3-ketoUDPG from 3-ketoglucose-1-phosphate.**

Reaction conditions: (a) UGPase, UTP, PPase,  $\text{MgCl}_2$ , no reaction; (b) DMF, pyr, trace product.

The condensation of glucose-1-phosphate with uridine 5'-monophosphomorpholide in the presence of base is another method used to prepare UDPG. The morpholide is first repeatedly azeotroped with dry pyridine to remove any water. Upon addition of the morpholide in pyridine to the 3-ketoglucose-1-phosphate, dry DMF was added and the reaction allowed to continue at room temperature. After 6 days, only traces of 3-ketoUDPG were observed, making this route undesirable (Figure 17).

### Synthesis of 3-ketoUDPG from UDPG using the standing cells of *A. tumefaciens*

It was originally presumed that 3-ketoUDPG could not be prepared using the wild type strain of *A. tumefaciens*. Fukui used the mutant strain M-24 with no indication whether an attempt was made using the native strain.<sup>83</sup> Similar to the oxidation of glucose-1-phosphate, the treatment of UDPG by the standing cells of *A. tumefaciens* originally resulted in  $\beta$ -elimination of UDP to form the endiolone (Figure 18). However removal of the Tris salts with cation exchange resin followed by lyophilization provided 3-ketoUDPG in 40% yield (Figure 18). The 3-ketoUDPG was characterized by  $^1\text{H}$  NMR,  $^{13}\text{C}$  NMR, GCOSY 2D NMR, and mass spec electrospray analysis. The final product

contained several impurities later confirmed by HPLC analysis to be uridine, UMP, and UDP. These impurities were presumably produced upon degradation of 3-ketoUDPG by the standing cells of *A. tumefaciens*. The 3-ketoUDPG produced was not purified beyond the removal of the Tris buffer for fear the desired product would not survive the purification.

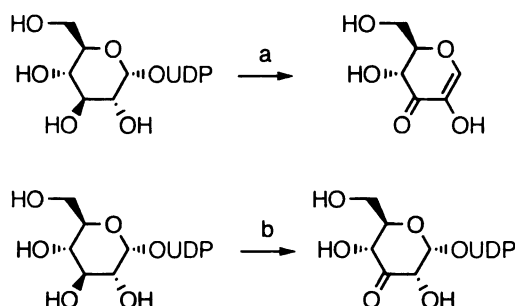


**Figure 18. Preparation of 3-ketoUDPG from UDPG using the standing cells of *A. tumefaciens*.**

Reaction conditions: (a) *A. tumefaciens* cells, 5 mM Tris-HCl, pH 8.2; (b) *i.* *A. tumefaciens* cells, 5 mM Tris-HCl, pH 8.2; *ii.* Dowex 50 (H<sup>+</sup> form).

#### **Reaction of 3-ketoUDPG with the cell-free extract of *A. mediterranei***

The analysis of 3-ketoUDPG intermediacy in the production of kanosamine by *A. mediterranei* required the preparation of *A. mediterranei* cell-free extract. A 4 L culture of *A. mediterranei* cells was grown on YMG medium for 2 days. The cells were harvested by centrifugation and resuspended in a 50 mM Tris-HCl buffer at pH 7.5 containing 20% glycerol and 1 mM PMSF. The cells were harvested by centrifugation and resuspended in 5 mL of the same buffer per gram of wet cells. The cells were lysed by two passes through a French pressure cell and the cellular debris was removed by centrifugation. The lysate was then dialyzed six times by repeated dilution and concentration using a 300 mL Amicon ultrafiltration system at 4°C. The lysate was then used directly for the cell-free reactions.



The prepared 3-ketoUDPG was treated with the cell-free lysate of *A. mediterranei* in the presence of NADH, glutamine, and  $\text{MgCl}_2$  at 28°C for 6 h. The protein was then removed by ultrafiltration. The supernatant was treated with ethanol to precipitate the product and remove the glycerol. The pellet was rinsed with ethanol and resuspended in d.d.  $\text{H}_2\text{O}$ . Kanosamine was produced in 6% yield as determined by  $^1\text{H}$  NMR analysis and the use of a calibration curve based on the  $\alpha$ -carbon. An interesting point with this reaction is that no 3-ketoUDPG was observed in the product mixture of this reaction. However UDPG and another product later identified as UDP-galactose were observed. As a positive control UDPG was reacted with NAD,  $\text{MgCl}_2$ , and glutamine using a portion of the same cell-free lysate to produce kanosamine in 8% yield.

### Role of NAD in *A. mediterranei* kanosamine biosynthesis

#### **Overview**

It has been presumed that during kanosamine biosynthesis the NADH cofactor produced upon oxidation of UDPG to 3-ketoUDPG by the oxidoreductase (presumably RifL) is used as a reducing factor during the transamination of 3-ketoUDPG to UDPK.<sup>72</sup> In doing so, the organism would be using a biosynthetic mechanism similar to that used by DHQ synthase during the isomerization of DAHP to DHQ in *E. coli*.<sup>87</sup> It has also been proposed that the two enzymes thought to be responsible for the oxidation and transamination steps, RifL and RifK, might form a complex,<sup>36</sup> which would further suggest a mechanism similar to that used by DHQ synthase.

A strategy was developed to determine if the oxidation/transamination reactions performed by *A. mediterranei* cell-free lysate utilize a DHQ synthase-type mechanism

through the incorporation of a  $^2\text{H}$  label into the starting UDPG. The oxidation of [3- $^2\text{H}$ ]-UDPG by the oxidoreductase would cause the  $^2\text{H}$  to be transferred to the NAD cofactor to form [ $^2\text{H}$ ]-NADH. If NADH is used as a reducing equivalent in the transamination of 3-ketoUDPG the  $^2\text{H}$  should be reincorporated into the product on some level. Also, the presence of  $^2\text{H}$  in the product kanosamine would lend some credence to the suggestion of a RifL/RifK complex *in vivo*.

### Synthesis of [3- $\text{H}^2$ ]-glucose

To prepare [3- $^2\text{H}$ ]-UDPG a chemical synthesis was first employed to prepare [3- $^2\text{H}$ ]-glucose from glucose (Figure 19). The collective protection of the C-1, C-2, C-4, and C-6 alcohols of glucose was accomplished through the treatment of glucose with acetone, zinc, and 85 %  $\text{H}_3\text{PO}_4$  to produce diisopropylidene glucose in 60% yield. The free hydroxyl group at C-3 was then oxidized with PDC to produce the ketone in 91% yield. The ketone was then reduced back to the alcohol in 60% yield with  $\text{NaBD}_4$  to incorporate a  $^2\text{H}$  label at C-3. Since the reduction of 3-ketoglucosides with  $\text{NaBH}_4$  gives the allo- configuration instead of the desired gluco-, the reduction was followed by a Mitsunobu reaction using DIAD to give the inverted alcohol in 44% yield. The  $^2\text{H}$ -labeled diisopropylidene glucose was then deprotected with 2N HCl to provide [3- $\text{H}^2$ ]-glucose in quantitative yield. The [3- $\text{H}^2$ ]-glucose was produced in 14% overall yield. The product was characterized by  $^1\text{H}$ ,  $^{13}\text{C}$  NMR, and mass spec.

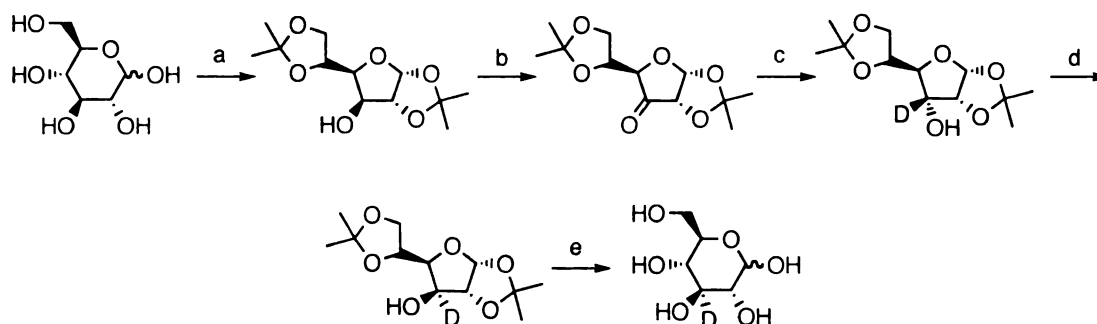


**Figure 19. Synthesis of [3-H<sup>2</sup>]-glucose from glucose.**

Reaction conditions: (a) acetone, ZnCl<sub>2</sub>, 85% H<sub>3</sub>PO<sub>4</sub>, r.t., 60%; (b) PDC, CH<sub>2</sub>Cl<sub>2</sub>, Ac<sub>2</sub>O, reflux, 91%; (c) NaBD<sub>4</sub>, EtOH:H<sub>2</sub>O (9:1), 60%; (d) *i.* DIAD, Ph<sub>3</sub>P, benzoic acid, benzene, *ii.* 1% NaOH/MeOH, 44%; (e) 2 N HCl, quant.

### Synthesis of [3-H<sup>2</sup>]-UDPG

Starting from glucose, a one-pot reaction can be used to prepare UDPG. The glucose is first phosphorylated to glucose-6-phosphate with hexokinase and UTP. The UDP produced in the phosphorylation is then recycled back to UTP with PEP by pyruvate kinase. The glucose-6-phosphate is then isomerized to glucose-1-phosphate using phosphoglucumutase. The glucose-1-phosphate is then converted to UDPG with UTP and UDPG pyrophosphorylase while the inorganic pyrophosphate produced in the reaction is converted to inorganic phosphate with inorganic pyrophosphorylase.

At the time of the study UDPG pyrophosphorylase (UGPase) was not commercially available as it was backordered and would not be available for some time. When purchased, the UGPase was expensive and the enzyme was provided in a powdered form, which made accurate unit calculation difficult. Overexpression of *galU*, the gene that encodes UGPase in *E. coli*, provided a solution to these problems. The gene *galU* was inserted into pJG7.248 (*T<sub>s</sub>*, *lacO*, *lacO*, 6 x *his*, *lacI<sup>r</sup>*, Amp<sup>r</sup>), derived from pQE30 (*T<sub>s</sub>*, *lacO*, *lacO*, 6 x *his*, Amp<sup>r</sup>), to form pHS3.244 (*T<sub>s</sub>*, *lacO*, *lacO*, 6 x *his*, *galU*, *lacI<sup>r</sup>*, Amp<sup>r</sup>). *E. coli* DH5α was transformed with pHS3.244 and *galU* was expressed by

the addition of IPTG. UGPase was purified from the cell-free lysate using  $\text{Ni}^{2+}$ -NTA resin. The specific activity was measured to be 64 U/mg (where one unit indicated the formation of NADH in  $\mu\text{mol}/\text{min}\cdot\text{mg}$ ).

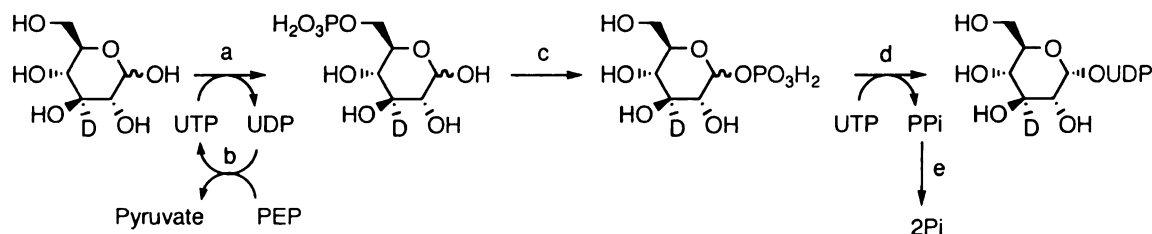


**Figure 20. One-pot enzymatic synthesis of [3- $\text{H}^2$ ]-UDPG from [3- $\text{H}^2$ ]-glucose.**

Enzymes: (a) Hexokinase; (b) Pyruvate kinase; (c) Phosphoglucomutase; (d) UDPase; (e) PPase. Abbreviations: UTP, uridine 5'-triphosphate; UDP, uridine 5'-diphosphate; PEP, phosphoenolpyruvate; PPI, inorganic pyrophosphate;  $\text{P}_i$ , inorganic phosphate.

[3- $\text{H}^2$ ]-glucose was treated in one pot with hexokinase, pyruvate kinase, phosphoglucomutase, UGPase, PPase, UTP, and PEP to produce [3- $\text{H}^2$ ]-UDPG (Figure 20). Initial attempts to purify the final product using an anion exchange resin failed to yield a clean product. The impurities were identified as UMP and UDP. To avoid producing the UMP and UDP it was thought the reaction might be run in stages where [3- $\text{H}^2$ ]-glucose-6-phosphate could be prepared first from [3- $\text{H}^2$ ]-glucose, purified, and then converted to [3- $\text{H}^2$ ]-UDPG using the remaining enzymes and UTP. Unfortunately UGPase activity is inhibited by a large concentration of glucose 6-phosphate and the reaction failed.

Using the original one-pot procedure with unlabeled glucose,<sup>86</sup> a variety of purification methods were attempted to remove the contaminating UMP and UDP (Table 3). All of the methods using anion exchange resin failed to provide pure product. Silica gel radial chromatography did provide clean UDPG, however the method was difficult to repeat as the amount of water in the eluant often caused the silica gel to break away from

the base plate. Paired ion chromatography using reverse phase HPLC did provide clean material after the salts ( $\text{NaHCO}_3$  and tetrabutylammonium hydrogen carbonate (TBAHC)) were removed by treatment with Dowex 50 ( $\text{H}^+$  form). The  $[3\text{-H}^2]\text{-UDPG}$  was prepared in 75% yield after purification with 86%  $\text{H}^2$  incorporation at C-3. The product was characterized using  $^1\text{H}$  and  $^{13}\text{C}$  NMR, 2D NMR analysis, and mass spec.

**Table 3. Methods used to purify  $[3\text{-H}^2]\text{-UDPG}$ .**

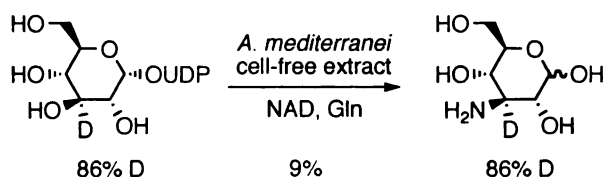
Entry	Purification media	Eluant
1	AG1-X8 ( $\text{HCO}_3^-$ form)	0 - 1 M TEAB pH 7.0
2	AG1-X8 ( $\text{CH}_3\text{CO}_2^-$ form)	0 – 4 M NaOAc pH 7.0
3	Dowex1x2-200 ( $\text{HCO}_3^-$ form)	0 – 1 M $\text{NaHCO}_3$ pH 7.0
4	Dowex1x2-200 ( $\text{HCO}_3^-$ form)	0.5 – 1 M $\text{NaHCO}_3$ pH 7.0
5	Silica gel radial chromatography	1:4 $\text{H}_2\text{O}$ :EtOH
6	HPLC C-18 reverse phase	50 mM $\text{NaHCO}_3$ , 2.5 mM TBAHC, $\text{H}_2\text{O}/\text{CH}_3\text{CN}$

#### **Reaction of $[3\text{-H}^2]\text{-UDPG}$ with *A. mediterranei* cell-free lysate**

*A. mediterranei* cell-free lysate was prepared as previously described. The  $[3\text{-H}^2]\text{-UDPG}$  was treated with the cell-free lysate in the presence of NAD,  $\text{MgCl}_2$ , and glutamine. The protein was removed by ultrafiltration after 6 h of stirring at  $28^\circ\text{C}$ . The supernatant was diluted with EtOH and the precipitate collected by ultrafiltration. The precipitate was rinsed with EtOH, dried, and dissolved in d.d.  $\text{H}_2\text{O}$ . The solution was absorbed onto a 10 mL column of Dowex 50 ( $\text{H}^+$  form) resin. The resin was washed with d.d.  $\text{H}_2\text{O}$ , and the product was eluted with a linear gradient of 0-2 N HCl. The fractions were assayed for amine content using a ninhydrin assay. The kanosamine produced in

the reaction was characterized by  $^1\text{H}$  NMR and mass spec analysis. The kanosamine was produced in 9% yield and contained 86%  $\text{H}^2$  incorporation. Since the substrate  $[3\text{-H}^2]\text{-UDPG}$  contained 86%  $\text{H}^2$  incorporation the  $[3\text{-H}^2]\text{-kanosamine}$  produced essentially retaining 100% of the label.

**Figure 21. Reaction of  $[3\text{-H}^2]\text{-UDPG}$  with the cell-free lysate of *A. mediterranei*.**



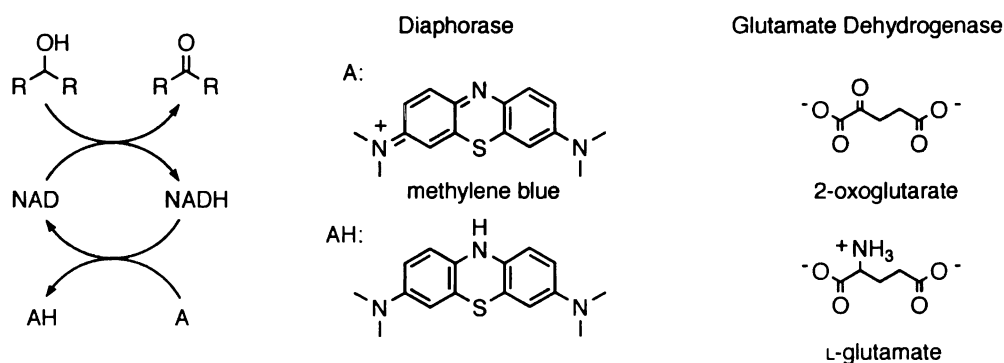
In order to better understand the enzymes performing the oxidation and transamination steps of kanosamine biosynthesis,  $[3\text{-H}^2]\text{-UDPG}$  was treated with *A. mediterranei* cell-free lysate in the presence of glutamine,  $\text{MgCl}_2$ , and a 1:1 ratio of NAD and NADH. If the enzymes form a complex as Floss and co-workers have indicated, the  $[^2\text{H}]\text{-NADH}$  formed during the oxidation might not be released into the reaction media, thereby giving the same  $\text{H}^2$  incorporation observed when no NADH was added to the reaction. However, if the  $[^2\text{H}]\text{-NADH}$  is released into the reaction supernatant, the  $\text{H}^2$  incorporation should be lower than that observed when no NADH is added to the reaction. However, the reaction yielded no kanosamine. The lack of kanosamine production was presumably due to inhibition by NADH of one of the proceeding enzymatic steps.

### NADH “trapping”

Another possible way to elucidate the mechanism of conversion of UDPG to UDPK through 3-ketoUDPG is through a “trapping” experiment.<sup>88</sup> If the mechanism

involves an enzyme complex, no NADH would be released during the course of reactions. However, if the enzymes perform the reactions separately, NADH would be released. The released NADH could then be “trapped,” and kanosamine would theoretically not be produced. In this case 3-ketoUDPG should be observed in the reaction mixture. In order to “trap” any NADH that might be produced in the reaction, two methods of NADH regeneration to NAD were employed (Figure 22). The first method attempted was the addition of diaphorase and methylene blue to the cell-free experiments. Upon treatment of UDPG, glutamine, NAD, and methylene blue with *A. mediterranei* cell-free extract and diaphorase; neither 3-ketoUDPG nor kanosamine was observed. To ensure that the lack of product produced with the *A. mediterranei* cell-free extract was not due to inhibition by methylene blue, a second regeneration technique using glutamate dehydrogenase, 2-oxoglutarate, and  $\text{NH}_4\text{OH}$  was used. Still no kanosamine or 3-ketoUDPG was observed in the reaction mixture with *A. mediterranei* cell-free extract. In conclusion it appears NADH is required for the transamination-reduction of 3-ketoUDPG to UDPK by enzymes in the cell-free lysate of *A. mediterranei*.

**Figure 22. Co-factors for the *in situ* regeneration of NAD from NADH**



## Expression and Analysis of RifL and RifK

### Overview

Purification of AHBA synthase, which aromatizes aminoDHS to form AHBA, and subsequent cloning of the encoding gene, *rifK*, by reverse genetics led the way for Floss and co-workers to clone, sequence, and analyze the 95 kb *rif* biosynthetic gene cluster responsible for rifamycin biosynthesis in *A. mediterranei*.<sup>26</sup> Further studies by Floss and co-workers identified seven genes of the rifamycin biosynthetic gene cluster, *rifG*, *-H*, *-J*, *-K*, *-L*, *-M*, and *-N*, which were involved in AHBA biosynthesis. Of those three, *rifG*, *-H*, and *-J*, encode homologs to shikimate pathway enzymes identified as aminoDHQ synthase, aminoDAHP synthase, and aminoDHQ dehydratase respectively.<sup>28</sup> The gene product of *rifN* was later identified by Floss as a kanosamine-specific kinase catalyzing the production of kanosamine-6-phosphate. The gene product of *rifM* shares sequence homology to phosphatases among the CBBY family and has been found to catalyze the specific cleavage of UDPK and kanosamine 1-phosphate to kanosamine.<sup>36</sup>

The remaining enzyme along the *rif* biosynthetic gene cluster, *rifL*, was found to be necessary for AHBA production in *A. mediterranei*. The gene product of *rifL* shares homology with a class of oxidoreductases that have been linked to the interconversion of hydroxyl and carbonyl groups.<sup>36</sup> This class of enzymes includes glucose-fructose oxidoreductase from *Zymomonas mobilis* and the gene product of *pur10* in *Streptomyces alboniger* puromycin biosynthesis. The gene product of *pur10* was found to be an NAD-dependent ATP dehydrogenase.<sup>74</sup> The subsequent amino transfer to the oxidized ATP,



presumably by the gene product of *pur4*, mirrors the presumed oxidation and transamination of UDPG to produce UDPK.

To confirm the remaining step in kanosamine biosynthesis requires the identification of the transaminase. Of the genes along the *rif* biosynthetic gene cluster two shared sequence homology to aminotransferases, *rifK* and *orf9*. The gene product of *orf9* shares sequence homology to the gene product of *yokM* from *B. subtilis*. However, *orf9* was excluded from expressing the required transaminase activity for kanosamine biosynthesis. The inactivation of *orf9* from the *A. mediterranei* genome did not have an effect on rifamycin production by intact cells and as such it was determined that *orf9* was not necessary for either AHBA or kanosamine production.<sup>36</sup>

On the other hand, the gene product of *rifK* was found to be a credible candidate for the desired transaminase. Although RifK has already been found to catalyze the isomerization of aminoDHS to AHBA, its homology to aminotransferases suggests a dual enzymatic role.<sup>26</sup> One homolog is the gene product of *stsC* from the streptomycin producer *Streptomyces griseus*, which catalyzes the aminotransfer between glutamate and *scyllo*-inosose to produce *scyllo*-inosamine and  $\alpha$ -keto-glutaramate, which cyclizes readily to 2-pyrrolidone-5-hydroxy-5-carboxylic acid.<sup>89</sup> Another homolog of RifK is ArnB involved in the modification of the lipid A moiety of the outer-membrane lipopolysaccharide in a polymyxin-resistant mutant of *E. coli* W3110. ArnB catalyzes the PLP and glutamate dependent transamination of 4-keto-UDP-L-arabinose to 4-amino-4-deoxy-UDP-L-arabinose prior to lipid A modification.<sup>90</sup> Other incidental indications that RifK is the transaminase responsible for the introduction of the amine in kanosamine biosynthesis include the close proximity of *rifK* to *rifL* along the *rif* gene cluster, the

existence of two homologs of *rifK* in the *asm* gene cluster, the combination of *rifK* and *rifL* homologs positioned identically in every AHBA biosynthetic gene cluster suggesting a close functional interaction, and the ability of RifK to bind both PMP and PLP equally well.<sup>37</sup>

### **Reaction of UDPG and 3-ketoUDPG with the cells free-lysates of RifL<sup>-</sup> and RifK<sup>-</sup> *A. mediterranei* mutants**

It was determined that reaction of *A. mediterranei* mutants lacking the ability to express *rifL* and *rifK* with UDPG and 3-ketoUDPG could help to elucidate the roles of these proteins in kanosamine biosynthesis. Floss and coworkers developed mutants of *A. mediterranei* where various genes among the *rif* gene cluster were disrupted through the deletion of fragments from the individual genes.<sup>28</sup>

To prepare a *rifL*-inactivated *A. mediterranei* mutant, the 1.6 kb *EcoRI-XhoI* and 1.65 kb *XhoI-BamHI* fragments containing the N and C termini of *rifL* were ligated and cloning into the plasmid pHGF008 to create the mutant pRM04 providing a *rifL* gene missing a 624-bp *XhoI* fragment. A suicide vector, pRM05, was then created by the insertion of a 1.7-kb *KpnI* fragment carrying a hygromycin resistance gene from pIJ5607 into pRM04 pre-treated with *KpnI*. This suicide vector was then transformed via electroporation into *A. mediterranei* S699 electrocompetent cells, which were plated onto YMG plates containing hygromycin. Colonies were screened using selective and non-selective plates to gain colonies resulting from several crossover recombination events while retaining hygromycin resistance. The genomic DNA was isolated and analyzed to

determine if the native *rifL* gene had been replaced with the inactivated *rifL*. The mutants containing an inactivated *rifL* were termed RM01.<sup>28</sup>

To prepare a *rifK* inactivated mutant of *A. mediterranei* the *rifK* gene was initially disrupted using a marker-replacement suicide vector, pSK-/AHBA2. This vector was prepared by inserting a hygromycin resistance gene into the 2.3 kb *XhoI* fragment of pSK-/AHBA1 at the only *BglII* site. Through electroporation pSK-/AHBA2 was transformed into *A. mediterranei* S699 competent cells. Through several screenings mutants were identified which could not produce rifamycin B. Through genetic analysis it was determined all of these mutants, HGF003, contained disrupted *rifK* in lieu of the native *rifK*.<sup>26</sup>

Both the RM01 and HGF003 mutants were obtained from Floss and their respective cell-free lysates were prepared according to the same method used to prepared *A. mediterranei* cell-free lysate. As expected, when UDPG was reacted with the cell-free lysate of *A. mediterranei* RM01 (*rifL*-) in the presence of NAD and glutamine, neither kanosamine nor 3-ketoUDPG was observed in the product mixture (Entry 1, Table 4). When 3-ketoUDPG was treated with the cell-free lysate of *A. mediterranei* RM01 (*rifL*-) in the presence of NADH and glutamine, surprisingly no kanosamine was observed (Entry 2, Table 4). When the same experiments were repeated with the cell-free lysate of *A. mediterranei* HGF003 (*rifK*-) no kanosamine was observed (Entries 3-4, Table 4).

**Table 4. Reactions of UDPG and 3-ketoUDPG with the cell-free lysate of *A. mediterranei* mutants lacking *rifL* and *rifK*.**

Entry	Substrate	Reaction Conditions	Yield Kanosamine (%)
1	UDPG	<i>A. mediterranei</i> RM01 ( <i>rifL</i> -) cell-free lysate, L-glutamine, NAD	0
2	UDPG	<i>A. mediterranei</i> HGF003 ( <i>rifK</i> -) cell-free lysate, L-glutamine, NAD	0
3	3-ketoUDPG	<i>A. mediterranei</i> RM01 ( <i>rifL</i> -) cell-free lysate, L-glutamine, NADH	0
4	3-ketoUDPG	<i>A. mediterranei</i> HGF003 ( <i>rifK</i> -) cell-free lysate, L-glutamine, NADH	0

### Heterologous expression and purification of RifL

Two plasmids were obtained to express RifL heterologously in *E. coli*. The first plasmid, pRM030 ( $T_7$ , *6xhis*, *rifL*, Amp<sup>r</sup>, *lacI*<sup>n</sup>) derived from pRSET ( $T_7$ , *6xhis*, Amp<sup>r</sup>), was obtained from Heinz Floss. The second plasmid, pJG7.275 ( $P_{lac}$ , *rifL*, *lacI*<sup>Q</sup>, Amp<sup>r</sup>), derived from pJF118EH ( $P_{lac}$ , *rifL*, Amp<sup>r</sup>, *lacI*<sup>Q</sup>), was prepared previously by Jiantao Guo in this research group. Due to the  $T_7$  promoter pRM030 was transformed into BL21(DE3) while pJG7.275 was transformed into JM109. Both strains were cultured in LB/Amp media until the OD<sub>600</sub> at 37°C until the OD<sub>600</sub> reached 0.6. At which time IPTG was added to 1 mM. The cultures were incubated another 4 h in a 37°C shaker before the cells were harvested by centrifugation at 4°C. The cell pellets obtained upon centrifugation were resuspended in 50 mM Tris-HCl at pH 7.5 and lysed by two passes through a French pressure cell. The cell-free lysates were obtained after the cellular debris was removed by centrifugation.

Once the cell-free lysates were prepared, they were used in an attempt to prepare 3-ketoUDPG from UDPG. UDPG and NAD were incubated with the cell-free lysates of BL21(DE3)/pRM030 and JM109/pJG7.275 at 28°C for 6 hr. No 3-ketoUDPG was

observed in either case. When 3-ketoUDPG was treated with the cell-free lysate of JM109/pJG7.275 in the presence of NADH, UDPG was produced in 3% yield. However, the same reaction run with BL21 (DE3)/pRM030 cell-free lysate failed to yield any UDPG. As a control, 3-ketoUDPG was treated with the cell-free lysate of JM109 in the presence of NADH and no UDPG was observed.

Since the oxidation of UDPG by JM109/pJG7.275 cell-free lysate in the presence of NAD did not yield high levels of 3-ketoUDPG, alternative reaction conditions were considered. UDPG was reacted with the cell-free extract of JM109/pJG7.275 using 2,6-dichloroindolphenol (DCIP) and phenazine methosulfate (PMS) as cofactors (Figure 23). Under these conditions, PMS acts as an intermediate electron carrier and the decrease in the optical density at 600 nm as DCIP acts as the terminal electron acceptor can be followed. Initially, no 3-ketoUDPG was produced. However, when the incubation of the JM109/pJG7.275 cells after IPTG addition was extended from 4 to 18-24 h 3-ketoUDPG was produced in 8% yield. No 3-ketoUDPG was produced when the cell-free lysate of JM109 was used in place of JM109/pJG7.275.

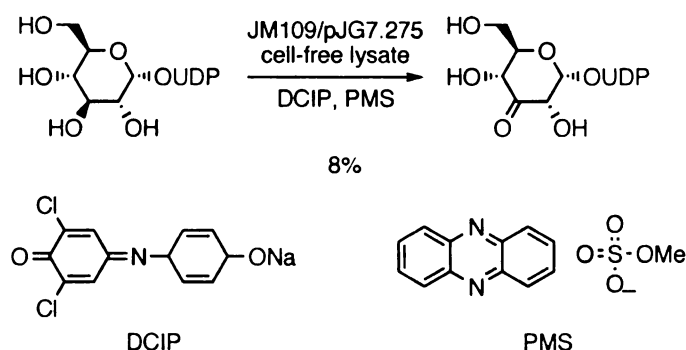


**Figure 23. Reaction of UDPG with DCIP, PMS, and the cell-free lysate of JM109/pJG7.275.**

Abbreviations: DCIP, 2,6-dichloroindolphenol; PMS, phenazine methosulfate.

An attempt was made to purify RifL from the cell-free lysate of JM109/pJG7.275 using an FPLC. Presumably, the purification would eliminate any background activity related to the reduction of 3-ketoUDPG with NADH and enhance the activity from the oxidation of UDPG to 3-ketoUDPG. The cell-free lysate was applied to a MonoQ column and eluted with a linear gradient from 0-600 mM NaCl in 20 mM Tris-HCl buffer at pH 7.5. Using a DCIP/PMS assay for oxidoreductase activity using UDPG as the substrate, no active fractions were observed. The lack of activity could indicate the activity of the expressed RifL was lost or that no active RifL had been produced after all.

Taking into account the preferred GC-rich codon usage of organisms like *A. mediterranei* and *Streptomyces* in comparison to *E. coli*, the GC content of *rifL* was calculated. The gene of interest *rifL* had a higher incidence of arginine (CCC) and proline codons (CGG) per 1000 amino acids than either *A. mediterranei* or *E. coli* (Table 5). Due to the high GC content of *rifL*, pJG7.275 was transformed into BL21 Codon Plus RP (*E. coli* B F<sup>-</sup>, *ompT*, *hsds*(*r<sub>B</sub>*<sup>-</sup> *m<sub>B</sub>*<sup>-</sup>), *dcm*<sup>+</sup>, Tet<sup>r</sup>, *gal*, *endA*, *the*, [*argU*, *proL*, Cm<sup>r</sup>]), which contains overexpressed tRNA synthetase genes for proline and arginine to provide the GC excess required to effectively express *rifL*. Again attempts to purify RifL by FPLC from the cell-free lysate of BL21 Codon Plus RP failed to yield active enzyme.

**Table 5. Arginine and proline codon frequencies of *E. coli*, *A. mediterranei*, and *rifL*.**

Entry	DNA sequence	CCC <sup>a</sup>	CGG <sup>a</sup>
1	<i>E. coli</i> K12 genomic DNA	5.5	5.4
2	<i>A. mediterranei</i> genomic DNA	15.9	36.5
3	<i>A. mediterranei rifL</i>	22.2	44.3

(a) Frequency of codon usage per 1000 amino acids of the analyzed DNA sequence.

3-ketoUDPG was produced in 16% yield when UDPG was reacted with the cell-free extract of BL21 Codon Plus RP/pJG7.275 in the presence of DCIP, PMS, and

MgCl<sub>2</sub>. Later, it was found that when preparing the cell-free lysate of BL21 Codon Plus RP, incubation of the cells for 12 h after IPTG induction instead of 18-20 h provided 3-ketoUDPG in 48% yield with no remaining UDPG. An attempt to reduce 3-ketoUDPG to UDPG in the presence of NADH using BL21 Codon Plus RP/pJG7.275 cell-free lysate failed, contradicting an earlier result with JM109/pJG7.275 cell-free lysate.

### **Specific activity of RifL**

Several assays were used to gauge the specific activity of RifL. The first method using the cell-free lysate of JM109/pJG7.275 followed the NADH loss and formation. To measure the specific activity of the RifL oxidation of UDPG to produce 3-ketoUDPG the absorbance at 340 nm was followed over one minute. Unfortunately the slope of NADH formation was not linear using either JM109/pJG7.275 or JM109 cell-free lysate. The loss of NADH was also followed as 3-ketoUDPG was reduced to UDPG by the cell-free lysate of both JM109 and JM109/pJG7.275. Using JM109/pJG7.275 cell-free lysate the specific activity of 3-ketoUDPG reduction was measured to be 0.057 U/mg where one unit is equal to  $\mu\text{mol}$  NADH produced per minute per mg of protein. The background activity using JM109 cell-free lysate was measured to be 0.037 U/mg leaving a RifL specific activity of 3-ketoUDPG reduction of 0.02 U/mg (Entry 1, Table 6).

The second method used to determine the specific activity of RifL followed the change in absorbance at 600 nm when UDPG is oxidized in the presence of DCIP, PMS, and the cell-free lysate of BL21 Codon Plus RP/pJG7.275. This method was used in the hopes of eliminating any reversibility of RifL. Using these conditions the specific activity of UDPG oxidation by RifL was calculated to be 0.012 U/mg (Entry 2, Table 6).

Lastly the specific activity of the RifL oxidation of UDPG to 3-ketoUDPG was determined by following the production of 3-ketoUDPG. 3-ketoUDPG was incubated with the cell-free lysate of BL21 Codon Plus RP in the presence of DCIP, PMS, MgCl<sub>2</sub>, and *p*-hydroxybenzoic acid to act as an internal standard. At 15-minute increments 400  $\mu$ L of the reaction mixture was removed and quenched with 100  $\mu$ L 10% TCA solution. The precipitated protein was removed by centrifugation and a portion of the supernatant was diluted by 13 to prepare a 1 mL solution. A 10  $\mu$ L portion of the diluted sample was then injected onto a Zorbax Bonus RP (amide-C14) analytical HPLC column. The sample was eluted with a linear gradient of eluant A (50 mM KH<sub>2</sub>PO<sub>4</sub>/2.5 mM TBAHS in water, pH 6.9) and eluant B (50 mM KH<sub>2</sub>PO<sub>4</sub>/2.5 mM TBAHS in CH<sub>3</sub>CN:H<sub>2</sub>O (1:1), pH 6.9) and analyzed at 254 nm. A response factor prepared with UDPG was used to calculate the  $\mu$ mol of 3-ketoUDPG produced over time. Using this assay the specific activity of the RifL oxidation of UDPG was measured to be 0.015 U/mg after 60 min with a slight drop to 0.012 U/mg after 120 min (Entry 3, Table 6).

**Table 6. Specific activity determinations of RifL.**

Entry	RifL Assay Conditions	Sp. Act (U/mg) <sup>a</sup>
1	Loss of NADH during 3-ketoUDPG reduction	0.02
2	DCIP reduction during UDPG oxidation to 3-ketoUDPG	0.012
3	3-ketoUDPG formation followed by HPLC	0.015

(a) One Unit refers to  $\mu$ mol conversion per min.

The results of all three methods used to assay RifL activity are presented in Table 6. Of the three assays used to determine RifL activity the assays using BL21 Codon Plus RP/pJG7.275 cell-free lysate to follow both DCIP reduction and 3-ketoUDPG formation are the most accurate. These results were much more consistent and the expression of RifL using BL21 Codon Plus RP provided more active enzyme.



### **Initial attempts to produce UDPK using RifK or a combination of RifK/RifL**

In the *rif* biosynthetic gene cluster, two genes, *rifK* and *orf9*, were found by Blast analysis to have sequence homology to known aminotransferase genes.<sup>26,28</sup> RifK is known to be the 3-amino-5-hydroxybenzoic acid synthase, but is homologous to other aminotransferase enzymes, which utilize pyridoxal 5'-phosphate as a cofactor. Another possible aminotransferase could be encoded by *orf9*, however gene inactivation experiments indicated that *orf9* was not necessary for AHBA production, and RifK was proposed to act both as the aminotransferase converting 3-ketoUDPG to UDPK and as the AHBA synthase. The plasmid pJG7.259a (*T5*, *rifK*, *6xhis*, *Ap<sup>R</sup>*, *lacI<sup>M</sup>*) was obtained and transformed into *E. coli* JM109. RifK was expressed by the addition of IPTG using the same conditions as for RifL. 3-ketoUDPG was treated with the cell-free extract of JM109/pJG7.259a in the presence of glutamine, pyridoxal 5'-phosphate and NAD or NADH. No UDPK was produced. When RifK purified by Ni<sup>2+</sup>-NTA resin was used in place of JM109/pJG7.259A cell-free extract with the addition of MgCl<sub>2</sub>, no UDPK was produced. Upon addition of JM109/pJG7.275 cell-free extract to the above reactions in the presence of NADH, 3-ketoUDPG was reduced to UDPG. A summary of the reactions incubating 3-ketoUDPG with heterologously expressed RifK is shown in Table 7.

**Table 7. Reactions of 3-ketoUDPG with heterologously expressed RifK from JM109/pJG7.259a.**

Entry	Substrate	Reaction conditions <sup>a</sup>	Yield UDPK (%)
1	3-ketoUDPG	JM109/pJG7.259a cell-free lysate, PLP, NADH, L-glutamine	0
2	3-ketoUDPG	JM109/pJG7.259a cell-free lysate, PLP, NAD, L-glutamine	0
3	3-ketoUDPG	RifK, PLP, NADH, MgCl <sub>2</sub> , L-glutamine	0
4	3-ketoUDPG	RifK, PLP, NAD, MgCl <sub>2</sub> , L-glutamine	0
5	3-ketoUDPG	JM109/pJG7.275 cell-free lysate, RifK, NADH, PLP, MgCl <sub>2</sub> , L-glutamine	0
6	3-ketoUDPG	JM109/pJG7.275 cell-free lysate, RifK, NAD, PLP, MgCl <sub>2</sub> , L-glutamine	0
7	UDPG	JM109/pJG7.275 and JM109/pJG7.259a cell-free lysates, PMS, DCIP, L-glutamine	0
8	UDPG	JM109/pJG7.275 and JM109/pJG7.259a cell-free lysates, DCIP, PMS, PLP, L-glutamine	0
9	UDPG	JM109/pJG7.275 and JM109/pJG7.259a cell-free lysates, NAD, PLP, DCIP, PMS, L-glutamine	0
10	UDPG	JM109/pJG7.259a cell-free lysate, RifK, PLP, DCIP, PMS, L-glutamine	0

(a) RifK was purified from JM109/pJG7.259.

When UDPG was treated with both the cell-free extracts of JM109/pJG7.275 (RifL) and JM109/pJG7.259a in the presence of DCIP, PMS, and glutamine, the presence of 3-ketoUDPG was not observed, however whether UDPK was produced was inconclusive as the anomeric proton of UDPK appears at approximately the same position as that of UDPgalactose. Attempts to use HPLC paired ion chromatography to

determine whether UDPK was produced were also inconclusive. The same was found when UDPG was treated with JM109/pJG7.275 cell-free extract and RifK in the presence of DCIP, PMS, and glutamine.

**Table 8. Reactions of 3-ketoUDPG with RifK obtained from BL21 C+ RP/pJG7.259a.**

Entry	Reaction Conditions <sup>a</sup>	Yield UDPK (%)
1	BL21 C <sup>+</sup> RP/pJG7.259a cell-free lysate, PLP, NADH, MgCl <sub>2</sub> , L-glutamine	5
2	BL21 C <sup>+</sup> RP cell-free lysate, PLP, NADH, MgCl <sub>2</sub> , L-glutamine	0
3	RifK, PLP, NADH, L-glutamine, MgCl <sub>2</sub>	1
4	RifK, L-glutamine, NADH, MgCl <sub>2</sub>	0
5	BL21 C <sup>+</sup> RP/pJG7.259a cell-free lysate, NADH, L-glutamine, MgCl <sub>2</sub>	1
6	BL21 C <sup>+</sup> RP cell-free lysate, NADH, L-glutamine, MgCl <sub>2</sub>	0

(a) All reactions were run at 30°C in 50 mM Tris-HCl buffer at pH 7.5 containing 20% glycerol. RifK was purified from JM109/pJG7.259.

Due to the high GC content of the *A. mediterranei* genome in comparison to *E. coli*, pJG7.259a (*T5*, *lacO*, *lacO*, *rifK*, *6xhis*, *lacI<sup>R</sup>*, *Ap<sup>R</sup>*) was transformed into BL21Codon Plus RP, which contains additional arginine and proline codons. Treatment of 3-ketoUDPG with the cell-free extract of BL21C<sup>+</sup>RP/pJG7.259a in the presence of NADH, L-glutamine, pyridoxal 5-phosphate (PLP), and MgCl<sub>2</sub> yielded UDPK in 8% yield. The same experiment performed with the cell-free extract of BL21 C<sup>+</sup> RP without pJG7.259a did not yield any UDPK. Performing the transamination reaction as above in the absence of PLP gave a 1% yield of UDPK with BL21 C<sup>+</sup> RP/pJG7.259a cell-free extract, and no UDPK with BL21 C<sup>+</sup> RP cell-free extract. (Table 8)

RifK was purified using Ni<sup>2+</sup>-NTA resin by stepwise elution with increasing concentrations of imidazole. An attempt was made to measure the specific activity of the RifK transamination of 3-ketoUDPG by following the loss of NADH, however the measured activity was extremely low. Upon treatment of 3-ketoUDPG with RifK in the presence of NADH, PLP, Mg<sup>2+</sup>, and glutamine, UDPK was produced in 1% (trace) yield. No UDPK was produced when PLP was omitted from the reaction. Due to the purified enzyme's instability and subsequently lower observed yield, cell-free extract was used for the remaining experiments.

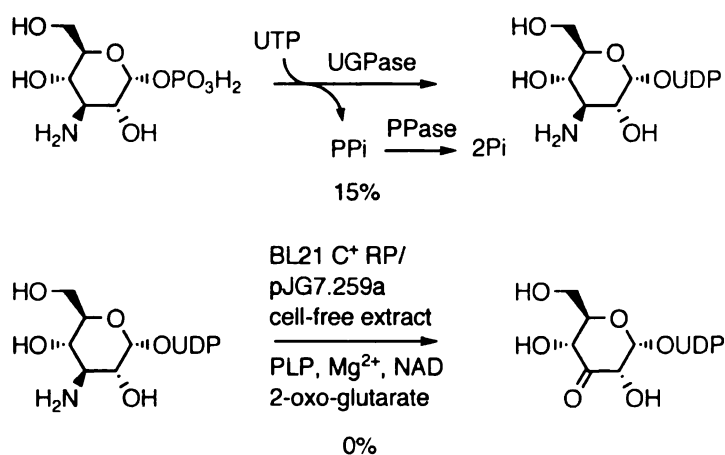
In order to securely identify the product produced in the above reaction as UDPK, the <sup>1</sup>H NMR evidence needed to be verified, and a second line of evidence needed to be established. To verify that the peak in the NMR presumed to represent the anomeric proton of UDPK was correct, a standard sample of UDPK, synthesized by Xiaofie Jia, was added to an NMR sample of a reaction thought to produce UDPK. No new peaks appeared in the NMR spectrum, however the presumed peak did not increase significantly since the amount of UDPK added was only ~1 mg.

Since the cell-free reactions to produce UDPK yield a complex mixture of products, a direct mass spectrum analysis of the crude reaction could not be obtained and the second line of evidence chosen was HPLC. The reaction sample was first partially purified by HPLC using a semi-preparative reverse phase HPLC column. The product was eluted using paired-ion chromatography with phosphate buffer and tetrabutyl ammonium hydrogen sulfate (TBAHS) as the paired ion.<sup>91</sup> Under these conditions the UDPK elutes from the column with an  $\alpha$  value of 0.4 or essentially within the first 3 min after the UV indicates sample is eluting from the column. The partially purified sample

was then injected onto an analytical Zorbax Bonus RP column (amide-C14 instead of C18 backbone) and eluted again with the same paired-ion buffers. Co-injection of the semi-purified sample with standard UDPK indicates UDPK is being produced in the cell-free reactions. Also, a small amount of this product was collected and analyzed by  $^1\text{H}$  NMR. The NMR coincided with a standard UDPK  $^1\text{H}$  NMR sample.

In order to determine if the reverse reaction from UDPK to 3-ketoUDPG might give a higher yield, UDPK was synthesized from kanosamine 1-phosphate using UDPG pyrophosphorylase purified from DH5 $\alpha$ /pHS3.244 and inorganic pyrophosphorylase. The purified UDPK was obtained in 15% yield (Figure 24), with the low yield being due to loss of product during work-up. The UDPK was then treated with BL21 C $^+$  RP/pJG7.259a cell-free extract in the presence of PLP, NAD, MgCl $_2$ , and 2-oxoglutarate in an attempt to produce 3-ketoUDPG (Figure 24). No 3-ketoUDPG was produced. It is possible this reaction needs to be repeated using glutamate instead of 2-oxoglutarate.

**Figure 24. Preparation of UDPK and the reaction of UDPK with BL21 C $^+$  RP/pJG7.259a to produce 3-ketoUDPG.**



### **Optimization of RifK expression in *E. coli***

A series of experiments were performed to increase the yield of UDPK from 3-ketoUDPG using BL21 C<sup>+</sup> RP/pJG7.259a cell-free extract. In these experiments a variety of variables were tested: buffer, stabilizing agent, growth media, temperature, and pH (Table 9). Unfortunately, the yield was not significantly increased by more than a factor of 2 for any of the conditions tested. However, one experiment not shown (Table 9) was to omit NADH from the reaction mixture. This was done along side a control (containing NADH) at pH 8.5 and a temperature of 37°C. The reaction without NADH yielded a slightly higher yield of UDPK, 9%. This was an interesting result, which could indicate that NADH is not the reducing factor needed for the transamination catalyzed by RifK.

**Table 9. Optimization of RifK transamination of 3-ketoUDPG.**

Entry <sup>a</sup>	pH	Temp. (°C)	Media	Reaction Buffer	Additive <sup>b</sup>	% UDPK
1	7.5	30	LB	phosphate	PMSF	6
2	7.5	30	LB	MOPS	PMSF	11
3	7.5	30	LB	HEPES	PMSF	8
4	7.5	30	LB	Bis-Tris propane	PMSF	4
5	7.5	30	LB	EPPS (HEPPS)	PMSF	13
6	7.5	30	LB	Tris-HCl	PMSF	9
7	7.5	30	LB	PIPES	PMSF	7
8	7.5	30	LB	triethanolamine	PMSF	16
9	7.5	30	LB	triethanolamine	PMSF, EDTA	2
10	7.5	30	LB	triethanolamine	PMSF, DTT	12
11	7.5	30	LB	triethanolamine	PMSF, BSA	14
12	7.5	30	LB	triethanolamine	PMSF, EDTA, DTT, BSA	2
13	7.5	30	TB	MOPS	PMSF	5
14	7.5	30	YT	MOPS	PMSF	13
15	7.5	30	NZCYM	MOPS	PMSF	12
16	8.5	37	LB	triethanolamine	PMSF	6
17 <sup>c</sup>	8.5	37	LB	triethanolamine	PMSF	9

(a) Reaction conditions: 3-ketoUDPG, BL21 C<sup>+</sup> RP/pJG7.259a cell-free lysate, NADH, MgCl<sub>2</sub>, PLP, L-glutamine; (b) Additives were added to help stabilize enzymes in the cell-free lysate; <sup>c</sup> No NADH was added to this reaction

To further optimize the reaction conditions and improve the reaction yield, the temperature and pH were adjusted in varying combinations. According to Floss the

optimal assay conditions for heterologously expressed RifK are pH 8.5 and 37°C. Changing these conditions did not improve the reaction yield. The cofactor was also changed from PLP to PMP in an attempt to improve the yield. This also did not provide a significant improvement (Table 10).

**Table 10. Optimization of RifK transamination of 3-ketoUDPG.**

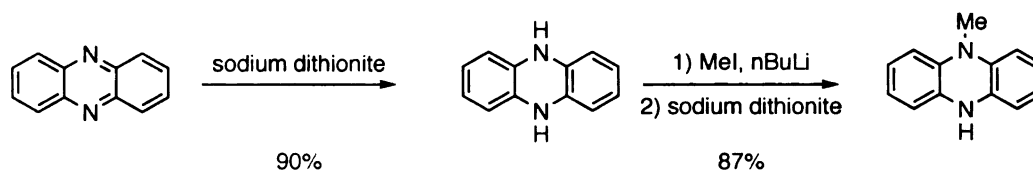
Entry <sup>a</sup>	pH	Temp. (°C)	Cofactor	Yield UDPK (%)
1	7.5	30	PLP	24
2	7.5	37	PLP	21
3	8.5	30	PLP	17
4	7.5	30	PMP	22
5 <sup>b</sup>	7.5	30	PMP	30

(a) All reactions contained BL21 C<sup>+</sup> RP/pJG7.259a cell-free lysate (cells cultured in YT medium), 3-ketoUDPG, RifK, MgCl<sub>2</sub>. Entries 1-4 contain glutamine; <sup>b</sup> Glutamine was omitted from this reaction.

Since it was discovered that NADH was not necessary for the conversion of 3-ketoUDPG to UDPK efforts were made to explore whether an alternative reducing agent could be used instead. It was thought that since NADH wasn't acting as a reducing agent there may be some other cofactor involved. Since phenazine methosulfate was a better oxidant than NAD for the oxidation of UDPG to 3-ketoUDPG, 5,10-dihydro-5-methyl phenazine (DHMP) (Figure 25) was synthesized to act as the reducing equivalent. DHMP was synthesized from phenazine by first reduction with sodium dithionite, followed by methylation with methyl iodide and *n*-BuLi with an overall yield of 78%. DHMP did not prove to be a useful reducing agent in the conversion of 3-ketoUDPG to UDPK as the yield decreased slightly (Figure 25).



**Figure 25. Preparation of DHMP.**



Sodium dithionite can be used in vitro to reduce FADH• to FADH<sub>2</sub>. Since the purified RifK is bright yellow in color it was thought that RifK might be an FAD requiring enzyme. In case RifK needs activation, sodium dithionite was added to the reaction (Table 11), however no increase in yield was observed. Adding either FAD or FMN with sodium dithionite also made no effect. Since PLP utilizing transaminases don't always require a reducing equivalent, it was determined at this point that a reducing equivalent may not be needed for this transamination.

**Table 11. Screening for RifK reducing equivalents.**

Entry <sup>a</sup>	Cofactors	Yield UDPK (%)
1	PLP, DHMP	13
2	PLP, Na <sub>2</sub> S <sub>2</sub> O <sub>4</sub>	17
3	PLP, Na <sub>2</sub> S <sub>2</sub> O <sub>4</sub> , FAD	16
4	PLP, Na <sub>2</sub> S <sub>2</sub> O <sub>4</sub> , FMN	17

(a) Each reaction contained 3-ketoUDPG, MgCl<sub>2</sub>, L-glutamine, and BL21 C<sup>+</sup> RP/pJG7.259a cell-free lysate in 50 mM triethanolamine buffer at pH 7.5 containing 1 mM PMSF and 10% w/v glycerol. Each reaction was run at 30°C for 8 h.

### Specific activity of RifK

The specific activity of heterologously expressed RifK was calculated using two separate assays. The first assay was used to measure the AHBA synthase activity of the heterologously expressed RifK and compare that activity with that reported by Floss. The generation of AHBA was followed over 60 min by measuring the absorbance at 296 nm when aminoSA was treated with the cell-free lysate of BL21 Codon Plus RP/pJG7.259a cells grown on YT medium. The measured AHBA synthase specific

activity was 0.0051  $\mu\text{mol}/\text{min}\cdot\text{mg}$ , which coincides with the reported crude AHBA synthase activity reported by Floss of 0.0052  $\mu\text{mol}/\text{min}\cdot\text{mg}$ .

The second assay was used to determine the transaminase activity of the heterologously expressed RifK. The specific activity was determined by following the formation of UDPK and the subsequent loss of 3-ketoUDPG using the same assay conditions used to measure the RifL specific activity. The measured transaminase specific activity of the crude cell-free extract, calculated over 120 min, was 0.0054  $\mu\text{mol}/\text{min}\cdot\text{mg}$  as determined for production of UDPK and 0.0051  $\mu\text{mol}/\text{min}\cdot\text{mg}$  as determined for the loss of 3-ketoUDPG.

### The source of nitrogen in *A. mediterranei* kanosamine biosynthesis

#### **Overview**

Upon demonstrating iminoE4P is derived via kanosamine biosynthesis and establishing a connection between kanosamine biosynthesis and the aminoshikimate pathway, attention turned toward elaborating the source of the aminoshikimate pathway's nitrogen atom. A previous report investigating the nitrogen source for rifamycin biosynthesis in *Nocardia mediterranei* U-32 indicated the amide nitrogen of glutamine would likely act as the donor. However, other PLP-dependent aminotransferases sharing homology with RifK and catalyzing similar reactions have been found to utilize L-glutamate as the nitrogen source.<sup>89,90,92</sup>

Through an experiment performed by another group member, the major components of the product mixture produced when UDPG was treated with dialyzed *A. mediterranei* cell-free lysate in the presence of NAD and L-glutamine were identified.

The byproducts of L-glutamine were found to be L-glutamic acid,  $\alpha$ -ketoglutaric acid and  $\alpha$ -ketoglutaramic acid. This would suggest the original theory was correct to indicate the amide nitrogen as the source.<sup>93</sup>

To further confirm the amide nitrogen as the source of nitrogen in the aminoshikimate pathway a series of  $^{15}\text{N}$  labeling experiments were performed by Jiantao Guo. Again using the dialyzed *A. mediterranei* cell-free lysate, UPDG was incubated with NAD in the presence of either [amine- $^{15}\text{N}$ ]-L-glutamine or [amide- $^{15}\text{N}$ ]-L-glutamine. The kanosamine produced was isolated, purified, and analyzed by HRMS to determine the enrichment of  $^{15}\text{N}$ . When [amine- $^{15}\text{N}$ ]-L-glutamine was used as the nitrogen source the kanosamine produced contained a  $^{15}\text{N}$  enrichment of 12%. When [amide- $^{15}\text{N}$ ]-L-glutamine was used as the nitrogen source the kanosamine produced contained 89%  $^{15}\text{N}$  enrichment (Table 12).<sup>94</sup>

#### **Investigation of the kanosamine biosynthetic nitrogen source using 3-ketoUDPG and heterologously expressed RifK**

With access to 3-ketoUDPG and the transaminase, RifK, the labeling study was repeated to help confirm that the nitrogen source was the amide nitrogen. 3-ketoUDPG was reacted with either [amide- $^{15}\text{N}$ ]-L-glutamine or [amine- $^{15}\text{N}$ ]-L-glutamine in the presence of PLP with the cell-free lysate of BL21 Codon Plus RP/pJG7.259a. The UDPK produced was analyzed by HRMS to determine the  $^{15}\text{N}$  incorporation. When [amide- $^{15}\text{N}$ ]-L-glutamine was used, as the nitrogen source the UDPK produced contained no  $^{15}\text{N}$ . When [amine- $^{15}\text{N}$ ]-L-glutamine was used as the nitrogen source, the UDPK contained 35%  $^{15}\text{N}$  incorporation (Table 12).

**Table 12.  $^{15}\text{N}$  enrichments in kanosamine produced using *A. mediterranei* cell-free lysate and in UDPK produced using BL21 C<sup>+</sup> RP/pJG7.259a cell-free lysate.**

Entry	Nitrogen Source	$^{15}\text{N}$ Enrichment in Kanosamine (%) <sup>a,c</sup>	$^{15}\text{N}$ Enrichment in UDPK (%) <sup>b,c</sup>
1	[amine- $^{15}\text{N}$ ]-L-glutamine	12	35
2	[amide- $^{15}\text{N}$ ]-L-glutamine	89	0

(a) Reaction conditions: UDPG,  $\beta$ -NAD, nitrogen source, *A. mediterranei* cell-free lysate pH 6.8 (after 6 cycles of dialysis); (b) Reaction conditions: 3-ketoUDPG, PLP, nitrogen source,  $\text{MgCl}_2$ , BL21 C<sup>+</sup> RP/pJG7.259a cell-free lysate, pH 6.8; (c)  $^{15}\text{N}$  enrichments were determined by electrospray mass spectrometry.

Due to the seemingly contradictory results between the different labeling experiments a series of experiments were performed to investigate the nitrogen source required for kanosamine biosynthesis using RifK as the aminotransferase. According to the previous results using *A. mediterranei* cell-free lysate when L-glutamine was replaced with L-glutamic acid, no UDPK should have been produced. However, UDPK was produced in 16% yield when 3-ketoUDPG was reacted with the cell-free lysate of *E. coli* BL21 Codon Plus RP/pJG7.259 cell-free lysate in the presence of PLP and L-glutamate (entry 2, Table 13). This result using L-glutamate as the nitrogen source was essentially equivalent to that produced when L-glutamine was used as the nitrogen source. When PLP was excluded from the reaction, the yield of UDPK dropped slightly to 12% (entry 3, Table 13). This is not necessarily surprising considering RifK is known to contain 0.6 mol PLP per mol of protein, and as such RifK should be able to catalyze the transamination without the addition of PLP. The yield of UDPK dropped significantly to 2% when neither nitrogen source was added. When neither nitrogen source nor PLP was added to the reaction the yield of UDPK again dropped to 2% (entries 4 and 5, Table 13). When the BL21 Codon Plus RP/pJG7.259 cell-free lysate was replaced with RifK

(purified from BL21 Codon Plus RP/pJG7.259) UDPK was produced in 8% yield in the presence of L-glutamic acid and PLP (Entry 6, Table 13). However, when L-glutamic acid was omitted the yield of UDPK dropped to 0% (Entry 7, Table 13).

The production of small amounts of UDPK when no nitrogen source was added to the reaction is presumably due to incomplete rinsing of the bacterial cells before lysis. Taken as a whole it appears RifK utilizes the  $\alpha$ -amine of glutamine, not the amide, in the transamination of 3-ketoUDPG to UDPK. This data is actually more consistent with that of other PLP-dependent transaminases sharing homology with RifK and catalyzing similar conversions.

The above results using heterologously expressed RifK seem to contradict those generated with the cell-free lysate of *A. mediterranei*. This contradiction may suggest another enzyme exists in the cell-free lysate of *A. mediterranei* that can also catalyze the transamination of 3-ketoUDPG to UDPK. The results with *A. mediterranei* cell-free lysate indicate this alternate transaminase could be acting as the dominant species catalyzing the transformation. This dominance could be the result of naturally higher aminotransferase specific activity or it could be that during extensive dialysis of the *A. mediterranei* cell-free lysate the specific activity of RifK drops significantly enough to limit its role in the transamination. Therefore, although RifK appears to use the  $\alpha$ -amine nitrogen of L-glutamine or L-glutamate, *A. mediterranei* can utilize either the amide or  $\alpha$ -amine nitrogen in the transamination of 3-ketoUDPG.

**Table 13. Nitrogen source and PLP dependence of the RifK catalyzed transamination of 3-ketoUDPG.**

Entry <sup>a,b</sup>	Nitrogen source <sup>c</sup>	PLP <sup>d</sup>	Yield UDPK (%)
1	L-glutamine	-	12
2	L-glutamic acid	+	16
3	L-glutamic acid	-	12
4	-	+	2
5	-	-	2
6 <sup>e</sup>	L-glutamic acid	+	8
7 <sup>e</sup>	-	+	0

(a) Reaction conditions: 3-ketoUDPG, MgCl<sub>2</sub>, nitrogen source (if added), PLP (if added), BL21 C<sup>+</sup> RP/pJG7.259a cell-free lysate; (b) bacterial cells were rinsed with 0.9% NaCl solution prior to lysis to remove contaminating nitrogen sources; (c) (-) indicates no nitrogen source was added to the reaction; (d) (+) indicates PLP was added to the reaction, (-) indicates PLP was omitted from the reaction. (e) Reactions were performed with RifK purified from BL21 C<sup>+</sup> RP/pJG7.259 cell-free lysate by Ni-NTA affinity chromatography.

#### Kanosamine biosynthesis through 3-ketoUDPG by *B. pumilus*

The *B. pumilus* cell-free lysate was prepared immediately prior to incubation of 3-ketoUDPG. *B. pumilus* cells were grown from a single colony at 28°C for 2 days with shaking in 4 L of a rich media containing peanut meal. Initially attempts were made to recover the bacterial cells by gentle centrifugation followed by scraping the cells carefully from the surface of the pellet. Later the process was improved by first filtering the cell culture through 5 layers of cheesecloth. The cell suspension obtained was then centrifuged to pellet the cells and any remaining peanut meal. The cells could be isolated easier as the cheesecloth removed the majority of the peanut meal. The collected cells were resuspended in a 50 mM Tris-HCl buffer at pH 7.5 containing 1 mM PMSF and 10% w/v glycerol. The cells were lysed by two passes through French pressure cell followed by centrifugation to remove cellular debris. The supernatant was used immediately for cell-free experiments.

When UDPG was treated with the cell-free lysate of *B. pumilus* in the presence of NAD and L-glutamine, kanosamine was produced in 7% yield. Kanosamine was produced in 3% yield when 3-ketoUDPG was treated with *B. pumilus* cell-free lysate in the presence of NADH, MgCl<sub>2</sub>, and L-glutamine. Unlike the reaction performed with *A. mediterranei* cell-free lysate the remaining 3-ketoUDPG was not reduced back to UDPG.

**Table 14. Reaction of [3-<sup>2</sup>H]-UDPG with *B. pumilus* cell-free lysate.**

Entry <sup>a</sup>	Co-factor	Yield Kanosamine (%)	% <sup>2</sup> H in Product
1	NAD	5	11
2	1:1 NAD/NADH	7	15

(a) Reaction conditions: [3-<sup>2</sup>H]-UDPG, L-glutamine, *B. pumilus* cell-free lyate.

As with *A. mediterranei* it was determined that treatment of [3-<sup>2</sup>H]-UDPG with the cell-free lysate of *B. pumilus* could aid in elucidating the mechanism of UDPG oxidation to 3-ketoUDPG. When [3-<sup>2</sup>H]-UDPG was incubated with NAD, L-glutamine, and *B. pumilus* cell-free lysate kanosamine was produced in 5% yield with a <sup>2</sup>H incorporation of 11% as determined by HRMS (Entry 1, Table 14). When [3-<sup>2</sup>H]-UDPG was treated with *B. pumilus* cell-free lysate in the presence of L-glutamine and a 1:1 mixture of NAD and NADH, kanosamine was produced in 7% yield containing 15% <sup>2</sup>H incorporation (Entry 2, Table 14). These results were quite the opposite of that obtained with *A. mediterranei* cell-free lysate.

As with *A. mediterranei* NADH trapping experiments were performed with *B. pumilus* cell-free lysate in an attempt to further determine the mechanism in which kanosamine is biosynthesized from UDPG. When UDPG was treated with *B. pumilus* cell-free lysate in the presence of NAD, L-glutamine, diaphorase and methylene blue, kanosamine was produced in 11% yield (Entry 3, Table 15). When UDPG was reacted

with *B. pumilus* cell-free lysate in the presence of NAD, L-glutamine, NH<sub>4</sub>OH, and 2-oxo-glutarate the yield of kanosamine produced increased to 19% (Entry 4, Table 15).

**Table 15. *B. pumilus* NADH trapping experiments.**

Entry	Reaction Conditions <sup>a</sup>	Yield Kanosamine (%)
1	NAD	7
2	NAD/NADH (1:1)	15
3	NAD, diaphorase, methylene blue	11
4	NAD, glutamate dehydrogenase, NH <sub>4</sub> OH, 2-oxoglutarate	19

(a) Reaction conditions: *B. pumilus* cell-free lysate, UDPG, L-glutamine.

### Discussion

In this chapter the intermediacy of 3-ketoUDPG during kanosamine biosynthesis from UDPG by both *A. mediterranei* and *B. pumilus* was investigated. The direct oxidation of UDPG at C-3 by *A. tumefaciens* provided 3-ketoUDPG. It has been demonstrated that both the cell-free lysate of *A. mediterranei*, and that of *B. pumilus* can produce kanosamine from 3-ketoUDPG.

The role of NAD in kanosamine biosynthesis was investigated for both *A. mediterranei* and *B. pumilus*. It was hypothesized that the NADH produced during the oxidation of UDPG to 3-ketoUDPG would be utilized as a reducing equivalent during the subsequent transamination to UDPK. The complete incorporation of <sup>2</sup>H into the kanosamine produced from [3-<sup>2</sup>H]-UDPG by the cell-free lysate of *A. mediterranei* suggested NADH is used during the transamination to form UDPK. This suggestion was elaborated by the lack of kanosamine produced during the NADH trapping experiments.



However later experiments using heterologously expressed RifL and RifK contradict this assumption. The RifL catalyzed oxidation of UDPG was found to utilize cofactors typically associated with FAD-dependent dehydrogenases such as G3DH from *A. tumefaciens*. The RifK catalyzed transamination of 3-ketoUDPG to UDPK did not require and was actually inhibited by the presence of NADH. The reason for this contradiction was not immediately apparent.

Unlike *A. mediterranei*, when the  $^2\text{H}$  labeling experiments were performed using the cell-free lysate of *B. pumilus* very little  $^2\text{H}$  was incorporated into the kanosamine produced. This result indicated that NADH is not utilized during the transamination of 3-ketoUDPG by the *B. pumilus* enzyme. This conclusion was further supported by the lack of effect on the yield of kanosamine when a 1:1 mixture of NAD/NADH was used in the reaction. The NADH trapping reagents also had no effect on the yield of kanosamine which lends further credence to the idea that *B. pumilus* does not directly recycle the NADH produced during the oxidation of UDPG. The isolation and sequencing of the *B. pumilus* dehydrogenase thought to be responsible for the oxidation of UDPG to 3-ketoUDPG by Jiantao Guo provided further clues to this process. The dehydrogenase itself was found to be FAD-dependent, not NAD-dependent. The NAD may be required as a cofactor for another enzyme utilized by the microbe to recycle the  $\text{FADH}_2$  produced during the oxidation back to FAD in order to regenerate the dehydrogenase. This process would actually mirror the process used by G3DH from *A. tumefaciens*.

Analyses of the enzymes, RifL and RifK, thought to be responsible for the oxidation of UDPG to 3-ketoUDPG and its subsequent transamination to UDPK were performed through their respective heterologous expression in *E. coli*. Using the *E. coli*

cell-free lysate containing RifL, it was found that RifL did catalyze the oxidation of UDPG to 3-ketoUDPG in the presence of DCIP and PMS. It was found also that heterologously expressed RifK was capable of catalyzing the transamination of 3-ketoUDPG to UDPK. It was found that RifK could catalyze the transamination in the presence of PLP or PMP, but did not require the exogenous addition of either. This result is understandable considering the report by Floss that RifK contains 0.6 mol of PLP per mol of enzyme.

Once it was confirmed that RifK could act as the enzyme responsible for the transamination of 3-ketoUDPG to UDPK efforts turned toward identifying the source of the *A. mediterranei* aminoshikimate pathway's nitrogen atom. Previous results obtained with the cell-free lysate of *A. mediterranei* suggested the amide nitrogen of L-glutamine was incorporated into the kanosamine produced.  $^{15}\text{N}$  labeling experiments with heterologously expressed RifK displayed a slight preference for incorporation of the  $\alpha$ -amine nitrogen of L-glutamine into the produced kanosamine. The finding that RifK could utilize L-glutamate as a nitrogen source further implicated the  $\alpha$ -amine as the nitrogen source, not the amide of L-glutamine.

Clearly the experiments performed using the cell-free lysate of *A. mediterranei* indicate the amide nitrogen of L-glutamine as the source for the aminoshikimate pathway's amine nitrogen, while the experiments with heterologously expressed RifK implicate the  $\alpha$ -amine nitrogen of L-glutamine or L-glutamate as the source. This apparent contradiction mirrors the contradiction introduced when the earlier  $^2\text{H}$  labeling results using  $[3\text{-}^2\text{H}]\text{-UDPG}$  indicated  $[^2\text{H}]\text{-NADH}$  was used by *A. mediterranei* for the transamination of 3-ketoUDPG resulting in  $[3\text{-}^2\text{H}]\text{-kanosamine}$ . It was later realized

RifK does not require and is inhibited by the presence of NADH. Another possible contradiction was found seeing that Floss insinuated RifL and RifK might form a complex *in vivo* while experiments performed by Jiantao Guo using a Bacteriomatch-two-hybrid system indicate no interaction between these two proteins. Taken as a whole, it seems the contradiction is likely due to a difference in the systems involved. RifK catalyzes both the transamination of 3-ketoUDPG to UDPK and the isomerization of aminoDHS to AHBA. The RifK-catalyzed transamination requires a nitrogen source, L-glutamate or L-glutamine, but does not require NADH or complex formation with RifL.

The most probable explanation for the opposite results obtained using the dialyzed cell-free lysate of *A. mediterranei* and the heterologously expressed RifK is that at least one other enzyme exists within the *A. mediterranei* cell, which can catalyze this transamination. Through extensive dialysis of the *A. mediterranei* cell-free lysate, RifK is most likely deactivated to some degree thereby allowing the characteristics of another transaminase to surface in the experimental results. A possible candidate for the other transaminase is the gene product of *orf9*, which is homologous to the transaminase YokM from *B. subtilis* (Table 1). The gene product of *orf9* was originally eliminated as a candidate for involvement in kanosamine biosynthesis due to the gene deactivation experiments performed by Floss and coworkers, which indicated that the deactivation of *orf9* had no effect on AHBA production. It should be taken into consideration that the gene deactivation experiments were performed by analyzing the level of AHBA observed in the culture supernatant of *A. mediterranei* mutants grown on a rich media. Also, we now know that RifK can act as the aminotransferase catalyzing the production of UDPK from 3-ketoUDPG, so deactivation of one aminotransferase in the presence of another

would quite reasonably have no effect on the production of AHBA, especially under rich conditions when any necessary co-factors should be present. This is especially logical since these whole cell experiments could not indicate whether RifK is necessary for the transamination of 3-ketoUDPG as RifK is known to catalyze the formation of AHBA, a later step in AHBA biosynthesis. Because Floss and co-workers were analyzing AHBA production, any lack of AHBA formation using a mutant of *A. mediterranei* where *rifK* is deactivated only indicates RifK is required for AHBA biosynthesis. This method does not indicate whether or not RifK is required at any step earlier than the production of AHBA from aminoDHS.

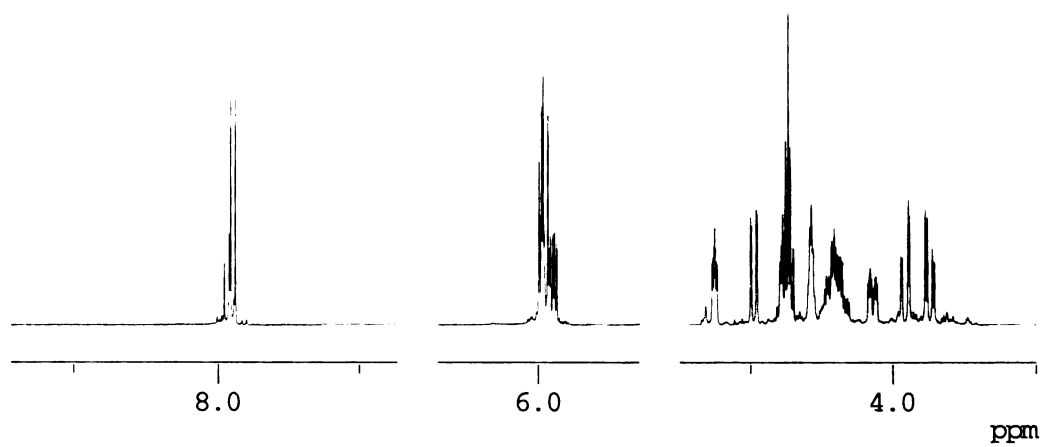


**Figure 26. <sup>1</sup>H NMR spectrum of 3-ketoUDPG produced by the oxidation of UDPG by *A. tumefaciens*.**

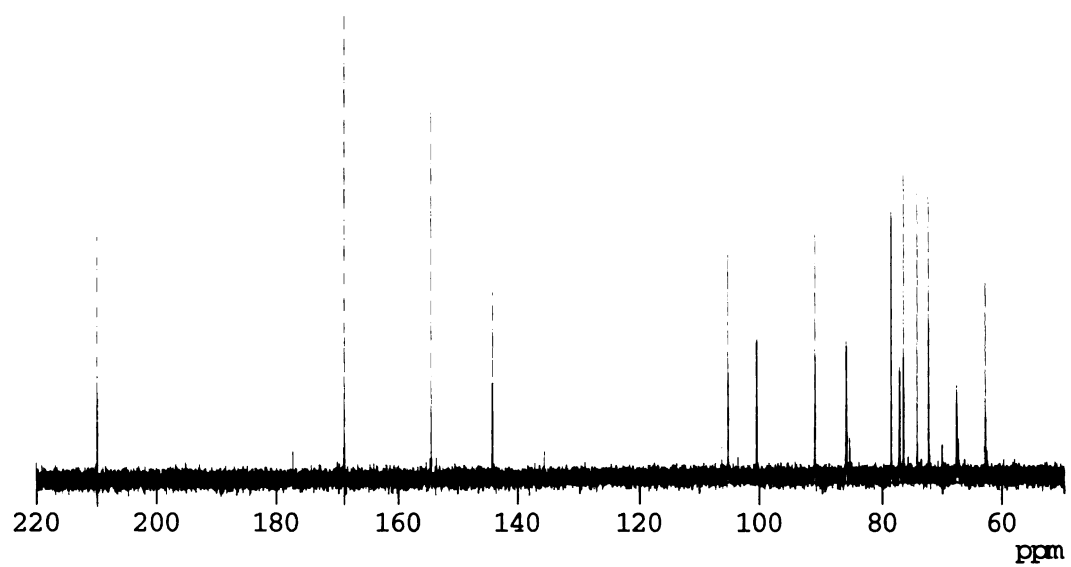


**Figure 27.  $^{13}\text{C}$  NMR spectrum of 3-ketoUDPG produced through the oxidation of UDPG by *A. tumefaciens*.**

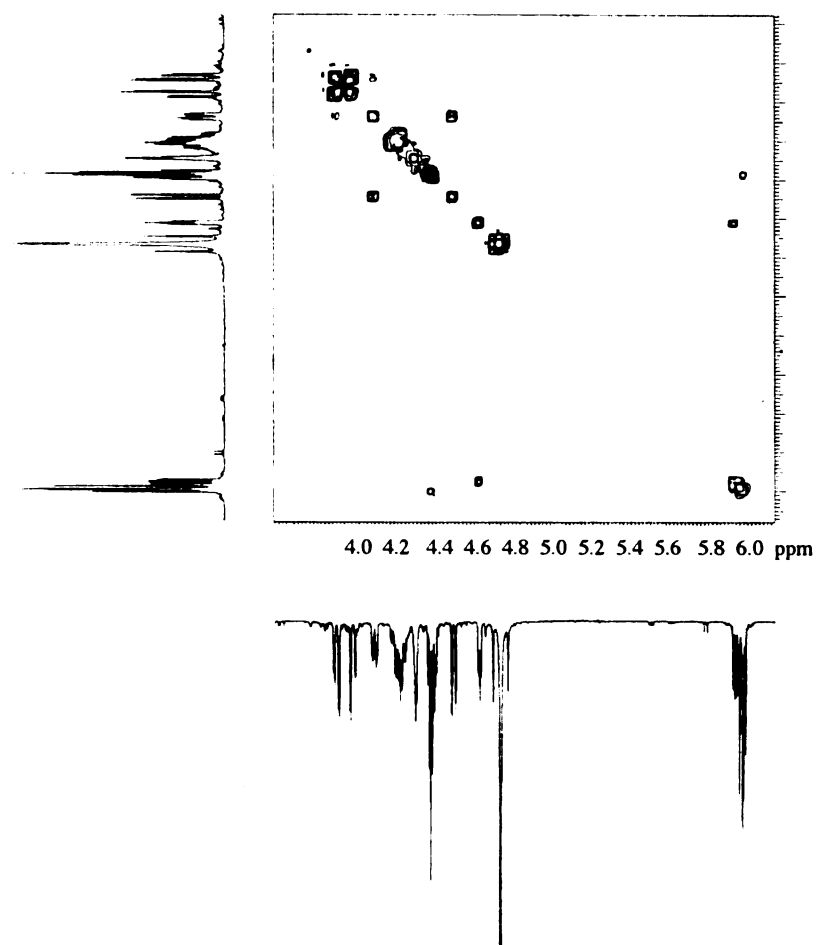


**Figure 28.** 2D-COSY spectrum of 3-ketoUDPG produced by *A. tumefaciens*.

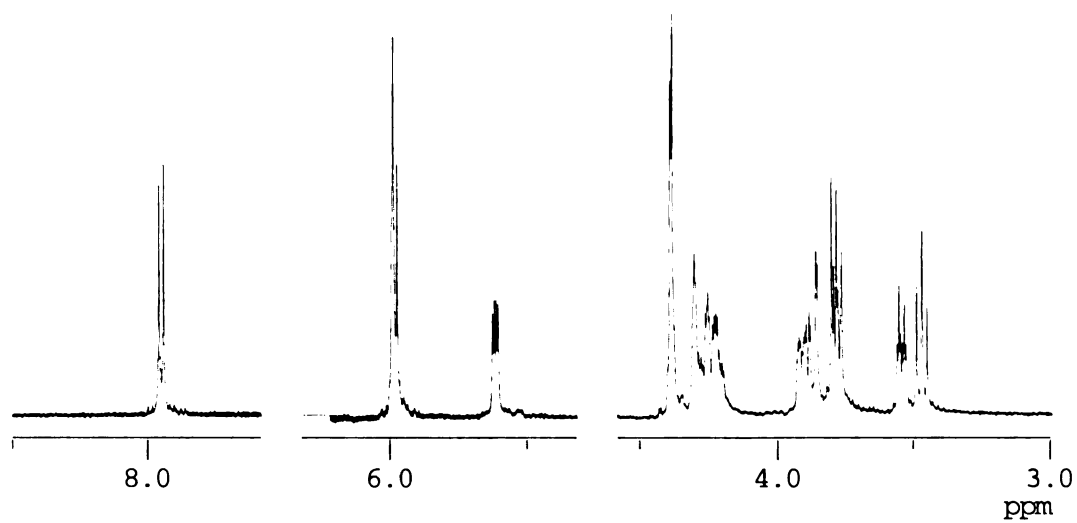


**Figure 29. Standard <sup>1</sup>H NMR spectrum of UDPG.**



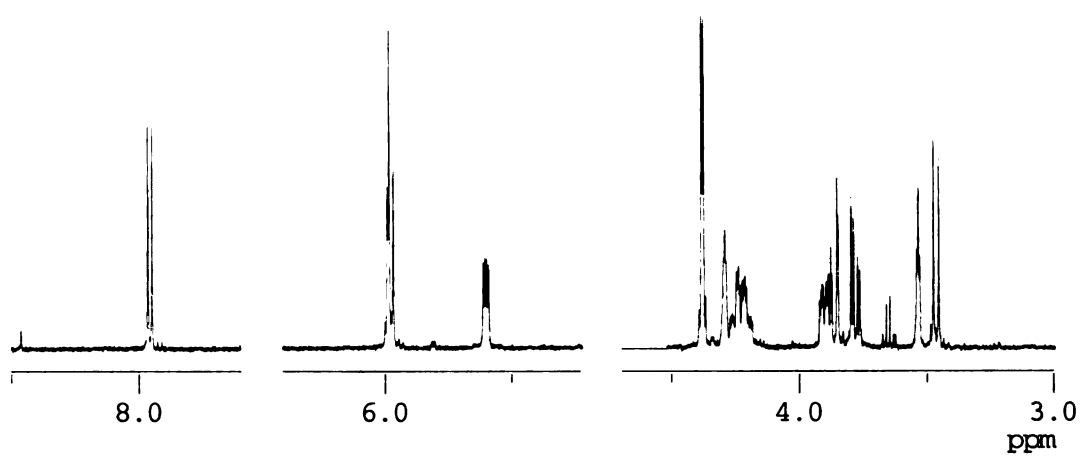


**Figure 30.  $^1\text{H}$  NMR spectrum of  $[3\text{-}^2\text{H}]\text{-UDPG}$ .**

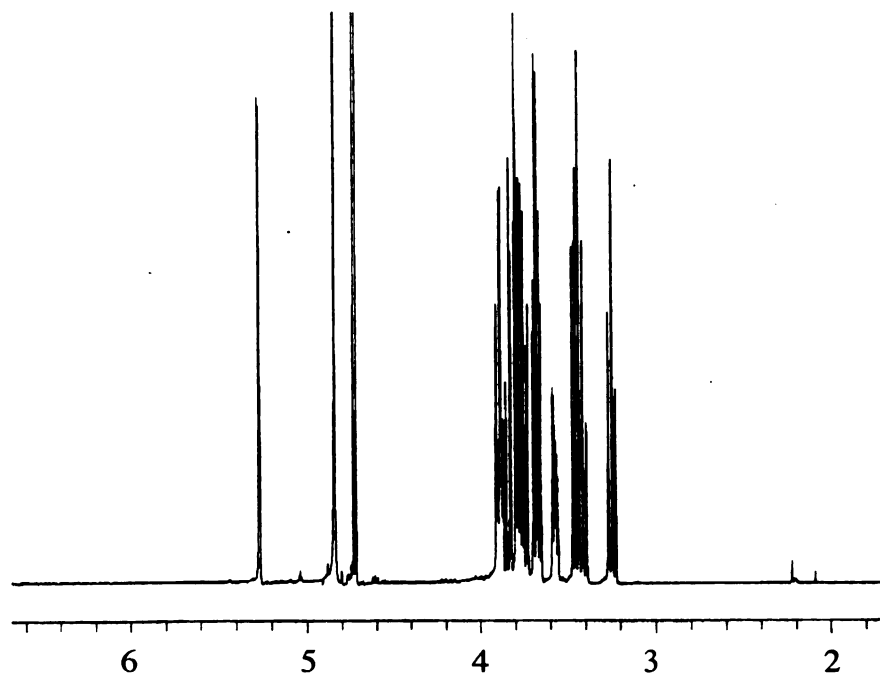


**Figure 31.**  $^1\text{H}$  NMR spectrum of kanosamine.

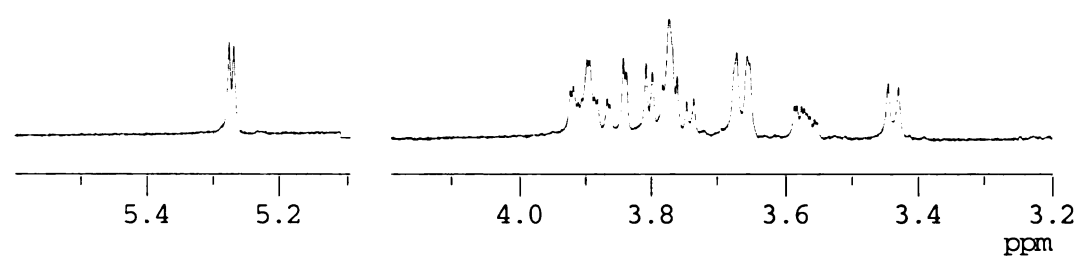


**Figure 32.**  $^1\text{H}$  NMR spectrum of [3- $^2\text{H}$ ]-kanosamine.

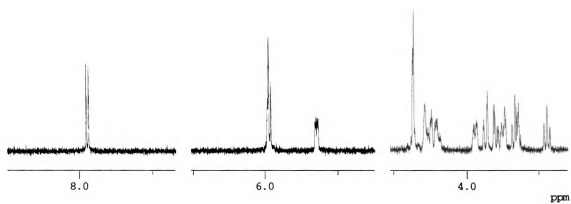


**Figure 33.**  $^1\text{H}$  NMR spectrum of UDPK.

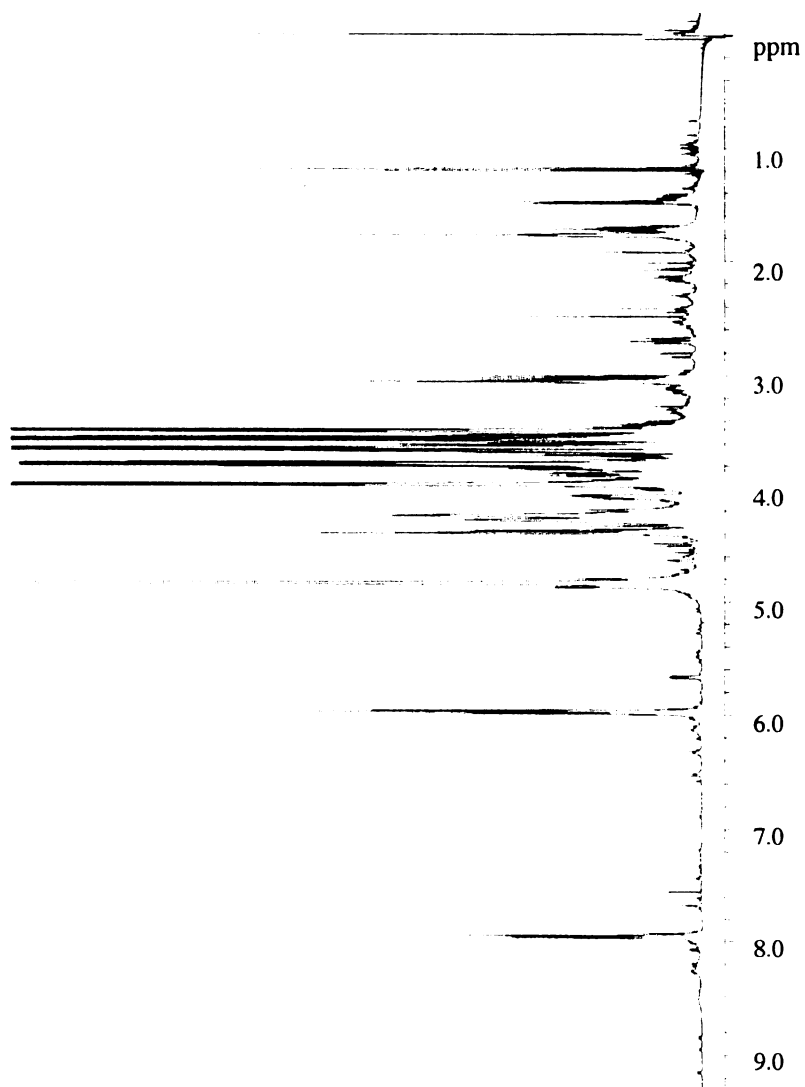


**Figure 34.  $^1\text{H}$  NMR of the crude product mixture obtained upon the RifK catalyzed transamination of 3-ketoUDPG.**

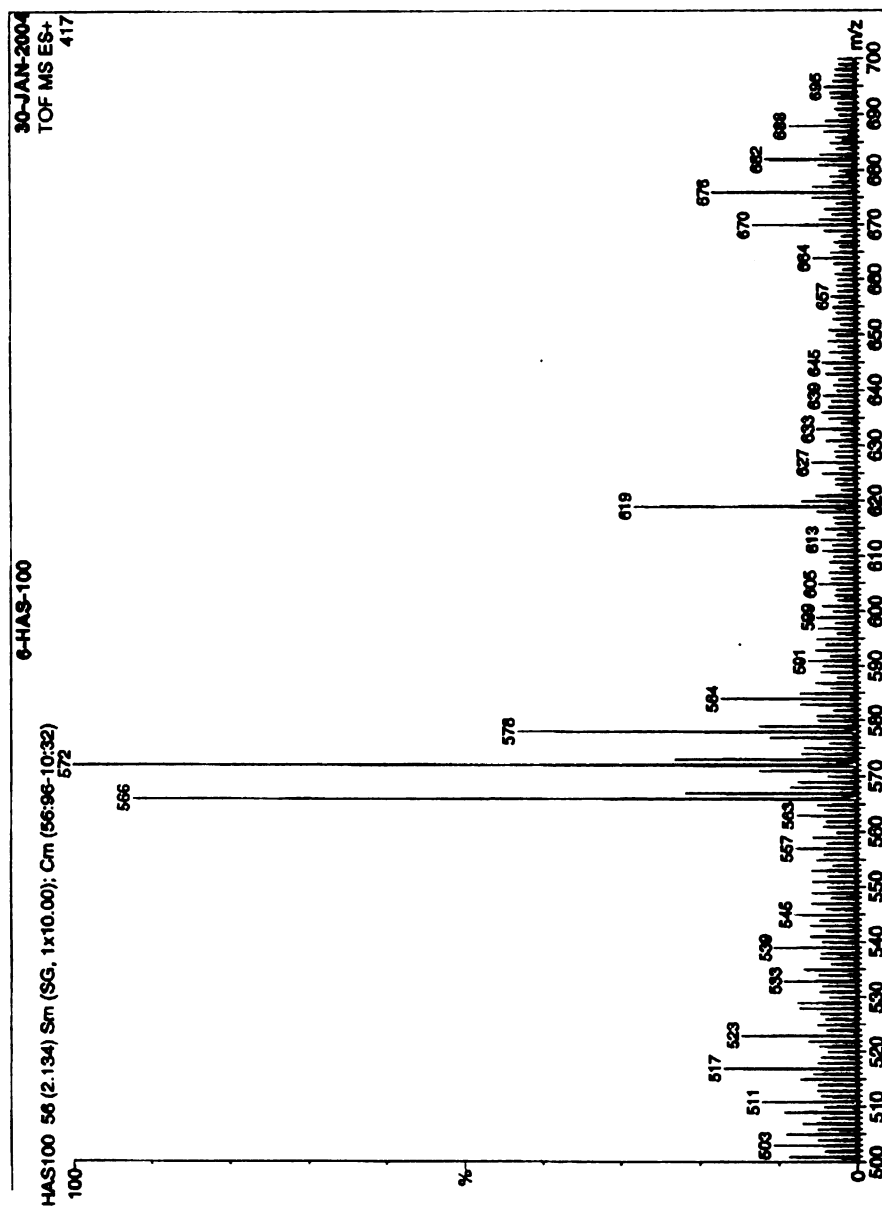


**Figure 35. Mass Spectrum of UDPK produced from the RifK catalyzed transamination of 3-ketoUDPG in the presence of L-glutamine.**

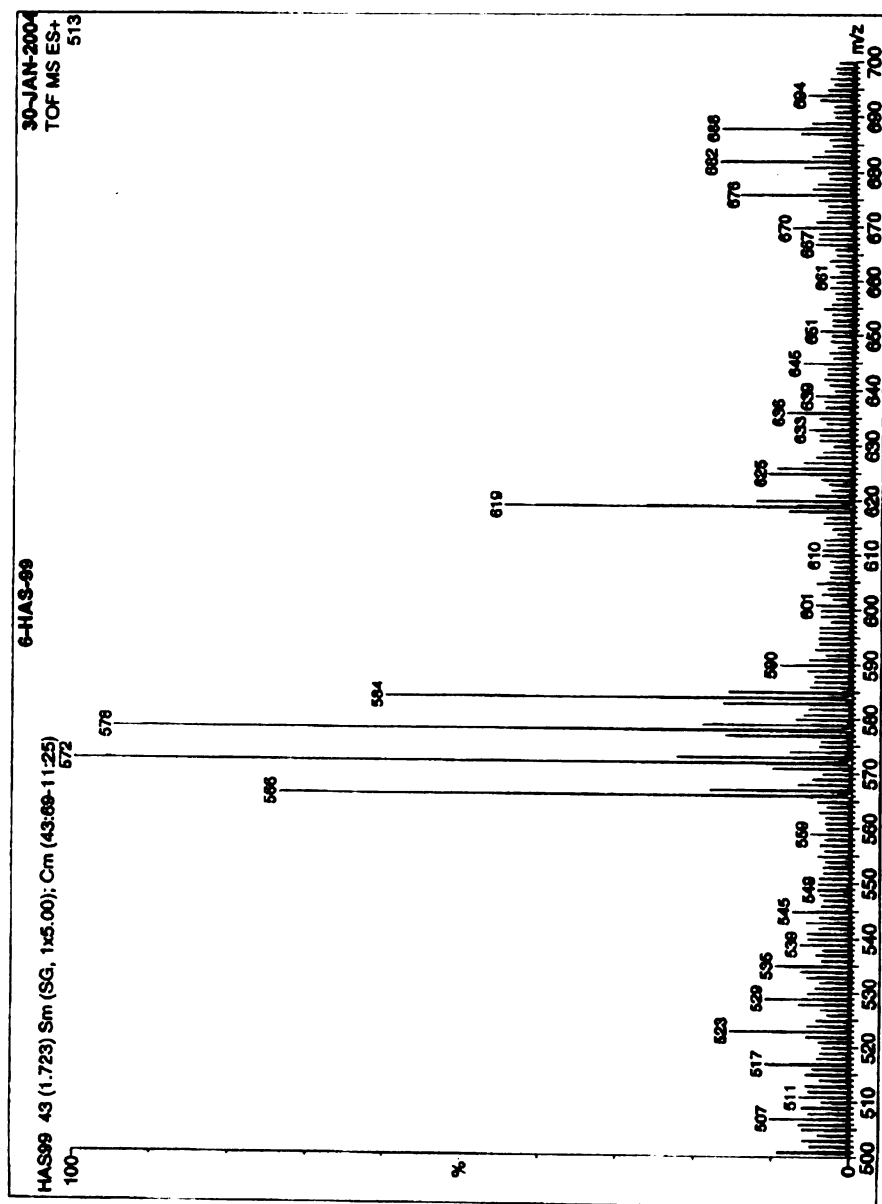


**Figure 36. Mass Spectrum of UDPK produced from the RifK catalyzed transamination of 3-ketoUDPG in the presence of [amide-<sup>15</sup>N]-L-glutamine.**

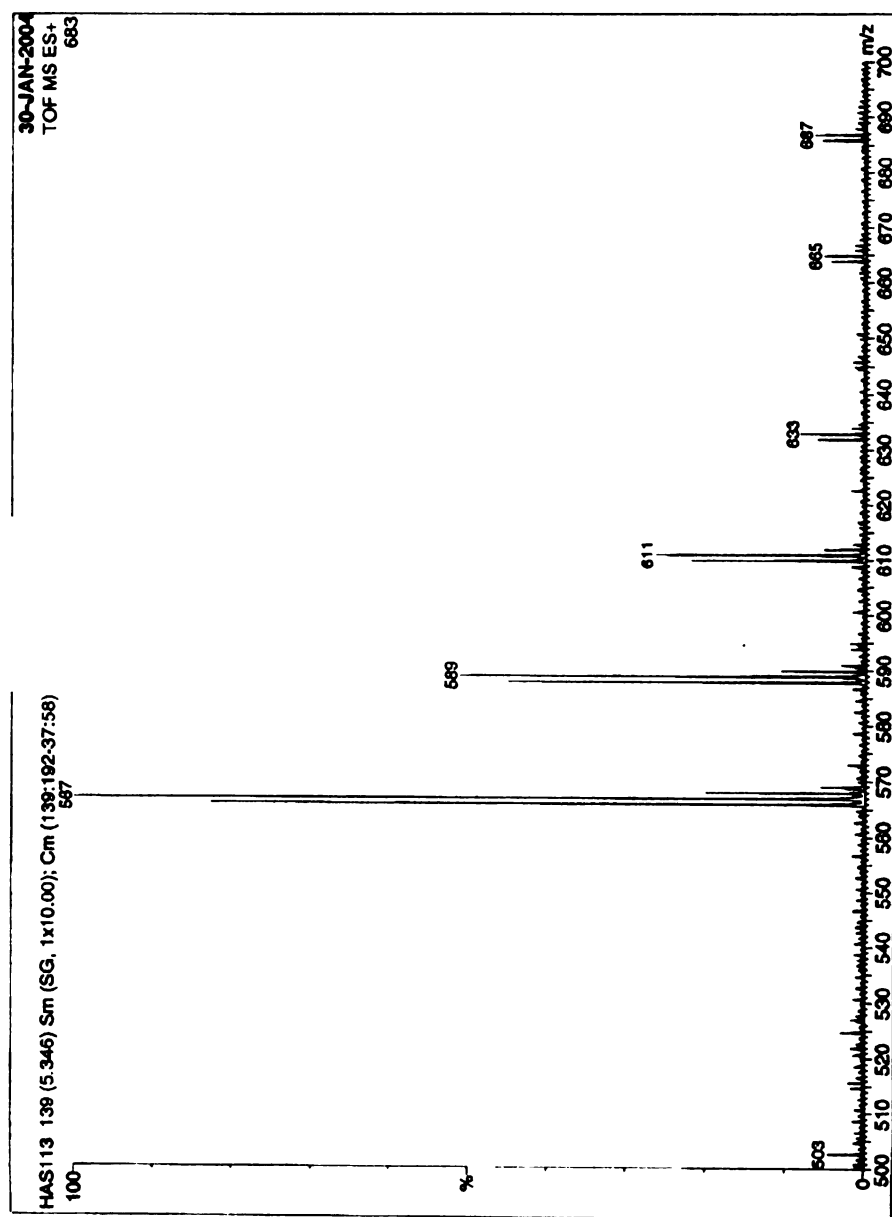


**Figure 37. Mass Spectrum of UDPK produced upon the RifK catalyzed transamination of 3-ketoUDPG in the presence of [alpha-<sup>15</sup>N]-L-glutamine.**



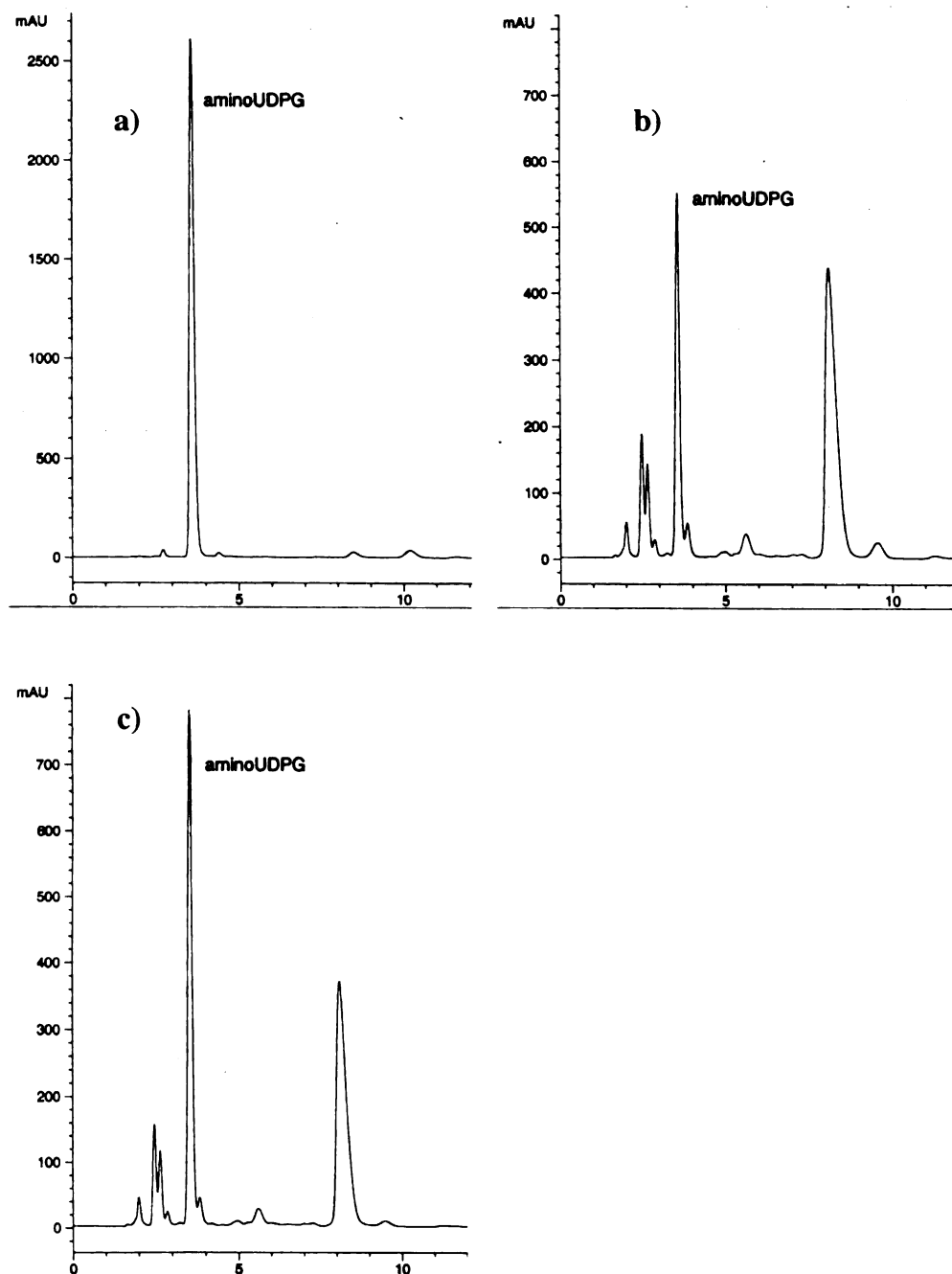


**Figure 38. HPLC analysis of UDPK produced by the RifK catalyzed transamination of 3-ketoUDPG.**

a) Standard: synthesized UDPK (3.5 min).; b) Sample taken from the reaction of 3-ketoUDPG with BL21 Codon Plus RP/pJG7.259 cell-free lysate in the presence of PLP and L-glutamine.; c) Co-injection of standard UDPK sample and a sample from the same reaction as shown in B. All three samples were eluted by the increase in  $\text{CH}_3\text{CN}$  using a 50 mM  $\text{Na}_2\text{HPO}_4$  buffer (pH 6.9) containing TBAHS as a paired ion. In B and C *p*-hydroxybenzoic acid (8.0 min) was added to the reaction sample as an internal standard for quantification.

## CHAPTER THREE

# **3-DEHYDROQUINATE BIOSYNTHESIS VIA THE ARCHAEAL SHIKIMATE PATHWAY OF METHANOCALDOCOCCLUS JANNASCHII**

### Introduction

The common pathway of aromatic amino acid biosynthesis, termed the shikimate pathway (Figure 1), in eukarya and eubacteria is well known where the genes, enzymes, and intermediates have been studied extensively.<sup>1</sup> In archaeal methanogens, however, this pathway is not fully understood. Early <sup>13</sup>C labeling experiments indicate E4P may not be a precursor to aromatic amino acid biosynthesis by some *Archaea*.<sup>95</sup> This suggestion was further supported by the discovery that among some archaeal methanogens, several shikimate pathway enzymes could not be identified.<sup>63</sup> In *Methanocaldococcus jannaschii* the first two enzymes of the pathway, DAHP synthase and DHQ synthase, are “missing”.<sup>59</sup> DAHP synthase catalyzes the condensation of E4P and PEP to form DAHP. The DAHP is then isomerized to DHQ by the action of DHQ synthase (Figure 1). Although DHQ has been identified as an intermediate in the archaeal shikimate pathway of *M. jannaschii*, several common intermediates, including DAHP, E4P, PEP, and pyruvate, were eliminated as precursors of DHQ biosynthesis by *M. jannaschii*.<sup>66</sup> These discoveries all promote a theory that the early steps of the shikimate pathway in these archaeal methanogens may vary utilizing different precursors and enzymes.

During early studies of the shikimate pathway in *Eukarya*, DDTH was considered as a possible precursor to DHQ.<sup>68</sup> Although DDTH was eliminated as a precursor in the common shikimate pathway, Frost proposed that DDTH could be the precursor to DHQ biosynthesis by the novel archaeal shikimate pathway. He suggested DDTH could be produced by the condensation of hydroxyacetone and oxaloacetaldehyde. The DDTH produced could then cyclize either spontaneously or enzymatically to form DHQ (Figure 39). Another possible source of DHQ would be through the condensation of L-aspartate semialdehyde (ASA) and either hydroxyacetone or some other precursor to form ATTH, which could then be converted to DDTH through transamination (Figure 41).

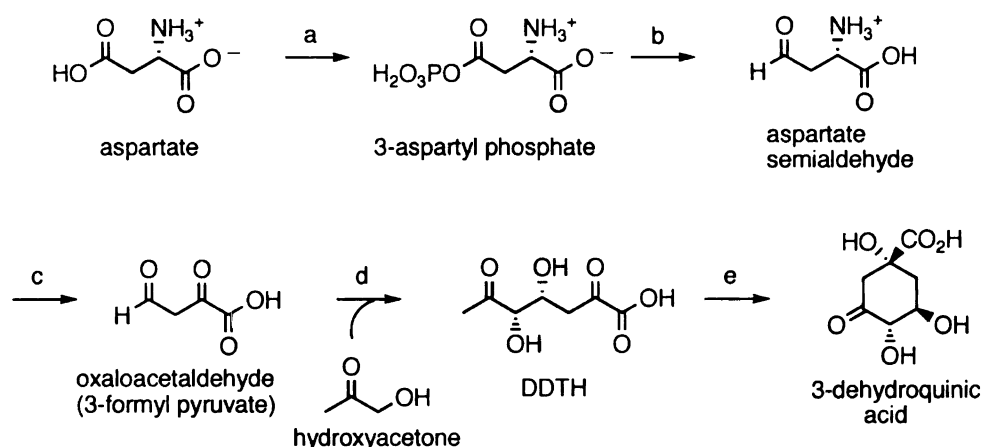


**Figure 39. Early proposal by Frost for alternate DHQ biosynthetic precursors.**

Enzymes: (a) aspartate kinase; (b) aspartate semialdehyde dehydrogenase; (c) amino acid aminotransferase; (d) putative aldolase MJ0400; (e) putative aldolase MJ1249.

It is important to note how the above biosynthetic route proposed by Frost would relate to the <sup>13</sup>C labeling patterns of the aromatic amino acids observed using various archaeal methanogens (Figure 40). First, aspartic acid or oxaloacetaldehyde would likely be prepared biosynthetically from oxaloacetate. As is the case of some archaeal methanogens oxaloacetate would be produced via a reductive, incomplete TCA cycle.

By the reductive TCA cycle, pyruvate is produced from the condensation of CO<sub>2</sub> and acetyl CoA (acetate). Pyruvate is then condensed with CO<sub>2</sub> to form oxaloacetate. Hydroxyacetone would likely be prepared by the cleavage of a hexose or the reduction of pyruvate. Based on the probable biosynthesis of oxaloacetate and hydroxyacetone from [1-<sup>13</sup>C]-pyruvate, [1-<sup>13</sup>C]-acetate, and [2-<sup>13</sup>C]-acetate, the expected labeling patterns of the intermediate DDTH, DHQ, and the aromatic amino acids L-tyrosine and L-tryptophan were predicted as seen in Figure 40. An important point of this prediction is that the predicted labeling patterns of the aromatic amino acids via Frost's proposed route mirror the labeling patterns observed using varying archaeal methanogens.

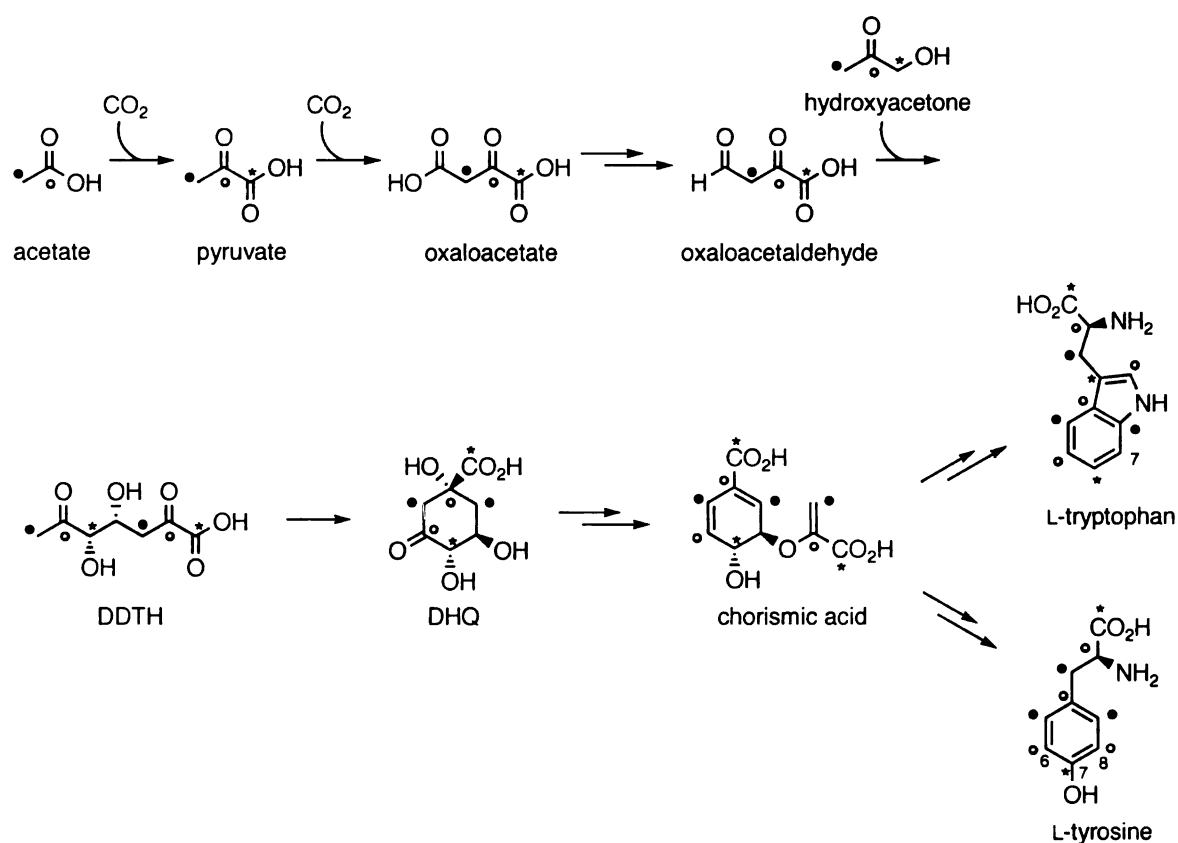


**Figure 40. Predicted <sup>13</sup>C labeling patterns of tyrosine and phenylalanine from acetate and pyruvate through the DHQ biosynthetic route proposed by Frost.**

The indicated labeling patterns were predicted based on the known biosynthesis of oxaloacetate, pyruvate, and hexoses from acetate and pyruvate by archaeal methanogens. Label key: (\*), [1-<sup>13</sup>C]-pyruvate; (o), [1-<sup>13</sup>C]-acetate; (•), [2-<sup>13</sup>C]-acetate.

In order to establish the precursors to this archaeal shikimate pathway, White performed a series of experiments with *M. jannaschii* cell-free lysate as well as two novel aldolases, MJ0400 and MJ1249.<sup>66</sup> MJ0400 and MJ1249 were identified by their genetic proximity to shikimate biosynthetic enzymes. The results of these experiments led White to propose a hypothetical pathway for DHQ biosynthesis in *M. jannaschii* (Figure 41). White proposed DHQ biosynthesis occurs through first the condensation of L-aspartate semialdehyde (ASA) and another intermediate, 6-deoxy-5-ketofructose 1-phosphate (DKFP), to form the amino acid intermediate ATTH by MJ0400. This condensation would be followed by the MJ1249 catalyzed reductive transamination of ATTH to form DDTH. Also under the influence of MJ1249, DDTH was proposed to cyclize producing DHQ (Figure 41).

Prior to the start of research toward this thesis the condensation of ASA and DKFP as described by White had not been confirmed. Also the intermediate ATTH had not been synthesized or demonstrated to be a precursor to DDTH biosynthesis by MJ1249. The possible intermediacy of oxaloacetaldehyde also has not been explored.

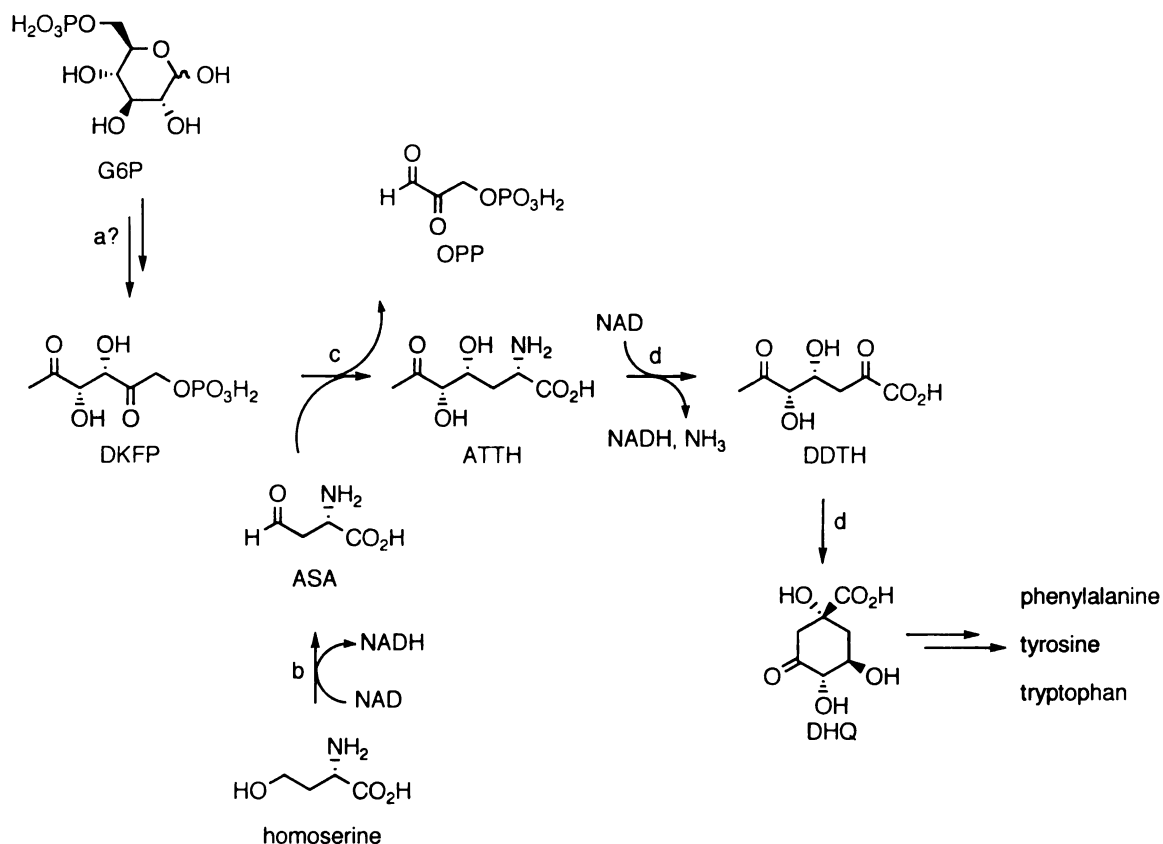


**Figure 41. Hypothetical *M. jannaschii* biosynthetic route to DHQ proposed by White.**

Enzymes: (a) MJ1055; (b) MJ1602; (c) MJ0400; (d) MJ1249. Abbreviations: G6P, glucose-6-phosphate; DKFP, 6-deoxy-5-ketofructose 1-phosphate; ASA, L-aspartate semialdehyde; ATTH, 2-amino-2,3,7-trideoxy-6-oxo-4,5-D-threo-heptanoic acid; DDTH, 3,7-dideoxy-D-threo-hepto-2,6-diulosonic acid; DHQ, 3-dehydroquinic acid.

This chapter will address attempts to verify the likelihood that DHQ biosynthesis by *M. jannaschii* proceeds through the intermediacy of ASA/DKFP and ATTH. The preparation of ASA and its subsequent reaction with DKFP in the presence of MJ0400 will be discussed first. A discussion of various attempts to prepare the proposed intermediate ATTH will follow.

### L-Aspartate semialdehyde intermediacy

Early attempts to provide evidence for or against White's proposal for DHQ biosynthesis centered on the condensation of DKFP and ASA using MJ0400. Since

neither compound is commercially available, each needed to be prepared synthetically or enzymatically from available materials. Once prepared attempts were made to condense DKFP and ASA using MJ0400 (heterologously expressed from *E. coli*), and identify any products produced.

### Preparation of ASA

Several syntheses of ASA from aspartic acid and other materials have been reported,<sup>96</sup> the ozonolysis of L-allyl glycine appears to be the most popular method of ASA preparation. L-Allyl glycine is unfortunately prohibitively expensive, so it was determined the L-form could be isolated from the much less expensive DL-allyl glycine. Racemic allyl glycine was purchased and reacted with acetic anhydride and sodium hydroxide to produce *N*-acetyl allyl glycine in 90% yield. The L-allyl glycine was then isolated in 39% yield by selective deacylation of the *N*-acetyl-L-allyl glycine with porcine kidney acylase (Figure 42).

The prepared L-allyl glycine was then oxidized to ASA through ozonolysis at 0°C in 1 N HCl (Figure 42). ASA is known to be very unstable and could not be isolated or analyzed by <sup>1</sup>H NMR analysis. To analyze ASA the reaction was performed in 1 N HCl in D<sub>2</sub>O to avoid destruction of the ASA upon reaction work-up, however no ASA was observed in the product mixture.

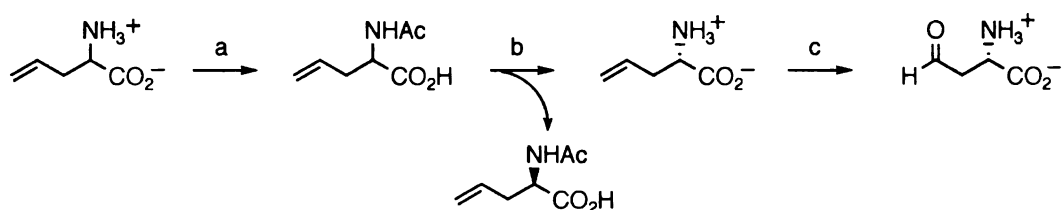


**Figure 42. Preparation of ASA from racemic allyl glycine.**

Reaction Conditions: (a)  $\text{Ac}_2\text{O}$ ,  $\text{NaOH}$ , 0°C, 90%; (b) porcine kidney acylase, pH 7.9, 37°C, 36% L-form; (c)  $\text{O}_3$ , 1 N HCl, 0°C.

Since ozonolysis using the free L-allyl glycine could not be confirmed, it was thought ozonolysis of a protected derivative might provide an indication of whether the aldehyde was being formed. Ozonolysis of the *N*-acetyl-DL-allyl glycine also failed to yield stable material for  $^1\text{H}$  NMR analysis. The *N*-acetyl-DL-allyl glycine was protected further using diazomethane at  $0^\circ\text{C}$  to yield the methyl ester in quantitative yield. Ozonolysis of this fully protected olefin followed by dimethyl sulfide quench provided a 1:1.8 mixture of the aldehyde and the dimethyl acetal respectively. Attempts to cleave the dimethyl acetal and recover the aldehyde using either IR-120 ( $\text{H}^+$  form) cation exchange resin or *p*-toluenesulfonic acid failed.

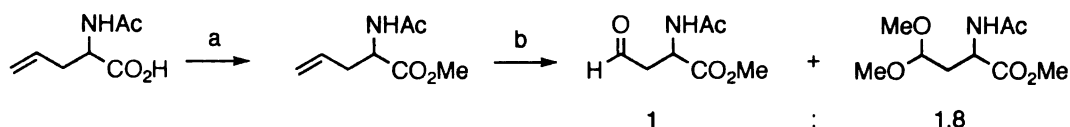


**Figure 43. Ozonolysis of Protected allyl glycine.**

Reaction conditions: (a)  $\text{CH}_2\text{N}_2$ , EtOAc,  $\text{Et}_2\text{O}$ ,  $0^\circ\text{C}$ , 96%; (b) *i.*  $\text{O}_3$ ,  $\text{CH}_2\text{Cl}_2/\text{MeOH}$  (4:1),  $-78^\circ\text{C}$ , *ii.*  $(\text{CH}_3)_2\text{S}$ .

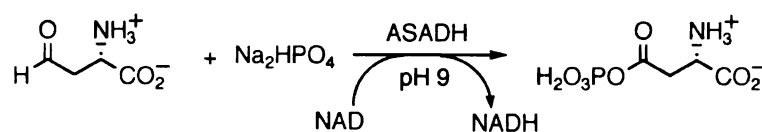
Since it was determined the ozonolysis reaction was working efforts again turned toward the preparation of the unprotected aldehyde. The reaction of L-allyl glycine was attempted again using EtOH as the solvent instead of water so the reaction could be cooled to  $-78^\circ\text{C}$  instead of  $0^\circ\text{C}$ . The reaction was quenched by the addition of zinc powder and acetic acid. Again the product could not be isolated for spectral confirmation, so an attempt was made to prepare the dinitrophenyl hydrazone. The ozonolysis product was treated with dinitrophenyl hydrazine, however none of the desired hydrazone was observed.

Another method, which could confirm the production of ASA upon ozonolysis of L-allyl glycine, was to assay for aspartate semialdehyde dehydrogenase (ASADH)



activity. The assay would also provide a method for quantifying the concentration of ASA in the product mixture. ASADH catalyzes the conversion of L-aspartyl phosphate to ASA and phosphate in the presence of NADH.<sup>97</sup> The gene encoding ASADH, *asd*, was amplified by PCR from *E. coli* W3110 genomic DNA and inserted into pJG7.246 ( $T_5$ , *lacO*, *lacO*, 6 *x his*, *lacI<sup>r</sup>*, Amp<sup>r</sup>) to provide the plasmid pHS7.098 ( $T_5$ , *lacO*, *lacO*, 6 *x his*, *asd*, *lacI<sup>r</sup>*, Amp<sup>r</sup>). The plasmid pHS7.098 was transformed into DH5 $\alpha$  competent cells. The production of ASADH was induced by the addition of IPTG to 0.1 mM at OD<sub>600</sub> = 0.6. The ASADH was purified by affinity chromatography using Ni<sup>2+</sup>-NTA resin. The presence of ASADH was verified by SDS-PAGE analysis. Using ASA produced from the ozonolysis of L-allyl glycine, the ASADH activity was determined by following the increase in NADH concentration at A<sub>340</sub> in the presence of phosphate. The specific activity of ASADH was measured to be 1.0 U/mg, where one unit was equivalent to 1  $\mu$ mol NADH produced per minute. The ASADH produced was stored at -20°C in 200  $\mu$ L aliquots to be thawed and used as needed.

**Figure 44. ASADH activity assay.**



### Preparation of DKFP

DKFP was prepared by Jiantao Guo through the condensation of DHAP and methylglyoxal. DHAP was first prepared as described by Whitesides through the enzymatic phosphorylation of DHA by glycerol kinase (GK) in the presence of ATP. In order to shift the reaction equilibrium toward product formation the ADP produced during the phosphorylation was recycled back to ATP by the action of pyruvate kinase

(PK) in the presence of PEP to form pyruvate.<sup>98</sup> DKFP was then prepared following the method of Kuchel where DHAP was condensed with methylglyoxal using RAMA.<sup>99</sup> The DKFP was isolated after purification by anion exchange chromatography. The yield of 20% was estimated based on <sup>1</sup>H NMR resonances.

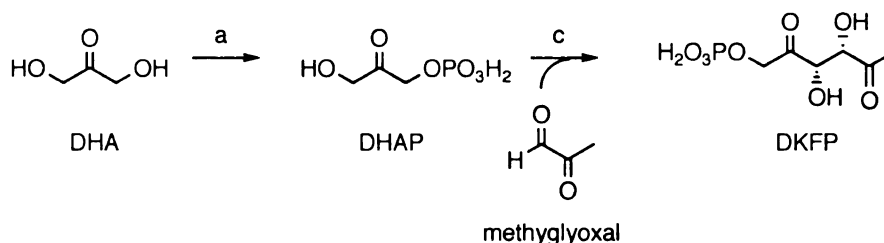


**Figure 45. Preparation of DKFP.**

Reaction conditions: (a) glycerol kinase, pyruvate kinase, ATP, PEP, 73%; (b) Rabbit muscle aldolase, methylglyoxal, 20%.

**Preparation of MJ0400.**

MJ0400 was obtained through the heterologous expression of *mj0400* in *E. coli*. The desired plasmid, pMJ0400 (*T7*, *mj0400*, Amp<sup>r</sup>), was obtained from White. The plasmid, MJ0400, was then transformed into BL21 Codon Plus (DE3) RIL competent cells obtained from Strategene. BL21 Codon Plus (DE3) RIL cells contain additional tRNA codons to compensate for the higher percentage of A and T in the *M. jannaschii* genome over that of *E. coli*. Expression of *mj0400* was induced by the addition of lactose at OD<sub>600</sub> = 1.0. After induction the cells were incubated at 28°C an additional 6 h, before being harvested by centrifugation. The cells were resuspended in degassed 50 mM phosphate buffer at pH 7.0 and lysed by two passes through a French pressure cell. After removal of cellular debris by centrifugation the majority of the *E. coli* enzymes were removed by heating the cell-free lysate at 60°C for 20 min followed by centrifugation. The production of MJ0400 was confirmed by SDS-PAGE analysis.

### **Reaction of ASA and DKFP with MJ0400.**

The prepared ASA and DKFP were then reacted with MJ0400 at 70°C and pH 7.0 for 30 minutes. An attempt to assay for the byproduct 2-oxo-propionaldehyde 3-phosphate (OPP) using glyceraldehyde 3-phosphate dehydrogenase in the presence of NADH failed. Attempts to isolate the product and determine through  $^1\text{H}$  NMR analysis if the desired amino acid, ATTH, was formed also failed.

White reported that upon condensation of ASA and DKFP with MJ0400, the proposed product ATTH cyclizes spontaneously to form a cyclic imine.<sup>66</sup> White reported  $\text{NaBH}_4$  treatment of the condensation product mixture obtained provided a cyclic amine, 4,5-dihydroxy-6-methyl-piperidine-2-carboxylic acid (DMPCA) (Figure 46). In preparation of GC-MS analysis the reduced product mixture was derivatized by treatment with trifluoroacetic anhydride in methanol and dichloromethane. White observed four GC peaks, which he determined represented four stereoisomers of derivatized DCMPCA. All four GC peaks yielded MS peaks of 477, 446, 418, 336, 276, and 190 m/z.<sup>66</sup> In an attempt to repeat White's results, ASA and DKFP were reacted with MJ0400 under the same reaction conditions. The product mixture was subjected to  $\text{NaBH}_4$  reduction followed by derivatization to the presumed tri-trifluoroacetate methyl ester derivative. GC-MS analysis of the product mixture did yield four GC peaks at 6.73, 7.20, 7.43, and 7.68 min, which all produced peaks at 418, 336, 276, and 190 m/z in the MS spectra. Attempts to purify the product either before or after derivatization did not provide better GC-MS results. Attempts to obtain a high-resolution MS spectra for the product mixture also failed, presumably due to the instability of the trifluoroacetate groups. None of the further attempts obtained contained the two highest two mass peaks (477 and 446). The

yield of DMPCA produced overall from the condensation of ASA and DKFP could not be determined without standard material, nor did White report a yield. The production of DCMPCA through the MJ0400 condensation of ASA and DKFP also could not be confirmed using a second line of evidence.

It was then hypothesized that the replacement of ASA with a more stable derivative might allow for the acquisition of more definitive evidence for the production of ATTH. ASA was thus replaced in the MJ0400 condensation reaction with *N*-acetyl-ASA. However, analysis of the GC-MS spectra produced by this product mixture did not provide the expected product peak at 633 *m/z* or any other peaks that might be formed by fragmentation of the desired product.

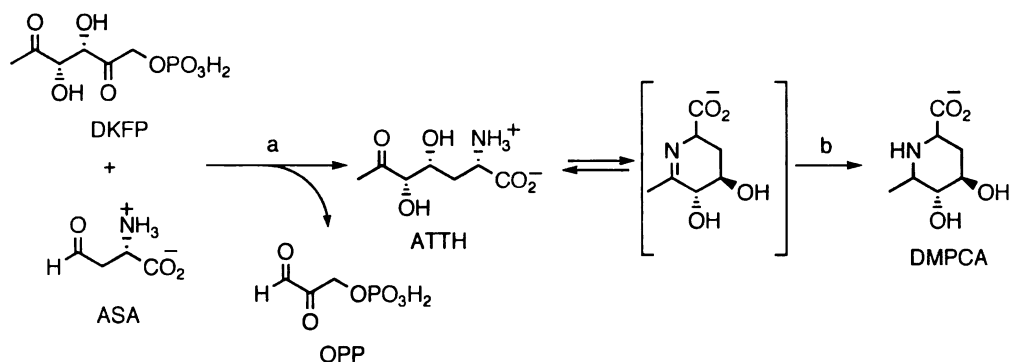


**Figure 46. Reaction of DKFP and ASA with MJ0400 as proposed by White.** Reaction Conditions: (a) MJ0400, 70°C, pH 7.0; (b) NaBH<sub>4</sub>. Abbreviations: DKFP, 6-deoxy-5-ketofructose 1-phosphate; ASA, L-aspartate semialdehyde; OPP, 2-oxo-propionaldehyde 3-phosphate; ATTH, 2-amino-2,3,7-trideoxy-6-oxo-4,5-D-threo-heptanoic acid; DMPCA, 4,5-dihydroxy-6-methyl-piperidine-2-carboxylic acid.

One reason for lack of discernable evidence substantiating the presence of DMPCA is the yield was small. A small yield of DMPCA might have been obtained due to a low production of ASA either because of inadequate resolving of the L-allyl glycine with porcine kidney acylase, or due to the instability of product and decomposition during reaction work-up. When the ozonolysis was performed on racemic allyl glycine

purchased from sigma, the concentration of ASA was found to be 0.3 mM by enzyme assay (a yield of 60%). When the same assay was used to determine the amount of ASA from L-allyl glycine, the yield of ASA was 4%.

### **Expression of *hdhI* and *thrA***

It was presumed that the apparently low production of ATTH was due in part to a low production of ASA, so it was hypothesized the oxidation of homoserine to generate ASA might provide a better result. By the oxidation of homoserine with homoserine dehydrogenase the ASA could be produced separately or *in situ*. In *E. coli* there are two bifunctional enzymes which contain homoserine dehydrogenase activity, ThrA and MetL (Figure 47). Recently, Viola and James, in an effort to generate new bifunctional enzymes by domain swapping, independently cloned and expressed the homoserine dehydrogenase portion of the *thrA* gene along with an interface region (*hdhI*<sup>+</sup>), which lies between the regions responsible for aspartokinase and homoserine dehydrogenase activities (Figure 48).<sup>100</sup> The homoserine dehydrogenase activity of the newly formed monofunctional enzyme (HDHI<sup>+</sup>) displayed a 10-fold increase in  $k_{cat}$  (3.30 s<sup>-1</sup>), a 2-fold increase in  $K_m$  (0.68 mM), and a 20-fold increase in  $k_{cat}/K_m$  (4.9 x 10<sup>3</sup> M<sup>-1</sup>s<sup>-1</sup>) over that of the native bifunctional enzyme ( $k_{cat}$  = 0.24 s<sup>-1</sup>;  $K_m$  = 1.2 mM;  $k_{cat}/K_m$  = 2.1 x 10<sup>2</sup> M<sup>-1</sup>s<sup>-1</sup>). Due to the increased activity of this monofunctional enzyme and the possibility of avoiding possible problems posed by the aspartokinase activity of the native bifunctional enzyme, an attempt was made to clone and express the homoserine dehydrogenase portion of the *thrA* along with the interface region from *E. coli* W3110 genomic DNA.

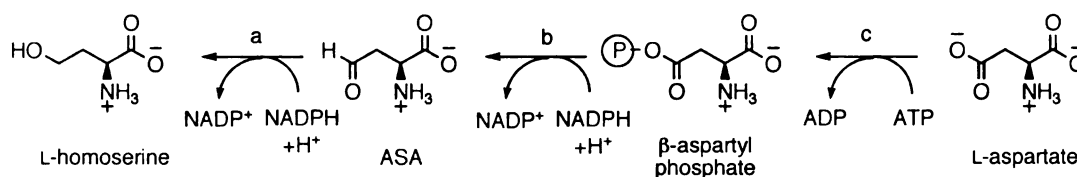


**Figure 47. Reactions catalyzed by homoserine dehydrogenase and aspartate kinase.** Enzymes (gene): (a) homoserine dehydrogenase I and II, *thrA*, *metL*; (b) aspartate semialdehyde dehydrogenase, *asd*; (c) aspartate kinase, *thrA*, *metL*, *lysC*.

To prepare the monofunctional homoserine dehydrogenase, the desired region of *E. coli* genomic DNA was PCR amplified. The DNA fragment produced was then inserted into pJG7.246 ( $T_5$ , *lacO*, *lacO*, *6xhis*, *lacI<sup>R</sup>*, *Amp<sup>r</sup>*) to form pHS8.080 ( $T_5$ , *lacO*, *lacO*, *6xhis*, *hdhI<sup>+</sup>*, *lacI<sup>R</sup>*, *Amp<sup>r</sup>*) (figure 2). The resulting plasmid was transformed into DH5 $\alpha$  competent cells. Expression of HDHI $^{+}$  (+ stands for the interface region) by the addition of 0.1 mM IPTG did not yield any of the desired protein. Expression was also attempted by the addition of 28 mM lactose, however none of the desired protein was produced again. It is interesting to note that upon induction the cells essentially stopped growing and acquired a white color and chunky consistency upon harvesting. Owing to the possible toxicity of the modified enzyme to the DH5 $\alpha$  cells, the plasmid was transformed into BL21 and JM109 competent cells and attempts were made to express the protein again. When JM109 was used, again the cells stopped growing upon induction and no HDHI $^{+}$  production was observed. In the case of BL21, the cells grew very well on induction, but still did not produce observable quantities of the desired protein.

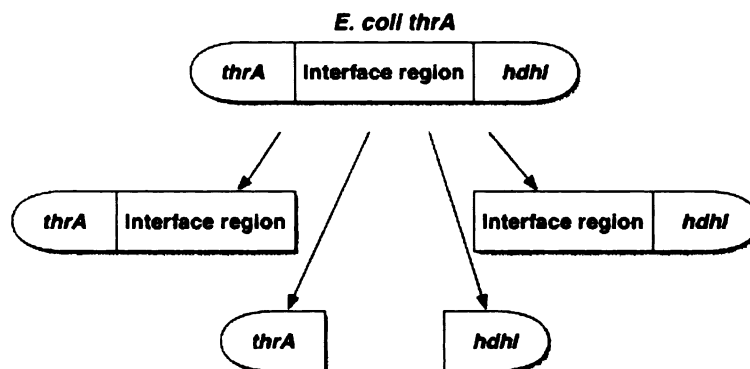


**Figure 48. Division of *thrA* into different gene segments for individual expression or recombination to produce new bifunctional enzymes.**

Instead of immediately pursuing additional cloning of *hdhI*<sup>+</sup>, it was decided an attempt should be made to over-express the native ThrA protein. The *thrA* gene was PCR amplified from *E. coli* W3110 genomic DNA and inserted into pET-15b (*T7*, *lacO*, *6xhis*, *lacI*<sup>r</sup>, *Amp*<sup>r</sup>) to form pHS8.216 (*T7*, *lacO*, *6xhis*, *thrA*, *lacI*<sup>r</sup>, *Amp*<sup>r</sup>).

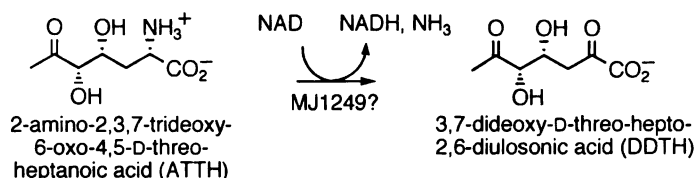
### Expression of *mjl602*

Along with the cloning and expression of the *E. coli* homoserine dehydrogenase enzymes, it was thought it might be useful to heterologously express the putative homoserine dehydrogenase from *M. jannaschii*, MJ1602. The expression of this enzyme would help determine whether or not it is actually acting as a homoserine dehydrogenase and since it would be thermally stable could be used to produce ASA *in situ* from homoserine. The PCR amplification of *mjl602* proved difficult, but was finally accomplished and the resulting DNA fragment was inserted into pET-15b to produce pHS8.240 (*T7*, *lacO*, *6xhis*, *mjl602*, *lacI*<sup>r</sup>, *Amp*<sup>r</sup>).

## Expression of *mj1249*

While attempts were being made to amplify and express the various homoserine dehydrogenase-encoding genes, efforts were also made to heterologously express MJ1249, the putative oxidase/aminotransferase proposed to be responsible for the transamination of the amino acid ATTH to the keto-acid DDTH (Figure 49).

**Figure 49. Presumed aminotransfer catalyzed by MJ1249 to produce the ketoacid DDTH.**



The gene, *mj1249*, was PCR amplified from *M. jannaschii* genomic DNA and inserted into two vectors, pJG7.246 (*T<sub>7</sub>*, *lacO*, *lacO*, *6xhis*, *lacI<sup>s</sup>*, *Amp<sup>r</sup>*) and pET-15b (*T<sub>7</sub>*, *lacO*, *6xhis*, *lacI<sup>s</sup>*, *Amp<sup>r</sup>*), to form pHS8.072 and pHS8.101. Both plasmids were transformed into BL21 Codon Plus strains to account for a high percentage of A and T content within the gene. Attempts to express MJ1249 from BL21 Codon Plus RIL/pHS8.072 upon the addition of 0.1, 0.5, or 1.0 mM IPTG did not produce observable levels of the desired protein when the cells were grown at 37°C or 28°C. Also, production of MJ1249 could not be observed when gene expression was induced by the addition of 28 mM lactose at 37°C or 28°C.

Expression of the *mj1249* gene product from BL21 Codon Plus (DE3)/pHS8.101 was attempted by induction with 0.1, 0.5, 1.0 mM IPTG and 28 mM lactose at both 37°C and 28°C. Initial experiments failed to yield any of the desired MJ1249. Upon transformation of BL21 Codon Plus (DE3) competent cells with pHS8.101, two distinctly different size colonies formed upon overnight incubation of agar plates. Analysis of a



random selection of the colonies showed that all contained the correct plasmid and additional control experiments showed no contamination was occurring. It was found that only the smaller colonies could produce the desired MJ1249 when induced with IPTG (0.2 mM), however the levels produced were quite low. In an attempt to improve the levels of expression of MJ1249, the gene was ligated into pT7-7 (*T<sub>7</sub>*, *lacO*, *Amp<sup>r</sup>*, *ColEI*) to form pHS8.243 (*T<sub>7</sub>*, *lacO*, *mj1249*, *Amp<sup>r</sup>*, *ColEI*) where the start of the gene is now much closer to the promoter along the sequence. The choice of pT7-7 as the vector was motivated by this vector's use in the construction of pMJ0400 designed by White.

### ATTH intermediacy

#### **Overview**

The condensation of ASA and DKFP was proposed to form the amino acid intermediate ATTH by White. However, the only evidence to suggest this intermediate was GC-MS spectra, which could not adequately be reproduced in this lab using the same reaction conditions. Also, no secondary evidence to support the intermediacy of ATTH was presented by White, nor could any be obtained from the MJ0400 catalyzed condensation in this lab. Clearly further work was required to gain either further support for or against White's claim of ATTH intermediacy.

One solution to this problem was to prepare the proposed intermediates, ATTH and DDTH. Synthesis of ATTH, apart from the enzyme catalyzed condensation of ASA and DKFP, seemed especially pertinent. Once prepared, the proposed cyclization of the amino acid to the cyclic imine could be investigated. Also, a standard GC-MS spectrum could be obtained for comparison with the results obtained via the condensation of ASA

and DKFP by MJ0400. With the molecule in hand a second method of analysis, such as NMR or HPLC, could be used to determine if ATTH is a product of the MJ0400 catalyzed condensation. Also, with access to ATTH the proposed conversion of ATTH to DDTH by MJ1249 could be addressed.

Two synthetic routes were applied toward the preparation of ATTH. One route took advantage of the structurally intact amino acid moiety of aspartic acid, which would be condensed with another 3-carbon unit. The second route from D-tartaric acid would utilize the given diol stereochemistry of a 2-deoxy-xylose intermediate to avoid the use of a stereoselective aldol or dihydroxylation reaction.

#### Synthesis of ATTH from *N*-Cbz-Aspartic acid

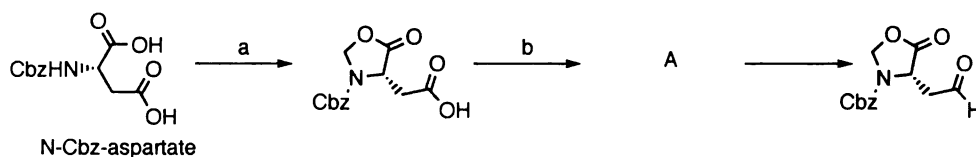


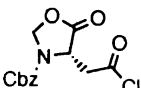
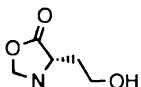
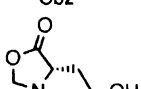
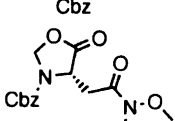
**Figure 50. Preparation of the oxazolidine aldehyde.**

Reaction conditions: (a) paraformaldehyde, pTSA, PhCH<sub>3</sub>, reflux, 88%; (b) see Table 16.

The  $\alpha$ -carboxylic acid group of *N*-Cbz-L-aspartic acid was first selectively converted to the oxazolidinone acid in 88% yield in the presence of *para*-formaldehyde and *p*-toluenesulfonic acid in toluene with the azeotropic removal of water (Figure 50). Several conditions were then applied to convert the free carboxyl group of the oxazolidine acid into a desirable intermediate for reduction to the aldehyde. Both acid chlorides and Weinreb amides are known to form aldehyde under reducing conditions, while a primary alcohol can be selectively oxidized to the aldehyde. The oxazolidine acid chloride was produced in 90% crude yield by treating the oxazolidine acid with distilled oxalyl chloride in dichloromethane with catalytic addition of DMF

(entry 1, Table 16). Attempts to produce the primary alcohol resulted in complex mixtures of products presumably due to side reactions involving reduction of the ester in the oxazolidine ring (entry 2 and 3, Table 16). In order to use this route a bulkier protecting group would be required, therefore the reduction/oxidation route was abandoned. The Weinreb amide was successfully produced in 70% yield by treating the oxazolidine acid with (N, O)-dimethyl hydroxylamine, triethylamine, and BOP reagent (entry 4, Table 16).

**Table 16. Varying conditions used to prepare compound A as an intermediate to the *N*-Cbz-oxazolidine aldehyde.**

entry	reaction conditions	product A	yield (%)
1	oxalyl chloride, DMF, CH <sub>2</sub> Cl <sub>2</sub>		90 <sup>a</sup>
2	NaBH <sub>4</sub> , AcOH, MeOH		complex mixture
3	BH <sub>3</sub> •THF, -5°C		complex mixture
4	HN(OMe)Me, BOP•PF <sub>6</sub> , NEt <sub>3</sub>		70 <sup>b</sup>

(a) crude yield; (b) yield after flash column purification

Once the acid chloride and the Weinreb amide were prepared attempts were made to convert both to the aldehyde under varying hydrogenation conditions (Table 17). Attempts to reduce the acid chloride via a modified Rosemund reduction<sup>101</sup> in the presence of 5% Pd/BaSO<sub>4</sub> and 2,6-lutidine in dry THF and 50 psi H<sub>2</sub> failed to yield the desired aldehyde. Although the acid chloride was no longer present at the end of the reaction, an examination of the <sup>1</sup>H NMR spectra of the product revealed no aldehyde

hydrogen was present. Performing this hydrogenation at atmospheric pressures of hydrogen initially failed to produce the aldehyde as well, however, when the reaction was run with freshly purchased catalyst the aldehyde was produced. This suggests the original catalyst was somehow poisoned or inactivated. The previous, yet unidentified, product of the reduction was also present so the success of the reaction was gauged by the  $H_a/H_b$  ratio (Table 17). Under atmospheric pressure of  $H_2$  the modified Rosemund reduction gave a  $H_a/H_b$  ratio of 0.38, however further attempts to perform the reduction indicated that the ratio was not consistently reproducible. The  $H_a/H_b$  ratio was smaller upon each subsequent run of the reaction. Changing the catalyst to Pd/C failed to yield any aldehyde product. Also attempting to reduce the acid chloride with  $Li(OtBu)_3AlH$  failed to produce the desired aldehyde. The last set of conditions attempted to reduce the acid chloride involved refluxing the acid chloride in toluene with Pd/BaSO<sub>4</sub> under a constant stream of hydrogen. The desired aldehyde was produced with a  $H_a/H_b$  ratio of 0.53 (entry 5, Table 17). Under these conditions again the undesired compound was visible in the  $^1H$  NMR, however the results were reproducible. The higher success of this reaction over the modified Rosemund reduction is presumably due the removal of HCl by the hydrogen stream, which would protect the catalyst from poisoning. Attempts to reduce the Weinreb amide to the aldehyde either gave trace yields or resulted in no reaction so this route was abandoned.

**Table 17. Optimization of oxazolidine aldehyde preparation.**

Entry	A	Conditions	<sup>1</sup> H NMR peak at 9.6 ppm	Integration ratio (H <sub>a</sub> /H <sub>b</sub> )
1		5% Pd/BaSO <sub>4</sub> , 2,6-lutidine, THF, 50 psi, H <sub>2</sub>	None	N/A
2	“	5% Pd/BaSO <sub>4</sub> , 2,6-lutidine, THF, H <sub>2</sub> , atmos	Yes	0.38
3	“	10% Pd/C, 2,6-lutidine, THF, atmos	None	N/A
4	“	Li(OtBu) <sub>3</sub> AlH, THF, rt	None	N/A
5	“	5% Pd/BaSO <sub>4</sub> , toluene, reflux, H <sub>2</sub> stream	Yes	0.53
6		DIBAL, THF/Hexanes, -78°C	Yes	Trace
7	“	Li(OtBu) <sub>3</sub> AlH, THF, -78°C-rt	None, NR	N/A

NR = No reaction; N/A = Not attempted

Although the reduction of the acid chloride in toluene at reflux provided a higher yield of the aldehyde, the consistency was still not at an acceptable level. Also, the presence of a contaminating byproduct might cause difficulties in later synthetic steps. It was considered that drying the acid chloride under vacuum may not have been capable of removing contaminating HCl. Several attempts were made to distill the acid chloride under vacuum as a means to remove any possible HCl, however only decomposition

occurred. The contaminating HCl was removed through resuspension of the acid chloride in solvent ( $\text{CH}_2\text{Cl}_2$  or  $\text{CHCl}_3$  (alcohol free)) followed by washing the organic layer with a dilute solution of sodium bicarbonate. The yield of acid chloride from the oxazolidine suffered lowering to 64%, however the  $H_a/H_b$  ratio of the aldehyde produced from the washed acid chloride was on average 0.75 or higher (Figure 51). Also, the undesired and unknown contaminating product of the hydrogenation was no longer produced leaving mainly aldehyde to be used for the next step of the synthesis.

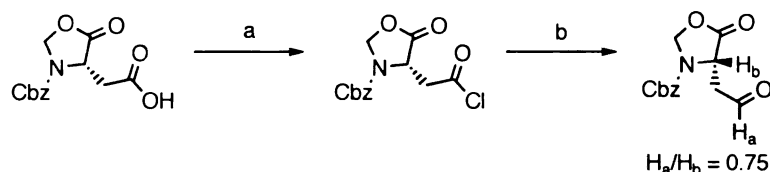


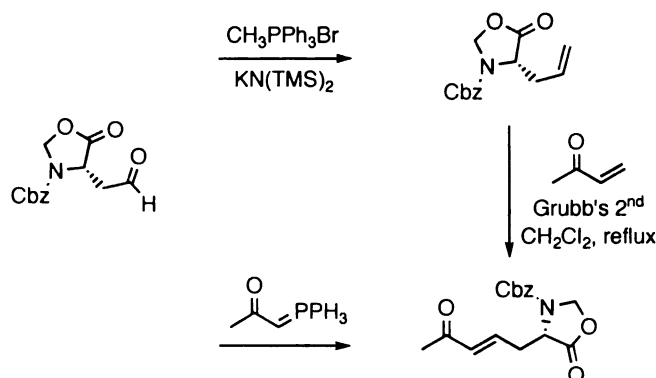
**Figure 51. Optimized of oxazolidine aldehyde preparation from the acid chloride.**  
 Reaction conditions: (a) *i.* oxalyl chloride, DMF,  $\text{CH}_2\text{Cl}_2$ , *ii.* dilute  $\text{NaHCO}_3$  wash, 64%;  
 (b)  $\text{H}_2$ , 5%  $\text{Pd/BaSO}_4$ , toluene, reflux.

The next step of the synthesis required the condensation of the oxazolidine aldehyde with another species through an aldol condensation or an Horner-Wadsworth Emmons or cross-metathesis reaction to form an  $\alpha,\beta$ -unsaturated ketone. The majority of selective aldol reactions in the literature either would not produce the correct stereochemistry of the diol, or require the preparation of additional intermediates. An attempt to condense the oxazolidine aldehyde with dihydroxyacetone phosphate using rabbit muscle aldolase failed, presumably due to the insolubility of the product in water.

The other option considered was to form an  $\alpha,\beta$ -unsaturated ketone via an Horner-Wadsworth Emmons condensation or a cross-metathesis reaction. The cross-metathesis reaction would require the condensation of the oxazolidine aldehyde first with a Wittig reagent to provide protected allyl glycine. The allyl glycine would then be

condensed with but-3-en-2-one via a cross-metathesis reaction with Grubb's second generation catalyst. A second method involved the formation of the enone in a single step by condensing the aldehyde with triphenylphosphoranyl-2-propanone (TPP). Since the latter route required the least number of reaction steps, it was attempted first (Figure 52).

**Figure 52. Synthetic strategy for enone preparation from the oxazolidine aldehyde.**



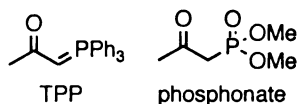
Early attempts to perform the condensation of the aldehyde with TPP at room temperature failed, so a test reaction was run to save starting material, and ensure the reaction was being performed correctly. Benzaldehyde was reacted with TPP at reflux, producing the desired enone in 95%. However, when the oxazolidine *N*-Cbz-aspartate semialdehyde was reacted with TPP at reflux the yield was a meager 7% (entry 1, Table 18). The temperature was then lowered in steps to 90, 60, and 40°C in an attempt to improve the yield. Running the condensation at 60°C gave the highest yield of 51% from the acid chloride (entries 2, 3, and 4, Table 18). It was a concern that the condensation might not produce exclusively the *trans* double bond so further reactions were performed to ensure the stereoselectivity for the *trans* double bond. Several conditions of Horner-Wadsworth Emmons condensations utilizing the phosphonate shown below (Table 18) have been reported for the selective preparation of the *trans* double bond.<sup>102</sup> However,

several conditions attempted failed to produce any of the enone product (entries 5, 6, and 7, Table 18).

**Table 18. Condensation of oxazolidine aldehyde with TPP to produce the enone.**

Entry	Reaction Conditions	% Yield Enone <sup>a</sup>
1	TPP, toluene, reflux	7
2	TPP, toluene, 90°C	10
3	TPP, toluene, 60°C	51
4	TPP, toluene, 40°C	27
5	Phosphonate, Ba(OH) <sub>2</sub> , THF/H <sub>2</sub> O	0
6	Phosphonate, LiCl, DBU, dry CH <sub>3</sub> CN	0
7	Phosphonate, LiCl, NEt <sub>3</sub> , dry CH <sub>3</sub> CN	0

(a) yield calculated based on mmol acid chloride used for hydrogenation

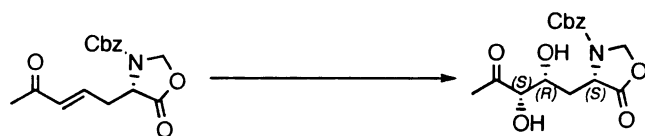


The next step of the synthesis required the *syn*-dihydroxylation of the enone to produce the vicinal diol with 4R, 5S stereochemistry. The route utilized most often in the literature is the Sharpless asymmetric dihydroxylation using the (DHQD)<sub>2</sub>PHAL ligand and OsO<sub>4</sub>. However, the dihydroxylation tends to be more difficult with α,β-unsaturated carbonyl compounds due to cleavage of the double bond and/or the deactivated double bond being unreactive towards dihydroxylation.<sup>103</sup> One reference reported the standard dihydroxylation conditions did not work and reported an alternative method using stoichiometric quantities of the ligand and OsO<sub>4</sub> followed by treatment with HCl/MeOH to cleave the osmate ester produced in the reaction.<sup>104</sup> Attempts to perform the dihydroxylation under these conditions with subsequent HCl/MeOH treatment (at room temperature or at reflux) failed to yield any product (entries 1 and 2, Table 19). A variety of procedures and conditions are reported for performing the dihydroxylation so attempts



were made to repeat as many of those conditions as possible. The treatment of the enone with AD-mix- $\beta$  at 0°C in tBuOH:H<sub>2</sub>O (1:1) failed to yield the diol (entry 3, Table 19). Adding the components of the AD-mix separately also failed (entry 5, Table 19). It has been reported by Sharpless that enones require buffering to avoid cleavage of the double bond. Attempting those conditions at 0 or 4°C failed to produce the diol using OsO<sub>4</sub> (entry 5 and 6, Table 19). Exchanging the Osmium catalyst to the more stable and easy to handle K<sub>2</sub>OsO<sub>4</sub>•2H<sub>2</sub>O resulted in a recovery of starting material when run under an inert atmosphere (entry 8, Table 19). Omitting the added K<sub>2</sub>OsO<sub>4</sub>•2H<sub>2</sub>O under inert conditions also led to a recovery of starting material (entry 9, Table 19). When buffered Sharpless conditions were used with the K<sub>2</sub>OsO<sub>4</sub>•2H<sub>2</sub>O in air the reaction yielded a 4% yield of a product presumed to be the diol (entry 10, Table 19). This yield, however, is not useful for the continuation of the synthesis so still more conditions were attempted. It was thought that lowering the temperature of the reaction might help to deter cleavage of the double bond, however running the reaction in either tBuOH:H<sub>2</sub>O or CH<sub>2</sub>Cl<sub>2</sub> at -20°C resulted in a recovery of starting material (entries 11 and 12, Table 19). Several groups have reported RuO<sub>4</sub> complexes formed *in situ* from RuCl<sub>3</sub> and NaIO<sub>4</sub> can catalyze the *syn* dihydroxylation, however these conditions again failed to produce the desired diol (entry 13, Table 19). Changing the co-oxidant from K<sub>3</sub>Fe(CN)<sub>6</sub> to NMO improved the yield of the presumed diol 10 fold (entry 14, Table 19), however the reaction produced a mixture of products which were not separable using a standard flash column. When the chiral ligand was added a mixture of products was again obtained (entry 15, Table 19) and the yield suffered slightly.

**Table 19. Dihydroxylation of the enone.**



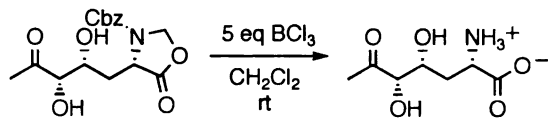
Entry	Reaction Conditions	Yield Diol (%)
1	i. OsO <sub>4</sub> , (DHQD) <sub>2</sub> PHAL, CH <sub>2</sub> Cl <sub>2</sub> /Et <sub>2</sub> O, -20°C-rt ii. HCl/MeOH, rt	0
2	i. OsO <sub>4</sub> , (DHQD) <sub>2</sub> PHAL, CH <sub>2</sub> Cl <sub>2</sub> /Et <sub>2</sub> O, -20°C-rt ii. HCl/MeOH, reflux	0
3	AD-mix-β, tBuOH:H <sub>2</sub> O (1:1), 0°C	0
4	OsO <sub>4</sub> , K <sub>3</sub> Fe(CN) <sub>6</sub> , K <sub>2</sub> CO <sub>3</sub> , (DHQD) <sub>2</sub> PHAL, tBuOH:H <sub>2</sub> O (1:1)	0
5	AD-mix-β, OsO <sub>4</sub> , NaHCO <sub>3</sub> , MeSO <sub>4</sub> NH <sub>2</sub> , tBuOH:H <sub>2</sub> O (1:1), 4°C	0
6	AD-mix-β, MeSO <sub>4</sub> NH <sub>2</sub> , NaHCO <sub>3</sub> , tBuOH:H <sub>2</sub> O (1:1), 0°C	0
7	AD-mix-β, OsO <sub>4</sub> , MeSO <sub>4</sub> NH <sub>2</sub> , NaHCO <sub>3</sub> , tBuOH:H <sub>2</sub> O (1:1), 0°C	0
8	AD-mix-β, K <sub>2</sub> OsO <sub>4</sub> •2H <sub>2</sub> O, MeSO <sub>4</sub> NH <sub>2</sub> , NaHCO <sub>3</sub> , tBuOH:H <sub>2</sub> O (1:1), 0°C, Ar	NR
9	AD-mix-β, MeSO <sub>4</sub> NH <sub>2</sub> , NaHCO <sub>3</sub> , tBuOH:H <sub>2</sub> O (1:1), 0°C, Ar	NR
10	AD-mix-β, K <sub>2</sub> OsO <sub>4</sub> •2H <sub>2</sub> O, MeSO <sub>4</sub> NH <sub>2</sub> , NaHCO <sub>3</sub> , tBuOH:H <sub>2</sub> O (1:1), 0°C	4
11	AD-mix-β, K <sub>2</sub> OsO <sub>4</sub> •2H <sub>2</sub> O, MeSO <sub>4</sub> NH <sub>2</sub> , NaHCO <sub>3</sub> , tBuOH:H <sub>2</sub> O (1:1), -20 to 0°C	NR
12	AD-mix-β K <sub>2</sub> OsO <sub>4</sub> •2H <sub>2</sub> O, MeSO <sub>4</sub> NH <sub>2</sub> , NaHCO <sub>3</sub> , CH <sub>2</sub> Cl <sub>2</sub> , -20°C	NR
13	RuCl <sub>3</sub> •H <sub>2</sub> O, H <sub>2</sub> O, NaIO <sub>4</sub> , EtOAc:CH <sub>3</sub> CN:H <sub>2</sub> O (3:3:1), 0°C	0
14	NMO, K <sub>2</sub> OsO <sub>4</sub> •2H <sub>2</sub> O, THF:tBuOH:H <sub>2</sub> O, 0°C-rt	44 <sup>a</sup>
15	NMO, K <sub>2</sub> OsO <sub>4</sub> •2H <sub>2</sub> O, (DHQD) <sub>2</sub> PHAL, THF:tBuOH:H <sub>2</sub> O, 0°C-rt	27 <sup>a</sup>

(a) Added enone all at once, product after chromatography was a mixture of diastereomers. NR = No reaction.

With the presumed diol in hand the next step of the synthesis involved removal of the oxazolidine ring and Cbz group. It has been reported that BCl<sub>3</sub> (5 eq) can remove both the Cbz group and open the oxazolidine ring to produce the free amino acid at room

temperature (Figure 53).<sup>105</sup> However, all attempts using these conditions resulted in decomposition of the product/starting material.

**Figure 53. Simultaneous removal of Cbz group and cleavage of oxazolidine ring.**



Throughout the synthesis the NMR spectra contained broad undefined peaks. Possible problems which were proposed that might have caused the poor spectra included the contamination of metals, which could be chelating to the synthetic or poor solubility of the intermediates in the NMR solvent. In order to remove any possible metal contamination, the oxazolidine acid was passed through small columns of cation exchange resins (Dowex 50 (H<sup>+</sup> form) or IR-120 (H<sup>+</sup> form)). However, the spectra did not improve. In an attempt to solve the possible issue of solubility, the oxazolidine acid was analyzed by <sup>1</sup>H NMR in a variety of NMR solvents, including CDCl<sub>3</sub>, CD<sub>3</sub>OD, DMSO-d<sub>6</sub>, and acetone-d<sub>6</sub>. Again little improvement of the NMR spectra was observed. Increasing the temperature of the NMR analysis when the oxazolidine acid was dissolved in acetone-d<sub>6</sub> did, however, improve the spectra significantly. The temperature was first raised to 40°C followed by 50°C (the instrument maximum allowable limit). Since 50°C gave the best result, all subsequent spectra were taken in acetone-d<sub>6</sub> at 50°C. All intermediates preceding the diol gave good spectra under these conditions. The diol however again gave poor spectra.

Further attempts were made to improve the selectivity of the dihydroxylation of the enone in the hopes of obtaining a cleaner product mixture. The substrate was added slowly over 12 to 18 h using a syringe pump in order to keep the concentration of the

substrate low enough to avoid reaction of osmium without the presence of the ligand. The equivalent of ligand was increased from 0.01 eq to 0.25 eq with no effect on the composition of the product mixture, however the yield decreased as the ligand equivalents increased (Table 20). Cooling the reaction to 0°C or running the reaction under an inert atmosphere also did not make a difference in the yield or product mixture composition.

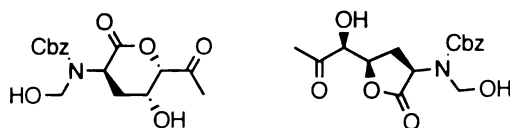
**Table 20. Optimization of enone dihydroxylation.**

Entry	Ligand <sup>a</sup>	Addition Time (h)	Atmos.	Temp. (°C)	Yield Product (%)
1	0.01	12	air	r.t.	48
2	0.01	12	argon	r.t.	42
3	0.01	12	air	0	45
4	0.02	18	air	r.t.	25
5	0.25	12	air	r.t.	11

(a) Equivalent of the ligand added to the reaction.

The product mixture was purified by HPLC using a C18 reverse phase column. The purified product was analyzed by mass spectral analysis and was found to have the mass expected for the diol product. However, the <sup>1</sup>H NMR spectra did not contain a peak expected for the oxazolidine methylene. This raised the question of whether the desired product was actually formed. Attempts were made to protect the presumed diol as a way of confirming the diol was present as expected. However preparation of the BBA protected diol failed to yield the desired product and instead produced a methyl ester. An attempt at preparing the benzyl diether also failed. It was thought perhaps the oxazolidine ring was opening during the dihydroxylation reaction to produce a cyclic product as seen in Figure 54.

**Figure 54. Possible alternate dihydroxylation products.**



### Synthesis of ATTH from *N*-Boc-Asp(Obz)-OH

With the realization the oxazolidine ring might be opening it was thought changing the protecting group on the alpha acid may provide a better result to the dihydroxylation. The mono boc and benzyl protected aspartate was purchased and the alpha ester protected as a *t*-butyl ester in 90% yield. A *t*-butyl ester was used since this protecting group is bulky and not highly susceptible to base catalyzed cleavage. In order to avoid any possible problems associated with the free hydrogen the amine group was protected with a second Boc group. The protection was attempted using Boc<sub>2</sub>O and NaH at reflux in THF, however the reaction yield was only 41%. When the conditions were changed to use DMAP as the base in CH<sub>3</sub>CN at room temperature the yield increased to 64%. The benzyl ester was then deprotected quantitatively using H<sub>2</sub> gas in the presence of 0.01 mol % Pd/C in MeOH at room temperature. An attempt to produce the acid chloride under the same conditions as the previous oxazolidine synthesis failed, presumably due to the acid sensitivity of the Boc carbamate and the *t*-butyl ester. As an alternative the carboxylic acid was treated with *N*, *O*-dimethylhydroxylamine, TEA, and BOP reagent to give the Weinreb amide in 75% yield. The amide was reduced to the aldehyde in 86% yield with DIBAL at -78°C followed by condensation of the aldehyde with TPP to produce the protected enone in 77% yield. The asymmetric dihydroxylation of the enone was attempted first using OsO<sub>4</sub>, NMO, and (DHQD)<sub>2</sub>PHAL ligand in a 3:1:1.7 *t*BuOH-H<sub>2</sub>O-THF solution. The dihydroxylation gave a clear 1:1 mixture of diol

diastereomers in 34% yield. The presence of two separate isomers was established using a 2D TOCSY experiment. There was no evidence of the loss of the protecting groups as witnessed previously with the oxazolidine-protected amino acid. The Sharpless conditions using AD-mix- $\beta$ ,  $K_2OsO_4$ , and methylsulfonamide with sodium bicarbonate as buffer were attempted to improve the stereoselectivity of the dihydroxylation. While the yield improved to 67%, the diastereoselectivity of the reaction was not improved. Attempts to purify the mixture into independent diastereomers by flash column chromatography failed. On all attempts the two compounds ran together.

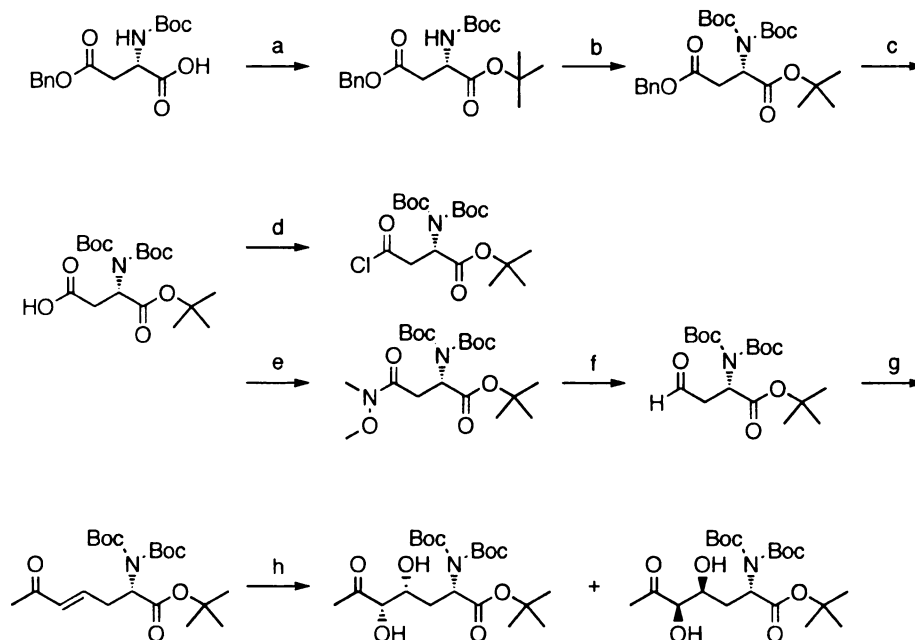


**Figure 55. Synthesis of ATTH from *N,N*-diboc-Asp-OtBu.**

Reaction conditions: (a) *t*BuOH, DMAP, DCC,  $CH_2Cl_2$ ,  $0^\circ C$  – r.t. 90%; (b)  $Boc_2O$ , DMAP,  $CH_3CN$ , 64%; (c)  $H_2$ , Pd/C, MeOH, r.t., quant.; (d) oxalyl chloride, DMF,  $CH_2Cl_2$ , r.t.; (e) BOP• $PF_6$ ,  $HN(OMe)Me$ , TEA,  $CH_2Cl_2$ , 75%; (f) DIBAL, THF/Hexanes,  $-88^\circ C$ , 86%; (g) TPP, toluene, reflux, 77%; (h) AD-mix- $\beta$ ,  $K_2OsO_4 \cdot 2H_2O$ ,  $NaHCO_3$ ,  $H_2NSO_2Me$ , *t*BuOH- $H_2O$  (1:1), 67%

In an attempt to both confirm diol production as well as find a method to purify the diastereomers, the diol product was subjected to varying protection conditions (Table

21). Any attempts to create the dibenzyl ethers failed. The diacetate diastereomers were produced in 84% yield, but still could not be separated. The isopropylidene and dibenzoyl ester diastereomers also could not be separated. The diol mixture was treated with trifluoroacetic acid to remove the boc and *t*-butyl groups. The product however did not resemble the expected amino acid.

**Table 21. Protection of protected ATTH in an attempt to separate the diol diastereomers.**

Entry	Reaction Conditions	R-	Yield (%)
1	Ac <sub>2</sub> O, pyr, r.t.	Ac-	84
2	BnBr, Bu <sub>4</sub> NI, NaH, 0°C- r.t.	Bn-	0
3	BnBr, NaH, THF, 0°C – r.t.	Bn-	0
4	2,2-dimethoxypropane, pTSA	isopropylidene	0
5	BzCl, pyr, r.t.	Bz-	38

In an attempt to reduce the steric hindrance during the dihydroxylation caused by the bulky boc groups, the synthesis of ATTH was performed without the second boc group. The exclusion of the second boc group would also allow the use of milder deprotection conditions at the end of the synthesis. The yields of several of the synthetic steps dropped slightly with this alteration and unfortunately there was no observed improvement in the selectivity of the dihydroxylation of the enone. Again the diastereomers were inseparable. Upon benzylation of the diol product mixture however the two diastereomers could be separated easily using silica gel.

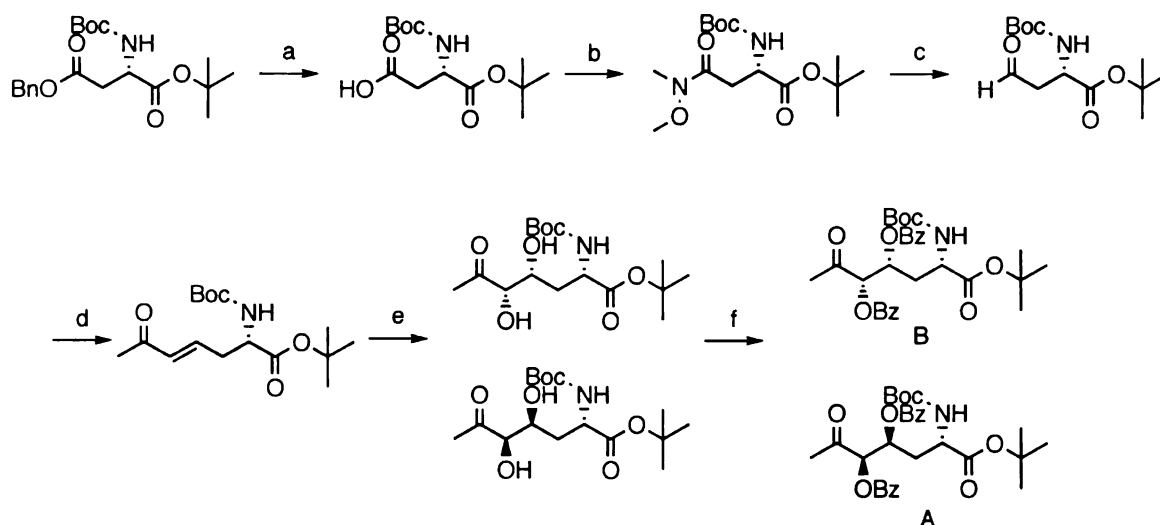


**Figure 56. ATTH from *N*-*boc*-Asp-OBn-OtBu.**

(a)  $\text{H}_2$ , Pd/C. MeOH, quant.; (b) BOP•PF<sub>6</sub>, HN(OMe)Me, TEA, CH<sub>2</sub>Cl<sub>2</sub>, 49%; (c) DIBAL, THF, -88°C, 68%; (d) TPP, toluene, 90°C, 57%; (e) AD-mix-β, K<sub>2</sub>OsO<sub>4</sub>•2H<sub>2</sub>O, H<sub>2</sub>NSO<sub>2</sub>Me, NaHCO<sub>3</sub>, *t*BuOH:H<sub>2</sub>O (1:1), 0°C, 48%; (f) BzCl, pyr, CH<sub>2</sub>Cl<sub>2</sub>, r.t., 72%.

In an attempt to determine which isomer was isolated from the asymmetric dihydroxylation of the mono-Boc protected enone, the reaction was performed using AD-mix-α. The reasoning being the ligand in AD-mix-α should have produced a diol with the opposite stereochemistry as the desired product. Thus a discernable excess of one diastereomer over the other would indicate that isomer contained the wrong stereochemistry. When AD-mix-β was replaced with AD-mix-α, the product mixture contained a 2.7:1 A:B ratio suggesting B was the desired isomer.

Attempts to deprotect the desired dibenzol ester to form the free amino acid using trifluoroacetic acid resulted in decomposition of the starting material. A variety of conditions were employed to remove the benzoyl esters, including the use of sodium methoxide and sodium bicarbonate, however the desired diol product was not obtained.

In an attempt to avoid keto-enol tautomerization of the hydroxyl group adjacent to the carbonyl, an attempt was made to convert the ketone into a cyclic ketal with ethylene



glycol and pTSA in refluxing benzene. Unfortunately, the benzoyl groups proved too sensitive for these conditions, and again product decomposition occurred. The ketal could be formed by reacting the protected  $\alpha,\beta$ -unsaturated ketone under the same reaction conditions. By protecting the carbonyl at this earlier stage of the synthesis the olefin would likely be more reactive toward the dihydroxylation conditions, and possibly better stereoselectivity could be obtained.

### **Synthesis of ATTH from D-tartaric acid through deoxy-xylose intermediacy**

A second synthetic route explored to produce ATTH utilized the built-in stereochemistry of 2-deoxyxylose. Two possible routes could be used to obtain the 2-deoxyxylose intermediate: synthetic from D-tartaric acid or chemo-enzymatic from glucose utilizing the 2-deoxyxylose producer SP1.1/pPV4.230. The chemo-enzymatic route would yield 2-deoxyxylose in amounts of 16 g/L, which would unfortunately be contaminated with as much as 2 g/L of 2-C-methylerythrose. Since the synthetic route starting from D-tartaric acid could be performed on a large scale giving clean, protected 2-deoxyxylose in approximately the same amount of time it was thought the synthetic route might be preferable.

The D-tartaric acid was first treated with 2,2-dimethoxy propane, pTSA, methanol, and cyclohexane with azeotropic removal of acetone to provide the isopropylidene dimethyl ester of D-tartaric acid in 76% yield. The dimethyl ester was then cautiously treated with  $\text{LiAlH}_4$  in diethyl ether to provide the isopropylidene diol in 59% yield. Using 1 equivalent of TBDMSCl provided the mono-TBDMS ether in 86% yield. The remaining alcohol was oxidized under Swern conditions to the aldehyde in 85% yield, which was immediately treated with the  $\text{MeMgBr}$  to give the secondary

alcohol in 48% yield. The secondary alcohol produced was then oxidized to the ketone in the presence of NMO, TPAP, and crushed, activated 4 Å molecular sieves in 88% yield. The preparation of the ketal however failed to produce the fully protected 2-deoxyxylose. The TBDMS group was apparently not able to survive the reaction conditions required to protect the ketone either using ethylene glycol or 1,3-propanedithiol. The replacement of the TBDMS group with a triisopropylsilyl or diphenylmethylsilyl group could alleviate this problem. However the isopropylidene could not survive the dithiane protection conditions. When the primary alcohol was protected as the TIPS ether the yield of the protection dropped to 23%. The subsequent oxidation of the second alcohol to the aldehyde under Swern conditions also experienced a yield decrease to 44%. The oxidation was followed by the Grignard reaction to provide the secondary alcohol in 19% yield.

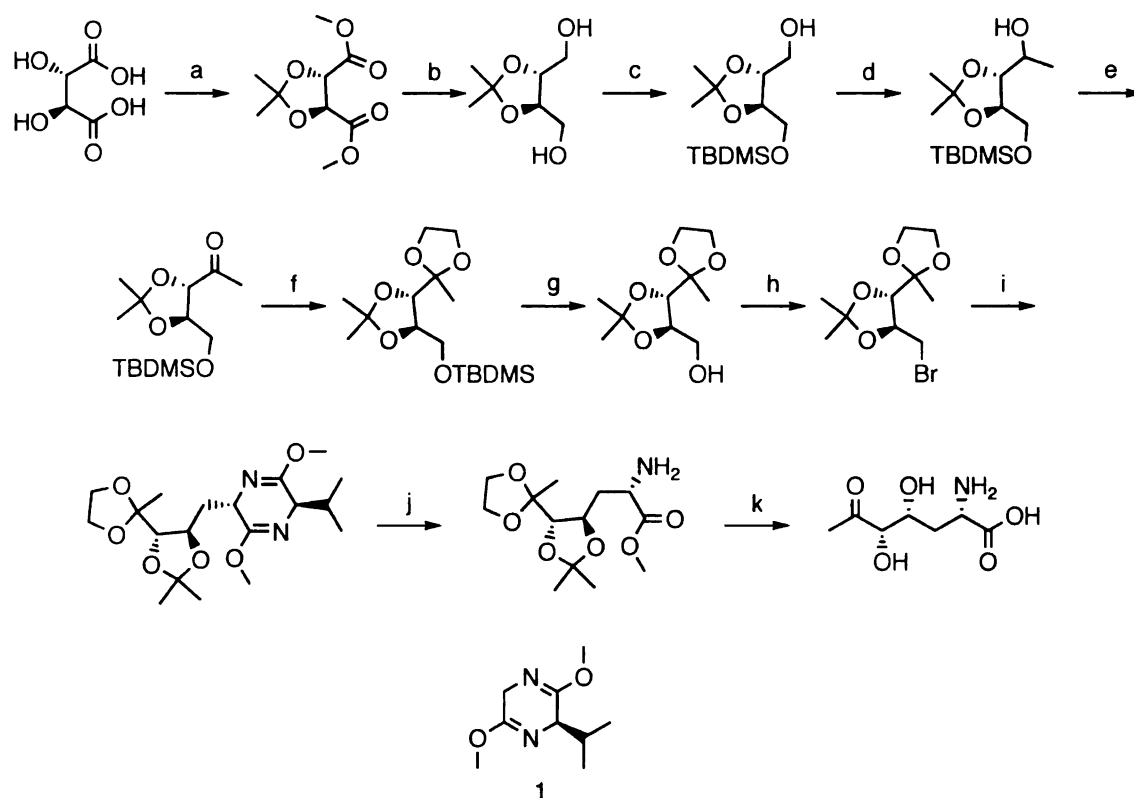


**Figure 57. ATTH synthesis from D-tartaric acid through 2-deoxy-xylose intermediacy.**

Reaction conditions: (a) 2,2-dimethoxypropane, MeOH, pTSA, cyclohexane, reflux, 76%; (b) *i.* LiAlH<sub>4</sub>, Et<sub>2</sub>O *ii.* H<sub>2</sub>O, NaOH, 59%; (c) TBDMSCl, NaH, THF, 0°C – r.t., 86%; (d) *i.* DMSO, oxalyl chloride, TEA, -78°C – r.t., 85%, *ii.* MeMgBr, THF, -78°C – r.t. 48%; (e) NMO, TPAP, CH<sub>2</sub>Cl<sub>2</sub>, 4 Å MS, 88%; (f) ethylene glycol, pTSA, benzene, reflux; no product; (g) TBAF, THF, r.t.; (h) PBr<sub>3</sub>; (i) *n*-BuLi, 1; (j) 0.25 N HCl; k. TMSI

## Discussion

The work presented in this chapter sought to provide evidence for the intermediacy of ATTH in the biosynthesis of DHQ by *M. jannaschii*. The work can be divided into two routes. The first route attempted was the examination of the product mixture obtained upon reaction of ASA and DKFP by MJ0400. The second route entailed the synthesis of the proposed intermediate ATTH to be used as both a standard for spectral analysis and a substrate for the enzymes in question (MJ0400 and MJ1249).

Unfortunately the attempt to condense ASA with DKFP using the heterologously expressed ATTH was not successful. The only evidence obtained which might lend credence to White's claim that ATTH was produced from this condensation was the GC-MS spectrum. However this spectrum did not contain all of the mass peaks reported by White and no further evidence could be obtained which might suggest this intermediate was being produced.

Several points can be made which may explain these poor results. Both the substrates and products are relatively unstable and could decompose under the reaction conditions. This decomposition would decrease the concentration of the desired ATTH in the product mixture making spectral analysis difficult. Another point to consider is the unmeasured specific activity of MJ0400. The possibility remains that the specific activity of heterologously expressed MJ0400 may be low under these reaction conditions. Low activity may be due to a variety of factors. Since no activity assay has been developed and the product cannot be adequately quantified, there is no way to determine the optimum temperature, pH, buffer, or other stabilizing cofactors. Another possible reason for a low activity of this enzyme could be substrate specificity. Oxaloacetaldehyde was never eliminated as a precursor to DHQ biosynthesis. White reported the preparation of DHQ from ASA and DKFP by the action of both MJ1249 and MJ0400, but no evidence has been reported to establish that MJ1249 does catalyze the transamination of ATTH. The transamination could occur prior to the condensation, preparing oxaloacetaldehyde from ASA. Thus the possibility remains that the condensation of DKFP and oxaloacetaldehyde by MJ0400 could lead to the synthesis of DDTH, which would then cyclize to DHQ.

Upon failing to provide adequate evidence for the production of ATTH by the MJ0400 catalyzed condensation of ASA and DKFP, it was determined the preparation of ATTH was required to be used as a standard or a substrate for the transamination by MJ1249. Unfortunately the synthetic efforts failed to provide the desired ATTH. The protected ATTH was produced from aspartic acid, however once prepared the protecting groups could not be removed without product decomposition. The synthesis starting from D-tartaric acid also failed to provide the desired product. Further synthetic efforts will need to be made to prepare the proposed intermediate.

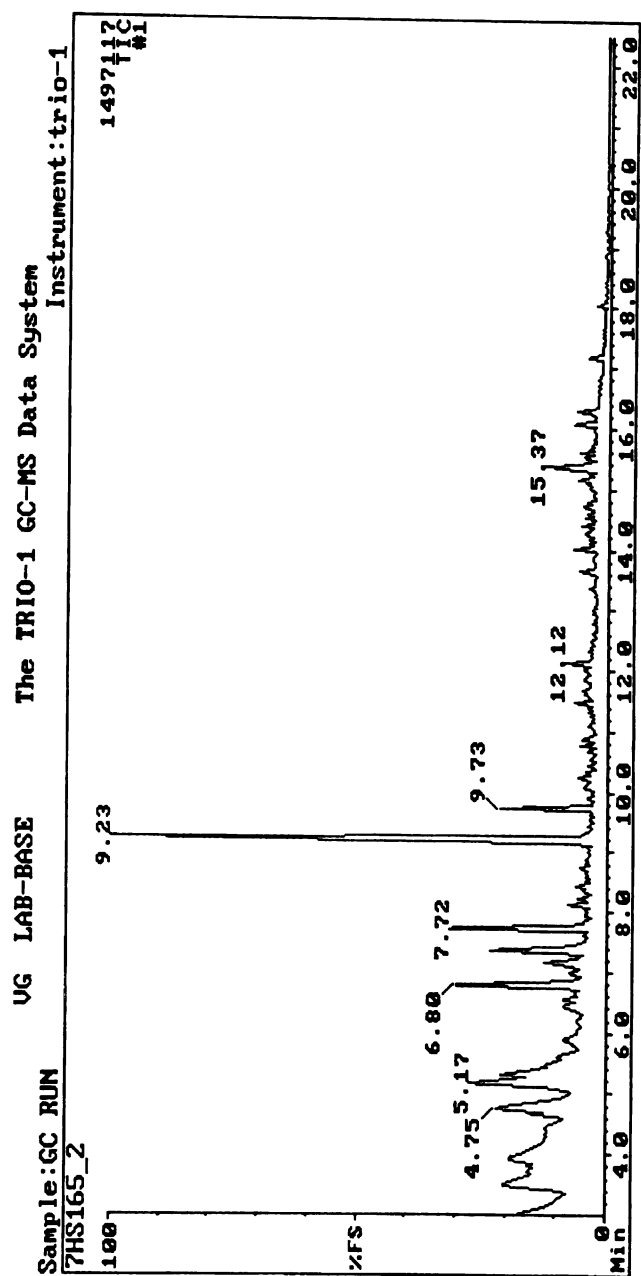


Figure 58. GC spectrum obtained from the MJ0400 catalyzed condensation of ASA and DKFP.

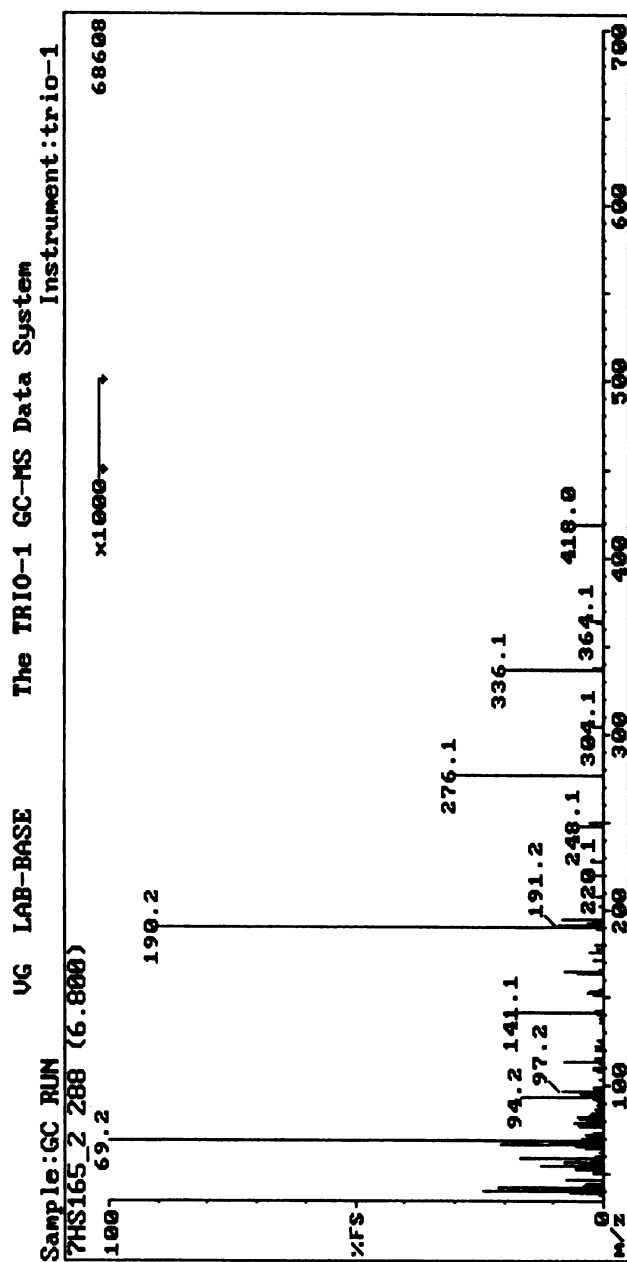
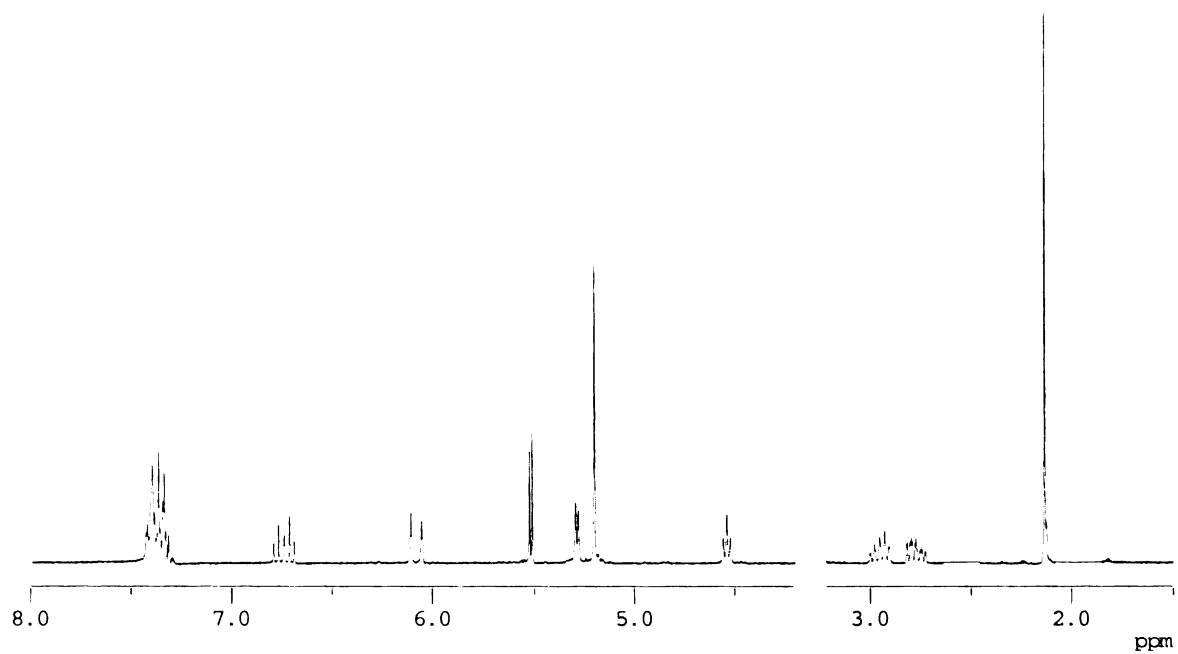
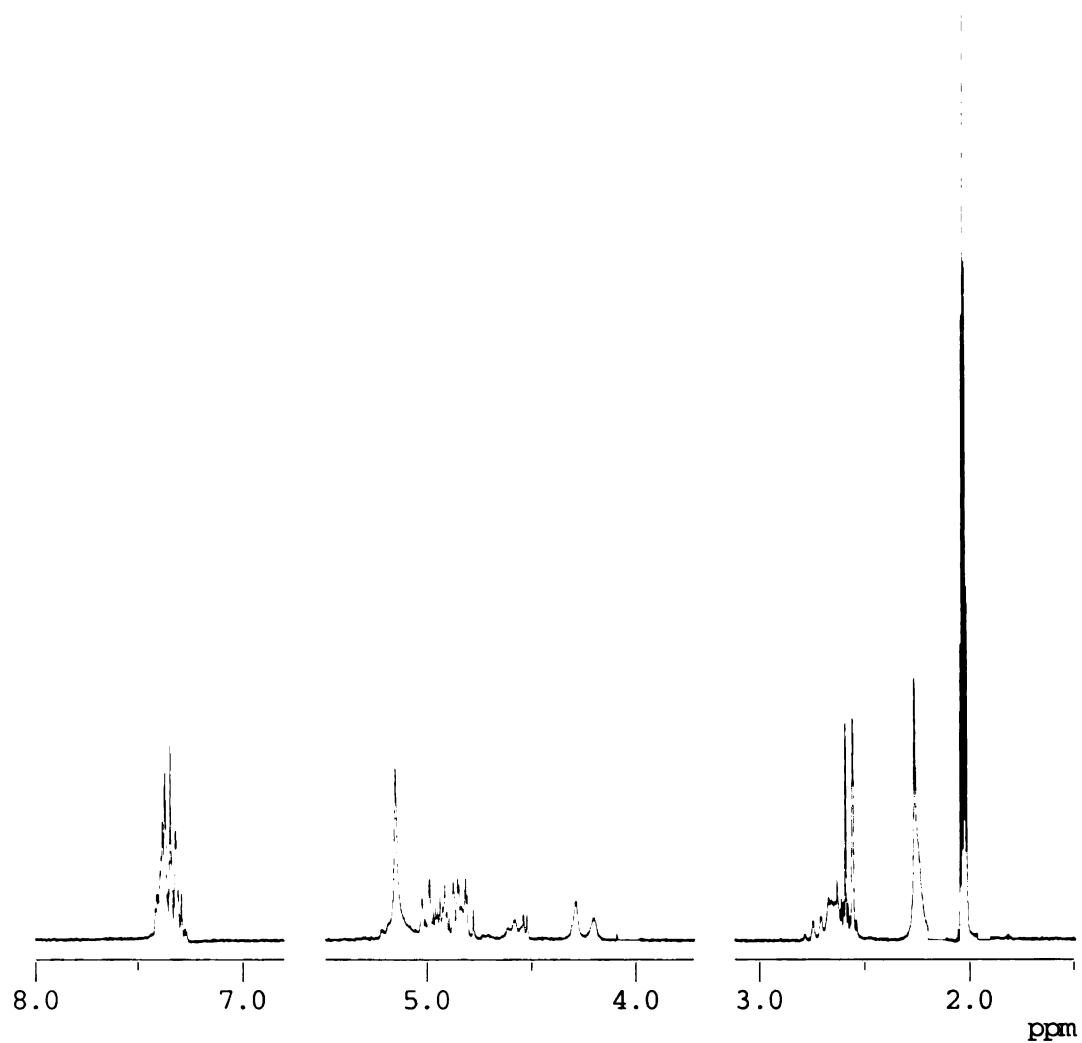


Figure 59. Example of a mass spectrum obtained from the GC-MS analysis of the MJ0400 catalyzed condensation of ASA and DKFP.



**Figure 60.**  $^1\text{H}$  NMR spectrum of (4S)-3-carbobenzyloxy-5-oxo-4-(4-oxo-pent-2-enyl)-oxazolidine.





**Figure 61.** <sup>1</sup>H NMR spectrum of the product mixture produced upon asymmetric dihydroxylation of (4S)-3-carbobenzyloxy-5-oxo-4-(4-oxo-pent-2-enyl)-oxazolidine.

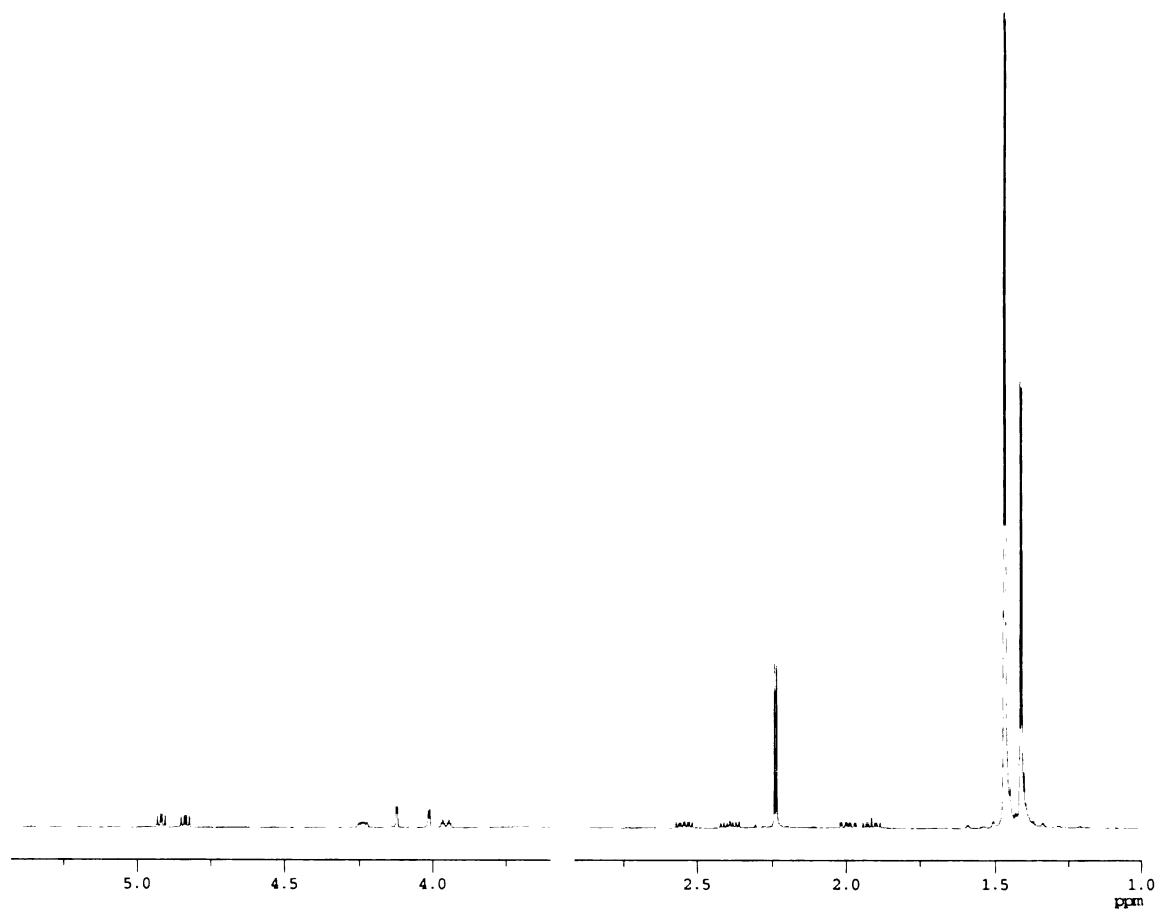


**Figure 62.** <sup>1</sup>H NMR spectrum of the diol mixture obtained upon Sharpless asymmetric dihydroxylation of *N,N*-Bis(*tert*-Butoxycarbonyl)amino-6-oxo-hept-4-enoic acid *tert*-butyl ester.

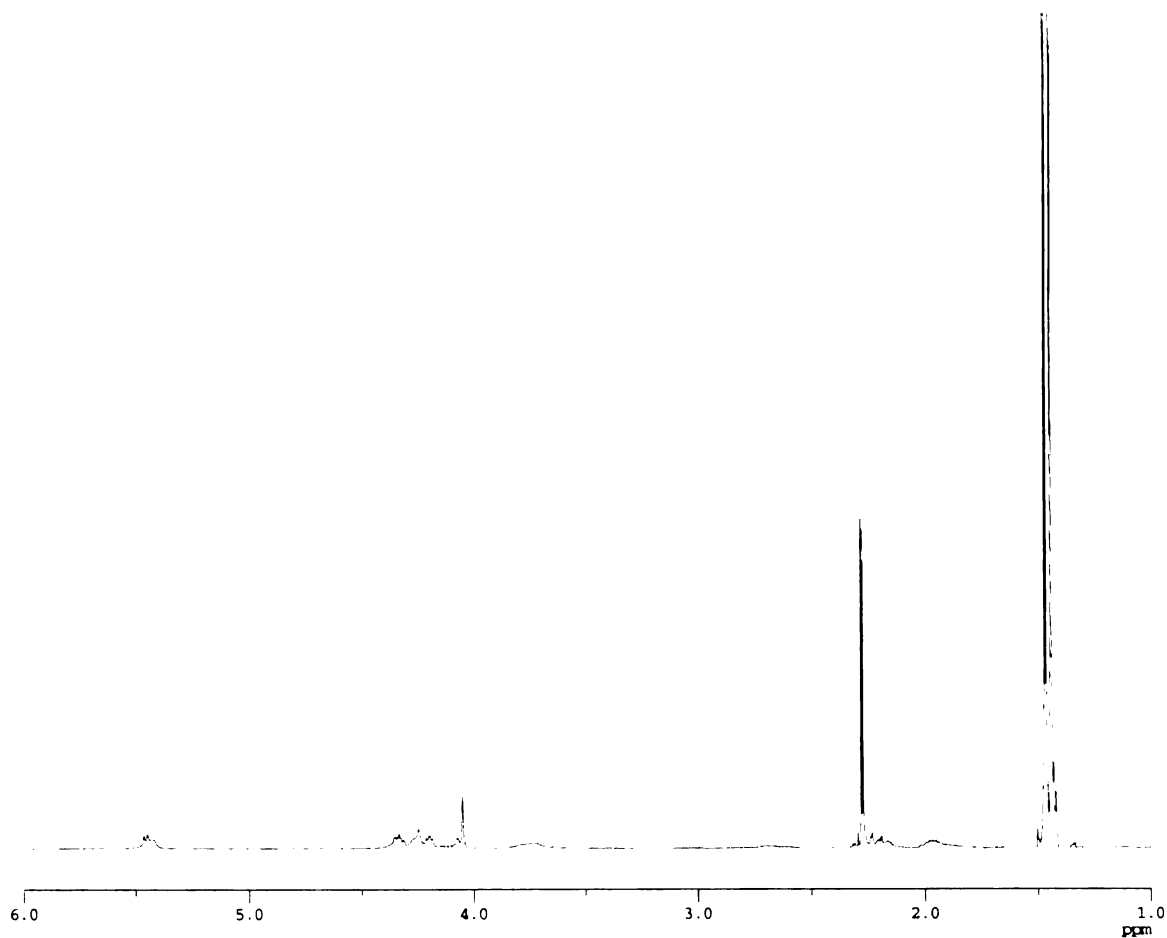


**Figure 63.**  $^1\text{H}$  NMR spectrum of diol mixture produced upon Sharpless asymmetric dihydroxylation of N-tert-Butoxycarbonylamino-6-oxo-hept-4-enoic acid tert-butyl ester.

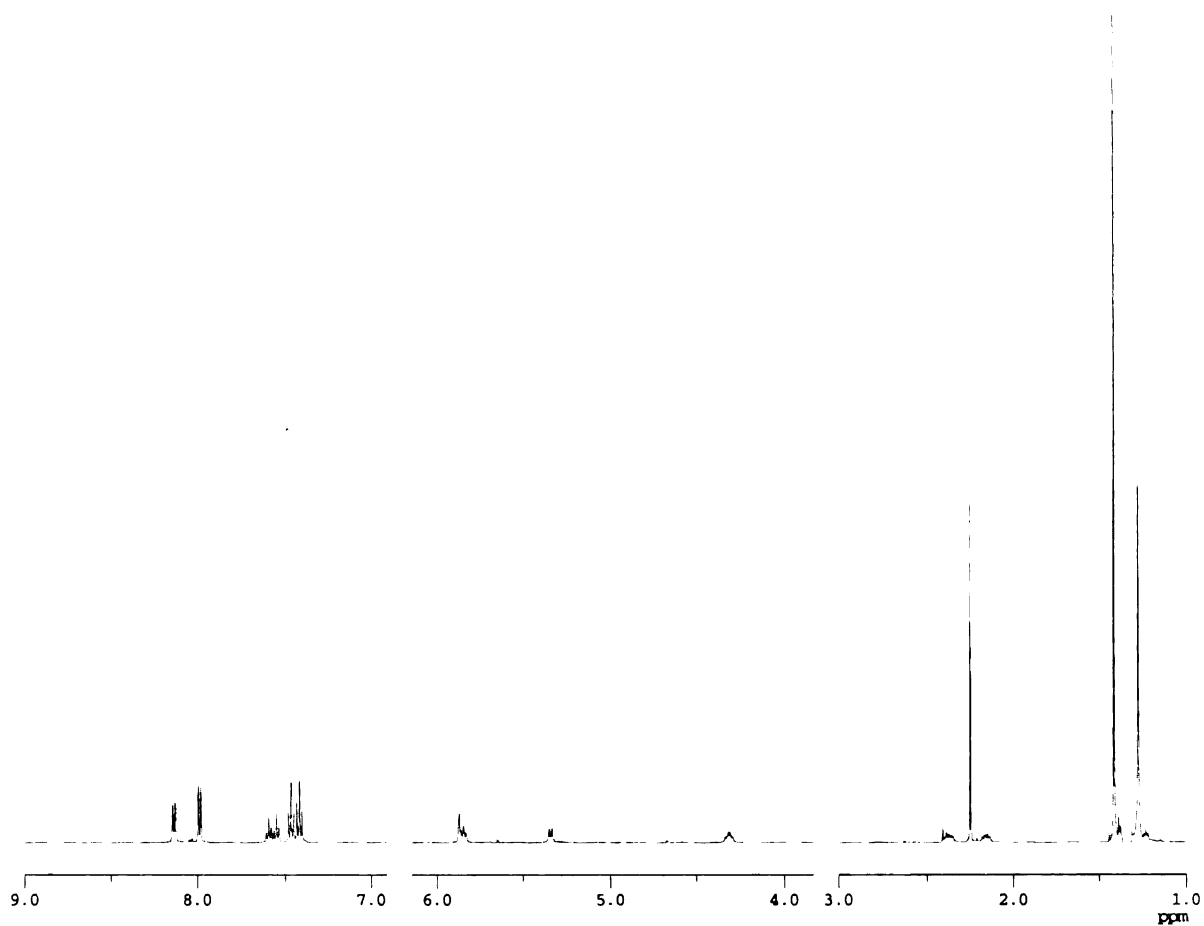


**Figure 64.** <sup>1</sup>H NMR spectrum of compound A isolated upon benzylation of the mono-boc protected diol mixture.

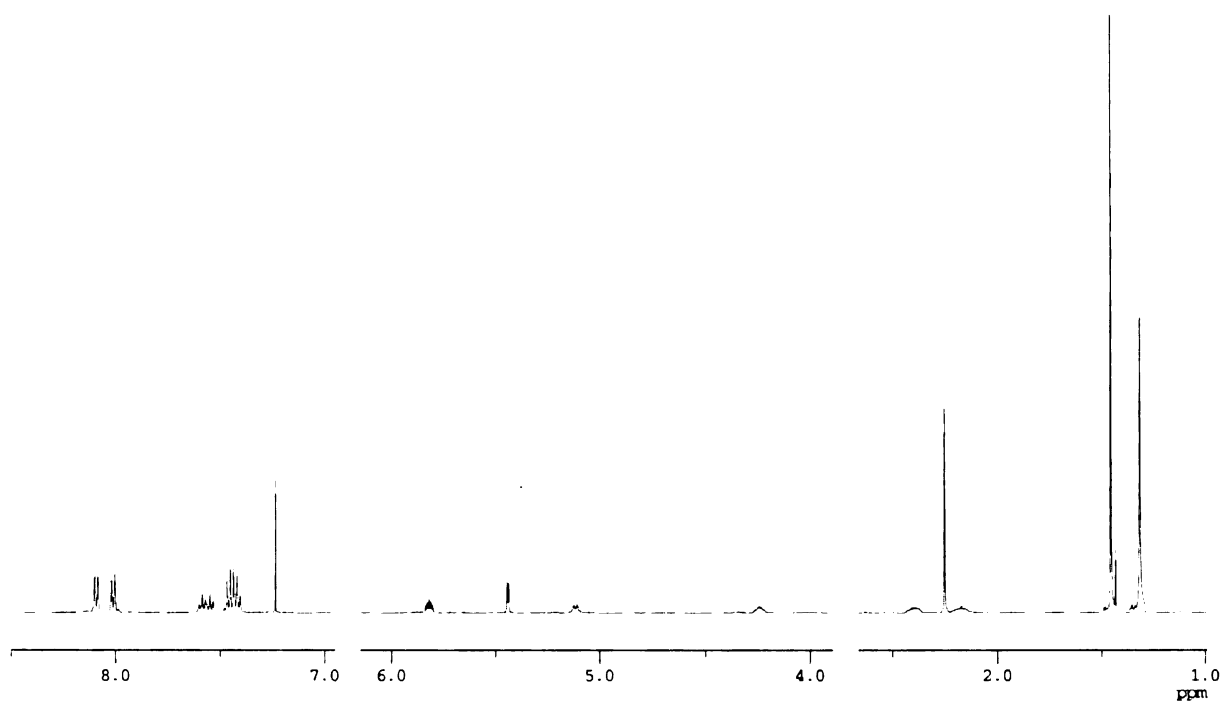


**Figure 65. <sup>1</sup>H NMR spectrum of compound B isolated upon the benzylation of the mono-boc protected diol mixture.**

## CHAPTER FOUR

### **EXPERIMENTALS**

#### GENERAL METHODS

##### **General Chemistry**

All reactions sensitive to air and moisture were carried out in flame-dried glassware under a positive atmosphere of argon. Air or moisture sensitive reagents and solvents were transferred to reaction flasks fitted with rubber septa via oven-dried syringes or cannula. Unless otherwise specified, all reactions were carried out at room temperature. Solvents were removed using either a Büchi rotary evaporator at water aspirator pressure or under high vacuum (0.5 mm Hg).

Acetone was dried over anhydrous  $\text{ZnCl}_2$ .  $\text{CH}_2\text{Cl}_2$ ,  $\text{Et}_3\text{N}$ , and pyridine were distilled from calcium hydride under argon. Tetrahydrofuran was distilled under argon from sodium/benzophenone. Methanol, ethyl ether, acetonitrile and toluene were distilled over sodium. Acetic anhydride was distilled over  $\text{P}_2\text{O}_5$ . Oxalyl chloride and 2,6-lutidine were distilled prior to use. Water used in synthesis was glass-distilled and deionized. All other reagents and solvents were used as available from commercial sources. Organic solutions of products were dried over anhydrous  $\text{Na}_2\text{SO}_4$  or  $\text{MgSO}_4$ . The sodium salt of 3-(trimethylsilyl)propionic-2,2,3,3- $d_4$  acid (TSP) was purchased from Lancaster Synthesis Inc. [Amine- $^{15}\text{N}$ ]-L-glutamine and [amide- $^{15}\text{N}$ ]-L-glutamine, were obtained from Cambridge Isotope Laboratories, Inc. [3- $^2\text{H}$ ]-glucose was purchased from Omicron Biochemicals Inc. *N*-Cbz-L-aspartic acid was purchased from EMD Biosciences, Inc. *N*-Boc-L-aspartic acid  $\beta$ -benzyl ester was purchased from Chem-Impex

International, Inc. All other reagents were purchased from Sigma-Aldrich or the MSU Chemistry stockroom.

### **Chromatography**

HPLC analysis was performed on an Agilent 1100 series HPLC with ChemStation acquisition software (Rev. A.08.03). Columns used include Agilent ZORBAX C-18 reverse phase analytical column (4.6 mm x 150mm), Agilent ZORBAX Bonus RP amide C-14 reverse phase analytical column (Agilent, 4.6 mm x 150 mm), Alltech C-18 reverse phase semi-prep column (22 mm x 250 mm), AXpak WA-624 weak anion exchange column (Showa Denko, 6 mm x 150 mm), and sugar KS-801 strong cation exchange column (Showa Denko, 8 mm x 300 mm). Solvents and samples were routinely filtered through 0.22- $\mu$ m membranes (Gelman Science). Analytes were detected at 254 nm.

Protein purification utilized an AKTA Purifier FPLC system with Unicorn acquisition software 4.10 (Amersham Biosciences). Columns used include HiPrep DEAE FF column (16 mm x 100 mm, 16 mL), a Resource Q column (6.4 mm x 30 mm, 1 mL and 16 mm x 30 mm, 6 mL), HiLoad Superdex 200 (prep grade) column (16 mm x 600 mm). All the columns were purchased from Amersham Biosciences. Solvents were routinely filtered through 0.22- $\mu$ m membranes (Gelman Science) and degassed under reduced pressure for 30 min prior to use. Proteins were detected at 260 nm.

AG1-X8 (acetate form and chloride form) was purchased from Bio-Rad. Ni-NTA resin was purchased from Qiagen. Dowex 1 (200-400 mesh, chloride form) and Dowex 50 (200-400 mesh, H<sup>+</sup>) were purchased from Sigma-Aldrich.

Radial chromatography was performed on a Harrison Associates Chromatotron (model 7924), using 1, 2 or 4 mm layers of silica gel 60 PF<sub>254</sub> containing gypsum (E. Merck). Silica gel 60 (40-63  $\mu\text{m}$ , E. Merck) was used for flash chromatography. Analytical thin-layer chromatography (TLC) utilized precoated glass plates of silica gel 60 F-254 (0.25 mm, Whatman). TLC plates were visualized by UV or by immersion in anisaldehyde stain (by volume: 93% ethanol, 3.5% sulfuric acid, 1% acetic acid, and 2.5% anisaldehyde) or phosphomolybdic acid stain (10% phosphomolybdic acid in absolute ethanol, w/v) followed by heating.

### Spectroscopic measurements

$^1\text{H}$  NMR and  $^{13}\text{C}$  NMR spectra were recorded on a Varian VX-300 FT-NMR or a Varian VX-500 FT-NMR spectrometer. Chemical shifts for  $^1\text{H}$  NMR spectra are reported (in parts per million) relative to internal tetramethylsilane ( $\text{Me}_4\text{Si}$ ,  $\delta = 0.0$  ppm) with  $\text{CDCl}_3$  as solvent and to sodium 3-(trimethylsilyl)propionate-2,2,3,3- $d_4$  (TSP,  $\delta = 0.0$  ppm) when  $\text{D}_2\text{O}$  was the solvent. When DMSO or acetone were used as the solvent the chemical shifts were reported relative to the solvent peaks. The following abbreviations are used to describe spin multiplicity: s (singlet), d (doublet), t (triplet), q (quartet), m (unresolved multiplet), dd (doublet of doublets), b (broad).  $^{13}\text{C}$  NMR spectra were recorded at 125 MHz. Chemical shifts for  $^{13}\text{C}$  NMR spectra are reported (in parts per million) relative to internal tetramethylsilane ( $\text{Me}_4\text{Si}$ ,  $\delta = 0.0$  ppm) with  $\text{CDCl}_3$  as solvent and to sodium 3-(trimethylsilyl)propionate-2,2,3,3- $d_4$  (TSP,  $\delta = 0.0$  ppm) when  $\text{D}_2\text{O}$  was the solvent, or the solvent peak for acetone- $d_6$ .  $^{31}\text{P}$  NMR spectra were recorded on a 121 MHz Varian spectrometer and chemical shifts are reported (in parts per million)



relative to external 85% phosphoric acid (0.0 ppm). UV and visible measurements were recorded on a Perkin-Elmer Lambda 3b UV-Vis spectrophotometer or on a Hewlett Packard 8452A Diode Array Spectrophotometer equipped with HP 89532A UV-Visible Operating Software. Fast atom bombardment (FAB) mass spectra were obtained on a double focusing Kratos MS50 mass spectrometer at Michigan State University and electrospray ionization (ESI) mass spectra were obtained on a direct infusion electrospray mass spectrometer at Department of Chemistry and Biochemistry at University of South Carolina.

Concentrations of culture and cell-free reaction products were determined by comparison of the integrals corresponding to each compound with the integral corresponding to TSP ( $\delta=0.00$  ppm) in the  $^1\text{H}$  NMR. Compounds were quantified using the following resonances: kanosamine ( $\delta$  5.27, d, 0.45 H), UDPG ( $\delta$  5.55, dd, 1.0 H), 3-ketoUDPG ( $\delta$  4.49, dd, 1.0 H). UDPK ( $\delta$  5.67, dd, 1.0 H). Concentrations of above compounds derived from their respective  $^1\text{H}$  NMR integral values tended to be overestimated and their precise concentrations were calculated by application of the following formulas:  $[\text{kanosamine (mM)}]_{\text{actual}} = 0.78 \times [\text{kanosamine (mM)}]_{\text{NMR}} + 0.15$ ;  $[\text{UDP-glucose (mM)}]_{\text{actual}} = 0.93 \times [\text{UDP-glucose (mM)}]_{\text{NMR}} + 0.10$ ;  $[\text{3-ketoUDPG } (\mu\text{M})]_{\text{actual}} = 1.01 \times [\text{3-ketoUDPG } (\mu\text{M})]_{\text{NMR}} - 0.96$ . The formula for UDPG was used for UDPK. These equations were obtained as follows: A known quantity of each compound was dissolved in 10 mL of  $\text{D}_2\text{O}$  to obtain a stock solution. Various known volumes of the stock solution of each compound were concentrated under reduced pressure and redissolved in 1 mL of  $\text{D}_2\text{O}$  containing 10 mM TSP and their  $^1\text{H}$  NMR spectra were recorded. The solute concentration in each sample that was estimated for  $^1\text{H}$  NMR was

plotted against the calculated concentration for that sample resulting in the calibration curve. The equation for 3-ketoUDPG was obtained as follows: Samples of known concentration of UDPG were prepared and injected on the HPLC. A calibration curve was generated by plotting the peak area against the sample concentration. Several NMR samples containing different concentrations of 3-ketoUDPG were then injected onto the HPLC. Using the calibration curve generation for UDPG the sample concentrations were calculated. The HPLC generated concentrations of 3-ketoUDPG were then plotted against the concentrations calculated by  $^1\text{H}$  NMR to create a calibration curve.

## **Chemical Assays**

### **Organic and Inorganic Phosphate Assay**

Reagents used to quantify both organic phosphate and inorganic phosphate include 10 %  $\text{Mg}(\text{NO}_3)_2$  (w/v, dissolved in ethanol), 0.5 M HCl, 10% ascorbic acid (w/v, dissolved in  $\text{H}_2\text{O}$ ), and 0.42%  $(\text{NH}_4)_2\text{MoO}_4$  (w/v, dissolved in 1 M  $\text{H}_2\text{SO}_4$ ). The assay solution (freshly mixed) consists of one volume of 10% ascorbic acid and six volumes of 0.42%  $(\text{NH}_4)_2\text{MoO}_4$ .

To assay for organic phosphate, 100  $\mu\text{L}$  of 10%  $\text{Mg}(\text{NO}_3)_2$  was added to a test tube (13 mm x 100 mm) containing 100  $\mu\text{L}$  of sample. The resulting mixture was then evaporated to dryness over a flame, leaving a white solid. To this test tube was added 600  $\mu\text{L}$  of 0.5 M HCl. After the white solid was dissolved, the solution was heated at 100  $^\circ\text{C}$  for 15 min in a boiling water bath. Assay solution (1400  $\mu\text{L}$ , described above) was added to the cooled sample and the resulting mixture was kept at 45  $^\circ\text{C}$  for 20 min. If the

original sample contains either inorganic phosphate or any organic phosphate, a blue color will develop.

To assay for inorganic phosphate, 600  $\mu\text{L}$  of 0.5 M HCl and 1400  $\mu\text{L}$  of assay solution were directly added to a test tube containing 100  $\mu\text{L}$  of sample. The resulting reaction mixture was then heated at 45 °C for 20 min. Blue color is developed if sample contains inorganic phosphate.

The phosphate concentration of a sample was quantified by comparing the absorbance at 820 nm of the sample to a standard curve that is prepared using a phosphorous standard solution (0.65 mM in 0.05 M HCl, Sigma 661-9).

#### **Ninhydrin assay**

The ninhydrin reagent contains NaOAc (15%, w/v), sulfolane (40%, v/v), ninhydrin (2%, w/v), and hydrindantin (0.36%, w/v) in  $\text{H}_2\text{O}$ . The pH of the reagent was adjusted to 2.5 with glacial acetic acid and the reagent was then filtered through filter paper.

An aliquot (50  $\mu\text{L}$ ) of the sample was added to a test tube (13 mm x 100 mm) containing 500  $\mu\text{L}$  of ninhydrin reagent. The resulting mixture was heated at 100 °C for 5 min. A purple color develops if the sample contains free amino group. The concentration of amino group containing compound in a sample was quantified by comparing the absorbance at 570 nm of the sample to a standard curve that is prepared using glycine as the standard.

## Bacterial Strains and Plasmids

*E. coli* DH5 $\alpha$  [F' *endA1 hsdR17(r<sub>K</sub>m<sup>+</sup><sub>K</sub>) supE44 thi-1 recA1 gyrA relA1  $\phi$ 80lacZ $\Delta$ M15  $\Delta$ (lacZYA-argF)<sub>U169</sub>] and JM109 [*el4*-(*McrA*-) *recA1 endA1 gyrA96 thi-1 hsdR17(r<sub>K</sub>m<sup>+</sup><sub>K</sub>) supE44 relA1  $\Delta$ (lac-proAB)* [F' *traD36 proAB lacI<sup>Q</sup>DM15*]] were obtained previously by this laboratory. *Amycolatopsis mediterranei* (ATCC 21789) and *B. pumilus* (ATCC 21143) were purchased from the American Type Culture Collection (ATCC). *A. tumefaciens* (NCPPB 396) was obtained from the National Collection of Plant Pathogenic Bacteria (NCPPB). *A. mediterranei* RM01 (Rif<sup>L</sup>) and *A. mediterranei* HGF003 (Rif<sup>K</sup>) were obtained previously from Professor Heinz G. Floss (University of Washington). Plasmid constructions were carried out in *E. coli* DH5 $\alpha$ . BL21 Codon Plus RP (F' *ompT hsdS*(r<sub>B</sub><sup>-</sup> m<sub>B</sub><sup>-</sup>) *dcm*<sup>+</sup> Tet<sup>r</sup> *gal endA* Hte [*argU proL* Cam<sup>r</sup>]), BL21 (DE3) Codon Plus RIL (F' *ompT hsdS*(r<sub>B</sub><sup>-</sup> m<sub>B</sub><sup>-</sup>) *dcm*<sup>+</sup> Tet<sup>r</sup> *gal  $\lambda$* (DE3) *endA* Hte [*argU ileY leuW* Cam<sup>r</sup>] ), and BL21 Codon Plus RIL (F' *ompT hsdS*(r<sub>B</sub><sup>-</sup> m<sub>B</sub><sup>-</sup>) *dcm*<sup>+</sup> Tet<sup>r</sup> *gal endA* Hte [*argU ileY leuW* Cam<sup>r</sup>]) were obtained from Stratagene. *Agrobacterium tumefaciens* NCPPB 396 was obtained from the National Collection of Plant Pathogenic Bacteria. The plasmid pMJ0400 was obtained from Prof. Robert H. White. The plasmids pJG7.259 (*T<sub>5</sub>, lacO, lacO, 6xhis, rifK, lacI<sup>Q</sup>, Amp<sup>r</sup>*), pJG7.275 (*P<sub>lac</sub>, rifL, lacI<sup>Q</sup>, Amp<sup>r</sup>*), and pJG7.246 (*T<sub>5</sub>, lacO, lacO, 6xhis, lacI<sup>Q</sup>, Amp<sup>r</sup>*) were obtained from Jiantao Guo. The plasmid pRM030 had previously been obtained from Prof. Heinz G. Floss.*

## Storage of Bacterial Strains and Plasmids

All bacterial strains were stored at -78 °C in glycerol. Plasmids were transformed into *E. coli* DH5 $\alpha$  for long-term storage. Glycerol samples were prepared by adding 0.75

mL of an overnight culture to a sterile vial containing 0.25 mL of 80% (v/v) glycerol. The solution was mixed, left at room temperature for 1h, and then stored at -78 °C.

### **Culture Medium**

Bacto tryptone, Bacto tryptone peptone, Bacto yeast extract, Bacto malt extract, agar, and soytone were purchased from Difco. Casein enzyme hydrolysate was obtained from Sigma. Meat extract was obtained from Fluka. Soy flour and peanut meal were purchased from ICN Bioscience. Nutrient agar was purchased from Oxoid.

All solutions were prepared in distilled, deionized water. LB medium<sup>106</sup> (1 L) contained Bacto tryptone (10 g), Bacto yeast extract (5 g), and NaCl (10 g). Terrific Broth (1 L) contained Bacto tryptone (12 g), Bacto yeast extract (24 g), glycerol (4 mL),  $\text{KH}_2\text{PO}_4$  (2.31 g), and  $\text{K}_2\text{HPO}_4$  (12.54 g). YT medium (1L) contained Bacto tryptone (16 g), Bacto yeast extract (10 g), NaCl (5 g). NZCYM medium (1 L) contained NZ amine (10 g), NaCl (5 g), Bacto yeast extract (5 g), CAS amino acids (1 g),  $\text{MgSO}_4 \cdot 7\text{H}_2\text{O}$  (2 g). Both YT and NZCYM media were adjusted to pH 7.0 with 50  $\mu\text{L}$  10 N NaOH solution before autoclaving. Antibiotics were added where required to the following final concentrations: chloramphenicol (Cm), 34  $\mu\text{g/mL}$ ; ampicillin (Ap), 50  $\mu\text{g/mL}$ ; kanamycin (Kan), 50  $\mu\text{g/mL}$ . Isopropyl  $\beta$ -D-thiogalactopyranoside (IPTG) or lactose was added to the culture medium of strains containing inducible promoters including  $P_{lac}$ ,  $P_{T7}$ , or  $P_{TS}$ . Inorganic salts, D-glucose, and  $\text{MgSO}_4$  solutions were autoclaved separately while antibiotics and IPTG were sterilized by passage through a 0.22- $\mu\text{m}$  membrane. Solid medium was prepared by the addition of 1.5% (w/v) agar to the liquid medium.

*A. mediterranei* was grown in YMG or vegetative medium. YMG medium (1 L) contained Bacto yeast extract (4 g), Bacto malt extract (10 g), and glucose (4 g). Vegetative medium<sup>107</sup> (1 L) contained meat extract (5 g), Bacto tryptone peptone (5 g), Bacto yeast extract (5 g), casein enzyme hydrolysate (2.5 g), glucose (20 g), and NaCl (1.5 g). Solid YMG was prepared by the addition of 1.5% (w/v) agar to the liquid medium.

*B. pumilus* was grown either on solid nutrient agar or in liquid SSNG medium. Nutrient agar plates were prepared by the addition of 2.8% (w/v) nutrient agar to H<sub>2</sub>O. SSNG medium<sup>108</sup> (1 L) contained soy flour (15 g), soytone (1 g), NaCl (6 g), and glucose (10 g). D-Glucose (20% w/v) was autoclaved separately.

*A. tumefaciens* was grown on solid MP medium or in liquid AB/sucrose medium. MP medium (1 L) contained Bacto peptone (5 g) and meat extract (3 g). AB sucrose medium (1 L) contained KH<sub>2</sub>PO<sub>4</sub> (5.4 g), Bacto yeast extract (0.5 g), Na<sub>2</sub>HPO<sub>4</sub> · 2H<sub>2</sub>O (10.8 g), and sucrose (20 g). After the medium cooled 10 mL of urea solution (0.9 g), and 10 mL of trace element solution containing MgSO<sub>4</sub> · 7H<sub>2</sub>O (0.15 g), CaCl<sub>2</sub> · 2H<sub>2</sub>O (0.025 g), FeSO<sub>4</sub> · 7H<sub>2</sub>O (0.01 g), and citric acid (0.16 g) at pH 7.0 were added. Sucrose (20% w/v) was autoclaved separately. Solid MP medium was prepared by the addition of 1.5% (w/v) agar to the liquid medium.

### **Analysis of culture supernatant**

Samples (1 mL) of the culture were taken at timed intervals and the cells were removed by microcentrifugation. Cell densities of *E. coli* were determined by

measurement of absorption at 600 nm ( $OD_{600}$ ) after dilution if necessary. Cell densities of *A. mediterranei* and *B. pumilus* were not measured.

Solute concentrations in the cell-free culture supernatant were determined by  $^1\text{H}$  NMR. Solutions were concentrated to dryness under reduced pressure, concentrated to dryness an additional time from  $\text{D}_2\text{O}$ , and then redissolved in  $\text{D}_2\text{O}$  containing a known concentration of the sodium salt of 3-(trimethylsilyl)propionic-2,2,3,3- $d_4$  acid (TSP). Concentrations were determined by comparison of the integrals corresponding to each compound with the integral corresponding to TSP ( $\delta=0.00$  ppm) in the  $^1\text{H}$  NMR. Compounds were quantified using the following resonances: kanosamine ( $\delta$  5.27, d, 0.45 H), UDPG ( $\delta$  5.55, dd, 1.0 H), and 3-ketoUDPG ( $\delta$  4.49, dd, 1.0 H). The concentrations of UDPG, 3-ketoUDPG, and kanosamine were calculated by application of the previously described calibration formulae.

## Genetic Manipulations

### General procedures

Standard protocols were used for construction, purification, and analysis of plasmid DNA. *E. coli* DH5 was used as the host strain for plasmid manipulations. dNTP's, and agarose (electrophoresis grade) were purchased from Invitrogen. *Pfu* turbo DNA polymerase and *pfu* DNA polymerase reaction buffer were purchased from Stratagene. Fastlink DNA ligase was purchased from Epicentre. Restriction enzymes were purchased from Invitrogen or New England Biolabs. Calf intestinal alkaline phosphatase was purchased from New England Biolabs. PCR amplifications were performed as described by Sambrook. <sup>Error! Bookmark not defined.</sup> Each reaction (0.50 mL)

contained 2.5  $\mu$ L of *pfu* DNA polymerase reaction buffer (10X concentration), dATP (0.2 mM), dCTP (0.2 mM), dGTP (0.2 mM), dTTP (0.2 mM), template DNA (0.02  $\mu$ g or 1  $\mu$ g), 0.5  $\mu$ M of each primer, 0.5 units of *pfu* Turbo polymerase, and 2  $\mu$ L DMSO. Primers were synthesized by the Macromolecular Structure Facility at Michigan State University.

SEVAG is a mixture of chloroform and isoamyl alcohol (24:1 v/v). TE buffer contained 10 mM Tris-HCl (pH 8.0) and 1 mM disodium EDTA (pH 8.0). Endostop solution (10X concentration) contained 50% glycerol (v/v), 0.1 M disodium EDTA (pH 7.5), 1% sodium dodecyl sulfate (SDS) (w/v), 0.1% bromophenol blue (w/v), and 0.1% xylene cyanole FF (w/v) and was stored at 4 °C. Prior to use, 0.12 mL of DNase-free RNase was added to 1 mL of 10X Endostop solution.

### **Determination of DNA concentration**

The concentration of DNA in a sample was determined as follows: an aliquot (10  $\mu$ L) of the DNA solution was diluted to 1 mL in TE and the absorbance at 260 nm was measured relative to the absorbance of TE. An absorbance of 1.0 at 260 nm corresponds to 50  $\mu$ g/mL of double stranded DNA.

### **Large scale purification of plasmid DNA**

Plasmid DNA was purified on a large scale using a modified lysis method as described by Sambrook et al. <sup>Error! Bookmark not defined.</sup> In a 2 L Erlenmeyer flask, 500 mL of LB medium containing the appropriate antibiotic was inoculated from a single colony, and the culture was incubated at 37 °C (*E. coli* strains harboring plasmids used for two-



hybrid experiments were grown at 30 °C) for approximately 12 h (24 h if culturing at 30 °C) with agitation at 250 rpm. In cases where the plasmid did not possess an antibiotic marker, 500 mL of M9 minimal medium was used and the culture was shaken (250 rpm) at 37°C for 24 h. Cells were harvested by centrifugation (4000g, 5 min, 4 °C) and then resuspended in 10 mL of cold solution 1 (50 mM glucose, 20 M Tris-HCl, pH 8.0, 10 mM EDTA, pH 8.0) into which lysozyme (5 mg/mL) had been added immediately before use. The suspension was stored at room temperature for 5 min. Addition of 20 mL of solution 2 (1% SDS (w/v) in 0.2 N NaOH) was followed by gentle mixing and storage on ice for 15 min. Fifteen milliliters of ice cold solution 3 (prepared by mixing 60 mL of 5 M KOAc, 11.5 mL of glacial acetic acid, and 28.5 mL of water) was added. Vigorous shaking resulted in formation of a white precipitate. After the suspension was stored on ice for 10 min, the cellular debris was removed by centrifugation (48000g, 20 min, 4 °C). The supernatant was transferred to two centrifuge bottles and isopropanol (0.6 volumes) was added to precipitate the DNA. After the samples were left at room temperature for 15 min, the DNA was recovered by centrifugation (20000g, 20 min, 4 °C). The DNA pellet was rinsed with 70% ethanol and dried.

The isolated DNA was dissolved in TE (3 mL) and transferred to a Corex tube. Cold 5 M LiCl (3 mL) was added and the solution was gently mixed. The sample was centrifuged (12000g, 10 min, 4 °C) to remove high molecular weight RNA. The clear supernatant was transferred to a Corex tube and isopropanol (6 mL) was added followed by gentle mixing. The precipitated DNA was collected by centrifugation (12000g, 10 min, 4°C). The DNA was then rinsed with 70% ethanol and dried. After redissolving the DNA in 0.5 mL of TE containing 20 µg/mL of RNase, the solution was transferred to a

1.5 mL microcentrifuge tube and stored at rt for 30 min. DNA was precipitated from the solution upon addition of 500  $\mu$ L of 1.6 M NaCl containing 13% PEG-8000 (w/v). The solution was mixed and microcentrifuged (10 min, 4 °C) to recover the precipitated DNA. The supernatant was removed and the DNA was then redissolved in 400  $\mu$ L of TE. The sample was extracted sequentially with phenol (400  $\mu$ L), phenol and SEVAG (400  $\mu$ L each), and finally SEVAG (400  $\mu$ L). Ammonium acetate (10 M, 100  $\mu$ L) was added to the aqueous DNA solution. After thorough mixing, 95% ethanol (1 mL) was added to precipitate the DNA. The sample was left at rt for 5 min and then microcentrifuged for 5 min at 4 °C. The DNA was rinsed with 70% ethanol, dried, and then redissolved in 250-500  $\mu$ L of TE.

Large scale purifications of plasmid DNA were also performed by using the Maxi Kit (Qiagen) following the protocol supplied by the manufacturer.

### **Small scale purification of plasmid DNA**

An overnight culture (5 mL) of the plasmid-containing strain was grown in LB medium containing the appropriate antibiotics. In cases where nutritional pressure was used to maintain plasmid, 5 mL of M9 minimal medium was used and the culture grown for 24 h. Cells from 3 mL of the culture were collected in a 1.5 mL microcentrifuge tube by microcentrifugation. The harvested cells were resuspended in 0.1 mL of cold solution 1 into which lysozyme (5 mg mL<sup>-1</sup>) was added immediately before use. The suspension was incubated on ice for 10 min and then treated with solution 2. The mixture was shaken gently and kept on ice for 5-10 min. To this sample was added 0.15 mL of cold solution 3, and the mixture was shaken vigorously, resulting in formation of a thick white

precipitate. The sample was stored on ice for 5 min, after which the precipitate was removed by microcentrifugation (15 min, 4°C). The supernatant was transferred to another microcentrifuge tube and extracted with equal volumes of phenol and SEVAG (0.2 mL each). The aqueous phase (approximately 0.5 mL) was transferred to a microfuge tube and the DNA was precipitated by addition of 95% ethanol (1 mL). The sample was left at room temperature for 5 min before microcentrifugation (15 min, rt) to isolate the DNA. The DNA pellet was rinsed with 70% ethanol, dried, and redissolved in 50-100 µL TE. DNA isolated from this method was used for restriction enzyme analysis.

### **Restriction enzyme digest of DNA**

A typical digest (10 µL) contained approximately 7.5 µL of DNA (0.1 µg/µL in TE), 1 µL of restriction enzyme buffer (10X concentration), 1 µL of restriction enzyme, and 0.5 µL of bovine serum albumin (BSA, 2 mg/mL). Reactions were incubated at 37 °C for 1 h. Digests were terminated by addition of 1 µL of Endostop solution (10X concentration) and subsequently analyzed by agarose gel electrophoresis.

When DNA was required for subsequent cloning, restriction digests were terminated by addition of 1 µL of 0.5 M EDTA (pH 8.0) followed by extraction of the DNA with equal volumes of phenol and SEVAG and precipitation of the DNA. DNA was precipitated by addition of 0.1 volume of 3 M NaOAc (pH 5.2) followed by thorough mixing and the addition of 3 volumes of 95% ethanol. Samples were stored for at least 1 h at -78 °C. Precipitated DNA was recovered by microcentrifugation (15 min, 4 °C). Ethanol (70%) was added and the sample was microcentrifuged for 10 min at 4°C. Ethanol was then discarded, and the DNA was air dried and redissolved in TE.

Alternatively, the DNA was isolated from the reaction mixture using Zymoclean DNA Clean and Concentrate Kit (Zymo Research).

### **Agarose gel electrophoresis**

Agarose gels were run in TAE buffer containing 40 mM Tris-acetate and 2 mM EDTA (pH 8.0). Gels typically contained 0.7% agarose (w/v) in TAE buffer. Lower concentrations of agarose (0.3%) were used to resolve genomic DNA and electrophoresis was conducted at 4 °C instead of rt. Ethidium bromide (0.5 µg/ml) was added to the agarose to allow visualization of DNA fragments under a UV lamp. The size of the DNA fragments were determined by comparison to DNA fragments contained in the following: λ DNA digested with *Hind*III (23.1-kb, 9.4-kb, 6.6-kb, 4.4-kb, 2.3-kb, 2.0-kb, and 0.6-kb) and λ DNA digested with *Eco*RI and *Hind*III (21.2-kb, 5.1-kb, 5.0-kb, 4.3-kb, 3.5-kb, 2.0-kb, 1.9-kb, 1.6-kb, 1.4-kb, 0.9-kb, 0.8-kb, and 0.6-kb).

### **Isolation of DNA from agarose**

Zymoclean DNA Isolation Kit (Zymo Research) was used to isolate DNA from agarose. The band of agarose containing the DNA of interest was excised from the gel with a razor and transferred to a 1.5 mL microfuge tube. Three volumes of agarose dissolving buffer was added to each volume of agarose gel and the resulting suspension was incubated at 42°C with intermittent vortexing until the gel was completely dissolved. DNA in the dissolved agarose solution was subsequently purified using a Zymo-Spin Column.

### **Treatment of vector DNA with calf intestinal alkaline phosphatase (CIAP)**

Following restriction enzyme digestion, vectors were dephosphorylated to prevent self-ligation. Digested vector DNA was dissolved in TE (88  $\mu\text{L}$ ). To this sample was added 10  $\mu\text{L}$  of dephosphorylation buffer (10X concentration) and 2  $\mu\text{L}$  of calf intestinal alkaline phosphatase (2 units). The reaction was incubated at 37 °C for 1 h. Phosphatase was inactivated by the addition of 1  $\mu\text{L}$  of 0.5 M EDTA (pH 8.0) followed by heat treatment (65 °C, 20 min). The sample was extracted with phenol and SEVAG (100  $\mu\text{L}$  each) to remove the protein, and the DNA was precipitated as previously described and redissolved in TE. Alternatively, the DNA was isolated from the reaction mixture by using Zymoclean DNA Clean and Concentrator Kit.

### **Ligation of DNA**

DNA ligations were designed so that the molar ratio of insert DNA to vector DNA was 3 to 1. A typical ligation reaction contained 0.03 to 0.1  $\mu\text{g}$  of vector DNA and 0.05 to 0.2  $\mu\text{g}$  of insert DNA in a combined volume of 7  $\mu\text{L}$ . To this sample, 2  $\mu\text{L}$  of ligation buffer (5X concentration) and 1  $\mu\text{L}$  of T4 DNA ligase (2 units) were added. The reaction was incubated at 16 °C for at least 4 h and then was used to transform competent cells. In an alternative method, the Fast-link DNA Ligation Kit (Epicentre) was used according to the manufacturer's protocol.

### **Preparation and transformation of *E. coli* competent cells**

Competent cells were prepared using a procedure modified from Sambrook et al. A single colony was inoculated into 5 mL of LB containing the necessary antibiotics.

After overnight growth, an aliquot (1 mL) of the culture was transferred to a 500 mL Erlenmeyer flask containing 100 mL of LB containing the necessary antibiotics. The cells were cultured at 37 °C with shaking at 250 rpm until an OD<sub>600</sub> of 0.4-0.6 was reached. The entire culture was transferred to a centrifuge bottle that was sterilized with bleach and rinsed exhaustively with sterile water. The cells were harvested by centrifugation (4000g, 4 °C, 5 min) and the culture medium was discarded. All manipulations were carried out on ice during the remainder of the procedure. Harvested cells were resuspended in 100 mL of ice cold 0.9% NaCl. After centrifugation at 4000g and 4 °C for 5 min, the cells were resuspended in ice cold 100 mM CaCl<sub>2</sub> (50 mL) and stored on ice for 30 min. The cells were then collected by centrifugation (4000g, 5 min, 4 °C) and resuspended in 4 mL of ice cold 100 mM CaCl<sub>2</sub> containing 15% glycerol (v/v). Aliquots (0.25 mL) of competent cells were transferred to 1.5 mL microfuge tubes, frozen in liquid nitrogen, and stored at -78 °C.

In order to perform a transformation, frozen competent cells were thawed on ice for 5 min prior to use. A small aliquot (1 to 10 mL) of plasmid DNA or a ligation reaction was added to the thawed competent cells (0.1 mL). The solution was gently mixed and stored on ice for 30 min. The cells were then heat shocked at 42 °C for 2 min and then placed on ice for 2 min. LB (0.5 mL) was added to the cells, and the sample was incubated at 37 °C for 1 h (or 30 °C for 1.5 h with agitation). After incubation, cells were collected by microcentrifugation. If the transformation was to be plated onto LB plates, 0.5 mL of the culture supernatant was removed. The cells was then resuspended in the remaining 0.1 mL of LB and spread onto LB plates containing the appropriate antibiotics. If the transformation was to be plated onto minimal medium plates, all the

culture supernatant was removed. The cells were washed with 0.5 mL of M9 salts and collected by microcentrifugation. After removal of all the supernatant, the cells were resuspended in 0.1 mL of M9 salts and spread onto the appropriate plates. A sample of competent cells with no DNA added was also carried through the transformation procedure as a control. These cells were used to check the viability of the competent cells and to verify the absence of growth on selective medium.

## **General Enzymology**

### **General information**

*E. coli* and *B. pumilus* cells were harvested at 4000g for 5 min at 4°C and *A. mediterranei* were harvested at 11000g for 5 min at 4°C. Cells lysis was achieved by two passages through a French pressure cell (SLM Aminco) at 16,000 psi. Cellular debris was removed from the lysate by centrifugation (30000g, 30 min, 4 °C). Protein solutions were concentrated by ultrafiltration using either Millipore PM-10 membranes (10,000 MWCO) or Centricon concentrators (Amicon). Protein concentrations were determined using the Bradford dye-binding procedure<sup>109</sup> using protein assay solution purchased from Bio-Rad. The assay solution was prepared by diluting 20 mL of the Bio-Rad concentrate to 100 mL with water followed by gravity filtration of the resulting solution. Assay solution (5 mL) was added to an aliquot of protein containing solution (diluted to 0.1 mL) and the sample was vortexed. After allowing the color to develop for 5 min, the absorbance at 595 nm of the solution was measured. Protein concentrations were determined by comparison to a standard curve prepared using bovine serum albumin

Protein solutions were concentrated by ultrafiltration using Millipore PM-10 membranes. This type of membrane was also used to remove proteins from reaction mixtures. Cell lysis was achieved by two passes through a French pressure cell (SLM Amico) at 16000 psi. Cellular debris was separated from the lysate by centrifugation at 48 000g for 20 min at 4 °C. Protein concentrations were quantified using the Bradford dye-binding procedure with the assay solution from Bio-Rad. The presence of heterologously expressed proteins was confirmed by SDS-PAGE analysis. AHBA synthase activity was measured by using the procedure reported by Floss.

#### ***E. coli* UGPase (GalU) assay**

The UGPase specific activity was measured using a coupled enzyme assay at r.t. by monitoring the production of NADH at 340 nm. A typical assay solution contained 100 mM Triethanolamine HCl buffer (pH 8.0), NAD (1.4 mM),  $\text{MgCl}_2 \cdot 6 \text{H}_2\text{O}$  (4 mM), UDPG (1 mM), PPI (1.8 mM), glucose-6-phosphate dehydrogenase (3 units), phosphoglucomutase (3 units), and an appropriate amount of UGPase. The final assay volume was 1 mL. The increase in absorbance was monitored for 1 min. One unit of activity was defined as the amount necessary to produce 1  $\mu\text{mol}$  of NADH per min at r.t. and pH 8.0. A molar extinction coefficient of  $3440 \text{ L mol}^{-1} \text{ cm}^{-1}$  was used for activity calculations.

#### ***A. tumefaciens* glucoside-3-dehydrogenase activity assay**

UDP-3-keto-D-glucose dehydrogenase activity was measured at rt by monitoring the reduction of 2,6-dichloroindophenol (DCIP) at 600 nm in the presence of phenazine



methosulfate (PMS).<sup>110</sup> A typical reaction mixture contained 10 mM phosphate buffer (pH 7.0), 60  $\mu$ M 2,6-dichloroindophenol, 1 mM phenazine methosulfate, 1.5 mM UDP-glucose, and an appropriate amount of enzyme. The final assay volume was 1 mL. The decrease in absorbance at 340 nm was monitored for several minutes. One unit of enzyme activity was defined as the amount necessary to reduce 1  $\mu$ mol of 2,6-dichloroindophenol per min at 25°C and pH 7.0. A molar extinction coefficient for 2,6-dichloroindophenol of 21,000 L mol<sup>-1</sup> cm<sup>-1</sup> was used for activity calculations.<sup>111</sup>

#### ***A. mediterranei* UDPG dehydrogenase (Rif<sup>r</sup>) assay**

##### Assay Condition #1: DCIP/PMS assay

UDP-3-keto-D-glucose dehydrogenase activity was measured at rt by monitoring the reduction of 2,6-dichloroindophenol (DCIP) at 600 nm in the presence of phenazine methosulfate (PMS).<sup>112</sup> A typical reaction mixture contained 10 mM phosphate buffer (pH 7.0), 60  $\mu$ M 2,6-dichloroindophenol, 1 mM phenazine methosulfate, 1.5 mM UDP-glucose, and an appropriate amount of enzyme. The final assay volume was 1 mL. The decrease in absorbance at 340 nm was monitored for several minutes. One unit of enzyme activity was defined as the amount necessary to reduce 1  $\mu$ mol of 2,6-dichloroindophenol per min at 25°C and pH 7.0. A molar extinction coefficient for 2,6-dichloroindophenol of 21,000 L mol<sup>-1</sup> cm<sup>-1</sup> was used for activity calculations.<sup>113</sup>

##### Assay Condition #2: HPLC assay

UDP-glucose (0.054 g, 89  $\mu$ mol) was incubated with 10 mL BL21 Codon Plus RP/pJG7.275 cell-free lysate in the presence of DCIP (0.003 g, 9  $\mu$ mol), PMS (0.038 g,

124  $\mu\text{mol}$ ),  $\text{MgCl}_2 \cdot 6\text{H}_2\text{O}$  (0.012 g, 64  $\mu\text{mol}$ ), and *p*-hydroxy benzoic acid (0.02 g, 144  $\mu\text{mol}$ ) at 30°C for 2 h. The *p*-hydroxy benzoic acid (PHBA) was added as an internal reference. 400  $\mu\text{L}$  samples were removed every 15 min for 1 h and quenched with 50  $\mu\text{L}$  10% TCA. The samples were vortexed and the precipitated proteins were removed by centrifugation (14000g, 1 min). 300  $\mu\text{L}$  supernatant were diluted to 640  $\mu\text{L}$  with distilled deionized  $\text{H}_2\text{O}$ . 200  $\mu\text{L}$  were then diluted again to 1 mL with distilled deionized  $\text{H}_2\text{O}$ . The samples were filtered through 0.22  $\mu\text{m}$  filters and 10  $\mu\text{L}$  were injected onto the HPLC. The specific activity was measured by following the formation of 3-ketoUDPG over time. One unit of specific activity was defined as the amount necessary to produce 1  $\mu\text{mol}$  of 3-ketoUDPG per min at 30°C and pH 7.5.

#### ***A. mediterranei* transaminase (RifK) assay**

UDP-3-keto-glucose (0.026 mg, 46  $\mu\text{mol}$ ) was incubated with 10 mL BL21 Codon Plus RP/pJG7.259 cell-free lysate in the presence of PLP (0.008 mg, 32  $\mu\text{mol}$ ), L-glutamine (0.013 g, 89  $\mu\text{mol}$ ),  $\text{MgCl}_2 \cdot 6\text{H}_2\text{O}$  (0.01 g, 49  $\mu\text{mol}$ ) at 30°C for 2 h. 250  $\mu\text{L}$  aliquots were removed every 30 minutes and quenched with 50  $\mu\text{L}$  10% TCA. After removal of the proteins by centrifugation (14000g, 1 min), 200  $\mu\text{L}$  supernatant was diluted with 300  $\mu\text{L}$  distilled deionized  $\text{H}_2\text{O}$  and 100  $\mu\text{L}$  PHBA solution (1.2 mg/mL). After filtration 20  $\mu\text{L}$  of each sample was injected onto the HPLC. The specific activity was measured by following both the formation of UDPK and the loss of 3-ketoUDPG over time at 254 nm. A unit of specific activity was defined as the amount necessary to convert 1  $\mu\text{mol}$  of 3-ketoUDPG to UDPK per min at 30°C and pH 7.5.

### ***A. mediterranei* AHBA synthase (RifK) activity**

The AHBA synthase activity was measured at 30°C by monitoring the production of AHBA. A typical reaction contained 50 mM Tris·HCl (pH 7.5), 0.5 mM PMSF, 0.5 mM DTT, 5% w/v glycerol, 25 mM KCl, 0.3 mM aminoDHS, and an appropriate amount of BL21 Codon Plus RP/pJG7.259 cell-free lysate. The final reaction volume was 1 mL. The sample was incubated at 30°C for 1 h before the addition of 200  $\mu$ L 10% (w/v) TCA solution. The protein was removed by microcentrifugation, and the absorbance of the solution was measured at 296 nm. One unit of enzyme activity was defined as the amount necessary to produce 1  $\mu$ mol AHBA per min at 30°C and pH 7.5. A molar extinction coefficient for AHBA of 1891 L mol<sup>-1</sup> cm<sup>-1</sup> was used for calculations.

### **SDS-PAGE protein gel**

SDS-PAGE analysis was followed the procedure described by Harris et al.<sup>114</sup> The separating gel was prepared by mixing 3.33 mL of 30% acrylamide stock solution (w/v in H<sub>2</sub>O), 2.5 mL of 1.5 M Tris-HCl (pH 8.8), and 4 mL of distilled deionized water. After degassing the solution using a water aspirator for 20 min, 0.1 mL of 10% ammonium persulfate (w/v in H<sub>2</sub>O), 0.1 mL 10% SDS (w/v in H<sub>2</sub>O), and 0.005 mL of N, N, N', N'-tetramethylethylenediamine (TEMED) was added. After mixing gently, the separating gel was poured into the gel cassette to about 1.5 cm below the top of the gel cassette. *t*-Amyl alcohol was overlaid on the top of the solution and the gel was allowed to polymerize for 1 h at rt. The stacking gel was prepared by mixing 1.7 mL of 30% acrylamide stock solution, 2.5 mL of 0.5 M Tris-HCl (pH 6.8), and 5.55 mL of distilled deionized water. After degassing for 20 min, 0.1 mL of 10% ammonium persulfate, 0.1

mL 10% SDS, and 0.01 mL of TEMED was added, and the solution was mixed gently. *t*-Amyl alcohol was removed from the top of the gel cassette, which was subsequently rinsed with water and wiped dry. After insertion of the comb, the gel cassette was filled with stacking gel solution, and the stacking gel was allowed to polymerize for 1 h at rt. After removal of the comb, the gel cassette was installed into the electrophoresis apparatus. The electrode chamber was then filled with electrophoresis buffer containing 192 mM glycine, 25 mM Tris base, and 0.1% SDS. Each protein sample (10  $\mu$ L) was diluted with Laemmli sample buffer<sup>115</sup> (10  $\mu$ L, Sigma S-3401) consisting of 4% SDS, 20% glycerol, 10% 2-mercaptoethanol, 0.004% bromophenol blue, and 125 mM Tris-HCl (pH 6.8). Samples and markers (MW-SDS-200, Sigma) were loaded into the sample well and the gel was run under constant current at 30 mA when the blue tracking dye (bromophenol blue) was within stacking gel. After the blue tracking dye reached the separating gel, a higher current (50 mA) was applied to the gel. At the completion of electrophoresis (blue tracking dye reaches the bottom of the gel), the gels were removed from the cassettes and fixed in a solution of 10% (w/v) aqueous trichloroacetic acid for 30 min. After staining in a solution containing 0.1% (w/v) Coomassie Brilliant Blue R, 45% (v/v) MeOH, 10% (v/v) HOAc in H<sub>2</sub>O for 3 h, the protein gels were destained in a solution of 45% (v/v) MeOH, 10% (v/v) HOAc in H<sub>2</sub>O. The gels were then sealed in a sheet protector.

## CHAPTER TWO

### Synthetic preparations

#### Synthesis of [3-<sup>2</sup>H]-glucose

**1,2:5,6-Di-*O*-isopropylidene- $\alpha$ -D-glucofuranose.** To a solution of D-glucose (20 g, 111 mmol) in dry acetone (200 mL) was added ZnCl<sub>2</sub> (16 g, 117 mmol) and 85% H<sub>3</sub>PO<sub>4</sub> (0.6 mL). The reaction was stirred at r.t. for 40 h. The reaction mixture then filtered through Celite and the filtrate was adjusted to pH 7.0 with NaOH. The solvent was removed by rotary evaporation and the residue was extracted with in CH<sub>2</sub>Cl<sub>2</sub> (3 x 50 mL). The organic layer was washed with H<sub>2</sub>O (2 x 50 mL) and the organic layer was dried over Na<sub>2</sub>SO<sub>4</sub>. The solution was filtered and the CH<sub>2</sub>Cl<sub>2</sub> was removed by rotary evaporation to provide a white solid. The solid was recrystallized from EtOAc and hexanes to afford 1,2:5,6-Di-*O*-isopropylidene- $\alpha$ -D-glucofuranose (17.3 g, 60%). <sup>1</sup>H NMR (CDCl<sub>3</sub>):  $\delta$  5.90 (d, *J* = 3.5 Hz, 1 H), 4.49 (d, *J* = 3.5 Hz, 1 H), 4.29 (m, 2 H), 4.13 (dd, *J* = 8.5, 6 Hz, 1 H), 4.03 (dd, *J* = 8, 3 Hz, 1 H), 3.95 (dd, *J* = 8.5, 5 Hz, 1 H), 2.57(d, *J* = 4 Hz, 1 H), 1.46 (s, 3 H), 1.41 (s, 3 H), 1.34 (s, 3 H), 1.29 (s, 3 H). <sup>13</sup>C NMR (CDCl<sub>3</sub>):  $\delta$  111.9, 109.7, 105.3, 85.1, 81.2, 75.3, 73.5 67.7, 26.9, 26.8, 26.2, 25.2.

**1,2:5,6-Di-*O*-isopropylidene-3-keto- $\alpha$ -D-glucofuranose.** Acetic anhydride (23 mL, 209 mmol) was added to pyridinium dichromate (28 g, 74.4 mmol) in dry CH<sub>2</sub>Cl<sub>2</sub> (200 mL). 1,2:5,6-Di-*O*-isopropylidene- $\alpha$ -D-glucofuranose (19 g, 72.9 mmol) in 50 mL of CH<sub>2</sub>Cl<sub>2</sub> was added via canula to the reaction and the mixture was heated in an oil bath at 75°C for 6 h. After the completion of the reaction, the mixture was diluted with EtOAc (500 mL) and the precipitate was filtered. After evaporation of the solvent,

diethyl ether was added (250 mL) and the mixture was filtered again. Drying and concentration gave a yellow oil. Purification by flash chromatography (EtOAc/hexane, 1:1, v/v) afforded the ketone as a colorless oil (14.7 g, 91%).  $^1\text{H}$  NMR ( $\text{CDCl}_3$ ):  $\delta$  6.14 (d,  $J = 4.5$  Hz, 1 H), 4.39 (d,  $J = 4.5$  Hz, 1 H), 4.35–4.38 (m, 2 H), 4.01–4.03 (m, 2 H), 1.46 (s, 3 H), 1.43 (s, 3 H), 1.34 (s, 6 H).  $^{13}\text{C}$  NMR ( $\text{CDCl}_3$ ):  $\delta$  208.8, 114.3, 110.4, 103.1, 79.0, 77.3, 76.4, 64.3, 27.6, 27.2, 26.0, 25.3.

**1,2:5,6-Di-*O*-isopropylidene-[3- $^2\text{H}$ ]- $\alpha$ -D-allofuranose.** The 1,2:5,6-di-*O*-isopropylidene-3-keto- $\alpha$ -D-glucofuranose (5.0 g, 19.4 mmol) was dissolved in 31 mL of 90% EtOH.  $\text{NaBD}_4$  (2.0 g, 50 mmol) was added and the mixture was stirred at r.t. for 1 h. After destroying unreacted borohydride by addition of an excess of  $\text{NH}_4\text{Cl}$ , the mixture was extracted with  $\text{CH}_2\text{Cl}_2$  (3 x 25 mL). The extracts were combined and washed with water (2 x 10 mL). Drying and concentration gave a yellow oil. Purification by flash chromatography (EtOAc/hexane, 1:2, v/v) afforded the 1,2:5,6-di-*O*-isopropylidene-[3- $^2\text{H}$ ]- $\alpha$ -D-allofuranose as a white solid (3.0 g, 60%).  $^1\text{H}$  NMR ( $\text{CDCl}_3$ ):  $\delta$  5.82 (d,  $J = 4$  Hz, 1 H), 4.61 (dd,  $J = 5, 4$  Hz, 1 H), 4.3 (m, 1 H), 4.00–4.10 (m, 3 H), 3.82 (dd,  $J = 6.5, 5$  Hz, 1 H), 2.56 (d,  $J = 8$  Hz, 1 H), 1.58 (s, 3 H), 1.47 (s, 3 H), 1.39 (s, 3 H), 1.37 (s, 3 H).  $^{13}\text{C}$  NMR ( $\text{CDCl}_3$ ):  $\delta$  112.9, 109.9, 104.0, 79.9, 79.0, 75.7, 72.6, 66.0, 26.6, 26.5, 26.3, 25.3.

**1,2:5,6-Di-*O*-isopropylidene-[3- $^2\text{H}$ ]- $\alpha$ -D-glucofuranose.** DIAD (0.26 g, 1.3 mmol) in 4 mL benzene was added via cannula to a solution of 1,2:5,6-di-*O*-isopropylidene-[3- $^2\text{H}$ ]- $\alpha$ -D-allofuranose (0.30 g, 1.1 mmol) and  $\text{PPh}_3$  (0.33 g, 1.3 mmol)

in 8 mL of benzene under argon. After the reaction was stirred for 2 min, benzoic acid (0.15 g, 1.3 mmol) in 4 mL of benzene was added. The reaction was stirred overnight at r.t.. The solvent was removed by rotary evaporation and the product was passed through a flash column (1:2 EtOAc/Hex). The fractions containing the desired product were combined and the solvent was removed. The residue was resuspended in 5 mL 1% NaOH/MeOH and stirred at r.t. for 1 h. Water (10 mL) was added to the solution and the aqueous layer was extracted with EtOAc (3 x 5 mL). The organic layer was dried with Na<sub>2</sub>SO<sub>4</sub> and the solvent was removed by rotary evaporation. The residue was purified by flash chromatography (1:2 EtOAc/Hex) to yield 1,2:5,6-di-*O*-isopropylidene-[3-<sup>2</sup>H]-α-D-glucofuranose (0.13 g, 44%).

**[3-<sup>2</sup>H]-D-glucose.** 1,2:5,6-Di-*O*-isopropylidene-[3-<sup>2</sup>H]-α-D-glucofuranose (0.14 g, 0.52 mmol) was treated with 2 N HCl (10 mL) for 20 min at r.t. The solvent was removed by hi-vacuum rotary evaporation to yield [3-<sup>2</sup>H]-glucose (0.13 g, 100%). <sup>1</sup>H NMR (D<sub>2</sub>O): δ 5.23 (d, 10.7 Hz, 0.4 H), 4.64 (d, 8.8 Hz, 0.6H), 3.81 (m, 70 Hz, 5 H), 3.46 (m, 47.6 Hz, 4 H), 3.24 (d, 7.9 Hz, 1 H). <sup>13</sup>C NMR: δ 97.0, 93.2, 77.0, 76.9, 75.3, 73.9, 72.6, 70.8, 61.9, 61.8.

#### **Uridine 5'-diphospho-[3-<sup>2</sup>H]-D-glucose**

A 60 mL solution of 100mM triethanolamine buffer (pH 8.0) was degassed with argon over 30 min. [3-<sup>2</sup>H]-glucose (0.02 g, 0.11 mmol), UTP (0.06 g, 0.11 mmol), PEP (0.025 g, 0.12 mmol), glucose 1,6-bisphosphate (0.001 g, 0.002 mmol), MgCl<sub>2</sub>·6H<sub>2</sub>O (0.049 g, 0.24 mmol), β-mercaptoethanol (0.042 mL), hexokinase (100 Units), pyruvate

kinase (200 units), phosphoglucomutase (100 Units), UDP-glucose pyrophosphorylase (200 Units), and inorganic pyrophosphatase (200 Units) were added to the buffer. The reaction was gently stirred at room temperature until UTP could no longer be detected by TLC. Additional [3-<sup>2</sup>H]-glucose (0.02 g), UTP (0.06 g), and PEP (0.025 g) were added to the reaction. The reaction was allowed to stir at room temperature overnight. The reaction solution was absorbed onto a Dowex 1-X200 (HCO<sub>3</sub><sup>-</sup> form) column (50 mL) and the column was washed with 100 mL d.d. H<sub>2</sub>O. The UDP-[3-<sup>2</sup>H]-glucose was eluted with a linear gradient (250 mL x 250 mL) 0-1 M NaHCO<sub>3</sub>, followed by an additional 150 mL of 1 M NaHCO<sub>3</sub>. Fractions containing UDP-[3-<sup>2</sup>H]-glucose were pooled and treated with Dowex 50 (H<sup>+</sup> form) at 4 °C until bubbling ceased. Upon removal of the resin, the supernatant was concentrated, adjusted to pH 7, and lyophilized to yield 110 mg of UDP-[3-<sup>2</sup>H]-glucose in 89% yield. <sup>1</sup>H NMR (D<sub>2</sub>O): δ 7.596 (d, *J* = 8.1 Hz, 1H, H-5''), δ 5.99 (d, 1H, H-1'), δ 5.95 (d, 1H, H-6''), δ 5.61 (dd, *J* = 7.1, 3.5 Hz, 1H, H-1), δ 4.38 (m, 2H, H-2', 3'), δ 4.29 (m, 1H, H-4'), δ 4.23 (m, 2H, H-5'), δ 3.91 (ddd, *J* = 14, 4.3, 2.3 Hz, 1H, H-5), δ 3.87 (dd, *J* = 12, 2.4 Hz, 1H, H-6), δ 3.79 (dd, *J* = 12, 4.6 Hz, 1H, H-6), δ 3.54 (dd, *J* = 6.4, 3.4 Hz, 1H, H-4), δ 3.47 (d, *J* = 10 Hz, 1H, H-2). <sup>13</sup>C NMR: δ 169.1, 154.7, 144.5, 105.5, 98.4 (d, *J* = 6.2 Hz), 91.3, 86.1 (d, *J* = 9.2), 76.6, 75.7, 74.4, 74.3, 72.5, 71.9, 67.8 (d, *J* = 5.7 Hz), 63.2. HRMS (ES) calcd for C<sub>15</sub>H<sub>22</sub>DN<sub>2</sub>O<sub>17</sub>P<sub>2</sub> (M-H): 566.0535. Found: 566.0544.



## Genetic manipulations

### Plasmid pHS3.244.

The *galU* locus was amplified by PCR from *E. coli* W3110 genomic DNA using the following primers containing *Bam*HI terminal recognition sequences: 5'-CGGGATCCATGGCTGCCATTAATACGAAA and 5'-CGGGATCCTTACTTCTTAATGCCCATCTC. The amplified 0.9 kb PCR fragment was digested with *Bam*HI and ligated into the *Bam*HI site of pJG7.246 (*T<sub>5</sub>*, *lacO*, *lacO*, *6xhis*, *laq<sup>Q</sup>*, Amp<sup>r</sup>) to create plasmid pHS3.244 (*T<sub>5</sub>*, *lacO*, *lacO*, *6xhis*, *galU*, *lacI<sup>Q</sup>*, Amp<sup>r</sup>) in which the *galU* gene is oriented in the same directions as the *T<sub>5</sub>* promoter.

## Enzyme purifications

### Overexpressed *E. coli galU*-encoded UGPase.

The plasmid pHS3.244 was transformed into DH5 $\alpha$  competent cells. DH5 $\alpha$ /pHS3.244 was grown on LB/Ap agar 8-10 h at 37°C. A single colony was then used to inoculate 5 mL LB/Ap medium and the culture was incubated at 37°C overnight in a shaker. The 5 mL culture was then used to inoculate 100 mL LB/Ap. The culture was incubated at 37°C in a shaker at 250 rpm for 45 min until the OD<sub>600</sub> was 0.7 at which time IPTG was added to 1 mM. The culture was incubated an additional 5 h at 37°C and 250 rpm. The cells were harvested by centrifugation (4800 g, 4°C, 5 min) and the supernatant was poured away.

The cells were resuspended in 3 mL binding buffer (20 mM Tris-HCl (pH 8.0) containing 5 mM imidazole and 500 mM NaCl). The cells were lysed by two passes through a french pressure cell, and the cellular debris was removed by centrifugation

(48000 g, 4°C, 20 min). Ni<sup>2+</sup>-NTA resin (1 mL) was added to the supernatant, and the mixture was stirred at 4°C for 1 h. The supernatant was then eluted from the resin. The resin was washed with 3 mL binding buffer, followed by 6 mL of washing buffer (20 mM Tris-HCl (pH 8.0) containing 20 mM imidazole and 500 mM NaCl). The GalU protein was then eluted with 3 mL of eluting buffer (20 mM Tris-HCl (pH 8.0) containing 100 mM imidazole and 500 mM NaCl). The resulting solution was dialyzed against 20 mM Tris-HCl (1 L) to remove imidazole and assayed. The presence of GalU was confirmed by SDS-PAGE analysis (MW 38,000 kDa). The final protein concentration was 1.1 mg/mL with a specific activity of 57 U/mg.

#### ***A. tumefaciens* glucoside 3-dehydrogenase.**

*A. tumefaciens* was grown on MP agar at 28°C for 24 h. A single colony was used to inoculate 5 mL AB/sucrose medium and incubated at 30°C at 250 rpm overnight (12 h). A portion (2 mL) of the overnight culture was used to inoculate 100 mL AB/sucrose. The 100 mL culture was incubated at 28°C and 250 rpm for 10 h. The 100 mL culture was then used to inoculate 1 L AB/sucrose, which was incubated at 28°C and 250 rpm until OD<sub>600</sub> of 2.5.

The cells were harvested by centrifugation (4800 g, 4°C, 10 min) and the supernatant was poured away. The cells were washed with 0.05 M phosphate buffer (pH 7.0) and resuspended in of the same buffer (1 mL per gram cells). The cells were lysed by two passes through a french pressure cell. The cellular debris was removed by centrifugation (48,000 g, 4°C, 20 min).

The supernatant was retained, and powdered  $\text{NH}_4\text{SO}_4$  was added slowly at 4°C over 30 min to 50% saturation. The precipitate was removed by centrifugation (48,000 g, 4°C, 50 min). The supernatant was retained, and powdered  $\text{NH}_4\text{SO}_4$  was added slowly at 4°C over 30 min to 85% saturation. The suspension was allowed to stir at 4°C for 6 h before the precipitate was removed by centrifugation (48,000 g, 4°C, 50 min). The supernatant was poured away, and the precipitate was resuspended in 0.05 M phosphate buffer (pH 7) containing 0.01 M sucrose (13 mL). The solution then was dialyzed against 2 L 0.005 M phosphate buffer (pH 7.0) containing 0.01 M sucrose over a period of 2 days.

The protein solution was then applied to a column of DEAE cellulose resin (10 mL) pre-equilibrated with 0.005 M phosphate buffer (pH 7.0) containing 0.01 M sucrose. The protein was then eluted with a linear gradient (200 mL x 200 mL) from Buffer 1 (0.01 M phosphate (pH 7.0) containing 0.01 M sucrose) to Buffer 1 (0.01 M phosphate (pH 7.0) containing 0.01 M sucrose and 0.15 M KCl). The column was then eluted with and additional 250 mL Buffer 2. Fractions (5 mL) were collected and assayed for G3DH activity. The fractions displaying G3DH activity were pooled and concentrated to 7 mL using an Amicon ultrafiltration apparatus (300 mL). The protein solution was then dialyzed at 4°C against 0.005 M phosphate buffer (pH 7.0) containing 0.01 M sucrose (4 L total). The protein solution was concentrated finally to 3 mL. The presence of G3DH was verified by SDS-PAGE analysis (MW 85,000 kDa). The final protein concentration was 1.5 mg/mL and the specific activity was 0.75 U/mg.

## **Recombinant RifK**

### BL21 Codon Plus RP/pJG7.259

The plasmid pJG7.259 was transformed into BL21 Codon Plus RP competent cells and grown on LB/Ap/Cm agar at 37°C overnight (12 h). A single colony was used to inoculate 5 mL of LB/Ap/Cm media, and the culture was incubated at 37°C and 250 rpm overnight (12 h). An aliquot (2 mL) of the overnight culture was used to inoculate 2 L LB/Ap/Cm. The culture was incubated at 30°C and 250 rpm until the OD<sub>600</sub> reached 0.6. IPTG was added to 1 mM and the culture was incubated overnight (13 h) at 30°C and 250 rpm.

The cells were harvested by centrifugation (4800 g, 4°C, 10 min). The supernatant was poured away and the cells were resuspended in 30 mL binding buffer (20 mM Tris-HCl (pH 8.0), containing 10 mM imidazole and 300 mM NaCl). The cells were lysed by two passes through a french pressure cell, and the cellular debris was removed by centrifugation (48,000 g, 4°C, 20 min). Ni<sup>2+</sup>-NTA resin (5 mL) was added to the supernatant (50 mL), and the mixture was stirred at 4°C for 1 h. The supernatant was eluted from the resin. The resin was washed with six column volumes binding buffer followed by eight column volumes of washing buffer (20 mM Tris-HCl (pH 8.0) containing 20 mM imidazole and 300 mM NaCl). The protein was eluted from the resin with two column volume of eluting buffer (20 mM Tris-HCl (pH 8.0) containing 100 mM imidazole and 300 mM NaCl). The resulting protein solution was dialyzed against 1 L dialysis buffer (50 mM triethanolamine buffer (pH 7.5) containing 10% (w/v) glycerol) by repeated dilution and concentration using an Amicon ultrafiltrator (300 mL). The protein solution was concentrated to a final volume of 17 mL. The presence of RifK was

confirmed by SDS-PAGE analysis (MW 44,000 kDa). The final protein concentration was 13mg/mL.

#### JM109/pJG7.259

The plasmid pJG7.259 was transformed JM109 competent cells and grown on LB/Ap agar at 37°C overnight (12 h). A single colony was used to inoculate 5 mL of LB/Ap, and the culture was incubated at 37°C and 250 rpm overnight (12 h). An aliquot (2 mL) of the overnight culture was used to inoculate 2 L LB/Ap/Cm. The culture was incubated at 28°C and 250 rpm until the OD<sub>600</sub> reached 0.6. IPTG was added to 1 mM and the culture was incubated overnight (20 h) at 30°C and 250 rpm.

The cells were harvested by centrifugation (4800 g, 4°C, 10 min). The supernatant was poured away and the cells were resuspended in 5 mL binding buffer (20 mM Tris-HCl (pH 7.0), containing 10 mM imidazole and 500 mM KCl). The cells were lysed by two passes through a french pressure cell, and the cellular debris was removed by centrifugation (48,000 g, 4°C, 20 min). Ni<sup>2+</sup>-NTA resin (1.5 mL) was added to the supernatant, and the mixture was stirred at 4°C for 1 h. The supernatant was eluted from the resin. The resin was washed with six column volumes of binding buffer followed by twelve column volumes washing buffer (20 mM Tris-HCl (pH 7.0) containing 60 mM imidazole and 500 mM KCl). The protein was eluted from the resin with six column volumes of eluting buffer (20 mM Tris-HCl (pH 7.0) containing 130 mM imidazole and 500 mM KCl). The resulting protein solution was dialyzed against 1 L dialysis buffer (20 mM Tris-HCl (pH 7.5) containing 10% (w/v) glycerol) by repeated dilution and concentration using an Amicon ultrafiltrator (300 mL). The protein solution was

concentrated to a final volume of 17 mL. The presence of RifK was confirmed by SDS-PAGE analysis (MW 44,000 kDa). The final protein concentration was 23 mg/mL.

### **In vivo enzymatic reactions**

#### **Oxidation of glucosides to 3-ketoglucosides by *A. tumefaciens* Whole Cells**

*A. tumefaciens* NCPPB 396 was grown on MP agar plates at 28°C for 1 day. A single colony was used to inoculate 5 mL AB/sucrose medium. The culture was incubated at 30°C, 250 rpm overnight (~18 h). 500 mL of AB/sucrose was inoculated with the overnight culture. The culture was incubated in 2L baffled culture flask at 30°C, 250 rpm until OD<sub>600</sub> ~2-3 (8 h). The cells were harvested by centrifugation at 6000g at 4°C for 10 min. The supernatant was carefully poured away and the cells were resuspended gently in 20 mL 5 mM Tris HCl (pH 8.2). The desired glucoside (1.0 g) was added and the suspension shaken at 30°C until the glucoside was no longer detected by <sup>1</sup>H NMR. The cells were removed by centrifugation (48000g, 4°C, 10 min). When 3-ketoglucose 1-phosphate and 3-ketoUDPG were used as substrates, the supernatant was absorbed onto a 10 mL Dowex 50 (H<sup>+</sup> form) column and the column was washed with 20 column volumes of d.d. H<sub>2</sub>O. The resulting solution was degassed, adjusted to pH 4 with NaOH and lyophilized to yield the desired 3-ketoglucoside.

3-keto-UDPG was isolated as a yellow solid (0.40 g, 40% yield). <sup>1</sup>H NMR (D<sub>2</sub>O): δ 7.95 (d, *J* = 8.2 Hz, 1H, H-6''), δ 6.0 (d, *J* = 4.6 Hz, 1H, H-1'), δ 5.98 (d, *J* = 8.2 Hz, 1H, H-5''), δ 5.96 (dd, *J* = 7.3, 4.2 Hz, 1H, H-1), δ 4.64 (m, 1H, H-2), δ 4.49 (dd, *J* = 10, 1.5 Hz, 1H, H-4), δ 4.38 (m, 2H, H-2', 3'), δ 4.29 (m, 1H, H-4'), δ 4.21 (m, 2H, H-5'), δ 4.1

(ddd,  $J = 10, 3.8, 2$  Hz, 1H, H-5),  $\delta$  3.97 (dd,  $J = 13, 2.1$  Hz, 1H, H-6),  $\delta$  3.88 (dd,  $J = 13, 3.7$  Hz, 1H, H6).  $^{13}\text{C}$  NMR ( $\text{D}_2\text{O}$ ):  $\delta$  210.0, 169.1, 154.7, 144.5, 105.6, 100.8 (d,  $J = 6.3$  Hz), 91.3, 86.1 (d,  $J = 8.9$  Hz), 78.7, 77.3 (d,  $J = 8.2$  Hz), 76.6, 74.4, 72.5, 67.9 (d,  $J = 5.4$  Hz), 63.2. HRMS (ES) calcd for  $\text{C}_{15}\text{H}_{21}\text{N}_2\text{O}_{17}\text{P}_2$  (M-H<sup>+</sup>): 563.0315. Found 563.0306.

3-ketoglucose 1-phosphate was isolated as a yellow solid (0.36 g, 36%).  $^1\text{H}$  NMR ( $\text{D}_2\text{O}$ ):

### Cell-free lysate preparations

#### Cell-free lysate of *A. mediterranei*.

*A. mediterranei* was first grown<sup>25a</sup> on a YMG plate at 28°C for 4 days. This plate culture of *A. mediterranei* was then used to inoculate vegetative medium. A 50 mL vegetative culture was grown in a 500 mL flask with baffles for two days at 28°C and 250 rpm and then a portion of this vegetative culture (5 mL) was used to inoculate 50 mL of production medium in 500 mL flask with baffles. The synthesis of rifamycin B was checked by spectrophotometry<sup>116</sup> after 4 days of incubation at 28°C and 280 rpm. The culture that showed the highest synthesis of rifamycin B was used to inoculate 500 mL YMG medium. After 3 days of incubation at 28°C and 300 rpm, the mycelia were harvested by centrifugation (8600g, 4°C, 5 min). After washing the mycelia with 50 mM Tris-HCl buffer (pH 7.5), the cells were harvested by centrifugation (11000g, 4°C, 5 min). The mycelia were resuspended in Tris-HCl buffer (pH 7.5) (5 mL/g of wet cells) containing 1 mM PMSF and glycerol (20% (w/v)). Cells were then disrupted by two passages through a French press (16000 psi). The cell debris was removed by centrifugation (48000g, 4 °C, 25 min) and the supernatant was used directly in most of

the cell-free reactions. Dialysis were carried out after centrifugation. Dialysis was performed using a Millipore PM-10 membrane and an Aminco stirred cell (300 mL). The cell lysate (about 30 mL) was first diluted to 300 mL followed by concentration (to about 25 mL). More buffer (225 mL) was added to the concentrator. The sample was concentrated to 25 mL again and the process was repeated until the concentration of the micro solute was sufficiently reduced. Typically, 3 to 6 cycles were performed to remove most of initial salt content. Finally, the lysate was concentrated to about 30 mL.

#### **Cell-free lysate of *A. mediterranei* RM01 and HGF003.**

Same procedure as described for *A. mediterranei*.

#### **Cell-free lysate of *B. pumilus***

*B. pumilus* was first grow on a nutrient agar plate at 37 °C for 18-24 h. A single colony from the plate was used to inoculate SSNG medium. A 100 mL culture was grown in a 500 mL flask with baffles for 1.5 to 2 days at 30°C and 250 rpm. The whole 100 mL culture was then transferred to a 4 L flask with baffles containing 1 L of the same medium. After 2 days of incubation at 30°C and 250 rpm, cells were collected by first passing through four layers of cheesecloth followed by centrifugation (6400g, 4°C, 10 min) of the filtrate. After washing the cells with 50 mM Tris-HCl buffer (pH 7.5), the cells were harvested by centrifugation (6400g, 4°C, 10 min). The cells were resuspended in 2 mL of 50 mM phosphate buffer (pH 7.0) per 1 g of wet cells and were disrupted by two passages through a French press (16000 psi). The cell debris was removed by centrifugation (48000g, 4°C, 25 min).



### **JM109/pJG7.275 and JM109/pJG7.259a Cell-free Lysate.**

JM109 competent cells were transformed with either pJG7.275 or pJG7.259, and incubated overnight on LB/Ap agar at 37°C. LB/Ap (5 mL) was inoculated with a single colony of the strain of interest. The culture was incubated at 37°C overnight (12 h). Inoculated 1 L LB/Ap with 1.0 mL overnight culture and incubated at 28°C until the OD<sub>600</sub> reached 0.6. Added IPTG to 0.1 mM and incubated an additional 20 h. The cells were harvested by centrifugation (6400g, 4°C, 10 min) and resuspended in 10 mL buffer (50 mM Tris HCl, 20% glycerol, pH 7.0). The cells were lysed by two passes through a french pressure cell and the cellular debris was removed by centrifugation (48,000g, 4°C, 20 min). The cell-free lysate was used immediately for cell-free experiments.

### **BL21(DE3)/pRM030 cell-free lysate**

BL21(DE3) competent cells were transformed with pRM030, and incubated overnight at 37°C on LB/Ap agar plates. A single colony was used to inoculate 5 mL LB/Ap. The culture was incubated at 37°C overnight (12 h). Inoculated 1 L LB/Ap with 1.0 mL overnight culture and incubated at 28°C until the OD<sub>600</sub> reached 0.6. Added IPTG to 0.1 mM and incubated an additional 20 h. The cells were harvested by centrifugation (6400g, 4°C, 10 min) and resuspended in 10 mL buffer (50 mM Tris HCl, 20% glycerol, pH 7.0). The cells were lysed by two passes through a french pressure cell and the cellular debris was removed by centrifugation (48,000g, 4°C, 20 min). The cell-free lysate was used immediately for cell-free experiments.

### **Preparation of BL21 Codon Plus RP/pJG7.275 Cell-free Lysate (Rif<sup>r</sup>L)**

Inoculated 5 mL LB/Ap/Cm with a single colony of BL21 Codon Plus RP/pJG7.275. Incubated at 37°C overnight until turbid. Inoculated 1 L LB/Ap/Cm with the overnight culture and incubated at 28°C until the OD<sub>600</sub> reached 0.6. IPTG was added to 0.1 mM, and the culture was incubated at 28°C for an additional 20 h. The cells were harvested by centrifugation (6400g, 4°C, 10 min), resuspended in 20 mL buffer (50 mM Tris-HCl, 20% glycerol, pH 7). The cells were lysed and the cellular debris was removed by centrifugation (48,000g, 4°C, 20 min). The supernatant was used directly for the cell-free experiments.

### **Preparation of BL21 Codon Plus RP/pJG7.259 cell-free lysate (Rif<sup>r</sup>K)**

Inoculated 5 mL YT/Ap/Cm with a single colony of BL21 Codon Plus RP/pJG7.259. Incubated at 37°C overnight. Inoculated 1 L YT/Ap/Cm with 1 mL of the overnight culture. Incubated at 28°C until the OD<sub>600</sub> reached 1.0. Added IPTG to 0.1 mM and incubated overnight (14 h). The cells were harvested by centrifugation (6400g, 4°C, 10 min) and rinsed with 100 mL cold 0.9% NaCl solution. The cells pellet was resuspended in 50 mL buffer (50 mM triethanolamine, 1 mM PMSF, 10 % glycerol, pH 7.5) and lysed. The cellular debris was removed by centrifugation (48,000g, 4°C, 20 min) and the supernatant was used directly for the cell-free experiments.

## ***In vitro* enzymatic reactions**

### **Kanosamine Biosynthesis from UDPG**

UDP-D-glucose (54 mg, 0.096 mmol), L-glutamine (14 mg, 0.096 mmol), and  $\beta$ -NAD (132 mg, 0.192 mmol) were incubated in 10 mL of *A. mediterranei*, *A. mediterranei* RM01, *A. mediterranei* HGF003, or *B. pumilus* cell-free lysate at 28°C for 6 h. When required diaphorase (100 U), methylene blue (45 mg, 0.12 mmol), glutamate dehydrogenase (112 U),  $\alpha$ -ketoglutarate (28 mg, 0.198 mmol), and  $\text{NH}_4\text{OH}$  (2 drops) were added. Protein was subsequently removed by ultrafiltration and the protein-free solution was applied to Dowex 50 ( $\text{H}^+$ ) strong cation exchange resin (10 mL). The column was washed with water (75 mL) and eluted with a linear gradient (120 mL + 120 mL, 0-1 M) of HCl. Organic phosphate and ninhydrin assays were used to identify fractions. The products were quantified by  $^1\text{H}$  NMR.  $^1\text{H}$ NMR ( $\text{D}_2\text{O}$ ):  $\delta$  5.27 (d,  $J$  = 3.5 Hz, 0.4 H),  $\delta$  4.72 (d,  $J$  = 8 Hz, 0.6 H),  $\delta$  3.89 (m, 1H),  $\delta$  3.74-3.87 (m, 2H),  $\delta$  3.67 (ddd,  $J$  = 10, 10 Hz, 0.5H),  $\delta$  3.57 (ddd,  $J$  = 7.5, 5.5, 2, 0.5H),  $\delta$  3.45 (dd,  $J$  = 10, 8 Hz, 0.5H),  $\delta$  3.41 (dd,  $J$  = 10, 10 Hz, 0.5H),  $\delta$  3.25 (dd,  $J$  = 10, 10 Hz, 0.5H).  $^{13}\text{C}$  NMR ( $\text{D}_2\text{O}$ ):  $\delta$  99.0, 94.1, 79.9, 74.3, 73.4, 71.0, 68.9, 68.8, 63.2, 63.0, 58.1. HSMS (FAB) calcd for  $\text{C}_6\text{H}_{13}\text{NO}_5(\text{M}+\text{H}^+)$ : 180.0872. Found: 180.0868.

### **Kanosamine biosynthesis from 3-ketoUDPG**

3-ketoUDPG (54 mg, 0.096 mmol),  $\beta$ -NADH (142 mg, 0.192 mmol), and L-glutamine (14 mg, 0.096 mmol) were incubated with *A. mediterranei*, *A. mediterranei* RM01, *A. mediterranei* HGF003, or *B. pumilus* cell-free lysate (10 mL) containing 50 mM Tris-HCl, 1 mM DTT, 1 mM PMSF, and 20% w/v glycerol for 6 hr at 30°C. The

proteins were removed by ultrafiltration and the filtrate concentrated to 2 mL. To the resulting syrup was added 40 mL 100% EtOH, and the precipitate was collected by centrifugation (20000g, 4°C, 30 min). The pellet was rinsed twice with EtOH and dissolved in water. The solution was applied to a Dowex 50 (H<sup>+</sup> form) column (30 mL, 2.5 cm x 6 cm). The column was eluted with dd H<sub>2</sub>O (60 mL) followed by 1 N HCl (60 mL). Kanosamine was produced was confirmed by <sup>1</sup>H NMR and HRMS. Yields were calculated by from <sup>1</sup>H NMR integration in comparison with the TSP standard and response factors generated from known compounds.

#### **Kanosamine biosynthesis from [3-<sup>2</sup>H]-UDPG**

[3-<sup>2</sup>H]-UDPG (48 mg, 0.085 mmol), L-glutamine (14 mg, 0.096 mmol), and β-NAD (0.132 mg, 0.192 mmol) were incubated in 10 mL of *A. mediterranei* or *B. pumilus* cell-free lysate at 28°C for 6 h. Protein was subsequently removed by ultrafiltration and the protein-free solution was applied to Dowex 50 (H<sup>+</sup>) strong cation exchange resin (10 mL). The column was washed with water (75 mL) and eluted with a linear gradient (120 mL + 120 mL, 0-1 M) of HCl. Organic phosphate and ninhydrin assays were used to identify fractions. The products were quantified by <sup>1</sup>H NMR.

3-<sup>2</sup>H]-Kanosamine. <sup>1</sup>H NMR (D<sub>2</sub>O): δ 5.27 (d, *J* = 3.5 Hz, 0.5 H), δ 4.71 (d, *J* = 10 Hz, 1H), δ 3.90 (m, 1H), δ 3.74-3.87 (m, 2H), δ 3.67 (dd, *J* = 8.1, 1.8 Hz, 1H), δ 3.57 (ddd, *J* = 9.8, 5.7, 2.1, 0.5H), δ 3.43 (d, *J* = 7.7 Hz, 0.5H). HRMS: calcd for C<sub>6</sub>H<sub>12</sub>DNO<sub>5</sub> (M+H<sup>+</sup>): 181.0935. Found: 181.0868.

### **Kanosamine biosynthesis from UDPG in the presence of NAD and NADH**

[3-<sup>2</sup>H]-UDPG (48 mg, 0.085 mmol), L-glutamine (14 mg, 0.096 mmol), β-NAD (70 mg, 0.10 mmol), and β-NADH (70 mg, 0.098 mmol) were incubated in 10 mL of *A. mediterranei* or *B. pumilus* cell-free lysate at 28°C for 6 h. Protein was subsequently removed by ultrafiltration and the protein-free solution was applied to Dowex 50 (H<sup>+</sup>) strong cation exchange resin (10 mL). The column was washed with water (75 mL) and eluted with a linear gradient (120 mL + 120 mL, 0-1 M) of HCl. Organic phosphate and ninhydrin assays were used to identify fractions. The products were quantified by <sup>1</sup>H NMR.

### **Oxidation of UDPG to 3-ketoUDPG by heterologously expressed RifL**

#### NAD cofactor

UDP-glucose (54 mg, 0.089 mmol) was incubated with β-NAD (136 mg, 0.198 mmol), MgCl<sub>2</sub>·6H<sub>2</sub>O (0.012 g, 0.064 mmol), and 10 mL of JM109/pJG7.275 or BL21 Codon Plus RP/pJG7.275 cell-free lysate at 30 °C for 6 h. The protein was removed by ultrafiltration and the filtrate was concentrated to 2 mL. EtOH (40 mL) was added and the precipitate was collected by centrifugation (48000g, 4°C, 20 min). The pellet was rinsed with EtOH and dried. The sample analyzed by <sup>1</sup>H NMR.

#### DCIP/PMS cofactor

UDP-glucose (0.054 g, 0.089 mmol) was incubated with DCIP (0.003 g, 0.009 mmol), PMS (0.038 g, 0.124 mmol), MgCl<sub>2</sub>·6H<sub>2</sub>O (0.012 g, 0.064 mmol), and 10 mL of cell-free lysate (JM109/pJG7.275, BL21(DE3)/pJG7.275, or BL21 Codon Plus

RP/pJG7.275) at 30 °C for 5 h. The protein was removed by ultrafiltration and the filtrate was concentrated to 2 mL. EtOH (40 mL) was added and the precipitate was collected by centrifugation (48000g, 4°C, 20 min). The pellet was rinsed with EtOH and dried. The sample analyzed by <sup>1</sup>H NMR and HPLC in comparison to UDP-3-keto-glucose produced by *A. tumefaciens*.

### **UDPG from 3-ketoUDPG by heterologously expressed RifL**

UDP-glucose (25 mg, 0.041 mmol) was incubated with β-NADH (68 mg, 0.095 mmol), MgCl<sub>2</sub>·6H<sub>2</sub>O (0.012 g, 0.064 mmol), and 10 mL of cell-free lysate (JM109/pJG7.275, BL21(DE3)/pJG7.275, or BL21 Codon Plus RP/pJG7.275) at 28 °C for 6 h. The protein was removed by ultrafiltration and the filtrate was concentrated to 2 mL. EtOH (40 mL) was added and the precipitate was collected by centrifugation (48000g, 4°C, 20 min). The pellet was rinsed with EtOH and dried. The sample analyzed by <sup>1</sup>H NMR.

### **UDPK from 3-ketoUDPG.**

#### Heterologously expressed RifK and RifL

3-ketoUDPG (0.03 g, 0.053 mmol) was incubated with 5 mL cell-free lysate (BL21 Codon Plus RP/pJG7.259 or JM109/pJG7.259) or RifK solution and 5 mL cell-free lysate (JM109/pJG7.275, BL21(DE3)/pJG7.275, or BL21 Codon Plus RP/pJG7.275) containing 0.4 mM MgCl<sub>2</sub>·6H<sub>2</sub>O at 28°C. Varying combinations of β-NADH (0.035 g, 0.049 mmol), PLP (0.005 g, 0.020 mmol), L-glutamine (0.008 g, 0.054 mmol) or L-glutamic acid (0.008 g, 0.0054 mmol) were added as needed. After 6 h the protein was

removed and the supernatant concentrated to 2 mL. The solution was diluted with EtOH (100%) and the precipitate was collected by centrifugation. The pellet was rinsed with EtOH, dried, and analyzed by  $^1\text{H}$  NMR and HPLC in comparison to synthesized UDP-kanosamine. In the cases where [amine- $^{15}\text{N}$ ] and [amine- $^{15}\text{N}$ ]-glutamine were used the samples were analyzed additionally by HRMS and compared to a sample prepared with non-labeled glutamine.

#### Heterologously expressed RifK

3-ketoUDPG (0.03 g, 0.053 mmol) was incubated with 10 mL cell-free lysate (BL21 Codon Plus RP/pJG7.259 or JM109/pJG7.259) or 10 mL diluted RifK solution containing 0.4 mM  $\text{MgCl}_2 \cdot 6\text{H}_2\text{O}$  at 28°C. Varying combinations of  $\beta$ -NADH (0.035 g, 0.049 mmol), PLP (0.005 g, 0.020 mmol), L-glutamine (0.008 g, 0.054 mmol) or L-glutamic acid (0.008 g, 0.0054 mmol) were added as needed. After 6 h the protein was removed and the supernatant concentrated to 2 mL. The solution was diluted with EtOH (100%) and the precipitate was collected by centrifugation. The pellet was rinsed with EtOH, dried, and analyzed by  $^1\text{H}$  NMR and HPLC in comparison to synthesized UDP-kanosamine. In the cases where [amine- $^{15}\text{N}$ ] and [amine- $^{15}\text{N}$ ]-glutamine were used the samples were analyzed additionally by HRMS and compared to a sample prepared with non-labeled glutamine.

## Chromatography

### HPLC paired-ion chromatography Analysis of UDP-glucosides

The UDP-glucosides were effectively separated by paired-ion chromatography on a Zorbax Bonus RP (amide C-14) analytical column. The respective UDP-glucosides were eluted using a linear gradient from 97.5% eluant A to 70% eluant A over 15 min. Eluant A was an aqueous solution containing 50 mM  $\text{KH}_2\text{PO}_4$  and 2.5 mM TBAHS at pH 6.9. Eluant B contained 50 mM  $\text{KH}_2\text{PO}_4$  and 2.5 mM TBAHS at pH 6.9 in a 1:1 solution of  $\text{H}_2\text{O}/\text{CH}_3\text{CN}$ . The UDP-glucosides were detected by UV light at 254 nm and their concentrations were calculated based on calibration curves generated from known samples.

## CHAPTER THREE

### Synthetic Preparations

#### Synthesis of L-aspartate semialdehyde

***N*-acetyl-DL-allyl glycine.** Acetic anhydride (6.25 mL) was added in portions to a solution of DL-allyl glycine (5 g, 43.4 mmol) in 2 N NaOH (22 mL) over a time period of 1 h. 10 M NaOH (0.7 mL) was added periodically to keep the pH above 9. After 2 h of stirring at r. t., 16 mL of HCl (conc.) was added to the solution. The aqueous solution was extracted with EtOAc (6 x 50 mL). The organic layer was dried with  $\text{Na}_2\text{SO}_4$ , filtered, and concentrated by rotary evaporation. The resulting solid was recrystallized from hot acetone by the addition of petroleum ether. The resulting crystals were collected by vacuum filtration and dried to yield *N*-acetyl-DL-allyl glycine (6.1 g, 90%). MP: 106-110°C.  $^1\text{H}$  NMR ( $\text{D}_2\text{O}$ ):  $\delta$  5.79 (m, 1H), 5.17 (m, 2H), 4.42 (dd, 1H), 2.60 (m,



1H), 2.51 (m, 1H), 2.02 (s, 3H), <sup>13</sup>C NMR (D<sub>2</sub>O): δ 178.3, 177.1, 135.6, 121.7, 55.6, 37.8, 24.5.

***N*-acetyl-L-allyl glycine.** *N*-acetyl-DL-allyl glycine (1 g, 6.4 mmol) was dissolved in H<sub>2</sub>O (64 mL) and freshly prepared LiOH solution was added dropwise until the pH of the solution was 7.9. Hog kidney acylase (10 mg, 5530U) was added and the reaction was incubated in a shaker at 37°C and 250 rpm for 15 h. The pH was adjusted to 3 with glacial acetic acid and charcoak (0.5 g) was added. The solution was filtered and the solution was concentrated to 10 mL by hi-vacuum rotary evaporation. Absolute EtOH as added to the solution and the precipitate was isolated by vacuum filtration and dried to yield *N*-acetyl-L-allyl glycine (0.27 g, 73%). MP: >270°C. <sup>1</sup>H NMR (D<sub>2</sub>O): δ 5.77 (m, 1H), 5.28 (m, 2H), 3.81 (dd, 1H), 2.65 (m, 2H),

**Aspartate semialdehyde.** Allyl glycine (66 mg, 0.57 mmol) was suspended in 1 M HCl (0.3 mL) and cooled to 0°C. Ozone was bubbled through the solution for 3 h at 0°C, then argon was used to displace the ozone. Powdered zinc was added and the reaction was allowed to warm to r.t.. After 4 h the suspension as filtered to remove the zinc, and the filtrate was concentrated on the hi-vacuum rotary evaporator. The solution was used directly for reactions.

**Diazomethane.** A solution of Diazald (5.2 g, 24 mmol) in Et<sub>2</sub>O (50 mL) was added dropwise via an addition funnel to a refluxing suspension of KOH (24 mmol), 2'-(2-ethoxy)-ethoxy ethanol (8.4 mL), and Et<sub>2</sub>O (20 mL). The CH<sub>2</sub>N<sub>2</sub>/Et<sub>2</sub>O solution was

distilled and collected into a chilled (0°C) flask until the distillate was colorless. An additional 30 mL of Et<sub>2</sub>O were added and the distillation continued until the distillate was colorless. The solution of CH<sub>2</sub>N<sub>2</sub>/Et<sub>2</sub>O was chilled on ice and used immediately.

***N*-acetyl allyl glycine methyl ester.** A freshly prepared solution of CH<sub>2</sub>N<sub>2</sub> in Et<sub>2</sub>O was added dropwise to a stirred, chilled (0°C) solution of *N*-acetyl allyl glycine (1.5 g) in EtOAc (15 mL) until a yellow color persisted. Several drops of acetic acid were then added to quench any remaining CH<sub>2</sub>N<sub>2</sub>. The solvent was removed by rotary evaporator to yield *N*-acetyl allyl glycine methyl ester (1.6 g, quant.) <sup>1</sup>H NMR (CDCl<sub>3</sub>): 6.06 (d, 1H), 5.64 (m, 1H), 5.10 (m, 2H), 5.67 (m, 1H), 3.72 (s, 3H), 2.52 (m, 2H), 1.99 (s, 3H). <sup>13</sup>C NMR (CDCl<sub>3</sub>): 172.0, 169.5, 132.4, 119.2, 52.2, 51.4, 36.3, 22.9.

***N*-acetyl aspartate semialdehyde methyl ester.** *N*-Acetyl allyl glycine methyl ester (0.33 g, 1.9 mmol) was dissolved in 50 mL 4:1 CH<sub>2</sub>Cl<sub>2</sub>/MeOH and chilled to -78°C. Ozone was bubbled through the solution until a blue color persisted. Dimethyl sulfide (3.0 mL, 41 mmol) was added, and the reaction was allowed to warm to r.t.. The reaction was stirred at r.t. overnight and the solvent was removed by rotary evaporation. The product mixture was purified by flash chromatography (EtOAc). Fractions were pooled and concentrated by rotary evaporation. The colorless syrup was dried to yield a 1:5 ratio of the desired aldehyde and the dimethyl acetal of the aldehyde.

## Preparation of DKFP

**Dihydroxyacetone phosphate.** Dihydroxyacetone (0.9 g, 10 mmol), ATP (55 mg, 0.1 mmol),  $\text{MgCl}_2 \cdot 6\text{H}_2\text{O}$  (51 mg, 0.25 mmol), and PEP (2.06 g, 10 mmol) were dissolved in 50 mL  $\text{H}_2\text{O}$ . The pH was adjusted to 7.0 with 10 N NaOH and the solution was degassed with argon for 30 min. Glycerol kinase (2 mg, 180 U) and pyruvate kinase (0.1 mL, 1800 U) were added and the solution was stirred under argon at r.t. for 72 h. The protein was removed by ultrafiltration and activated charcoal was added. The solution was filtered through celite to remove the charcoal. The filtrate was adjusted to  $\text{pH} < 4$  with Dowex-50 ( $\text{H}^+$  form). The resin was removed and 800 mL of EtOH was added to the solution. The precipitate was collected by centrifugation (48,000 rpm,  $4^\circ\text{C}$ , 20 min) and resuspended in 5 mL of  $\text{H}_2\text{O}$ . The solution was filtered and lyophilized overnight. NMR spectra consistent with literature reported data.<sup>117</sup>

**6-Deoxy-2-ketofructose 1-phosphate.** Rabbit muscle aldolase (1 mL) was added to a solution of dihydroxyacetone phosphate (80 mg, 0.38 mmol) in 10 mL 50 mM Tris-HCl (pH 7.6). A 40% (w/v) solution of methyl glyoxal (0.12 mL, 0.76 mmol) was then added and the pH of the reaction solution was adjusted to 7.2 with NaOH. Throughout the reaction 0.5 M NaOH was added to maintain a pH of 6.8-7.2. Upon completion of the reaction, the protein was removed by ultrafiltration. The solution was applied to a column of Dowex-1 anion exchange resin (10 mL) and the column was washed with  $\text{H}_2\text{O}$ . The product was eluted with a linear gradient (0 – 1 M) of  $\text{NaHCO}_3$  solution (pH 7.6). The solution was concentrated by rotary evaporation to yield a solution of 6-deoxy-2-ketofructose 1-phosphate (19%). The concentration and yield were determined by  $^1\text{H}$

NMR analysis of the reaction solution, and were not adjusted using a calibration curve. The solution was filtered and lyophilized overnight. NMR spectra consistent with literature reported data.<sup>118</sup>

#### **Preparation of ATTH from *N*-Cbz-L-aspartic acid.**

**(4S)-3-Carbobenzyloxy-5-oxo-4-oxazolidineacetic acid.** Paraformaldehyde (7.3 g, 243 mmol) and pTSA (0.77 g, 4.5 mmol) were added to a suspension of *N*-Cbz-L-aspartic acid (10.3 g, 38.5 mmol) in 750 mL of toluene. The suspension was heated to reflux with a Dean Stark trap to remove H<sub>2</sub>O. The reaction was heated at reflux for 3 h, and then cooled slightly. The cooled solution was applied to a plug of silica gel. The silica gel was washed with toluene, and the product was eluted to with Et<sub>2</sub>O. The solvent was removed by rotary evaporation to yield a light yellow syrup which crystallized on standing to provide (4S)-*N*-carbobenzyloxy-5-oxo-4-oxazolidineacetic acid (10.6 g, 99%). <sup>1</sup>H NMR (Acetone-d<sub>6</sub>, 50°C): δ 7.33-7.42 (m, 5H), 5.34-5.51 (br, 2 H), 5.14-5.25 (m, 2H), 4.38 (br, 1 H), 3.06-3.40 (m, 2H). HRMS calculated for C<sub>13</sub>H<sub>13</sub>NO<sub>6</sub> (M-H): 278.0665. Found: 278.0669.

**(4S)-3-Carbobenzyloxy-4-(2-chloro-2-oxoethyl)-5-oxo-oxazolidine.** Freshly distilled oxalyl chloride (2 mL, 22.4 mmol) was added to a solution of (4S)-*N*-carbobenzyloxy-5-oxo-4-oxazolidineacetic acid (4.3 g, 15 mmol) in 15 mL dry CH<sub>2</sub>Cl<sub>2</sub>. One drop of DMF was added and the reaction was stirred at r.t. until the reaction was complete (TLC). The solvent was removed by rotary evaporation to yield a red-orange syrup. The syrup was redissolved in CH<sub>2</sub>Cl<sub>2</sub> and washed with dilute NaHCO<sub>3</sub>. The

organic layer was dried with Na<sub>2</sub>SO<sub>4</sub> and filtered. The solvent was removed by rotary evaporation to yield (4S)-*N*-carbobenzyloxy-4-(2-chloro-2-oxoethyl)-5-oxo-oxazolidine (2.7 g, 60%). <sup>1</sup>H NMR (acetone-d<sub>6</sub>, 50°C): <sup>13</sup>C NMR (CDCl<sub>3</sub>): δ 198.2, 171.3, 152.0, 137.3, 134.9, 128.7, 128.4, 128.3, 127.96, 127.93, 124.9, 77.9, 67.5, 49.4, 43.9, 42.9, 21.0. HRMS calculated for C<sub>13</sub>H<sub>12</sub>ClNO<sub>5</sub> (M): 297.0404. Found: 297.0405.

**(4S)-3-Carbobenzyloxy-5-oxo-4-(2-oxo-ethyl)-oxazolidine.** To a solution of oxazolidine acid chloride (2 g, 6.7 mmol) in 40 mL dry toluene under argon was added Pd/BaSO<sub>4</sub> (5% (w/v)), 0.85 g). The solution was heated to reflux under a flow of H<sub>2</sub>. The excess H<sub>2</sub> was bubbled through H<sub>2</sub>O. When the reaction was complete (TLC), the H<sub>2</sub> was replaced with argon and the reaction cooled. The suspension was filtered through celite and the solvent removed by rotary evaporation to yield the aldehyde as a syrup (1.4 g). <sup>1</sup>H NMR (acetone-d<sub>6</sub>, 50°C): δ 9.69 (dd, 1H), 7.73 (m, 5H), 5.53 (d, 1H), 5.17 (s, 2H), 4.50 (dd, 1H), 3.38 (dd, 1H), 3.08 (dd, 1H). <sup>13</sup>C NMR (CDCl<sub>3</sub>): δ 198.3, 171.4, 152.2, 137.5, 128.7, 128.0, 127.9, 77.9, 67.6, 51.2, 49.5, 42.9, 43.0. HRMS calculated for C<sub>13</sub>H<sub>13</sub>NO<sub>5</sub> (M): 263.0794. Found: 263.0793.

**(4S)-3-Carbobenzyloxy-5-oxo-4-(4-oxo-pent-2-enyl)-oxazolidine.** To a solution of the oxazolidine aldehyde (1.4 g) in toluene (40 mL) was added 1-(triphenylphosphoranylidene)-2-propanone (TPP) (1.5 g, 4.7 mmol). The suspension was heated to 60°C under argon. After 18 h the reaction was complete, and the reaction was concentrated by rotary evaporation. Et<sub>2</sub>O was added to the suspension, and the precipitate was removed by vacuum filtration. The solvent was removed and the

resulting syrup was purified by flash chromatography (1:1 EtOAc-hexanes) to yield the enone as a syrup (0.64 g, 62% from acid chloride).  $^1\text{H}$  NMR (acetone- $d_6$ , 50°C):  $\delta$  7.38 (m, 5H), 6.76 (ddd, 1H), 6.09 (dd, 1H), 5.53 (d, 1H), 5.30 (d, 1H), 5.21 (s, 2H), 4.56 (dd, 1H), 2.96 (m, 1H), 2.77 (m, 1H).  $^{13}\text{C}$  NMR ( $\text{CDCl}_3$ ):  $\delta$  197.9, 171.0, 152.8, 139.5, 139.4, 135.4, 128.3, 128.0, 97.8, 68.0, 54.1, 33.9, 33.5, 27.3. HRMS calculated for  $\text{C}_{16}\text{H}_{17}\text{NO}_5$  (M): 303.1107. Found: 303.1094.

**(4S)-3-Carbobenzyloxy-4-(2,3-dihydroxy-4-oxo-pentyl)-5-oxo-oxazolidine.**

The oxazolidine enone (0.6 g, 2 mmol) was added over 12 h to a suspension of NMO (0.3 g, 2.6 mmol), (DHQD) $_2$ PHAL ligand (16 mg, 0.02 mmol), and  $\text{OsO}_4$  (2.5% (w/v) in  $t\text{BuOH}$ , 0.2 mL) in a solution of  $t\text{BuOH}/\text{H}_2\text{O}$  (3:1) at r.t.. The reaction was stirred no enone remained (TLC). EtOAc was added and the reaction was washed with 1 M HCl, followed by brine. The organic layer was dried with  $\text{Na}_2\text{SO}_4$  and the concentrated by rotary evaporation. The product was purified by flash chromatography (3:7:2:0.5 EtOAc-hexanes- $\text{CH}_2\text{Cl}_2$ -MeOH) (0.3 g, 48%).  $^1\text{H}$  NMR (acetone- $d_6$ , 50°C): HRMS calculated for  $\text{C}_{16}\text{H}_{19}\text{NO}_7$  (M-H): 336.1084. Found: 336.1090.

**Preparation of ATTH from *N*-tert-butoxycarbonyl-L-aspartic acid  $\beta$ -benzyl ester**

***N*-tert-butoxycarbonyl-L-aspartic acid  $\alpha$ -tert-butyl  $\beta$ -benzyl ester.** To stirred a solution of *N*-tert-butoxycarbonyl-L-aspartic acid  $\beta$ -benzyl ester (16 g, 50 mmol), DMAP (0.5 g, 4.1 mmol), and  $t\text{BuOH}$  (5.1 mL, 55 mmol) in 250 mL  $\text{CH}_2\text{Cl}_2$  at 0°C was added DCC (12.4 g, 60 mmol). The reaction was stirred at 0°C for 2 h, warmed to r.t. and allowed to stir at r.t. overnight. The suspension was filtered and the filtrate diluted with

400 mL Et<sub>2</sub>O. The organic layer was washed with 1 M HCl (2 x 100 mL), sat. NaHCO<sub>3</sub> (2 x 100 mL), and finally H<sub>2</sub>O (2 x 100 mL). The organic layer was dried with Na<sub>2</sub>SO<sub>4</sub> and concentrated by rotary evaporation. The resulting syrup was purified by flash chromatography (7:3 EtOAc-hexanes) to yield a colorless syrup which crystallized on standing (17 g, 90%). MP 53-56°C. <sup>1</sup>H NMR (CDCl<sub>3</sub>): δ 7.33 (m, 5H), 5.43 (d, 1H), 5.11 (dd, 2H), 4.44 (m, 1H), 2.98-2.91 (ddd, 2H), 1.42 (s, 9H), 1.41 (s, 9H). <sup>13</sup>C NMR (CDCl<sub>3</sub>): δ 170.8, 169.9, 155.4, 135.5, 128.5, 128.3, 128.2, 82.3, 79.8, 66.6, 50.5, 37.0, 28.3, 27.8. HRMS calculated for C<sub>20</sub>H<sub>29</sub>NO<sub>6</sub> (M+H): 380.2073. Found: 380.2078.

***N,N*-Bis(*tert*-butoxycarbonyl)-L-aspartic acid α-*tert*-butyl β-benzyl ester.** To a solution of *N-tert*-butoxycarbonyl-L-aspartic acid α-*tert*-butyl β-benzyl ester (17.5 g, 46 mmol) in dry CH<sub>3</sub>CN (20 mL) under argon at r. t. was added Boc<sub>2</sub>O (16 g, 83 mmol), and DMAP (0.4 g, 3.3 mmol). The reaction was stirred at r. t. overnight (12 h) before concentration by rotary evaporation. The resulting syrup was purified by flash chromatography (19:1 hexanes-EtOAc) to yield the desired amino acid (17.1 g, 77%). <sup>1</sup>H NMR (CDCl<sub>3</sub>): δ 7.31 (br, 5H), 5.34 (dd, 1H), 5.11 (dd, 2H), 3.25 (dd, 1H), 2.70 (dd, 1H), 1.47 (s, 18H), 1.41 (s, 9H). <sup>13</sup>C NMR (CDCl<sub>3</sub>): δ 170.7, 168.6, 151.9, 128.5, 128.2, 128.1, 83.2, 81.9, 66.5, 55.5, 35.6, 27.9, 27.8. HRMS calculated for C<sub>25</sub>H<sub>37</sub>NO<sub>8</sub> (M+H): 502.2417. Found: 502.2411.

***N,N*-Bis(*tert*-butoxycarbonyl)-L-aspartic acid α-*tert*-butyl ester.** To a solution of the benzyl ester (0.43 g, 0.89 mmol) under argon in 10 mL MeOH was added 10% (w/v) Pd/C (9 mg, 8.9 μmol). The argon was replaced by H<sub>2</sub> and the reaction was stirred

under atmospheric H<sub>2</sub> until complete (TLC). The H<sub>2</sub> was then replaced with argon, and the suspension filtered through celite to remove the catalyst. The filtrate was concentrated by rotary evaporation to yield the acid (0.35 g, quant.). MP 104-107°C. <sup>1</sup>H NMR (CDCl<sub>3</sub>): 5.27 (dd, 1H), 3.25 (dd, 1H), 2.72 (dd, 1H), 1.49 (s, 18H), 1.43 (s, 9H). <sup>13</sup>C NMR: δ 175.7, 168.6, 151.9, 83.2, 82.2, 55.4, 35.2, 27.9, 27.8. HRMS calculated for C<sub>18</sub>H<sub>31</sub>NO<sub>8</sub> (M+H): 412.1947. Found: 412.1939.

***N-tert-Butoxycarbonyl-L-aspartic acid α-tert-butyl ester.*** To a solution of the benzyl ester (2.5 g, 6.6 mmol) under argon in 70 mL MeOH was added 10% (w/v) Pd/C (63 mg). The argon was replaced by H<sub>2</sub> and the reaction was stirred under atmospheric H<sub>2</sub> until complete (TLC). The H<sub>2</sub> was then replaced with argon, and the suspension filtered through celite to remove the catalyst. The filtrate was concentrated by rotary evaporation to yield the acid (1.9 g, quant.). <sup>1</sup>H NMR (CDCl<sub>3</sub>): δ 5.48 (d, 1H), 4.42 (m, 1H), 2.97 (dd, 1H), 2.76 (dd, 1H), 1.42 (s, 18H). HRMS calculated for C<sub>13</sub>H<sub>23</sub>NO<sub>6</sub> (M+H): 312.1423. Found: 312.1432.

***N,N-Bis(tert-butoxycarbonyl)-L-aspartic acid (α-tert-butyl ester) N-methoxy-N-methylamide.*** To a solution of *N,N*-bis(*tert*-butoxycarbonyl)-*L*-aspartic acid α-*tert*-butyl ester (3.2 g, 8.2 mmol) and TEA (1.3 mL, 9.3 mmol) in 85 mL CH<sub>2</sub>Cl<sub>2</sub> under argon at r.t. was added BOP reagent (4.1 g, 9.3 mmol). The reaction was allowed to stir for 20 min before the addition of TEA (1.3 mL, 9.3 mmol) and *N*, *O*-dimethylhydroxylamine·HCl (0.94 g, 9.6 mmol). The reaction was stirred for an additional 6 h before washing with 1 N HCl (3 x 100 mL), sat. NaHCO<sub>3</sub> (2 x 100 mL),



and brine. The organic layer was dried with Na<sub>2</sub>SO<sub>4</sub>, and the solvent was removed by rotary evaporation. The resulting syrup was purified by flash chromatography (7:3 Hexanes-EtOAc) to yield the wienreb amide (2.6 g, 73%). MP 63-67°C. <sup>1</sup>H NMR (CDCl<sub>3</sub>): δ 5.41 (dd, 1H), 3.67 (s, 3H), 3.38 (dd, 1H), 3.13 (s, 3H), 2.70 (dd, 1H), 1.48 (s, 18H), 1.41 (s, 9H). <sup>13</sup>C NMR (CDCl<sub>3</sub>): δ 169.0, 151.9, 83.0, 81.3, 61.0, 55.4, 33.5, 28.0, 27.8. HRMS calculated for C<sub>20</sub>H<sub>36</sub>N<sub>2</sub>O<sub>8</sub> (M+H): 455.2369. Found: 455.2359.

***N-tert-butoxycarbonyl-L-aspartic acid (α-tert-butyl ester) N-methoxy-N-methylamide.*** To a solution of *N-tert-butoxycarbonyl-L-aspartic acid α-tert-butyl ester* (4.8 g, 16.5 mmol) and TEA (4 mL, 28.5 mmol) in 170 mL CH<sub>2</sub>Cl<sub>2</sub> under argon at r.t. was added BOP reagent (8 g, 18 mmol). The reaction was allowed to stir for 20 min before the addition of TEA (4 mL, 28.7 mmol) and *N,O*-dimethylhydroxylamine·HCl (1.9 g, 19.8 mmol). The reaction was stirred for an additional 6 h before washing with 1 N HCl (3 x 50 mL), sat. NaHCO<sub>3</sub> (2 x 50 mL), and brine. The organic layer was dried with Na<sub>2</sub>SO<sub>4</sub>, and the solvent was removed by rotary evaporation. The resulting syrup was purified by flash chromatography (7:3 Hexanes-EtOAc) to yield the wienreb amide (3.6 g, 67%). <sup>1</sup>H NMR (CDCl<sub>3</sub>): δ 5.63 (d, NH), 4.41 (ddd, 1H), 3.66 (s, 3H), 3.13 (s, 3H), 3.10 (dd, 1H), 2.84 (dd, 1H), 1.42 (s 9H), 1.41 (s, 9H). <sup>13</sup>C NMR (CDCl<sub>3</sub>): δ 170.5, 155.7, 81.7, 79.4, 61.1, 50.3, 34.2, 28.3, 27.8. HRMS calculated for C<sub>15</sub>H<sub>28</sub>N<sub>2</sub>O<sub>6</sub> (M+H): 333.2025. Found: 333.2025.

***N,N-Bis(tert-butoxycarbonyl)-L-aspartate semialdehyde α-tert-butyl ester.***

To a solution of the weinreb amide (0.63 g, 1.5 mmol) in 6 mL dry THF at -90°C was

added dropwise 2.2 mL of DIBAL (1 M in hexanes). After 2.5 h at  $-90^{\circ}\text{C}$  the reaction was quenched by the addition of 0.35 M  $\text{NaHSO}_4$ , and partitioned between  $\text{NaHSO}_4$  solution and  $\text{Et}_2\text{O}$ . The aqueous layer was extracted with  $\text{Et}_2\text{O}$  (2 x 10 mL). The combined ether extracts were washed with 1 N  $\text{HCl}$  (10 mL), sat.  $\text{NaHCO}_3$  (3 x 10 mL), and finally brine. The organic layer was dried with  $\text{MgSO}_4$  and concentrated by rotary evaporation to yield the aldehyde (0.5 g, 92%).  $^1\text{H}$  NMR ( $\text{CDCl}_3$ ):  $\delta$  9.76 (dd, 1H), 5.27 (dd, 1H), 3.31 (dd, 1H), 2.73 (dd, 1H), 1.49 (s, 18H), 1.42 (s, 9H).  $^{13}\text{C}$  NMR ( $\text{CDCl}_3$ ):  $\delta$  200.6, 172.0, 155.5, 73.2, 70.6, 47.1, 42.2, 28.0, 27.7.

***N-tert-butoxycarbonyl-L-aspartate semialdehyde  $\alpha$ -tert-butyl ester.*** To a solution of the weinreb amide (3.6 g, 11 mmol) in 45 mL dry THF at  $-90^{\circ}\text{C}$  was added dropwise 17 mL of DIBAL (1 M in hexanes). After 3.5 h at  $-90^{\circ}\text{C}$  the reaction was quenched by the addition of 0.35 M  $\text{NaHSO}_4$ , and partitioned between  $\text{NaHSO}_4$  solution and  $\text{Et}_2\text{O}$ . The aqueous layer was extracted with  $\text{Et}_2\text{O}$  (2 x 10 mL). The combined ether extracts were washed with 1 N  $\text{HCl}$  (10 mL), sat.  $\text{NaHCO}_3$  (3 x 10 mL), and finally brine. The organic layer was dried with  $\text{MgSO}_4$  and concentrated by rotary evaporation. The residue was purified by flash chromatography (4:1 hexanes-EtOAc) to yield the aldehyde (1.5 g, 51%).  $^1\text{H}$  NMR ( $\text{CDCl}_3$ ):  $\delta$  9.72 (dd, 1H); 5.32 (d, 1H); 4.45 (m, 1H); 2.95 (ddd, 2H), 1.43 (s, 9H), 1.41 (s, 9H).  $^{13}\text{C}$  NMR ( $\text{CDCl}_3$ ):  $\delta$  200.5, 172.0, 157.5, 73.2, 70.6, 49.6, 45.0, 29.0, 28.7. HRMS calculated for  $\text{C}_{13}\text{H}_{23}\text{NO}_5$  ( $\text{M}+\text{H}$ ): 274.1654. Found: 274.1658.

***N,N-Bis(tert-Butoxycarbonyl)amino-6-oxo-hept-4-enoic acid tert-butyl ester.***  
To a solution of *N,N*-bis(*tert*-butoxycarbonyl)-L-aspartate semialdehyde  $\alpha$ -*tert*-butyl ester

(0.69 g, 1.8 mmol) in 35 mL dry toluene under argon was added 1-(triphenylphosphoranylidene)-2-propanone (TPP) (0.85 g, 2.5 mmol). The suspension was heated at reflux for 8 h and cooled to r. t.. The reaction was concentrated by rotary evaporation. Et<sub>2</sub>O was added to the suspension, and the precipitate was removed by vacuum filtration. The solvent was removed and the resulting syrup was purified by flash chromatography (1:1 EtOAc-hexanes) to yield the enone as a syrup (0.59 g, 78%). <sup>1</sup>H NMR (CDCl<sub>3</sub>): δ 6.71 (m, 1H), 6.01 (d, 1H), 4.86 (dd, 1H), 2.94 (m, 1H), 2.76 (m, 1H), 2.17 (s, 3H), 1.44 (s, 18H), 1.40 (s, 9H). <sup>13</sup>C NMR (CDCl<sub>3</sub>): δ 196.5, 172.0, 155.4, 141.9, 129.3, 73.1, 70.7, 54.6, 31.1, 28.1, 27.8, 26.4. HRMS calculated for C<sub>21</sub>H<sub>35</sub>NO<sub>7</sub> (M+Na): 436.2311. Found: 436.2313.

***N-tert-Butoxycarbonylamino-6-oxo-hept-4-enoic acid tert-butyl ester.*** To a solution of *N-tert-butoxycarbonyl-L-aspartate semialdehyde α-tert-butyl ester* (1.4 g, 5.1 mmol) in 100 mL dry toluene under argon was added 1-(triphenylphosphoranylidene)-2-propanone (TPP) (2.6 g, 8.2 mmol). The suspension was heated at reflux for 8 h and cooled to r. t.. The reaction was concentrated by rotary evaporation. Et<sub>2</sub>O was added to the suspension, and the precipitate was removed by vacuum filtration. The solvent was removed and the resulting syrup was purified by flash chromatography (4:1 EtOAc-hexanes) to yield the enone as a syrup (1.3 g, 81%). <sup>1</sup>H NMR (CDCl<sub>3</sub>): δ 6.67 (m, 1H), 6.08 (d, 1H), 5.11 (d, NH), 4.32 (m, 1H), 2.72 (m, 1H), 2.55 (m, 1H), 2.21 (s, 3H), 1.44 (s, 9H), 1.42 (s, 9H). <sup>13</sup>C NMR (CDCl<sub>3</sub>): δ 198.0, 170.3, 155.0, 142.0, 134.0, 82.6, 79.9, 52.9, 36.2, 28.2, 27.9, 26.6. HRMS calculated for C<sub>16</sub>H<sub>27</sub>NO<sub>5</sub> (M+H): 314.1967. Found: 314.1972.

***N,N*-Bis(*tert*-Butoxycarbonyl)amino-(4*S*,5*R*)-4,5-dihydroxy-6-oxo-heptanoic acid *tert*-butyl ester and *N,N*-Bis(*tert*-butoxycarbonyl)amino-(4*R*,5*S*)-4,5-dihydroxy-6-oxo-heptanoic acid *tert*-butyl ester.** Combined AD-mix  $\beta$  (0.98 g),  $K_2OsO_4 \cdot 2H_2O$  (4.2 mg, 1.1  $\mu$ mol),  $NaHCO_3$  (0.176 g, 2.1 mmol), and  $H_2NSO_4Me$  (66 mg, 0.7 mmol) in 7 mL  $tBuOH/H_2O$  (1:1). The suspension was stirred at r.t. for 5 min, then chilled to 0°C. *N,N*-bis(*tert*-butoxycarbonyl)amino-6-oxo-hept-4-enoic acid *tert*-butyl ester (0.29 g, 0.7 mmol) in  $CH_2Cl_2$  was added and the solution stirred at 0°C overnight (12 h). Upon completion of the reaction (TLC), the reaction was quenched by the addition of sat.  $Na_2S_2O_4$ . The reaction was stirred for an additional 20 min, then extracted with EtOAc (3 x 10 mL). The combined organic fractions were washed with 0.5 N HCl, 1 M  $NaHCO_3$ ,  $H_2O$ , and brine. The organic layer was dried with  $Na_2SO_4$  and concentrated by rotary evaporation. The resulting syrup was purified by flash chromatography (3.5:6:2.5:0.5 EtOAc-hexanes- $CH_2Cl_2$ -MeOH) to yield a 1:1 mixture of diol diastereomers A and B (0.21 g, 67%).  $^1H$  NMR ( $CDCl_3$ ):  $\delta$  4.92 (dd, 1H), 4.83 (dd, 1H), 4.24 (ddd, 1H), 4.12 (d, 1H), 4.05 (d, 1H), 3.96 (ddd, 1H), 2.55 (m, 1H), 3.39 (m, 1H), 2.24 (s, 3H), 2.23 (s, 3H), 1.99 (m, 1H), 1.92 (m, 1H), 1.45 (s, 36H), 1.39 (s, 18H).  $^{13}C$  NMR ( $CDCl_3$ ):  $\delta$  208.3, 207.9, 170.0, 169.7, 152.6, 152.4, 83.4, 83.1, 81.9, 81.5, 79.5, 79.0, 69.5, 69.3, 56.7, 55.7, 35.6, 33.8, 27.97, 27.93, 27.86, 27.81, 25.9, 25.1. HRMS calculated for  $C_{21}H_{37}NO_9$  (M+Na): 470.2366. Found: 470.2354.

***N-tert*-Butoxycarbonylamino-(4*S*,5*R*)-4,5-dihydroxy-6-oxo-heptanoic acid *tert*-butyl ester and *N-tert*-butoxycarbonylamino-(4*R*,5*S*)-4,5-dihydroxy-6-oxo-**

**heptanoic acid *tert*-butyl ester.** Combined AD-mix  $\beta$  (4.4 g),  $\text{K}_2\text{OsO}_4 \cdot 2\text{H}_2\text{O}$  (20 mg),  $\text{NaHCO}_3$  (0.8 g), and  $\text{H}_2\text{NSO}_4\text{Me}$  (0.3 g) in 70 mL  $\text{tBuOH}/\text{H}_2\text{O}$  (1:1). The suspension was stirred at r.t. for 5 min, then chilled to  $0^\circ\text{C}$ . *N-tert*-butoxycarbonylamino-6-oxo-hept-4-enoic acid *tert*-butyl ester (1.0 g, 3.2 mmol) in  $\text{CH}_2\text{Cl}_2$  was added and the solution stirred at  $0^\circ\text{C}$  overnight (12 h). Upon completion of the reaction (TLC), the reaction was quenched by the addition of sat.  $\text{Na}_2\text{S}_2\text{O}_4$ . The reaction was stirred for an additional 20 min, then extracted with EtOAc (3 x 10 mL). The combined organic fractions were washed with 0.5 N HCl, 1 M  $\text{NaHCO}_3$ ,  $\text{H}_2\text{O}$ , and brine. The organic layer was dried with  $\text{Na}_2\text{SO}_4$  and concentrated by rotary evaporation. The resulting syrup was purified by flash chromatography (3.5:6:2.5:0.5 EtOAc-Hex- $\text{CH}_2\text{Cl}_2$ -MeOH) to yield a 1:1 mixture of diol diastereomers (0.46 g, 41%).  $^1\text{H}$  NMR ( $\text{CDCl}_3$ ):  $\delta$  5.46 (m, 2H), 4.36 (m, 2H), 4.26 (m, 2H), 4.22 (dd, 1 H), 4.07 (m, 2H), 3.76 (br, 1H), 2.29 (s, 3H), 2.28 (s, 3H), 2.24-2.15 (m, 2H), 2.00-1.92 (m, 2H), 1.48 (s, 3H), 1.47 (s, 9H), 1.47 (s, 9H), 1.454 (s, 9H), 1.451 (s, 9H). HRMS calculated for  $\text{C}_{16}\text{H}_{29}\text{NO}_7$  (M+H): 348.2022. Found: 348.2037.

***N-tert*-Butoxycarbonylamino-(4S,5R)-4,5-dihydroxy-6-oxo-heptanoic acid *tert*-butyl ester and *N-tert*-butoxycarbonylamino-(4R,5S)-4,5-dihydroxy-6-oxo-heptanoic acid *tert*-butyl ester.** Combined AD-mix  $\alpha$  (0.9 g),  $\text{K}_2\text{OsO}_4 \cdot 2\text{H}_2\text{O}$  (4 mg),  $\text{NaHCO}_3$  (0.16 g), and  $\text{H}_2\text{NSO}_4\text{Me}$  (60 mg) in 14 mL  $\text{tBuOH}/\text{H}_2\text{O}$  (1:1). The suspension was stirred at r.t. for 5 min, then chilled to  $0^\circ\text{C}$ . *N-tert*-butoxycarbonylamino-6-oxo-hept-4-enoic acid *tert*-butyl ester (0.2 g, 0.6 mmol) in  $\text{CH}_2\text{Cl}_2$  was added and the solution stirred at  $0^\circ\text{C}$  overnight (12 h). Upon completion of the reaction (TLC), the reaction was quenched by the addition of sat.  $\text{Na}_2\text{S}_2\text{O}_4$ . The reaction was stirred for an additional 20

min, then extracted with EtOAc (3 x 10 mL). The combined organic fractions were washed with 0.5 N HCl, 1 M NaHCO<sub>3</sub>, H<sub>2</sub>O, and brine. The organic layer was dried with Na<sub>2</sub>SO<sub>4</sub> and concentrated by rotary evaporation. The resulting syrup was purified by flash chromatography (3.5:6:2.5:0.5 EtOAc-Hex-CH<sub>2</sub>Cl<sub>2</sub>-MeOH) to yield a 3:1 mixture of diol diastereomers (20 mg, 20%). Spectra same as found using AD-mix β.

**(4S,5R)-4,5-Diacetoxy-*N,N*-Bis(*tert*-butoxycarbonyl)amino-6-oxo-heptanoic acid *tert*-butyl ester and (4R,5S)-4,5-diacetoxy-*N,N*-bis(*tert*-butoxycarbonyl)amino-6-oxo-heptanoic acid *tert*-butyl ester.** Pyridine (1.6 mL) was added to a solution of the diol mixture (0.21 g, 0.47 mmol) in Ac<sub>2</sub>O (2.2 mL). The reaction was stirred overnight at r.t.. The solvent was removed by rotary evaporation and the resulting residue was azeotroped with EtOH (3 x). The resulting residue was purified by flash chromatography to provide an inseparable mixture of the two diastereomers (0.21 g, 84%). <sup>1</sup>H NMR (CDCl<sub>3</sub>): δ 5.52 (ddd, 1H), 5.24 (ddd, 1H), 5.23 (d, 1H), 4.98 (d, 1H), 4.89 (d, 1H), 4.72 (dd, 1H), 2.176 (s, 3H), 2.171 (s, 3H), 2.615 (s, 3H), 2.41(m, 3H), 2.21 (m, 1H), 2.11 (m, 1H), 2.02 (s 3H), 2.00 (s, 3H), 1.46 (s, 18H), 1.45 (s, 18H), 1.39 (s, 9H), 1.38 (s, 9H). HRMS calculated for C<sub>25</sub>H<sub>41</sub>NO<sub>11</sub> (M+Na): 554.2577. Found: 554.2568.

**(4S,5R)-4,5-Bis-benzoyloxy-*N,N*-Bis(*tert*-butoxycarbonyl)amino-6-oxo-heptanoic acid *tert*-butyl ester and (4R,5S)-4,5-bis-benzoyloxy-*N,N*-bis(*tert*-butoxycarbonyl)amino-6-oxo-heptanoic acid *tert*-butyl ester.** The diol mixture (70 mg, 0.16 mmol) was dissolved in pyridine (0.2 mL) and CH<sub>2</sub>Cl<sub>2</sub> (0.2 mL). Benzoyl chloride (50 μL) was added dropwise, and the reaction was stirred at r. t. for 24 h. The

pH of the reaction was adjusted to 8.0 by the addition of NaOH. The solution was then extracted with EtOAc (3 x 5 mL). The pooled organic fractions were washed with H<sub>2</sub>O (3 x 5 mL) followed by brine (1 x 5 mL). The organic layer was dried with Na<sub>2</sub>SO<sub>4</sub> and the solvent was removed by rotary evaporation. The resulting residue was purified by flash chromatography (5:1 hexanes-EtOAc) to yield an inseparable mixture diastereomers (38 mg, 36%). <sup>1</sup>H NMR (CDCl<sub>3</sub>): δ 8.12-7.99 (m, 8H), 7.61-7.39 (m, 12H), 5.86 (ddd, 1H), 5.67 (ddd, 1H), 5.61 (d, 1H), 5.37 (d, 1H), 5.02 (dd, 1H), 4.89 (dd, 1H), 2.75-2.67 (m, 2H), 2.50 (ddd, 1H), 2.35 (ddd, 1H), 2.255 (s, 3H), 2.249 (s, 3H), 1.424 (s, 18H), 1.412 (s, 18H), 1.406 (s, 18H), 1.389 (s, 18H).

**(4S,5R)-4,5-Bis-benzoyloxy-*N*-*tert*-butoxycarbonylamino-6-oxo-heptanoic acid *tert*-butyl ester and (4R,5S)-4,5-bis-benzoyloxy-*N*-*tert*-butoxycarbonylamino-6-oxo-heptanoic acid *tert*-butyl ester.** The diol mixture produced using AD-mix β (0.44 g, 1.2 mmol) was dissolved in pyridine (1.5 mL) and CH<sub>2</sub>Cl<sub>2</sub> (1.5 mL). Benzoyl chloride (0.4 mL) was added dropwise, and the reaction was stirred at r. t. for 24 h. The pH of the reaction was adjusted to 8.0 by the addition of NaOH. The solution was then extracted with EtOAc (3 x 5 mL). The pooled organic fractions were washed with H<sub>2</sub>O (3 x 5 mL) followed by brine (1 x 5 mL). The organic layer was dried with Na<sub>2</sub>SO<sub>4</sub> and the solvent was removed by rotary evaporation. The resulting residue was purified by flash chromatography (5:1 hexanes-EtOAc) to yield two diastereomers A (0.2 g, 30%)) and B (0.28 g, 42%).

Product A <sup>1</sup>H NMR (CDCl<sub>3</sub>): δ 8.14 (d, 2H), 7.99 (dd, 2H), 7.57 (ddd, 2H), 7.44 (ddd, 4H), 5.87 (d, 1H), 5.85 (dd, 1H), 5.34 (d, 1H), 4.31 (m, 1H), 2.37 (m, 1H), 2.25 (s,

3H), 2.15 (m, 1H), 1.42 (s, 9H), 1.28 (s, 9H).  $^{13}\text{C}$  NMR ( $\text{CDCl}_3$ ):  $\delta$  201.2, 170.2, 165.3, 165.2, 155.4, 133.3, 133.2, 129.7, 129.6, 129.0, 128.8, 128.3, 128.2, 82.3, 79.8, 77.9, 69.5, 50.6, 34.3, 27.9, 27.6, 27.5, 26.4. HRMS calculated for  $\text{C}_{30}\text{H}_{37}\text{NO}_9$  ( $\text{M}+\text{Na}$ ): 578.2366. Found: 578.2357.

Product B  $^1\text{H}$  NMR ( $\text{CDCl}_3$ ):  $\delta$  8.09 (d, 2H), 8.01 (d, 2H), 7.57 (ddd, 2H), 7.44 (m, 4H), 5.81 (m, 1H), 5.44 (d, 1H), 5.11 (d, 1H), 4.24 (m, 1H), 2.39 (m, 1H), 2.26 (s, 3H), 2.17 (m, 1H), 1.46 (s, 9H), 1.32 (s, 9H).  $^{13}\text{C}$  NMR ( $\text{CDCl}_3$ ):  $\delta$  202.0, 170.6, 165.7, 165.4, 133.6, 133.5, 130.3, 129.9, 129.7, 128.53, 128.47, 82.7, 79.9, 78.8, 69.4, 53.5, 51.1, 33.6, 28.2, 28.1, 27.9, 27.1. HRMS calculated for  $\text{C}_{30}\text{H}_{37}\text{NO}_9$  ( $\text{M}+\text{Na}$ ): 578.2366. Found: 578.2363.

**(4S,5R)-4,5-Bis-benzoyloxy-*N*-tert-butoxycarbonylamino-6-oxo-heptanoic acid *tert*-butyl ester and (4R,5S)-4,5-bis-benzoyloxy-*N*-tert-butoxycarbonylamino-6-oxo-heptanoic acid *tert*-butyl ester.** The diol mixture produced using AD-mix  $\alpha$  (20 mg, 6  $\mu\text{mol}$ ) was dissolved in pyridine (70  $\mu\text{L}$ ) and  $\text{CH}_2\text{Cl}_2$  (70  $\mu\text{L}$ ). Benzoyl chloride (20  $\mu\text{L}$ ) was added dropwise, and the reaction was stirred at r. t. for 24 h. The pH of the reaction was adjusted to 8.0 by the addition of NaOH. The solution was then extracted with EtOAc (3 x). The pooled organic fractions were washed with  $\text{H}_2\text{O}$  (3 x) followed by brine (1 x). The organic layer was dried with  $\text{Na}_2\text{SO}_4$  and the solvent was removed by rotary evaporation. The resulting residue was purified by flash chromatography (5:1 hexanes-EtOAc) to yield two diastereomers A (4 mg, 13%) and B (12 mg, 38%). Same spectra as above.



## ATTH from D-tartaric acid

**[4S,5S]-2,2-Dimethyl-[1,3]dioxolane-4,5-dicarboxylic acid dimethyl ester.** A solution containing D-tartaric acid (50 g, 333 mmol), 2,2-dimethoxy propane (95 mL, 770 mmol), and *p*-toluenesulfonic acid (0.2 g, 1.05 mmol) in 20 mL of MeOH was heated to reflux under argon for 1.5 h. Cyclohexane (225 mL) and additional 2,2-dimethoxypropane (48 mL, 385 mmol) were added. A vigreux column and a variable reflux distilling head were affixed and MeOH and acetone were azeotroped with cyclohexane over 2 days. The reaction was allowed to cool and NaHCO<sub>3</sub> was added slowly until a yellow color persisted. Any volatile components were removed by rotary evaporation. The residue was then distilled under vacuum (b.p. 120°C under vacuum) to yield the desired [4S,5S]-2,2-dimethyl-[1,3]dioxolane-4,5-dicarboxylic acid dimethyl ester as a yellow oil (55 g, 76%). <sup>1</sup>H NMR (CDCl<sub>3</sub>): δ 4.79 (s, 2H), 3.60 (s, 6H), 1.49 (s, 6H). <sup>13</sup>C NMR (CDCl<sub>3</sub>): 170.1, 113.9, 77.0, 52.8, 26.3. HRMS calculated for C<sub>9</sub>H<sub>15</sub>O<sub>6</sub> (M+H): 219.0869. Found: 219.0865.

**[2R,3R]-2,3-O-Isopropylidene-D-threitol.** A suspension of LiAlH<sub>4</sub> (16 g, 424 mmol) in dry Et<sub>2</sub>O (270 mL) was refluxed under a stream of argon for 45 min, then the heating mantle was removed. [4S,5S]-2,2-Dimethyl-[1,3]dioxolane-4,5-dicarboxylic acid dimethyl ester (55g, 252 mmol) in Et<sub>2</sub>O (130 mL) was added over 2 h via an addition funnel. The suspension was heated to reflux under argon for 5 h, then cooled to -5°C with an ice/acetone bath. Water (15 mL) was added carefully, followed by 15 mL 4 N NaOH solution. An additional 50 mL of water was then added and the suspension was stirred at r. t. until the gray color was gone. The suspension was filtered by vacuum

filtration, and the solid collected was washed with Et<sub>2</sub>O. The inorganic solid was extracted over 2 days with THF using a sohxlet apparatus. The combined organic extracts were combined and dried with MgSO<sub>4</sub>. The solvents were removed by rotary evaporation and the residue distilled under vacuum (1 mm Hg) to yield [2R,3R]-2,3-O-isopropylidene-D-threitol (b.p. 124°C) (24 g, 59%). <sup>1</sup>H NMR (CDCl<sub>3</sub>): δ 3.99 (m, 2H), 3.72 (dd, 4H), 2.17 (br, 2H), 1.40 (s, 6H). <sup>13</sup>C NMR (CDCl<sub>3</sub>): δ 101.6, 81.7, 62.5, 28.6. HRMS calculated for C<sub>7</sub>H<sub>15</sub>O<sub>4</sub> (M+H): 164.0490. Found: 163.0970.

**[2R,3R]-2,3-O-Isopropylidene-D-threitol 4-*tert*-butyl dimethyl silyl ether.**  
[2R,3R]-2,3-O-Isopropylidene-D-threitol (24 g, 148 mmol) in THF (130 mL) was added to a stirred suspension of NaH (60% immersion in oil) (6 g, 150 mmol) in 270 mL THF under argon at 0°C. The suspension was stirred for 10 min at 0°C before warming to r.t. and stirring for an additional 45 min. TBDMSCl (23 g, 150 mmol) in 130 mL THF was added over 20 min, and the suspension was stirred at r.t. an additional 3 h. The suspension was then poured into 300 mL sat. NaHCO<sub>3</sub> solution, and the organic phase was separated. The aqueous phase was extracted with EtOAc (3 x 200 mL). The organic fractions were combined and dried with MgSO<sub>4</sub>. The solvent was removed by rotary evaporation to yield [2R,3R]-2,3-O-isopropylidene-D-threitol 4-*tert*-butyl dimethyl silyl ether (35 g, 86%) as a yellow oil. <sup>1</sup>H NMR (CDCl<sub>3</sub>): δ 3.79 (m, 6H), 1.39 (s, 3H), 1.38 (s, 3H), 0.87 (s, 9H), 0.06 (s, 6H). <sup>13</sup>C NMR (CDCl<sub>3</sub>): δ 109.0, 80.1, 78.1, 63.6, 62.7, 26.9, 26.8, 25.8, 18.2, -5.5. HRMS calculated for C<sub>13</sub>H<sub>28</sub>O<sub>4</sub>Si (M+H): 277.1835. Found: 277.1841.

**[2R,3R]-2,3-O-Isopropylidene-D-threitol 4-triisopropyl silyl ether.** [2R,3R]-2,3-O-Isopropylidene-D-threitol (1.0 g, 5.9 mmol) in THF (3 mL) was added to a stirred suspension of NaH (60% immersion in oil) (0.3 g, 6.5 mmol) in 12 mL THF under argon at 0°C. The suspension was stirred for 10 min at 0°C before warming to r.t. and stirring for an additional 45 min. TIPSCl (1.3 mL, 6.2 mmol) was added over 15 min, and the suspension was stirred at r.t. an additional 3 h. The suspension was then poured into mL sat. NaHCO<sub>3</sub> solution, and the organic phase was separated. The aqueous phase was extracted with EtOAc (3 x 200 mL). The organic fractions were combined and dried with MgSO<sub>4</sub>. The solvent was removed by rotary evaporation to yield [2R,3R]-2,3-O-isopropylidene-D-threitol 4-*tert*-butyl dimethyl silyl ether (35 g, 86%) as a yellow oil. <sup>1</sup>H NMR (CDCl<sub>3</sub>): δ 3.86 (m, 4H), 2.36 (s, 1H), 1.40 (s, 3H), 1.38 (s, 3H), 1.05 (s, 18H), 1.04 (s, 3H). <sup>13</sup>C NMR (CDCl<sub>3</sub>): δ 109.3, 80.7, 78.4, 64.4, 63.0, 27.2, 27.1, 18.1, 12.0.

**[2R,3R]-5-(*tert*-Butyl-dimethyl-silanyloxymethyl)-2,2-dimethyl-[1,3]dioxolane-4-carbaldehyde.** DMSO (8 mL, 109 mmol) in CH<sub>2</sub>Cl<sub>2</sub> (212 mL) was added via an addition funnel to a stirred solution of oxalyl chloride (4.8 mL, 55 mmol) in 120 mL CH<sub>2</sub>Cl<sub>2</sub> at -88°C under argon. The solution was allowed to stir at -88°C for several minutes before the addition of [2R,3R]-2,3-O-isopropylidene-D-threitol 4-*tert*-butyl dimethyl silyl ether (11.6 g, 42 mmol) in 60 mL CH<sub>2</sub>Cl<sub>2</sub> via cannula. The solution was stirred at -88°C an additional 20 min before TEA (30 mL 210 mmol) was added. The reaction was allowed to warm to r.t. and stirred for an additional 1 h. H<sub>2</sub>O (100 mL) was added and the organic layer was dried with Na<sub>2</sub>SO<sub>4</sub>. The solvent was removed by rotary evaporation, and the resulting syrup was resuspended in 1:1 EtOAc-hexanes. The

solution was passed through a plug of silica gel plug. The solute was concentrated by rotary evaporation to yield the aldehyde (9.8 g, 85%). <sup>1</sup>H NMR (CDCl<sub>3</sub>): δ 9.75 (d, 1H), 4.31 (dd, 1H), 4.09 (m, 2H), 3.78 (d, 4H), 1.45 (s, 3H), 1.40 (s, 3H), 0.88 (s, 9H), 0.06 (s, 6H).

**[2R,3R]-5-(triisopropyl-silanyloxymethyl)-2,2-dimethyl-[1,3]dioxolane-4-carbaldehyde.** DMSO (0.24 mL, 3.4 mmol) in CH<sub>2</sub>Cl<sub>2</sub> (1 mL) was added to a stirred solution of oxalyl chloride (0.15 mL) in 7 mL CH<sub>2</sub>Cl<sub>2</sub> at –88°C under argon. The solution was allowed to stir at –88°C for several minutes before the addition of [2R,3R]-2,3-O-isopropylidene-D-threitol 4-triisopropylsilyl ether (0.4 g, 1.3 mmol) in 2 mL CH<sub>2</sub>Cl<sub>2</sub>. The solution was stirred at –88°C an additional 20 min before TEA (0.9 mL) was added. The reaction was allowed to warm to r.t. and stirred for an additional 1 h. H<sub>2</sub>O was added and the organic layer was dried with Na<sub>2</sub>SO<sub>4</sub>. The solvent was removed by rotary evaporation, and the resulting syrup was resuspended in 1:1 EtOAc-hexanes. The solution was passed through a plug of silica gel plug. The solute was concentrated by rotary evaporation to yield the aldehyde (0.18 g, 44%). <sup>1</sup>H NMR (CDCl<sub>3</sub>): δ 9.76 (d, 1H), 4.38 (dd, 1H), 4.11 (m, 1H), 3.86 (dd, 2H), 1.44 (s, 3H), 1.38 (s, 3H), 1.04 (s, 18H), 1.03 (s, 3H).

**[2R,3R]-1-[5-(*tert*-Butyl-dimethyl-silanyloxymethyl)-2,2-dimethyl-[1,3]dioxolan-4-yl]-ethanol.** Methyl magnesium bromide (3 M in hexanes, 35 mL, 105 mmol) was added to a solution of aldehyde (9.8 g, 35 mmol) in 350 mL THF at –78°C under argon. The solution was stirred at –78°C for 2 h, then warmed to r.t. and stirring

continued until the reaction was complete. The reaction was quenched by the addition of 100 mL of sat.  $\text{NH}_4\text{Cl}$ . The aqueous layer was extracted with  $\text{Et}_2\text{O}$  (3 x 100 mL). The organic layers were combined and dried with  $\text{MgSO}_4$ . The solvent was removed by rotary evaporation and the residue was purified by flash chromatography (1:9 EtOAc-hexanes) to yield the alcohol (5.9 g, 48%).  $^1\text{H}$  NMR ( $\text{CDCl}_3$ ): 4.29 (d, 1H), 4.03 (m, 1H), 3.79 (dd, 2H), 2.25 (s, 3H), 1.43 (s, 3H), 1.40 (s, 3H), 0.86 (s, 9H), 0.05 (s, 6H).

**[2R,3R]-1-[5-(triisopropylsilyloxy)-2,2-dimethyl-[1,3]dioxolan-4-yl]-ethanol.**

Methyl magnesium bromide (2.5 M in hexanes, 0.5 mL, 1.25 mmol) was added to a solution of aldehyde (0.18 g, 0.57 mmol) in 4 mL THF at  $-78^\circ\text{C}$  under argon. The solution was stirred at  $-78^\circ\text{C}$  for 2 h, then warmed to r.t., and stirring continued until the reaction was complete. The reaction was quenched by the addition of sat.  $\text{NH}_4\text{Cl}$ . The aqueous layer was extracted with  $\text{Et}_2\text{O}$  (3 x 2 mL). The organic layers were combined and dried with  $\text{MgSO}_4$ . The solvent was removed by rotary evaporation and the residue was purified by flash chromatography (1:9 EtOAc-hexanes) to yield the alcohol (35 mg, 19%).  $^1\text{H}$  NMR ( $\text{CDCl}_3$ ):  $\delta$  3.79 (m, 5H), 3.35 (s, 1H), 1.38 (s, 3H), 1.37 (s, 3H), 1.25 (d, 3H), 1.07 (s, 18H), 1.05 (s, 3H).  $^{13}\text{C}$  NMR ( $\text{CDCl}_3$ ):  $\delta$  84.3, 79.4, 68.1, 64.5, 26.9, 26.7, 19.4, 17.8, 11.7.

**1-[5-(*tert*-Butyl-dimethyl-silanyloxymethyl)-2,2-dimethyl-[1,3]dioxolan-4-yl]-ethanone.** To a solution of alcohol (5.9 g, 20 mmol) in  $\text{CH}_2\text{Cl}_2$  (65 mL) was added NMO (3.3 g, 28 mmol), crushed, activated 4Å molecular sieves (6.5 g), and TPAP (0.32 g, 1 mmol). The suspension was stirred at r.t. under argon for 2 h. The suspension was

concentrated by rotary evaporation. The resulting syrup was purified by flash chromatography (19:1 hexanes-EtOAc). The fractions containing the desired product were pooled and concentrated to yield the ketone (5.2 g, 88%) as a syrup. <sup>1</sup>H NMR (CDCl<sub>3</sub>): 4.29 (d, 1H), 4.03 (m, 1H), 3.79 (dd, 2H), 2.25 (s, 3H), 1.43 (s, 3 H), 1.40 (s, 3H), 0.86 (s, 9 H), 0.05 (s, 6H). HRMS calculated for C<sub>14</sub>H<sub>28</sub>O<sub>4</sub>Si (M+H): 289.1835. Found: 289.1826.

### Genetic manipulations

#### pHS7.098.

The *asd* locus was amplified by PCR from *E. coli* W3110 genomic DNA using the following primers containing *Bam*HI terminal recognition sequences: 5'-CGGGATCCATGAAAAATGTTGGTTTTATC and 5'-CGGGATCCTTACGCCAGTTGACGAAGCAT. The amplified 1.1 kb PCR fragment was digested with *Bam*HI and ligated into the *Bam*HI site of pJG7.246 (*T<sub>s</sub>*, *lacO*, *lacO*, *6xhis*, *laq<sup>o</sup>*, Amp<sup>r</sup>) to create plasmid pHS7.098 (*T<sub>s</sub>*, *lacO*, *lacO*, *6xhis*, *asd*, *lacl<sup>o</sup>*, Amp<sup>r</sup>) in which the *asd* gene is oriented in the same directions as the *T<sub>s</sub>* promoter.

#### pHS8.080.

The *hdhI* locus was amplified by PCR from *E. coli* W3110 genomic DNA using the following primers containing *Bam*HI terminal recognition sequences: 5'-CGCGGATCCGTGATGAAGACGAATTACC and 5'-CGCGGATCCTCAGACTCCTAACTTCCATG. The amplified 1.5 kb PCR fragment was digested with *Bam*HI and ligated into the *Bam*HI site of pJG7.246 (*T<sub>s</sub>*, *lacO*, *lacO*,

*6xhis*, *laq<sup>Q</sup>*, *Amp<sup>r</sup>*) to create plasmid pHS8.080 (*T<sub>5</sub>*, *lacO*, *lacO*, *6xhis*, *hdhI*, *lacI<sup>Q</sup>*, *Amp<sup>r</sup>*) in which the *hdhI* gene is oriented in the same directions as the *T<sub>5</sub>* promoter.

#### **pHS8.216.**

The *thrA* locus was amplified by PCR from *E. coli* W3110 genomic DNA using the following primers containing *Bam*HI and *Nde*I terminal recognition sequences: 5'-GGAATTCATATGGAGTGTTGAAGTTTCGGCG and 5'-CCGGATCCGACTCCTAACTTCCATGAGAGG. The amplified 2.46 kb PCR fragment was digested with *Bam*HI and *Nde*I and ligated into the *Bam*HI/*Nde*I sites of pET-15b (*T<sub>7</sub>*, *lacO*, *rbs*, *6xhis*, *Amp<sup>r</sup>*, *lacI<sup>Q</sup>*) to create plasmid pHS8.216 (*T<sub>7</sub>*, *lacO*, *rbs*, *6xhis*, *thrA*, *Amp<sup>r</sup>*) in which the *thrA* gene is oriented in the same directions as the *T<sub>7</sub>* promoter.

#### **pHS8.240.**

The *mjl602* locus was amplified by PCR from *M. jannaschii* genomic DNA using the following primers containing *Bam*HI terminal recognition sequences: 5'-CGGGATCCATATAATTATAGTAGGATTTG and 5'-CGGGATCCTTATTTTTTAGTAGAATTGTA. The amplified 1.0 kb PCR fragment was digested with *Bam*HI and ligated into the *Bam*HI site of pET-15b (*T<sub>7</sub>*, *lacO*, *rbs*, *6xhis*, *Amp<sup>r</sup>*, *lacI<sup>Q</sup>*) to create plasmid pHS8.240 (*T<sub>7</sub>*, *lacO*, *rbs*, *6xhis*, *mjl602*, *Amp<sup>r</sup>*, *lacI<sup>Q</sup>*) in which the *mjl602* gene is oriented in the same directions as the *T<sub>7</sub>* promoter.

### **pHS8.243.**

The *mj0400* locus was amplified by PCR from pMJ0400 using the following primers containing *Bam*HI terminal recognition sequences: 5'-CGCGGATCCG A A T T A T T T A A A G A C A T A A A G and 5'-CGCGGATCCTTATTTCTTCCTAATCTCTTT. The amplified 0.8 kb PCR fragment was digested with *Bam*HI and ligated into the *Bam*HI site of pET-15b (*T<sub>7</sub>*, *lacO*, *rbs*, *6xhis*, Amp<sup>r</sup>, *lacI*<sup>Q</sup>) to create plasmid pHS8.101 (*T<sub>7</sub>*, *lacO*, *rbs*, *6xhis*, *mj0400*, Amp<sup>r</sup>, *lacI*<sup>Q</sup>) in which the *mj0400* gene is oriented in the same directions as the *T<sub>7</sub>* promoter.

### **pHS8.101.**

The *mjl249* locus was amplified by PCR from *M. jannaschii* genomic DNA using the following primers containing *Bam*HI terminal recognition sequences: 5'-CGCGGATCCG G A T G G G T T A A T G T T A T T G G A and 5'-CGCGGATCCTCACTTTTCAATAATCGTCTC. The amplified 0.9 kb PCR fragment was digested with *Bam*HI and ligated into the *Bam*HI site of pET-15b (*T<sub>7</sub>*, *lacO*, *rbs*, *6xhis*, Amp<sup>r</sup>, *lacI*<sup>Q</sup>) to create plasmid pHS8.101 (*T<sub>7</sub>*, *lacO*, *rbs*, *6xhis*, *mjl249*, Amp<sup>r</sup>, *lacI*<sup>Q</sup>) in which the *mjl249* gene is oriented in the same directions as the *T<sub>7</sub>* promoter.

## **Enzyme Purifications**

### ***E. coli* aspartate semialdehyde dehydrogenase (ASADH)**

DH5 $\alpha$ /pHS7.098 was grown on LB/Amp agar plates at 37°C overnight. A single colony was used to inoculate 5 mL LB/Amp media, and the cultures were grown at 37°C in a shaker overnight. A 1 mL aliquot of the 5 mL overnight culture was used to



inoculate 500 mL of LB/Amp media. The 500 mL culture was incubated in a shaker at 37°C and 250 rpm until the OD<sub>600</sub> reached ~1. IPTG was added to a concentration of 0.1 mM, and the culture was incubated at 37°C and 250 rpm for an additional 12. The culture cells were harvested by centrifugation (6400 g, 4°C, 5 min), and the supernatant was discarded.

The cells were resuspended in 10 mL of binding buffer (20 mM Tris-HCl (pH 8.0) containing 10 mM imidazole and 300 mM NaCl). The cells were lysed by two passes through a french pressure cell and the cellular debris was removed by centrifugation (48,000g, 4°C, 30 min). Ni<sup>2+</sup>-NTA resin (1 mL) was added to the supernatant. The suspension was stirred at 4°C for 1 h, and the supernatant was eluted from the resin. The resin was washed with 5 column volumes of binding buffer, followed by 5 column volumes of wash buffer #1 (20 mM Tris-HCl (pH 8.0) containing 20 mM imidazole and 300 mM NaCl) and wash buffer #2 (20 mM Tris-HCl (pH 8.0) containing 100 mM imidazole and 300 mM NaCl). The desired ASADH was eluted with 5 column volumes of eluting buffer (20 mM Tris-HCl (pH 8.0) containing 200 mM imidazole and 300 mM NaCl). The presence of ASADH was determined by SDS-PAGE (MW 77.5 kDa, dimer), and fractions containing the desired protein were dialyzed against 20 mM Tris-HCl (pH 7.5) overnight. The final protein concentration was 7.9 mg/mL. The specific activity of the ASADH produced was measured to be 0.48 U/mg.

#### **MJ0400 from BL21 Codon Plus RIL//pMJ0400.**

The plasmid pMJ0400 was transformed into BL21 Codon Plus RIL competent cells, and the construct was grown at 37°C overnight on LB/Amp/Cm agar plates. A

single colony was used to inoculate 5 mL LB/Amp/Cm media. The 5 mL culture was incubated at 37°C in a shaker overnight. The 5 mL culture was used to inoculate 1 L LB/Amp/Cm media, and this culture was incubated at 37°C and 250 rpm until the OD<sub>600</sub> reached ~1. Lactose was added to 28 mM to induce MJ0400 expression. The culture was incubated an additional 3 h at 37°C before the cells were harvested by centrifugation (6400g, 4°C, 5 min).

The supernatant was discarded and the cells were resuspended in 15 mL of 20 mM Bis-Tris-HCl (pH 6.5). The cells were lysed by two passes through a french pressure cell and the cellular debris was removed by centrifugation (48,000g, 4°C, 25 min). The supernatant was heated at 70°C for 30 min and the precipitated proteins were removed by centrifugation (48,000g, 4°C, 20 min). The supernatant was dialyzed against 1 L 20 mM Tris-HCl (pH 7.5) overnight. The protein solution was concentrated to 2 mL containing 20 mg/mL protein. The presence of MJ0400 was determined by SDS-PAGE (29.7 kDa).

## **Enzyme Assays**

### **ASADH specific activity assay**

A solution of 1 M phosphate (pH 9.0) (10 µL) was diluted with 940 µL d.d. H<sub>2</sub>O. To this solution was added 10 µL NADP solution (6 mg/mL) and 20 µL ASA solution produced through the ozonolysis of L-allyl glycine. Upon addition of 10 µL ASADH solution the increase in the absorbance at 340 nm at r.t. was observed. An extinction coefficient of 6220 was used for specific activity calculations.

## **In vitro enzyme reactions**

### **Condensation of ASA and DKFP by MJ0400.**

A solution containing ASA (6 mg, 51  $\mu$ mol), DKFP (18 mg, 71  $\mu$ mol),  $\text{MgCl}_2 \cdot 2\text{H}_2\text{O}$  (17 mg, 84 mmol), 20 mM potassium phosphate buffer (degassed) (5 mL), and d.d.  $\text{H}_2\text{O}$  (4.4 mL) was prepared and degassed with argon. A solution of MJ0400 (1 mL, 20 mg protein) was added, and the solution was stirred at 60°C for 30 min.  $\text{NaBH}_4$  (0.5 mL of a 5.3 M solution in  $\text{H}_2\text{O}$ ) was added, and the reaction was stirred for an additional 1.5 h at r.t.. The reaction was acidified by the addition of HCl solution and the protein was removed by centrifugation. The solvent was removed by rotary evaporation, and the residue was azeotroped three times with MeOH. The residue was resuspended in  $\text{H}_2\text{O}$  and absorbed onto a column of Dowex 50 ( $\text{H}^+$  form) (1 mL). The column was washed with d.d.  $\text{H}_2\text{O}$  (15 column volumes) and the product was eluted with 1 N HCl (15 column volumes). The solvent was removed by rotary evaporation. The resulting residue was treated with 1 N HCl in MeOH overnight at r.t.. The solvent was removed by rotary evaporation, and the residue was resuspended in a 1:1 solution of trifluoroacetic anhydride- $\text{CH}_2\text{Cl}_2$ . The reaction was stirred at r.t. for 2 h and the solvent was removed under a stream of argon. The resulting residue was resuspended in methyl acetate (250  $\mu$ L). The product was analyzed by GC-MS analysis. GC peaks identified: 6.73, 7.20, 7.43, and 7.68 min.

## **GC-MS analysis**

### **Analysis of MJ0400 catalyzed condensation of ASA and DKFP.**

A 5  $\mu\text{L}$  aliquot of the product solution in methyl acetate was injected onto a GC-MS column at 95°C. The temperature was increased by 10°C per min to provide a linear gradient from 95 to 280°C. The samples were analyzed at 70 eV.

## REFERENCES

- <sup>1</sup> Pittard, A.J., *Biosynthesis of Aromatic Amino Acids*, in *Escherichia coli and Salmonella Cellular and Molecular Biology*, F.C. Neidhardt, Editor. 1996, ASM Press: Washington D.C. p. 458-484.; Bult. C. J.; et. Al. *Science* **1996**, 273, 1058-1073.
- <sup>2</sup> Floss, H.G. *Natural Product Reports* **1997**, 14(5), 433-452.
- <sup>3</sup> Rinehart, K. L.; Shield, L. S. *Forstchr. Chem. Org. Naturst.* 1976, 33, 231-307.
- <sup>4</sup> Prelog, V.; Oppolzer, W. *Helv. Chim. Acta* **1973**, 56, 2279-2287.
- <sup>5</sup> Funayama, S.; Cordell, G. A. *Stud. Nat. Prod. Chem.* **2000**, 23, 61-106.
- <sup>6</sup> Sensi, P.; Greco, A. M.; Ballotta, G. *Antibiot. Annu.* **1959**, 262-270.
- <sup>7</sup> Wehrli, W.; Knusel, F.; Nuesch, J.; Staehelin, M. *Proc. Natl. Acad. Sci. USA* **1968**, 61, 667-673.
- <sup>8</sup> (a) Ganguly, A. K.; *J. Chromatogr. Libr.* **1978**, 15, 39-68. (b) Mustaev, A.; Zaychikov, E.; Severinov, K.; Kashlev, M.; Polyakov, A.; Nikiforov, V.; Goldfarb, A. *Proc. Nat. Acad. Sci. USA* **1994**, 91, 12036-12040. (c) Wehrli, W., *Rev. Infect. Dis.* **1983**, 5, S407-S411. (d) Wegrzyn, A.; Szalewska-Palasz, A.; Blaszcak, A.; Liberek, K.; Wegrzyn, G. *FEBS Lett.* **1998**, 440, 172-174. (e) Pfannschmidt, T.; Link, G. *Mol. Gen. Genet.* **1997**, 257, 35-44. (f) Sodeik, B.; Griffiths, G.; Ericsson, M.; Moss, B.; Doms, R. W. *J. Virol.* **1994**, 68, 1103-1114. (g) Tomiyama, T.; Asano, S.; Suwa, Y.; Morita, T.; Kataoka, K.-I.; Mori, H.; Endo, N. *Biochem. Biophys. Res. Comm.* **1994**, 204, 76-83.
- <sup>9</sup> Sepkowitz, K. A.; Raffalli, J.; Riley, L.; Kiehn, T. E.; Armstrong, D. *Clin. Microbiol. Rev.* **1995**, 8, 180-199.
- <sup>10</sup> Corcoran, J. W.; Chick, M.; in *Biosynthesis of Antibiotics*; Academic Press: London, New York, 1966; Vol. 1; 159.
- <sup>11</sup> (a) Ghisalba, O.; Auden, J. A. Schupp, T.; Nuesch, J. in *Biotechnology of industrial Antibiotics* Vandamme, E. J., Ed; 1984, Vol 22, 281. (b) Allen, M. S.; McDonald, I. A.; Rickards, R. W. *Tetrahedron Lett.* 1981, 1145-1148. (c) White, R. J.; Martinelli, E.; Lancini, G. *Proc. Natl. Acad. Sci. USA* 1974, 71, 3260-3264. (d) Milavetz, B.; Kakinuma, K.; Rinehart, K. L.; Rolls, J. P.; Haak, W. J. *J. Am. Chem. Soc.* 1973, 95, 5793-5795. (e) Sugita, M.; Sasaki, T.; Furihata, K.; Seto, H.; Otake, N. *J. Antibiot.*

- 1982, 35, 1467-1473. (f) Johnson, R. D.; Haber, A.; Rinehart, K. L. *J. Am. Chem. Soc.* 1974, 96, 3316-3317.
- <sup>12</sup> Brufani, M.; Kluepfel, D.; Lancini, G. C.; Leitich, J.; Mesentseu, A. S.; Prelog, V.; Schmook, F. P.; Sensi, P. *Helv. Chim. Acta.* 1973, 56, 2315-2323.
- <sup>13</sup> (a) Johnson, R. D.; Haber, A.; Rinehart, K. L. *J. Am. Chem. Soc.* 1974, 96, 3316-3317. (b) Haber, A.; Johnson, R. D.; Rinehart, K. L. *J. Am. Chem. Soc.* 1977, 99, 3541-3544.
- <sup>14</sup> Lee, J. P.; Tsao, S.-W.; Chang, C. J.; Floss, H. G. *Can. J. Chem.* 1994, 72, 182-187.
- <sup>15</sup> (a) Allen, M. S.; McDonald, I. A.; Rickards, R. W. *Tetrahedron lett.* 1981, 1145-1148. (b) McDonald, I. A.; Rickards, R. W. *Tetrahedron lett.* 1981, 1149-1152.
- <sup>16</sup> Milavetz, B.; Kakinuma, K.; Rinehart, K. L.; Roll, J. P.; Haak, W. J. *J. Am. Chem. Soc.* 1973, 95, 5793-5795.
- <sup>17</sup> Lancini, G.; Grandi, M. In *Antibiotics*, Corcoran, J. W., Eds.; New York: Springer-Verlag, 1981, vol 4 (Biosynthesis), p12-40.
- <sup>18</sup> Ghisalba, O.; Nuesch, J. *J. Antibiot.* **1981**, 34, 64-71.
- <sup>19</sup> (a) Staley, A. L.; Rinehart, K. L. *J. Antibiot.* **1991**, 44, 218-224. (b) Hatano, K.; Akiyama, S.; Asai, M.; Richards, R. W. *J. Antibiot.* **1982**, 35, 1415-1417. (c) Anderson, M. G.; Kibby, J. J.; Rickards, R. W.; Rothschild, J. M. *J. Chem. Soc., Chem. Commun* **1980**, 1277-1278. (d) Herlt, A. J.; Kibby, J. J.; Rickards, R. W. *Aust. J. Chem.* **1981**, 34, 1319-1324.
- <sup>20</sup> (a) Karlsson, A.; Sartori, G.; White, R. J. *Eur. J. Biochem.* **1974**, 47, 251-256. (b) Haber, A.; Johnson, R. D.; Rinehart, K. L. *J. Am. Chem. Soc.* **1977**, 99, 3541-3544. (c) Hornemann, U.; Kehr, J. P.; Eggert, J. H. *J. Chem. Soc., Chem. Commun.* **1974**, 1045-1046. (d) Hornemann, U.; Eggert, J. H.; Honor, D. P. *J. Chem. Soc., Chem. Commun.* **1980**, 11-13.
- <sup>21</sup> a) Bezanson, G. S.; Vining, L. C. *Can. J. Biochem.* **1971**, 49, 911-918. b) Casati, R.; Beale, J. M.; Floss, H. G. *J. Am. Chem. Soc.* **1987**, 109, 8102-8104.
- <sup>22</sup> Meier, R. M.; Tamm, C. *J. Antibiot.* **1992**, 45, 400-410.

- 23 a) Ghisalba, O.; Nuesch, J. *J. Antibiot.* **1978**, *31*, 202-214. b) Ghisalba, O.; Fuhrer, H.; Richter, W. J.; Moss, J. *J. Antibiot.* **1981**, *34*, 58-63. c) Gyax, D.; Ghisalba, O.; Treichler, H.; Nuesch, J. *J. Antibiot.* **1990**, *43*, 324-326.
- 24 Hornemann, U.; Kehrer, J. P.; Eggert, J. H. *J. Chem. Soc., Chem. Commun.* **1974**, 1045-1046.
- 25 (a) Kim, C.-G.; Kirschning, A.; Bergon, P.; Zhou, P.; Su, E.; Sauerbrei, B.; Ning, S.; Ahn, Y.; Breuer, M.; Leistner, E.; Floss, H. G. *J. Am. Chem. Soc.* **1996**, *118*, 7486-7491. (b) Kim, C.-G.; Kirschning, A.; Bergon, P.; Ahn, Y.; Wang, J. J.; Shibuya, M.; Floss, H. G. *J. Am. Chem. Soc.* **1992**, *114*, 4941-4943.
- 26 Kim, C.-G.; Yu, T.-W.; Fryhle, C. B.; Handa, S.; Floss, H. G. *J. Biol. Chem.* **1998**, *272*, 6030-6040.
- 27 August, P. R.; tang, L.; Yoon, Y. J.; Ning, S.; Muller, R.; Yu, T. -W.; Taylor, M.; Hoffmann, D.; Kim, C. -G.; Zhang, X.; Hutchinson, C. R.; Floss, H. G. *Chem. & Biol.* **1998**, *5*, 69-79.
- 28 Yu, T.-W.; Muller, R.; Muller, M.; Zhang, X.; Draeger, G.; Kim, C.G.; Leistner, E.; Floss, H. G. *J. Biol. Chem.* **2001**, *276*, 12546-12555.
- 29 Jiao, R.; Liu, C.; Jin, Z.; Zhang, X.; Ni, L.; Lu, Z. *Sci. Sin. Ser. B (engl. Ed.)* **1984**, *27*, 380-390.
- 30 Muller, R.; Floss, H. G. unpublished results.
- 31 Personal communication with the Floss group at University of Washington.
- 32 (a) Muller, M.; Floss, H. G. unpublished results. (b) Guo, J.; Frost, J. W. unpublished results.
- 33 Guo, J.; Frost, J. F. *J. Am. Chem. Soc.* **2001**, *124*(4), 528-529.
- 34 a) Blackmore, P. F.; Williams, J. F.; MacLeod, J. K. *FEBS Lett.* **1976**, *64*, 222. b) Duke, C. C.; MacLeod, J. K.; Williams, J. F. *Carbohydr. Res.* **1981**, *95*, 1.
- 35 Guo, J.; Frost, J. F. *J. Am. Chem. Soc.* **2002**, *124*(36), 10642-10643.
- 36 Arakawa, K.; Müller, R.; Mahmud, T.; Yu, T-W.; Floss, H. G. *J. Am. Chem. Soc.* **2002**, *124*(36), 10644-10645.

- 37 a) Umezawa, S.; Umino, K.; Shibahara, S.; Hamasa, M.; Omoto, S. *J. Antibiot.* **1967**, *20*, 355. b) Umezawa, S.; Umino, K.; Shibahara, S.; Omoto, S. *Bull. Chem. Soc. Japan* **1967**, *40*, 2419. c) Umezawa, S.; Shibahara, S.; Omoto, S.; Takeuchi, T.; Umezawa, H. *J. Antibiot.* **1968**, *21*, 485.
- 38 Woese, C. R.; Fox, G. E. *Proc. Natl. Acad. Sci. USA* **1977**, *74*(11), 5088-5090.
- 39 Woese, C. R.; Kandler, O.; Wheelis, M. L. *Proc. Natl. Acad. Sci. USA* **1990**, *87*, 4576-4579.
- 40 Mayr, E. *Nature* **1990**, *348*, 491.
- 41 Margulis, L.; Guerreo, R. *New Sci.* **1991**, *348*, 491.
- 42 Cavalier-Smith, T. *Nature* **1992**, *356*, 570.
- 43 Brown, J. R.; Doolittle, W. F. *Microbiol. Mol. Biol. Rev.* **1997**, *61*(4), 456-502.
- 44 Cavalier-Smith, T. *J. Syst. Evol. Microbiol.* **2002**, *52*, 7-76.
- 45 Daniels, L. Zeikus, J. G. *J. Bacteriol.* **1978**, *136*, 75-84.
- 46 Stupperich, E.; Fuchs, G. *Arch. Microbiol.* **1984**, *139*, 8-13.
- 47 a) Zeikus, J. G.; Fuchs, G.; Kenealy, W.; Thauer, R. K. *J. Bacteriol.* **1977**, *132*(2), 604-613. b) Fuchs, G.; Stupperich, E. *Arch. Microbiol.* **1978**, *121*, 121-125.
- 48 a) Weimer, P. J.; Zeikus, J. G. *J. Bacteriol.* **1979**, *137*(1), 332-339. b) Ekiel, I.; Sprott, G. D.; Patel, G. B. *J. Bacteriol.* **1985**, *162*(3), 905-908.
- 49 a) Ekiel, I.; Smith, I. C.; Sprott, G. D. *J. Bacteriol.* **1983**, *156*(1), 316-326. b) Ekiel, I.; Jarrell, K. F.; Sprott, G. D. *Eur. J. Biochem.* **1985**, *149*, 437-444. c) Ekiel, I.; Sprott, G. D.; Patel, G. B. *J. Bacteriol.* **1985**, *163*(3), 905-908.
- 50 Ekiel, I.; Jarrell, K. F.; Sprott, G. D. *Eur. J. Biochem.* **1985**, *149*, 437-444.
- 51 Ekiel, I.; Smith, I. C.; Sprott, G. D. *J. Bacteriol.* **1983**, *156*(1), 316-326.
- 52 Zeikus, J. G.; Wolfe, R. S. *J. Bacteriol.* **1972**, *109*, 707-713.



- <sup>53</sup> Eisenreich, W.; Schwarzkopf, B.; Bacher, A. *J. Biol. Chem.* **1991**, 266(15), 9622-9631.
- <sup>54</sup> Eisenreich, W.; Bacher, A. *J. Biol. Chem.* **1991**, 266(35), 23840-23849.
- <sup>55</sup> Fuchs, G.; Stupperich, E. *Arch. Microbiol.* **1980**, 127, 267-272.
- <sup>56</sup> Sprott, G. D.; Ekiel, I.; Patel, G. B. *Appl. Environ. Microbiol.* **1993**, 59(4), 1092-1098.
- <sup>57</sup> Choquet, C. G.; Richards, J. C.; Patel, G. B.; Sprott, G. D. *Arch. Microbiol.* **1994**, 161, 481-488.
- <sup>58</sup> Yu, J. P.; Ladapo, J.; Whitman, W. B. *J. Bacteriol.* **1993**, 176(2), 325-332.
- <sup>59</sup> Tumbula, D. L.; Teng, Q.; Bartlett, M. G.; Whitman, W. B. *J. Bacteriol.* **1997**, 179(19), 6010-6013.
- <sup>60</sup> Doong, R. L.; Gander, J. E.; Ganson, R. J.; Jensen, R. A. *Physiol. Plant.* **1992**, 84, 352-360.
- <sup>61</sup> Fischer, R. S.; Bonner, C. A.; Jensen, R. A. *Arch. Microbiol.* **1993**, 160, 440-446.
- <sup>62</sup> Bult, C. J.; White, O.; Olsen, G. J.; Zhou, L.; Fleischmann, R. D.; Sutton, G. G.; Blake, J. A.; Fitzgerald, L. M.; Clayton, R. A.; Gocayne, J. D.; Kerlavage, A. R.; Dougherty, B. A.; Tomb, J.-F.; Adams, M. D.; Reich, C. I.; Overbeek, R.; Kirkness, E. F.; Weinstock, K. J.; Merrick, J. M.; Glodek, A.; Scott, J. L.; Geoghagen, N. S. M.; Weidman, J. F.; Fuhrman, J. L.; Nguyen, D.; Utterback, T. R.; Kelley, J. M.; Pererson, J. M.; Sadow, P. W.; Hanna, M. C.; Cotton, M. D.; Roberts, K. M.; Hurst, M. A.; Kaine, B. P.; Borodovsky, M.; Klenk, H.-P.; Fraser, C. M.; Smith, H. O.; Woese, C. R.; Venter, J. C. *Science* **1996**, 273, 1058-1073.
- <sup>63</sup> Higuchi, S.; Kawashima, T.; Suzuki, M. *Proc. Japan Acad. Ser. B.* **1999**, 75, 241-245.
- <sup>64</sup> Daugherty, M.; Vonstein, V.; Overbeek, R.; Osterman, A. *J. Bacteriol.* **2001**, 183(1), 292-300.
- <sup>65</sup> Woodard, R. W. *Bioorg. Chem.* **2004**, 32, 309-315.
- <sup>66</sup> White, R. H. *Biochemistry* **2004**, 43, 7618-7627.

- <sup>67</sup> John Frost, personal communication
- <sup>68</sup> Adlersberg, M.; Sprinson, D. B. *Biochemistry* **1964**, 3(12), 1855-1806.
- <sup>69</sup> (a) Brufani, M.; Fedeli, W.; Giacomello, G.; Vaciago, A. *Experientia* **1964**, 20, 339-342. (b) Oppolzer, W.; Prelog, V. *Helv. Chim. Acta* **1973**, 56, 2287-2314. (c) Higashide, E.; Asai, M.; Ootsu, K.; Tanida, S.; Kozai, Y.; Hagesawa, T.; Kishi, T.; Sugino, Y.; Yoneda, M. *Nature* **1977**, 270, 712-722. (d) Asai, M.; Mizuta, E.; Izawa, M.; Haibara, K.; Kishi, T. *Tetrahedron* **1979**, 35, 1079-1085.
- <sup>70</sup> Webb, J. S.; Cosulich, D. B.; Mowat, J. H.; Patrick, J. B.; Broschard, R. W.; Meyer, W. E.; Williams, R. P.; Wolf, C. F.; Fulmor, W.; Pidacks, C.; Lancaster, J. E. *J. Am. Chem. Soc.* **1962**, 84, 3183-3184.
- <sup>71</sup> Kim, C.-G.; Kirschning P.; Bergen, P.; Ahn, B. Y.; Wang, J. J.; Shibuya, M.; Floss, H. G. *J. Am. Chem. Soc.* **1992**, 114(12), 4941-4943.
- <sup>72</sup> (a) Umezawa, S.; Umino, K.; Shibahara, S.; Omoto, S. *Bull. Chem. Soc. Japan* **1967**, 40, 2419-2421. (b) Umezawa, S.; Shibahara, S.; Omoto, S. *J. Antibiot.* **1968**, 21(8), 485-491.
- <sup>73</sup> (a) Dolak, L. A.; Castle, T. M.; Dietz, A.; Laborde, A. L. *J. Antibiot.* **1980**, 33(8), 900-901. (b) Tsuno, T.; Ikeda, C.; Numata, K.; Tomita, K.; Konishi, M.; Kawaguchi, H. *J. Antibiot.* **1986**, 39, 1001-1003. (c) Fusetani, N.; Ejima, D.; Matsunaga, S.; Hashimoto, K.; Itagaki, K.; Akagi, Y.; Taga, N.; Suzuki, K. *Experientia* **1987**, 43, 464-465. (d) Milner, J. L.; Silo-Suh, L.; Lee, J. C.; He, H.; Clardy, J.; Handelsman, J. *Appl. Environ. Microbiol.* **1996**, 62, 3061-3065.
- <sup>74</sup> Tercero, J. A.; Espinosa, J. C.; Lacalles, R. A.; Jiménez, A. *J. Biol. Chem.* **1996**, 271(3), 1579-1590.
- <sup>75</sup> Pietsch, M.; Walter, M.; Buchholz, K. *Carb. Res.* **1994**, 254, 183-194.
- <sup>76</sup> Drummond, M. *Nature* **1979**, 281(4), 343-347.
- <sup>77</sup> Bernaerts, M. J.; De Ley, J. Antonie Van Leeuwenkoek, *J. Microbiol. Serol.* **1967**, 27, 247-256.
- <sup>78</sup> a) Fukui, S. *Biochem. Biophys. Res. Commun.* **1965**, 18(2), 186-191. b) Van Beeuman, J.; De Ley, J. *Eur. J. Biochem.* **1968**, 6, 331-343. c) Fukui, S. *J. Bacteriol.* **1969**, 97(2), 793-798. d) Hayano, K.; Fukui, S. *J. Bacteriol.* **1970**, 101(1), 692-697.

- 79 Van Beeuman, J.; De Ley, J. *Eur. J. Biochem.* **1968**, *6*, 331-343.
- 80 Hayano, K.; Fukui, S. *J. Bacteriol.* **1970**, *101*(1), 692-697.
- 81 Fukui, S. *J. Bacteriol.* **1969**, *97*(2), 793-798.
- 82 Miyairi, A.; Fukui, S. *J. Bacteriol.* **1973**, *113*(2), 658-665.
- 83 Fukui, S. *Agr. Biol. Chem.* **1970**, *34*(2), 321-324.
- 84 Chern, C.-K.; Fukui, S. *Agr. Biol. Chem.* **1974**, *38*(10), 2039-2040.
- 85 Fukui, S.; Hayano, K. *Agr. Biol. Chem.* **1969**, *33*(7), 1013-1017.
- 86 Ma, X.; Stöckigt, J. *Carb. Res.* **2001**, *333*, 159-163.
- 87 Rotenberg, S.; Sprinson, D. B. *J. Biol. Chem.* **1978**, *253*(7), 2210-2215.
- 88 Lee, L. G.; Whitesides, G. J. *Am. Chem. Soc.* **1985**, *107*(24), 6999.
- 89 Ahlert, J.; Distler, J.; Mansouri, K.; Piepersberg, W. *Arch. Microbiol.* **1997**, *168*, 102-113.
- 90 Breazeale, S. D.; Ribeiro, A. A.; Raetz, C. R. H. *J. Biol. Chem.* **2003**, *278*(27), 24731-24739.
- 91 Meynial, I.; Paquet, V.; Combes, D. *Anal. Chem.* **1995**, *67*, 1627-1631.
- 92 Chem, H.; Yeung, S-M.; Que, N. L. S.; Müller, T.; Schmidt, R. R.; Liu, H. *J. Am. Chem. Soc.* **1999**, *121*, 7166-7167.
- 93 Unpublished results by Jiantao Guo
- 94 Unpublished results by Jiantao Guo
- 95 a) Zeikus, J. G.; Fuchs, G.; Kenealy, W.; Thauer, R. K. *J. Bacteriol.* **1977**, *132*(2), 604-613. b) Fuchs, G.; Stupperich, E. *Arch. Microbiol.* **1978**, *121*, 121-125. c) Ekiel, I.; Smith, I. C.; Sprott, G. D. *J. Bacteriol.* **1983**, *156*(1), 316-326. d) Ekiel, I.; Jarrell, K. F.; Sprott, G. D. *Eur. J. Biochem.* **1985**, *149*, 437-444. e) Ekiel, I.; Sprott, G. D.; Patel, G. B. *J. Bacteriol.* **1985**, *163*(3), 905-908.

- <sup>96</sup> a) Lüscher, H.; Uzar, H. C. *Tetrahedron: Asymmetry* **2000**, *11*, 4965-4973. b) Paris, M.; Pothion, C.; Heitz, A.; Martinez, J.; Fehrentz, J.-A. *Tetrahedron Letters* **1998**, *39*, 1341-1344. c) Roberts, S. J.; Morris, J. C.; Renwick, C. J.; Gerrard, J. A. *Bioorg. Med. Chem. Lett.* **2003**, *13*, 265-267. d) Black, S.; Wright, N. G. *J. Biol. Chem.* **1955**, *213*, 39-50.
- <sup>97</sup> Hegeman, G. D.; Cohen, G. N.; Morgan, R. *Methods in Enzymology* **1970**, *17A*, 708-713.
- <sup>98</sup> Wong, C. H.; Whitesides, G. M. *J. Org. Chem.* **1983**, *48*, 3199-3205.
- <sup>99</sup> Bubbs, W. A.; Kuchel, P. W. *J. Biol. Chem.* **1992**, *267*(14), 9713-9717.
- <sup>100</sup> James, C.; Viola, R. E. *Biochemistry* **2002**, *41*, 3720-3725.
- <sup>101</sup> Burgstahler, A. W.; Weigel, L. O.; Shaefer, C. G. *Synth. Commun.* **1976**, 767-768.
- <sup>102</sup> a) Blanchette, M. A.; Choy, W.; Davis, J.; Essendorf, A. P.; Roush, W. R.; Sakai, T. *Tetrahedron Letters* **1984**, *25*(21), 2183-2186.; b) Ghosh, A. K.; Gong, G. *J. Am. Chem. Soc.* **2004**, *126*, 3704-3705.
- <sup>103</sup> Walsh, P. J.; Sharpless, K. B. *Synlett* **1993**, 605-606.
- <sup>104</sup> Cox, R.; de Andrés-Gómez, A.; Godfrey, C. R. A. *Org. Biomol. Chem.* **2003**, *1*, 3171-3177.
- <sup>105</sup> Allevi, P.; Criboiu, R.; Anastasia, M. *Tetrahedron: Asymmetry* **2004**, *15*, 1355-1358.
- <sup>106</sup> Miller, J. H. *Experiments in Molecular Genetics*; Cold Spring Harbor Laboratory: Cold Spring Harbor, NY, 1972.
- <sup>107</sup> Lancini, G. In *Biotechnology*; Rehm, H.-J., Reed, G., Eds.; VCH Verlagsgesellschaft: Weinheim, 1986; Vol. 4, Chapter 14.
- <sup>108</sup> Guo, J.; Frost, J. W. unpublished results.
- <sup>109</sup> Bradford, M. M. *Anal. Biochem.* **1976**, *72*, 248-254.
- <sup>110</sup> Singer, T. P. *Methods Biochem. Anal.* **1974**, *22*, 123-175.
- <sup>111</sup> Allen, R. G.; Keogh, B. P.; Tresini, M.; Gerhard, G. S.; Volker, C.; Pignolo, R. J.; Horton, J.; Cristofalo, V. J. *J. Biol. Chem.* **1997**, *272*, 24805-24812.

- <sup>112</sup> Singer, T. P. *Methods Biochem. Anal.* **1974**, 22, 123-175.
- <sup>113</sup> Allen, R. G.; Keogh, B. P.; Tresini, M.; Gerhard, G. S.; Volker, C.; Pignolo, R. J.; Horton, J.; Cristofalo, V. J. *J. Biol. Chem.* **1997**, 272, 24805-24812.
- <sup>114</sup> Harris, E. L. V.; Angal, S. In *Protein Purification Methods: A Practical Approach*; Oxford University Express: Oxford, New York, Tokyo, 1989.
- <sup>115</sup> Laemmli, U. K. *Nature* **1970**, 227, 680-685.
- <sup>116</sup> Pasqualucci, C. R.; Vigevani, A.; Radaelli, P.; Gallo, G. G. *J. Pharm. Sci.* **1970**, 59, 685-687.
- <sup>117</sup> Rae, C.; Bubb, W. A.; Kuchel, P. W. *J. Biol. Chem.* **1992**, 267(14), 9713-9717.
- <sup>118</sup> Rae, C.; Bubb, W. A.; Kuchel, P. W. *J. Biol. Chem.* **1992**, 267(14), 9713-9717.

MICHIGAN STATE UNIVERSITY LIBRARIES



3 1293 02845 8770